

**The role of Insulin Growth Factor axis in stem cell based  
periodontal regeneration under diabetic conditions**

Nancy Mohamed Sobeih Elsayed Hussein

Submitted in accordance with the requirements for the degree of  
Doctor of Philosophy

The University of Leeds  
Faculty of Medicine and Health  
School of Dentistry

June 2023

## Declaration

The candidate confirms that the work submitted is her own, except where work which has formed part of jointly authored publications has been included. The contribution of the candidate and the other authors to this work has been explicitly indicated below. The candidate confirms that appropriate credit has been given within the thesis where reference has been made to the work of others.

**The work in chapter 1 of the thesis has been published as a review paper as follows:**

The Effect of Diabetes Mellitus on IGF Axis and Stem Cell Mediated Regeneration of the Periodontium.

**Authors:** Nancy M. S. Hussein, Josie L. Meade, Hemant Pandit, Elena Jones and Reem El-Gendy

**Journal:** Bioengineering

**Year:** 2021

**Author Contributions:** Conceptualization, R.E.-G., E.J. Writing - original draft preparation, N.M.S.H. Writing - review and editing, R.E.-G., E.J., J.L.M., H.P., N.M.S.H. Supervision, R.E.-G., E.J., J.L.M., H.P. All authors have read and agreed to the published version of the manuscript.

This copy has been supplied on the understanding that it is copyright material and that no quotation from the thesis may be published without proper acknowledgement. The right of Nancy Mohamed Sobeih Elsayed Hussein to be identified as Author of this work has been asserted by her in accordance with the Copyright, Designs and Patents Act 1988.

© 2023 The University of Leeds and Nancy Mohamed Sobeih Elsayed Hussein

## Acknowledgement

I would like to offer a huge thank you to my main supervisor Dr Reem El-Gendy for her invaluable support and enthusiasm throughout my PhD. I am deeply grateful for her sincere advice, constant guidance and comprehensive training on tissue culture and qPCR techniques. Her exceptional cooperation, understanding and motivation were fundamental to this project and inspirational to me on different levels.

I also would like to thank Dr Josie Meade for her warmth and invaluable help with the flow cytometry experiments and the ELISA assays. I genuinely enjoyed all our discussions – not just about flow cytometry and immunology but also about English culture and her brilliant recommendations of books and novels. I am also indefinitely grateful to Dr Elena Jones for her compassionate and heartfelt guidance. Her feedback on my lab work and writing was always positive and insightful. The time I spent working with her group was a great experience which deeply enriched my PhD journey. A special and sincere thank you for Prof. Hemant Pandit, this work would not have been possible without his precious help and dedication.

I would like to thank all my colleagues at the Division of Oral Biology, especially Dr Sarah Myers, Ms Emma Black and Mr Michael Brookes for their kind support. I am also thankful for Ms Arwa Alghamdi, Ms Laura Whitehouse, Ms Essra Zawia, Ms Raghda Abdelgawad, Ms Dina Abdel Fattah, Ms Asmaa Harfoush, Ms Hend Alharbi and Dr Taghreed Mohamed for their friendliness; and Ms Julie McDermott and Ms Ruth Kaiman for their administrative assistance.

A big thank you for colleagues and friends at Leeds Institute of Rheumatic and Musculoskeletal Medicine (LIRMM) and Haematology Unit: Dr Payal Ganguly, Dr Dragos Ilas and Dr William Jones for their helpful advice. I am also grateful for Ms Rekha Palmer, Dr Sophie Stephenson and Ms Zoe Wigston for their generous help. A huge thank you goes to Ms Liz Strzynski, her expert technical help and patience were fundamental to the flow cytometry analyses.

I am also grateful for the Egyptian Ministry of Higher Education (Newton Mosharafa Program) for funding my PhD and for the Egyptian Cultural and

Educational Bureau in London for their cooperation and helpfulness during my stay in the UK. Same goes for Mansoura University, my home university in Egypt, especially my friends and colleagues at the Faculty of Dentistry.

Last but not least, I can never thank my husband Khaled enough for his unfailing and never ending support, encouragement and understanding, not just during the highs and lows of my PhD journey but ever since we met. Same goes for my parents, who were always there for me and to whom I owe a lot. I am also grateful for my brother and sister, their families, my in-laws and my friends Aya and Rana for being a source of constant support, best wishes and endless prayers.

## Abstract

Periodontitis and diabetes mellitus (DM) are two of the most common and challenging health problems worldwide, and they affect each other mutually and adversely. Current periodontal therapies have unpredictable outcome in diabetic patients. Periodontal tissue engineering is a challenging but promising approach that aims at restoring periodontal tissues using one or all of the following: stem cells, signalling molecules and scaffolds. Mesenchymal stem/stromal cells (MSCs) and Insulin-like growth factor (IGF) could be ideal candidates for stem cells and signalling molecules.

In this study, bone marrow mesenchymal stem/stromal cells (BM-MSCs) were isolated from patients with type 2 diabetes mellitus (T2DM) and non-diabetic controls. Both cell populations were compared for their clonogenicity, proliferation rates and percentage of MSC populations. Moreover, expression of osteogenic, periodontal markers and IGF axis genes was assessed under basal and osteogenic conditions after 1, 2 and 3 weeks in culture. Levels of IGFBP-2, -3 and -4 in conditioned media were evaluated using ELISA assays.

Diabetic and non-diabetic BM-MSCs exhibited similar clonogenic, proliferative and osteogenic potentials. Flow cytometry analysis showed both cell population contained comparable numbers of cells fitting the MSCs phenotype (CD73<sup>+</sup>, CD90<sup>+</sup>, CD105<sup>+</sup>, CD14<sup>-</sup>, CD19<sup>-</sup>, CD34<sup>-</sup>, CD45<sup>-</sup> and HLA-DR<sup>-</sup>). Diabetic BM-MSCs expressed lower levels of periodontal markers *POSTN* and *CEMP-1* as well as a number of IGFBPs (*IGFBP-2*, -3 and -4), although ELISA assays showed similar release levels of these IGFBPs by both diabetic and non-diabetic cells. These molecules could be targeted to enhance the periodontal regeneration potentials of diabetic BM-MSCs. Moreover, both diabetic and non-diabetic cells showed a upregulation of *IGFBP-2* in their osteogenic cultures along with downregulation of *IGF-1* and *IGFBP-5*, and these molecules could enhance the use of BM-MSCs in bone tissue engineering in general.

# Table of Contents

<b>Declaration</b> .....	<b>i</b>
<b>Acknowledgement</b> .....	<b>ii</b>
<b>Abstract</b> .....	<b>iv</b>
<b>Table of Contents</b> .....	<b>v</b>
<b>List of Figures</b> .....	<b>viii</b>
<b>List of Tables</b> .....	<b>xi</b>
<b>List of Abbreviations</b> .....	<b>xii</b>
<b>Chapter 1 Literature Review</b> .....	<b>1</b>
1.1 General introduction .....	1
1.2 Biology of periodontium .....	1
1.2.1 The periodontal ligament.....	2
1.2.2 The alveolar bone .....	3
1.2.3 The cementum .....	4
1.2.4 The gingiva.....	5
1.2.5 Development of periodontal tissues .....	5
1.3 Periodontitis.....	7
1.4 Diabetes .....	10
1.5 Reciprocal interaction between periodontitis and diabetes.....	12
1.6 Periodontal therapy .....	14
1.6.1 Non-surgical periodontal therapy .....	14
1.6.2 Surgical periodontal therapy.....	16
1.6.3 Regenerative periodontal therapy in diabetic animal models	17
1.6.4 Clinical trials in regenerative periodontal therapy in diabetic patients.....	18
1.6.5 Clinical trials in dental implant therapy in diabetic patients....	19
1.7 Tissue engineering and periodontal regeneration .....	20
1.7.1 Scaffolds in regenerative periodontal therapy .....	20
1.7.2 Stem cells in regenerative periodontal therapy .....	22
1.7.3 Growth factors in regenerative periodontal therapy.....	44
<b>Chapter 2 Aim and Objectives</b> .....	<b>55</b>
<b>Chapter 3 Materials and Methods</b> .....	<b>56</b>
3.1 Materials.....	56
3.1.1 Cell isolation, culture and staining.....	56
3.1.2 Flow cytometry .....	58

3.1.3	Quantitative polymerase chain reaction (qPCR) .....	60
3.1.4	Enzyme linked immunosorbent assay (ELISA) .....	63
3.1.5	Prepared buffers, fixatives and stains .....	64
3.1.6	Equipment .....	65
3.2	Methods.....	66
3.2.1	Isolation of human bone marrow mesenchymal stem cells ...	66
3.2.2	Cell culture, passaging, expansion and freezing .....	67
3.2.3	Colony forming unit fibroblasts (CFU-Fs) assay.....	68
3.2.4	Population doubling time assay.....	68
3.2.5	Flow cytometry analysis .....	69
3.2.6	Osteogenic differentiation of BM-MSCs .....	76
3.2.7	Analysis of gene expression using quantitative polymerase chain reaction (qPCR).....	79
3.2.8	ELISA assay for assessing protein levels of IGFBPs in conditioned media .....	82
3.2.9	Statistical analysis.....	86
<b>Chapter 4 Results Characterisation of diabetic BM-MSCs in comparison to non-diabetic controls .....</b>		<b>87</b>
4.1	Introduction.....	87
4.2	Results .....	88
4.2.1	Colony forming unit fibroblasts (CFU-Fs) assay of diabetic and non-diabetic BM-MSCs .....	88
4.2.2	Population doubling time (PDT) assay of diabetic and non- diabetic BM-MSCs .....	89
4.2.3	Flow cytometric analysis of stem cells surface markers of diabetic and non-diabetic BM-MSCs .....	92
4.3	Discussion .....	102
<b>Chapter 5 Results Osteogenic differentiation of diabetic and non- diabetic BM-MSCs with a vision for periodontal regeneration ....</b>		<b>109</b>
5.1	Introduction.....	109
5.2	Results .....	110
5.2.1	Alkaline phosphatase (ALP) staining of diabetic and non- diabetic BM-MSCs cultured under basal and osteogenic conditions .....	110
5.2.2	Alizarin Red (AR) staining and quantification of calcified nodules in diabetic and non-diabetic BM-MSCs cultured under basal and osteogenic conditions .....	113

5.2.3	Relative changes in the expression of osteogenic and periodontal markers genes in diabetic and non-diabetic BM-MSCs using qPCR .....	116
5.3	Discussion .....	138
<b>Chapter 6 Results IGF axis expression in diabetic and non-diabetic BM-MSCs .....</b>		<b>149</b>
6.1	Introduction.....	149
6.2	Results .....	151
6.2.1	Relative changes in the expression of IGF axis genes in diabetic and non-diabetic BM-MSCs .....	151
6.2.2	Protein levels of IGFBPs in conditioned media of diabetic and non-diabetic BM-MSCs .....	172
6.3	Discussion .....	176
6.3.1	Relative changes in the expression of IGF axis genes in diabetic and non-diabetic BM-MSCs .....	176
6.3.2	Protein levels of IGFBPs in conditioned media of diabetic and non-diabetic BM-MSCs .....	187
<b>Chapter 7 General discussion .....</b>		<b>192</b>
7.1	Discussion .....	192
7.2	Future work .....	197
7.3	Limitations .....	201
7.4	Conclusions.....	203
<b>References.....</b>		<b>204</b>
<b>Appendix.....</b>		<b>267</b>

## List of Figures

Figure 1-1: Diagram showing cross section of dental and periodontal tissues. ....	2
Figure 1-2: Different types of stem cells used for tissue engineering ..	23
Figure 1-3: Components of the IGF axis .....	45
Figure 3-1: Cells passaging, counting and expansion .....	68
Figure 3-2: Samples preparation for flow cytometry analysis .....	75
Figure 4-1: Representative CFU-Fs of early passage BM-MSCs isolated from a non-diabetic (A) and a diabetic donor (B).....	88
Figure 4-2: CFU-Fs in non-diabetic (ND) and diabetic (D) early passage BM-MSCs. ....	89
Figure 4-3: PDT assay of non-diabetic (ND) and diabetic (D) BM-MSCs	91
Figure 4-4: Flow chart showing sequential gating strategy for evaluation of MSCs surface markers expression on BM-MSCs .....	94
Figure 4-5: Expression of MSCs surface markers on non-diabetic BM-MSCs.....	95
Figure 4-6: Expression of MSCs surface markers on diabetic BM-MSCs .....	96
Figure 4-7: Expression of MSCs surface markers on non-diabetic (ND) and diabetic (D) BM-MSCs. ....	97
Figure 4-8: Flow chart showing gating strategy for MSCs enumeration in non-diabetic and diabetic BM-MSC.....	99
Figure 4-9: Sequential gating for enumeration of MSCs population in non-diabetic BM-MSCs .....	100
Figure 4-10: Sequential gating for enumeration of MSCs population in diabetic BM-MSCs.....	101
Figure 4-11: MSCs enumeration in non-diabetic (ND) and diabetic (D) BM-MSCs .....	102
Figure 5-1: BM-MSCs from diabetic (D) and non-diabetic (ND) donors cultured under basal (B) conditions and stained with alkaline phosphatase stain at Wk1, Wk2 and Wk3 time points .....	111
Figure 5-2: BM-MSCs from diabetic (D) and non-diabetic (ND) donors cultured under osteogenic (O) conditions and stained with alkaline phosphatase stain at Wk1, Wk2 and Wk3 time points .....	112
Figure 5-3: BM-MSCs from diabetic (D) and non-diabetic (ND) donors cultured under basal (B) conditions and stained with Alizarin Red stain at Wk1, Wk2 and Wk3 time points .....	114
Figure 5-4: BM-MSCs from diabetic (D) and non-diabetic (ND) donors cultured under osteogenic (O) conditions and stained with Alizarin Red stain at Wk1, Wk2 and Wk3 time points .....	115

Figure 5-5: Quantification of Alizarin Red stain in cultures of non-diabetic (ND) and diabetic (D) BM-MSCs .....	116
Figure 5-6: <i>ALPL</i> relative expression in BM-MSCs from non-diabetic (ND) and diabetic (D) donors normalized to <i>HPRT1</i> (A), <i>GAPDH</i> (B) and the average of both genes (C). .....	118
Figure 5-7: <i>COL1A1</i> relative expression in BM-MSCs from non-diabetic (ND) and diabetic (D) donors normalized to <i>HPRT1</i> (A), <i>GAPDH</i> (B) and the average of both genes (C). .....	119
Figure 5-8: Relative changes in gene expression of <i>ALPL</i> in non-diabetic and diabetic BM-MSCs.....	121
Figure 5-9: Relative changes in gene expression of <i>RUNX2</i> in non-diabetic and diabetic BM-MSCs.....	123
Figure 5-10: Relative changes in gene expression of <i>OCN</i> in non-diabetic and diabetic BM-MSCs.....	125
Figure 5-11: Relative changes in gene expression of <i>COL1A1</i> in non-diabetic and diabetic BM-MSCs.....	127
Figure 5-12: Relative changes in gene expression of <i>POSTN</i> in non-diabetic and diabetic BM-MSCs.....	129
Figure 5-13: Relative changes in gene expression of <i>CEMP-1</i> in non-diabetic and diabetic BM-MSCs.....	131
Figure 5-14: Relative changes in gene expression of <i>OPG</i> in non-diabetic and diabetic BM-MSCs.....	133
Figure 5-15: Relative changes in gene expression of <i>RANKL</i> in non-diabetic and diabetic BM-MSCs.....	135
Figure 5-16: <i>OPG/RANKL</i> ratio in non-diabetic and diabetic BM-MSCs .....	137
Figure 6-1: Relative changes in gene expression of <i>IGF-1</i> in non-diabetic and diabetic BM-MSCs.....	152
Figure 6-2: Relative changes in gene expression of <i>IGF-2</i> in non-diabetic and diabetic BM-MSCs.....	154
Figure 6-3: Relative changes in gene expression of <i>IGF-1R</i> in non-diabetic and diabetic BM-MSCs.....	156
Figure 6-4: Relative changes in gene expression of <i>IGF-2R</i> in non-diabetic and diabetic BM-MSCs.....	158
Figure 6-5: Relative changes in gene expression of <i>IGFBP-1</i> in non-diabetic and diabetic BM-MSCs.....	160
Figure 6-6: Relative changes in gene expression of <i>IGFBP-2</i> in non-diabetic and diabetic BM-MSCs.....	162
Figure 6-7: Relative changes in gene expression of <i>IGFBP-3</i> in non-diabetic and diabetic BM-MSCs.....	164
Figure 6-8: Relative changes in gene expression of <i>IGFBP-4</i> in non-diabetic and diabetic BM-MSCs.....	166

<b>Figure 6-9: Relative changes in gene expression of <i>IGFBP-5</i> in non-diabetic and diabetic BM-MSCs.....</b>	<b>168</b>
<b>Figure 6-10: Relative changes in gene expression of <i>IGFBP-6</i> in non-diabetic and diabetic BM-MSCs.....</b>	<b>170</b>
<b>Figure 6-11: Comparing the levels of IGF axis genes expression in non-diabetic and diabetic BM-MSCs at baseline (T0).....</b>	<b>171</b>
<b>Figure 6-12: IGFBP-2 levels in conditioned media of non-diabetic and diabetic BM-MSCs.....</b>	<b>173</b>
<b>Figure 6-13: IGFBP-3 levels in conditioned media of non-diabetic and diabetic BM-MSCs.....</b>	<b>174</b>
<b>Figure 6-14: IGFBP-4 levels in conditioned media of non-diabetic and diabetic BM-MSCs.....</b>	<b>175</b>

## List of Tables

<b>Table 1-1: Diagnostic criteria of prediabetes and diabetes.....</b>	<b>11</b>
<b>Table 1-2: Summary of studies of BM-MSCs cultured under simulated diabetic conditions .....</b>	<b>36</b>
<b>Table 1-3: Summary of studies of PDLSCs cultured under simulated diabetic conditions .....</b>	<b>40</b>
<b>Table 3-1: Materials used in cell isolation, culture and staining.....</b>	<b>56</b>
<b>Table 3-2: Materials used in flow cytometry .....</b>	<b>58</b>
<b>Table 3-3: Antibodies used in flow cytometry analysis .....</b>	<b>59</b>
<b>Table 3-4: Materials used in qPCR .....</b>	<b>60</b>
<b>Table 3-5: TaqMan<sup>®</sup> gene expression assays used in qPCR.....</b>	<b>61</b>
<b>Table 3-6: Kits used for the ELISA assays.....</b>	<b>63</b>
<b>Table 3-7: List of buffers, fixatives and stains .....</b>	<b>64</b>
<b>Table 3-8: Equipments used in different experiments .....</b>	<b>65</b>
<b>Table 3-9: Demographic data of BM-MSCs donors.....</b>	<b>66</b>
<b>Table 3-10: Surface markers used for MSCs identification through flow cytometric analysis.....</b>	<b>70</b>
<b>Table 3-11: Tubes used for compensation matrix setup .....</b>	<b>72</b>
<b>Table 3-12: FMO controls used in flow cytometry analysis .....</b>	<b>73</b>
<b>Table 3-13: Experimental design for assessment of osteogenic potentials of isolated BM-MSCs .....</b>	<b>77</b>
<b>Table 4-1: PD, APD and PDT of non-diabetic and diabetic BM-MSCs ...</b>	<b>90</b>
<b>Table 4-2: Proportions of cells expressing MSCs markers in non-diabetic and diabetic BM-MSCs.....</b>	<b>97</b>

## List of Abbreviations

2-hr PG	2 hours plasma glucose
ABL	Alveolar bone loss
AGEs	Advanced glycosylated endproducts
ALP	Alkaline phosphatase
<i>ALPL</i>	Alkaline phosphatase (gene)
ALS	Acid labile subunit
AMPK	AMP-activated protein kinase
APD	Accumulative population doubling
AR	Alizarin Red
AT-MSCs	Adipose tissue mesenchymal stem cells
BCP	Biphasic calcium phosphate
BG	Bioactive glass
BM	Bone marrow
BMA	Bone marrow aspirate
BMD	Bone mineral density
BMI	Body mass index
BM-MSCs	Bone marrow mesenchymal stem/stromal cells
BMP	Bone morphogenic protein
BOP	Bleeding on probing
BSA	Bovine serum albumin
CAD	Computer aided design
CAL	Clinical attachment loss
CAP	Cementum attachment protein
CBCT	Cone beam computed tomography
CD	Cluster of differentiation
cDNA	Complementary deoxyribonucleic acid

CEJ	Cementoenamel junction
CEMP-1	Cementum protein-1
CFU-Fs	Colony forming unit fibroblasts
CFU-Os	Colony forming unit osteoblasts
CLI	Critical limb ischemia
COL1	Collagen 1
COL1A1	Collagen 1 A1
CRP	C reactive protein
Ct	Threshold cycle
CVD	Cardiovascular disease
d	distilled
DFSCs	Dental follicle stem cells
DM	Diabetes mellitus
DMSO	Dimethyl sulfoxide
DNA	Deoxyribonucleic acid
DPSCs	Dental pulp stem cells
ECM	Extracellular matrix
ECs	Endothelial cells
ELISA	Enzyme linked immunosorbent assay
EMD	Enamel matrix derivative
eNOS	Endothelial nitric oxide synthase
EPCs	Endothelial progenitor cells
ESCs	Embryonic stem cells
FACS	Florescence activated cell sorting
FBG	Fasting blood glucose
FBS	Foetal bovine serum
FGF	Fibroblast growth factor
FMO	Fluorescence minus one

FSC	Forward scatter
FVS	Fixable viability stain
GAPDH	Glyceraldehyde-3-phosphate dehydrogenase
GBD	Global burden of disease
GFP	Green fluorescent protein
GH	Growth hormone
GHRH	Growth hormone releasing hormone
GOI	Gene of interest
GSCs	Gingival stem cells
GTR	Guided tissue regeneration
HA	Hydroxyapatite
HbA1c	Glycated haemoglobin
HERS	Hertwig's epithelial root sheath
HG	High glucose
HIF	Hypoxia inducible factor
HKG	Housekeeping gene
HLA-DR	Human Leukocyte Antigen – DR isotype
HPRT-1	Hypoxanthine Phosphoribosyltransferase 1
HRP	Horseradish peroxidase
HSCs	Hematopoietic stem cells
IFN- $\gamma$	Interferon- $\gamma$
Ig G	Immunoglobulin G
IGF	Insulin-like growth factor
IGF-1	Insulin-like growth factor-1
IGF1-R	Insulin-like growth factor-1 receptor
IGF-2	Insulin-like growth factor-2
IGF2-R	Insulin-like growth factor-2 receptor
IGFBP-1	Insulin-like growth factor binding protein-1

IGFBP-2	Insulin-like growth factor binding protein-2
IGFBP-3	Insulin-like growth factor binding protein-3
IGFBP-4	Insulin-like growth factor binding protein-4
IGFBP-5	Insulin-like growth factor binding protein-5
IGFBP-6	Insulin-like growth factor binding protein-6
IL	Interleukin
iPSCs	Induced pluripotent stem cells
IR	Insulin receptor
ISCT	International Society for Cell & Gene Therapy
L-G	L-glutamine
LJE	Long junctional epithelium
LNGFR	Low-affinity nerve growth factor receptor
LPS	Lipopolysaccharide
M6P	Mannose 6 phosphate
MACS	Magnetic activated cell sorting
MCP-1	Monocyte chemoattractant protein-1
M-CSF	Macrophage colony stimulating factor
MMPs	Matrix metalloproteinases
mRNA	Messenger ribonucleic acid
MSCs	Mesenchymal stem/stromal cells
NCCs	Neural crest cells
NF- $\kappa$ B	Nuclear factor kappa $\beta$ ligand
NSAIDs	Non-steroidal anti-inflammatory drugs
NSCs	Neural stem cells
OA	Osteoarthritis
OCN	Osteocalcin
OD	Optical density
OFD	Open flap debridement

ON	Osteonectin
OPG	Osteoprotegerin
OPN	Osteopontin
OSX	Osterix
P	passage
P/S	Penicillin/streptomycin
PAPP-A	Pregnancy associated plasma protein A
PBMCs	Peripheral blood mononuclear cells
PBS	Phosphate buffered saline
PCL	Polycaprolactone
PD	Population doubling
PDGF	Platelet derived growth factor
PDGFR $\beta$	Platelet-derived growth factor receptor $\beta$
PDL	Periodontal ligament
PDLSCs	Periodontal ligament stem cells
PDT	Population doubling time
PLA	Poly lactic acid
PLGA	Poly lactic-co-glycolic acid
POSTN	Periostin
PPAR- $\gamma$	Peroxisome proliferator-activated receptor- $\gamma$
PRF	Platelet rich fibrin
PRP	Platelet rich plasma
PSD	Polymicrobial synergy and dysbiosis
PTEN	Phosphatase and Tensin Homolog
qPCR	Quantitative polymerase chain reaction
RA	Rheumatoid arthritis
RAGEs	Receptor of advanced glycated endproducts
RANK	Receptor activator of nuclear factor $\kappa$ B

RANKL	Receptor activator of nuclear factor $\kappa$ B ligand
rh	Recombinant human
RM-ANOVA	Repeated measures one-way ANOVA
ROS	Reactive oxygen species
RT	Room temperature
RTP $\beta$	Receptor tyrosine phosphatase $\beta$
RUNX2	Runt related transcription factor 2
SA- $\beta$ -Gal	Senescence-associated $\beta$ -galactosidase
SCAP	Stem cells of apical papilla
SHC	Src homolog and collagen protein
SHED	Stem cells of human exfoliated deciduous teeth
SSC	Side scatter
STC	Stanniocalcin
STZ	Streptozotocin
T2DM	Type 2 diabetes mellitus
TCP	Tricalcium phosphate
TGF- $\beta$	Transforming growth factor- $\beta$
TLRs	Toll like receptors
TNF- $\alpha$	Tumour necrosis factor- $\alpha$
VEGF	Vascular endothelial growth factor
$\alpha$ -MEM	$\alpha$ -Modified Minimum Essential Medium

# Chapter 1 Literature Review

## 1.1 General introduction

Periodontitis is one of the most common chronic inflammatory diseases worldwide. It is characterized by destruction of periodontal tissues that provide support and anchorage for teeth: the cementum covering the root surface, the alveolar bone, the periodontal ligament (PDL) that attaches the tooth to the adjacent bone and the gingiva covering all these tissues (1). Type 2 diabetes mellitus (T2DM) is also one of the most prevalent metabolic disorders characterized by chronic hyperglycaemia attributed to insufficient insulin or lack of its cellular response (2). Both health problems affect each other mutually and adversely (3). Currently, periodontal surgery, including guided tissue regeneration therapies, are used to treat periodontal infrabony defects. However, postsurgical complications are encountered and include loss of membrane coverage and subsequent infection, with reports of T2DM possibly contributing to poor clinical outcomes (4).

Periodontal tissue engineering is a complex but promising process that aims at restoring periodontal tissues using one or combination of the following: stem cells, signalling molecules and scaffolds (5). Bone marrow mesenchymal stem/stromal cells (BM-MSCs) and periodontal ligament stem cells (PDLSCs) represent promising candidates for this purpose (6). However, the impact of T2DM on stem cells is not fully investigated particularly on the molecular level (7). Characterizing stem cells isolated from diabetics could help to enhance autologous stem cell based tissue regeneration in T2DM patients with periodontal disease. This thesis investigates how BM-MSCs and members of insulin-like growth factor (IGF) axis are affected in T2DM patients and whether these changes can be reversed to enhance cellular regenerative therapy of periodontitis.

## 1.2 Biology of periodontium

The periodontal tissues include 4 structures: the cementum covering the root surface, the alveolar bone, the PDL that attaches the tooth to the adjacent bone and the gingiva covering all these tissues (Figure 1-1). These tissues provide

teeth with attachment and are capable of enduring the masticatory load (8). The biology of each will be briefly touched upon in this section.

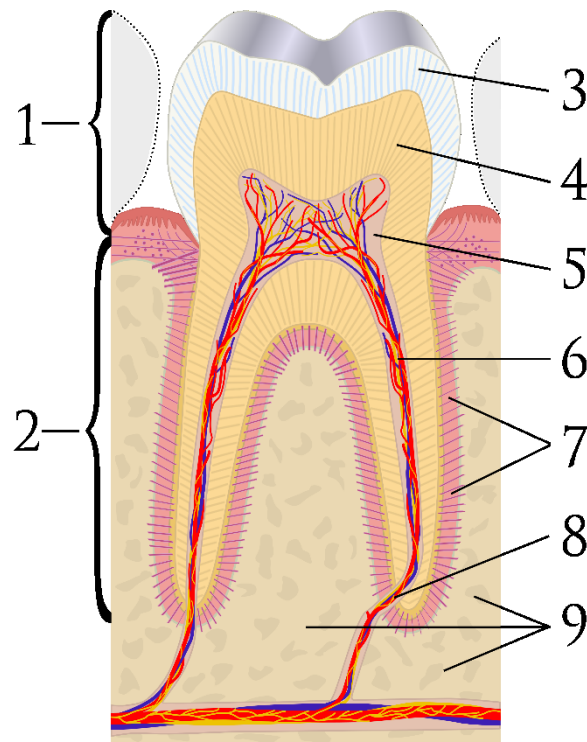


**Figure 1-1: Diagram showing cross section of dental and periodontal tissues.**

Diagram showing 1. Dental crown, 2. Dental root, 3. Dental enamel, 4. Dentine, 5. Pulp chamber, 6. Pulp root canal, 7. Periodontal ligament, 8. Dental apex and 9. Alveolar bone. This diagram is reproduced from [https://commons.wikimedia.org/wiki/File:Cross\\_sections\\_of\\_teeth\\_labels.png](https://commons.wikimedia.org/wiki/File:Cross_sections_of_teeth_labels.png) (Author: Ian Furst, Goran tek-en) and was changed by adding different description to the arrows. This file is licensed under the Creative Commons Attribution-Share Alike 3.0 Unported license.

### 1.2.1 The periodontal ligament

The PDL tissue occupies 100-400  $\mu\text{m}$  in between the root cementum and alveolar bone and is composed mainly of well-arranged bundles of collagen 1 (COL1) fibres. These fibres are called the principle fibres and they anchor the tooth in place. The ends of these fibres embedded within cementum and alveolar bone are called Sharpey's fibres (9). PDL is a connective tissue consisting of cells and extracellular matrix (ECM), with fibroblasts responsible for the synthesis of collagen fibres and representing the main cell type in the PDL (10). PDL tissue also contains a variety of other cell types including epithelial cells, endothelial

cells and stem cells, namely PDLSCs. PDLSCs can differentiate into cementoblasts, fibroblasts and osteoblasts for periodontal tissues maintenance. The PDL is highly vascularized with nerve endings responsible for proprioception and response to other sensory stimuli (11).

The PDL fibres are organized into 4 groups: apical, oblique, horizontal and alveolar crest fibres. Out of these the oblique fibres – which have apical insertion into root surface - represent the major group with the main function of resisting physiologic occlusal load, as well as intrusive and vertical forces (12). The PDL tissue also contains elastic fibres (such as Elastin and Oxytalan) and non-collagenous matrix proteins (including glycoproteins such as fibronectin) (13).

### **1.2.2 The alveolar bone**

The maxilla and mandible are formed of basal bone constituting the body of maxilla and mandible, the alveolar process that contains the teeth alveoli or sockets and the bone lining the alveolar sockets (14). The latter is called bundle bone because of the embedded bundles of PDL fibres and is also called alveolar bone proper or cribriform plate as it encloses the root portion of teeth and contains perforations to allow for innervation, vascularization and possibly BM-MSCs access of PDL tissue (15). The labial, lingual and palatal outer surfaces of alveolar bone are cortical plates of bone extending from the basal jaw bones with spongy cancellous bone situated between these outer plates and the alveolar bone proper (16). The structural unit of cortical or compact bone is the osteon with a central Haversian canal and Volkmann's canals connecting adjacent Haversian canals (17), while cancellous bone consists of a network of bone trabeculae with numerous bone marrow (BM) spaces (18).

Bone is formed in 2 stages: patterning of size and shape, followed by mesenchymal stem/stromal cells (MSCs) differentiation into chondroblasts and formation of cartilaginous template that is replaced by bone tissue and cells (endochondral ossification). Alternatively, MSCs can directly differentiate into osteoblasts (intramembranous ossification) (19). The axial skeleton and extremities are formed through endochondral ossification, while the skull, facial bones (including alveolar bone) and clavicles undergo intramembranous ossification (20). Bone mineralisation starts with the primary phase as osteoblasts produce mineralisation vesicles where calcium and phosphate ions induce crystal nucleation and growth. Ultimately these crystals penetrate the vesicles

membranes, form mineralised nodules and attach to collagen fibres. The secondary mineralisation involves a gradual increase in bone mineral density, possibly through transportation of calcium and phosphate ions through osteocytes canaliculi (21).

Structurally, bone is a hard calcified connective tissue of cells and ECM. The ECM of alveolar bone is comparable to other bony tissues and it consists mainly of a scaffold of interwoven collagen fibres with crystals of calcium phosphate (hydroxyapatite, HA) within and in-between these fibres (16). Bone contains 4 types of cells: osteoblasts, osteocytes, osteoclasts and bone lining cells. Osteoblasts are bone forming cells descending from MSCs with expression of Runt related transcription factor (*RUNX2*) and osterix (*OSX*) crucial for their differentiation and upregulation of osteoblasts-associated genes such as collagen 1 A1 (*COL1A1*), alkaline phosphatase (*ALPL*), bone sialoprotein (*BSP*) and osteocalcin (*OCN*) (22). Osteoblasts are cuboidal in shape and located on edges of newly formed bone with maximum activity during embryonic bone formation. Following bone deposition, osteoblasts either become osteocytes, quiescent bone lining cells or undergo apoptosis, and new osteoblasts could differentiate from MSCs (20).

Osteocytes are the bone residing cells arising from osteoblasts that get encapsulated with bone matrix during bone formation. They extend dendritic processes to communicate with adjacent osteocytes and other cell types, forming a cellular network that recognize mechanical stimuli (23), and respond accordingly by producing a wide range of signalling molecules crucial for bone homeostasis including both inhibitors (sclerostin, receptor activator of nuclear factor  $\kappa$ B ligand, RANKL, and macrophage-colony stimulating factor, M-CSF) and promoters (Osteoprotegerin, OPG) of bone deposition (24). Osteoclasts are large multinucleated cells which differentiate from monocytes/macrophages under influence of M-CSF. M-CSF also induces the expression of receptor activator of nuclear factor  $\kappa$ B (RANK) which is stimulated by RANKL, and this binding drives the chief osteoclastogenesis pathway in bone (25,26).

### **1.2.3 The cementum**

Cementum is the avascular, non-innervated mineralised connective tissue, covering outer surface of the dental root with thickness varying from 20-50  $\mu$ m cervically to 150-200  $\mu$ m apically (27). Cementum has been classified based on

the presence or absence of cementocytes (cellular versus acellular) and the type of embedded fibres (extrinsic or Sharpey's fibres which are produced by PDL fibroblasts and to some extent by cementoblasts, and intrinsic fibres which are an exclusive product of cementoblasts) into 2 major types: acellular extrinsic fibre cementum and cellular intrinsic fibre cementum (28). Acellular extrinsic fibre cementum, also known as acellular or primary cementum, is found on roots cervical portions and provide the strong attachment to PDL fibres. Cellular intrinsic fibre cementum, also known as cellular or secondary cementum, covers apical parts of roots and is responsible for post eruptive cementum formation (29). Cementoblasts, the cells within cementum forming the noncollagenous ECM proteins including BSP and fibronectin, express a number of markers, such as cementum attachment protein (*CAP*) and cementum protein-1 (*CEMP-1*), which contribute to cementoblasts differentiation and ECM mineralization (11).

#### **1.2.4 The gingiva**

The gingiva is the soft tissue that covers the alveolar bone up to or coronal to the cemento-enamel junction (CEJ) and is composed of 3 parts: attached gingiva, interdental gingiva and free gingival margin. Histologically, gingiva is formed of 2 layers: the connective tissue and the covering epithelium (30). The gingival epithelium acts as the first line of protection against invading pathogens through different guards: physical (stratified histology and intercellular junctions), chemical (antimicrobial peptides secreted by epithelial cells and found in saliva) and immunological (leucocytes found within epithelium and migrating into the gingival sulcus, the 'depression' enclosed between the tooth surface and the gingival margin) (31).

The junctional epithelium is a non keratinized stratified squamous epithelium directly attached to the tooth surface (enamel) in healthy periodontium (32). Junctional epithelium has a true basement membrane towards the gingival connective tissue (external basal lamina) and is attached to the tooth surface via hemidesmosomes (internal basal lamina) (33). The integrity of junctional epithelium is critical for maintaining a healthy periodontium and its disruption is a key event in development of periodontitis (13).

#### **1.2.5 Development of periodontal tissues**

A critical event in the embryonic development of oral tissues is the migration of neural crest cells (NCCs) from neural tube into the pharyngeal arches, which later form the craniofacial structures. The NCCs in craniofacial region are known as neural crest derived mesenchymal cells, ectodermal mesenchymal cells, or in short ectomesenchymal cells. These cells are responsible for formation of facial and jaw bones (34), in addition to teeth and surrounding periodontium (35).

The development of the tooth starts with thickening of oral epithelium to form dental lamina, which then invaginates into the ectomesenchyme beneath to form the tooth bud that matures into the enamel organ through cap and bell stages (36). The ectomesenchymal cells enclosed by the enamel organ form the dental papilla, while those surrounding the enamel organ and dental papilla constitute the dental follicle or sac (37).

The epithelial-ectomesenchymal interaction leads to differentiation of dental papilla cell into odontoblasts and subsequent dentine deposition, and differentiation of inner enamel epithelial cells of enamel organ into ameloblasts that carry on enamel formation. When enamel reaches the future CEJ junction, the apical portion of enamel organ extends to form the Hertwig's epithelial root sheath (HERS) (37).

HERS plays a fundamental role to induce differentiation of cells in the apical part of dental papilla into odontoblasts and radicular dentine deposition (38). When dental sac cells come in contact with this dentine, some of its cells attach to dentine surface and differentiate into cementoblasts that form acellular cementum covering root dentine (39). The cells of HERS are potential source of cementoblasts through epithelial mesenchymal transition. In addition to cementoblasts, cells of dental sac differentiate into periodontal ligament fibroblasts and osteoblasts (40).

The calcification of cementum matrix proceeds from dentine surface towards the centre of PDL tissue, but leaves some unmineralized fringe fibres where PDL fibres attach, forming Sharpey's fibres that represent the connection between PDL tissue and root surface. Surrounding alveolar bone is already calcified, but undergoes extensive remodelling where Sharpey's fibres can attach to bone (9). The central portion of PDL tissue is composed of loose connective tissue when Sharpey's fibres are formed. The stem cells in this part continue to differentiate into PDL fibroblasts that are responsible for the continuous remodelling of PDL

tissue, through production and degradation of collagen fibres. This goes through different phases from early root formation to tooth eruption and full occlusal load. The PDL tissue matures into a network of collagen bundles connecting cementum to alveolar bone (9).

### **1.3 Periodontitis**

Periodontitis is a chronic inflammatory disease that can lead to different degrees of destruction of periodontal tissues (1). It is caused by accumulation of dental plaque containing pathogenic bacteria in close proximity to periodontal tissues. Bacteria and their products activate a host inflammatory response and both lead to an extensive production of proinflammatory cytokines that ultimately causes damage to the collagen fibres and alveolar bone through the recruitment of immuno-inflammatory cells and uncoupling of bone remodelling (41,42). Severe periodontitis is estimated to affect around 10% of adults world population on average, a proportion that did not show significant change between 1990 and 2010 (43) with 796 million cases globally in 2017 (44). Consistently, The Global Burden of Diseases, Injuries, and Risk Factors Study 2016 (GBD 2016) ranked periodontitis the eleventh most common disease worldwide and the second most common oral disease after caries of permanent teeth in 2006 and 2016 analyses (45).

Periodontitis is diagnosed through measuring the tooth clinical attachment loss (CAL), radiographic alveolar bone loss (ABL) and periodontal pocketing. The loss of tooth supporting structures can lead in severe cases to tooth mobility and eventually tooth loss. The most recent classification system of periodontal diseases was published in 2018 (46) and describes periodontitis through a multi-dimensional system of staging and grading. Accordingly, periodontitis is classified into 4 stages (I – IV) based on the clinical presentation (CAL, ABL and tooth loss) and the subsequent complexity of treatment plan, for example in case of tooth mobility or advanced furcation involvement (The furcations are the anatomical area of root divergence in multirrooted teeth which pose greater clinical challenge when they become periodontally compromised because of their intricate anatomy and relatively difficult access of oral hygiene (47)). The extent or distribution is added to the stage to describe how much of the dentition is involved (localized, generalized or molar/incisor pattern). Furthermore, each stage is graded into 3 grades (A – C) representing biology or history of disease progression rate and

the grade modifiers (risk factors) smoking and diabetes. This reflects the expected treatment outcomes and possible influence on systemic health (48). This system replaces the widely accepted classification proposed in 1999 by Armitage (49) which had a number of limitations, such as categorical overlap, broad definitions and implementation difficulties (48). The UK implementation of this new classification for UK dental practice relies on interproximal bone loss to determine the staging of periodontitis while the grading depends on % bone loss/age (50).

The pathogenic bacterial species in subgingival plaque involved in initiation and progression of periodontitis were classified into red, orange, yellow and green complexes based on cluster analysis and community ordination. Bacteria of the red complex, *Porphyromonas gingivalis*, *Treponema denticola* and *Tannerella forsythia*, strongly related with each other and to parameters reflecting severity of periodontal disease such as probing depth and bleeding on probing (BOP) (51). This model, however, was later challenged by several findings. For instance, periodontitis associated bacterial populations were shown to be more diverse, and species like *Filifactor alocis* was associated with periodontitis at least equally to *P. gingivalis* and *T.denticola*, and far higher than *T. forsythia* (52).

Polymicrobial synergy and dysbiosis (PSD) model was proposed to reflect the concept that different members of oral microbiota play different and specific roles to transform it into a disease causing microbiota. The role of key pathogens, such as *P. gingivalis*, is to trigger this synergistic interaction between different bacterial communities and impair host immune response. The growing dysbiotic microbiota express virulence factors, leading to homeostasis disruption and eventual damage of periodontal tissues (53). This dysbiotic community evoke, tolerate and benefit from host inflammatory response initiating a vicious circle for periodontal disease continuation (54).

The host inflammatory response in periodontitis goes through different phases including neutrophil and then macrophages and dendritic cells recruitment, leading to the release of several proinflammatory cytokines, such as interleukin (IL)-1 $\beta$ , IL-17 and tumour necrosis factor- $\alpha$  (TNF- $\alpha$ ) (55). IL-17 recruits more immune cells and induces release of matrix metalloproteinase (MMPs), reactive oxygen species (ROS) and stimulates osteoblasts to express RANKL which is responsible for maturation of osteoclasts. Activated B and T lymphocytes, as well

as neutrophils, close enough to bone contribute further to bone loss through RANKL dependant mechanisms (55). Antibodies produced by B-lineage cells diffusing into periodontal pocket or remaining within the tissue side can, in theory, exert some protective effects. However, antibody dependant activation of immune cells leads to further inflammation and tissue damage. The activated B-lineage cells can also express MMPs, RANKL, IL-1, IL-6 and TNF, contributing to soft and hard tissue damage (56).

IL-17 produced by subsets of T helper cells, IL-1 and TNF produced by dendritic cells and macrophages as well as bacterial lipopolysaccharide (LPS) can all induce RANKL expression in inflamed periodontal tissues (57). Bone loss during periodontitis depends mainly on *RANKL* upregulation and *OPG* downregulation within PDL fibroblasts and osteoblasts with subsequent activation of osteoclasts and alveolar bone resorption (58). Other factors that could promote osteoclastogenesis in periodontitis include memory B cells and expression of the proinflammatory cytokine IL-22 (59).

The bone defects seen in periodontitis are generally classified based on their morphology into suprabony, infrabony and furcation defects. Suprabony defects are those with the base of periodontal pocket situated coronal to the alveolar crest, where in infrabony defects the pocket base is apical to the alveolar crest. The furcation or interradicular defects involve bone loss within the furcation area of multirrooted teeth (60). Unlike other types of oral bone defects, such as extraction sockets and periapical lesions that undergo healing through self-regeneration under proper clinical care (61), bone and subsequent PDL loss in periodontal disease is irreversible (62). This has led to the extensive study and application of various regenerative approaches for managing periodontal disease, which will be covered in the next sections of this review.

In 1989, Mattila et al. (63) proposed that poor oral health (using an index of both caries and periodontal disease), was associated with acute myocardial infraction, and this relationship remained valid after adjustment for other risk factors, such as age, diabetes, smoking, social background and serum lipid levels (63). Also in 1989, but in a different study, long term diabetic patients had more sites with gingivitis and periodontal pockets compared to non-diabetics, and long term diabetics aged 40-49 years had exhibited further alveolar bone loss than short term diabetic patients and non-diabetics (64).

Since then, and over the next 30 years, the evidence of association between periodontitis and systemic diseases has been growing steadily and exponentially through cross-sectional, longitudinal and interventional studies, and ultimately the term periodontal medicine was coined describing how periodontal disease influence systemic health (65). In fact, periodontitis has been suggested to be linked with 57 health problems (66), including cardiovascular disease (CVD) (67), adverse pregnancy outcomes (68,69), chronic kidney disease (70), chronic obstructive pulmonary disease (71), rheumatoid arthritis (RA) (72,73) and Alzheimer disease (74,75), with systemic inflammation as a common pathologic pathway in all these (65). The bidirectional relationship between periodontal disease and diabetes mellitus remains one of the most extensively investigated and will be briefly described in the following sections.

## **1.4 Diabetes**

Diabetes mellitus (DM) represents a heterogeneous group of chronic metabolic diseases manifested clinically by hyperglycaemia due to lack of insulin secretion, function or both. It is estimated that globally 422 million people had DM in 2014 with 20-69% expected increase by 2030 (76,77). DM is classified into type 1, type 2, hybrid forms of diabetes (slowly evolving, immune mediated diabetes of adults and ketosis-prone type 2 diabetes), hyperglycaemia first detected during pregnancy (gestational diabetes); and other specific forms of diabetes (including diabetes related to disease of the exocrine pancreatic tissues such as tumours and infections, diabetes due to destruction of  $\beta$  cells because of viral infection, drug or chemical induced diabetes and excess secretion of hormones antagonist to insulin) (78).

Type 1 diabetes mellitus (T1DM) is an autoimmune disease characterized by destruction of insulin producing pancreatic  $\beta$  cells. This is caused by production of autoantibodies from B lymphocytes and expansion of autoreactive T lymphocytes (79). T1DM main risk factor is genetic, as it is seen most commonly in individuals with HLA-DR3-DQ2 or HLA-DR4-DQ8 haplotypes, or both (80). Different environmental triggers have been suggested to be involved in T1DM pathogenesis, such as maternal and postnatal enteroviral infections and overweight, early childhood diet and psychological stress (81).

T2DM is manifested by insulin resistance and relative insulin deficiency associated with a wide spectrum of microvascular (retinopathy, nephropathy and

neuropathy) and macrovascular (CVD and strokes) complications (82). Risk factors of T2DM include age, ethnicity, obesity, family history, physical inactivity and diet rich in refined carbohydrates, processed meat and sugar sweetened drinks, but poor in fruits, vegetables and whole grains (83). The clear distinction between T1DM and T2DM diagnoses (depending on age at onset, presence of diabetes associated antibodies, extent of  $\beta$  cell loss of function and need for insulin therapy) has been diminishing. This is due the increased prevalence of obesity and T2DM in young people and the rising incidence of autoimmune T1DM in adults (78).

Diabetes and prediabetes (glucose levels that are too high to be normal, but not meeting criteria of diabetes diagnosis, usually associated with obesity, dyslipidaemia and hypertension and reflecting high risk for diabetes and CVD), are diagnosed using 3 types of laboratory investigations: fasting plasma glucose (FPG), 2 hour plasma glucose (2-hr PG) or glycated haemoglobin (HbA1c) (Table 1-1) (77).

**Table 1-1: Diagnostic criteria of prediabetes and diabetes.**

Test	Normal	Prediabetes	Diabetes
FPG	<100 mg/dl (< 5.6 mmol/L)	100-125 mg/dl (5.6 – 6.9 mmol/L)	$\geq$ 126 mg/dl ( $\geq$ 7 mmol/L)
2-hr PG	<140 mg/dl (< 7.8 mmol/L)	140-199 mg/dl (7.8 – 11.0 mmol/L)	$\geq$ 200 mg/dl ( $\geq$ 11.1 mmol/L)
HbA1c	< 5.7% (< 39 mmol/mol)	5.7 – 6.4% (39 – 47 mmol/mol)	$\geq$ 6.5% ( $\geq$ 48 mmol/mol)

2-hr PG: 2 hour plasma glucose. FPG: fasting plasma glucose. HbA1c: glycated haemoglobin.

Low grade chronic inflammation is associated with development and progression of T2DM. Expanding adipose tissue in obesity, a key risk factor of T2DM, produces a number of inflammatory cytokines, such as IL-1, -6, -10, TNF- $\alpha$ , angiotensinogen and adiponectin, with serum levels of some of these cytokines predictive of developing T2DM (84,85). TNF- $\alpha$  can contribute to insulin resistance in different ways, such as reducing expression of glucose transporter 4 in adipocytes and insulin receptor (IR) signalling pathways. TNF- $\alpha$  also promotes

production of C reactive protein (CRP), another inflammatory marker, by hepatocytes and adipocytes (86).

Advanced glycated endproducts (AGEs) represent a varied group of complex molecules found irreversibly in serum and tissues (87). Glucose interacts with proteins forming AGEs that accumulate and bind to their receptors on osteoblasts causing increased oxidative stress, RANKL expression and osteoclasts activation. Moreover, osteoblasts apoptosis is induced with the overall result of decreased bone mineralization and repair (88). AGEs also induces more damage of pancreatic  $\beta$  cells and is linked with insulin resistance, and the induced ROS promotes further production of AGEs (2).

The hyperglycaemia increases production of superoxide and other ROS in mitochondria. This oxidative stress leads to cell and tissue destruction and contributes to inflammation. ROS also increases AGEs formation as mentioned earlier, and also induces receptors for AGEs (RAGEs) expression and NF- $\kappa$ B pathway activation. This is associated with impaired insulin function and late diabetic complications (79).

The number of circulating endothelial progenitor cells (EPCs) that promote angiogenesis and vascular healing was reported to be reduced in DM patients. This could be due lowered release from BM, shorter survival in circulation, homing outside circulatory system or combination of all. DM also shifts EPCs differentiation potentials to an inflammatory phenotype (89), which has been characterized as EPCs enhanced ability to endocytose, stimulate naïve T cells and produce IL-12 (90).

### **1.5 Reciprocal interaction between periodontitis and diabetes**

DM and periodontitis share a two-way relationship where they affect each other reciprocally and adversely (91). DM is an established risk factor for chronic periodontitis and the morbidity and severity of periodontitis positively correlates with poorly controlled or long standing diabetes (92), and such pathological influence is even detectable before clinical diagnosis of DM, where prediabetes is associated with higher incidence, prevalence and severity of periodontitis (3).

Diabetes contributes to periodontitis through multiple mechanisms, one of which is altering the oral microbiota to a more pathogenic composition with increased levels of bacterial species associated with periodontitis and poor periodontal

healing in diabetic animals, and this 'diabetic' microbiota enhanced IL-6 production and osteoclasts differentiation, periodontal bone loss and inflammation when transferred to normoglycemic mice (93), and such microbiological changes can be seen even in clinically healthy and resolved periodontal sites in T2DM patients (94).

Diabetes is also suggested to alter the host response to the oral bacterial biofilm in multiple ways. Elevated levels of proinflammatory cytokines IL-6, IL-12, TNF- $\alpha$  as well as macrophage inflammatory protein-1a and granulocyte-macrophage colony-stimulating factor were detected in gingival crevicular fluid of healthy and inflamed periodontium of diabetic patients (95). Another way is stimulation of immune cells with AGEs leading to higher levels of proinflammatory cytokines secretions with periodontal tissues expressing RAGEs as well. Increased collagenase activity and reduced collagen synthesis are possible contributors (96). Specifically, hyperglycaemia and AGEs in gingival tissues were shown to activate Toll like receptors (TLRs) and NF- $\kappa$ B pathway (97). As mentioned earlier, hyperglycaemia can induce higher levels of ROS, which are also released by PMNs infiltrating inflamed periodontal tissues. These ROS can contribute to cellular damage within the periodontal tissues, as well as degradation of different ECM constituents, such as proteoglycans (98), and this oxidative stress can impair bone healing in diabetic animal models (99).

Conversely, DM is linked with reduced production of anti-inflammatory cytokines, such as IL-4, IL-10 and transforming growth factor  $\beta$  (TGF- $\beta$ ). The elevated levels of proinflammatory cytokines cause recruitment and activation of neutrophils with further tissue damage. Moreover, DM increases apoptosis of osteoblast and PDL cells and is linked with upregulation of apoptosis regulating genes (100), as well as delayed myofibroblasts differentiation during periodontal healing (101). All of the above mentioned changes cause exacerbated clinical presentation of periodontitis, even with a subgingival microbiome that has not changed much from healthy (94).

The effect of periodontitis on glycaemic control is evident in non-diabetic subjects with periodontitis, as they show higher levels of HbA1c and FBG levels and are at higher risk of developing T2DM compared to those with better periodontal status (102), and their HbA1c values positively correlated with CRP serum levels, probing depth and BOP (103). The serum levels of proinflammatory cytokines,

compared to anti-inflammatory ones were high in patients with periodontitis and even higher in patients with periodontitis and T2DM (104). This is associated with insulin dysfunctions, insulin resistance and ensuing hyperglycaemia (105).

Periodontitis has been linked to higher risk of CVD as well (106). In addition to elevated systemic inflammatory markers, the 'leakage' of periodontal pathogens through gingival ulceration into bloodstream stimulates atherogenesis. This could happen through bacteraemia or by using blood cells as vehicles (42). Indeed, *P. gingivalis* was found to be the most abundant bacteria in non-atherosclerotic human coronary vessels (107) and it contributed to atheroplaque formation independently of dietary lipids in mice (108).

Conversely, proper periodontal therapy has been shown to lower HbA1c levels in T2DM patients by 3-4 mmol/mol (0.3 - 0.4%), which is equivalent of adding a second antidiabetic drug, but without additional renal and hepatic pharmacological load (109). Periodontal therapy also reduced serum levels of CRP, IL-1 $\beta$ , IL-6 and TNF- $\alpha$  in diabetic T2DM patients (110,111) and their risk of developing CVD (112).

## **1.6 Periodontal therapy**

### **1.6.1 Non-surgical periodontal therapy**

The UK version of the European Federation for Periodontology Clinical Practice Guideline for treatment of periodontitis indicates that the first step of periodontal therapy aims at motivating the patient to perform removal of supragingival plaque and includes oral hygiene instructions, professional mechanical plaque removal, aiming at removal of supragingival plaque and calculus and their retentive factors, and controlling risk factors such as diabetes. The second step aims at controlling subgingival plaque mainly through subgingival instrumentation and may include adjunctive subgingival locally delivered antimicrobials or systemic antimicrobials. Both steps are considered non-surgical periodontal therapy (113). Non-surgical periodontal therapy aims at arresting periodontal inflammation and disease progression by removal of causative microorganisms (11) and inadequate removal of subgingival plaque has been linked with re-infection of periodontal pockets and recurrence of periodontitis since periodontal pathogens and their endotoxins have been detected within radicular cementum (114). This therapy is considered the cornerstone and a preliminary part of any periodontal therapy

(115) and in cases where no periodontal pockets  $\geq 4$  mm with BOP are detected after non-surgical periodontal therapy, patients should move to supportive periodontal care and periodontal surgery is not recommended (113).

Non-surgical periodontal therapy is valuable in T2DM patients, where it is linked with considerable reduction in HbA1c and inflammatory cytokines levels as mentioned earlier (116). Surgical intervention may not be necessary in diabetic patients. If they are planned, several factors have to be considered, such as level of glycaemic control, association of CVD, delayed wound healing with higher risks of infection, a problematic feature in diabetics (2), in addition to the physical and emotional stresses associated with surgery (117). On the other hand, healing following non-surgical periodontal therapy entails formation of long junctional epithelium (LJE) between the root surface and gingival tissues with little or no regeneration of bone, cementum or PDL tissues and unsurprisingly higher risk of disease recurrence (118). The formation of LJE is considered repair not regeneration, as it implies wound healing without restoring the normal form and function of periodontal apparatus (119).

Follow-up reports of non-surgical periodontal therapy in diabetic patients are mixed. T2DM patients with HbA1c levels ranging from 6.5% to 11% and without major diabetic complications treated with non-surgical periodontal therapy and systemic antibiotics showed less gain of clinical attachment, higher risk of gingival recession and higher proportions of periodontal pathogens compared to non-diabetics (120). In a similar setting (non-surgical periodontal therapy without antibiotics), no difference in clinical, immunological and microbiological outcomes was detected in diabetics versus non-diabetics. However, T2DM patients included in the study had slightly better glycaemic control (HbA1c between 4.4% and 10.6%) compared to the study mentioned above, and it is possible this could have contributed to these fairly positive outcomes (121). A systematic review of similar studies concluded that DM does not seem to influence the probing depth reduction or CAL gain following non-surgical periodontal therapy. However, the follow up periods in the included studies were relatively short (up to 6 months only) and the outcomes did not include assessment of bone regeneration which is not very commonly seen following non-surgical therapy. Other limitations of the reviewed studies included variable examination protocols and severity/extent of periodontitis cases in the included studies (122). Therefore, non-surgical

periodontal treatment is known to reduce the microbial load and can improve the periodontal condition and has a positive effect on the glycaemic control but it is not enough for treating advanced periodontal cases with extensive tissue damage.

### **1.6.2 Surgical periodontal therapy**

Surgical periodontal therapy included both historical, non-regenerative approaches, such as pocket elimination with osseous resection and modified Widman flap with pocket closure (123), as well as regenerative techniques that aim at restoring the form and function of periodontal tissues. These include bone grafts, root surface conditioning, the application of enamel matrix derivative (EMD) and guided tissue regeneration (GTR) using barrier membranes beneath the soft tissue flap to prevent gingival epithelial cells from contacting the root surface and allow for the PDL cells to fill the wound and regenerate periodontal tissues (124). The outcome of these regenerative procedures is evaluated clinically (measuring probing depth and CAL which are indicative of soft tissue healing) and radiographically to assess bone healing with surgical re-entry rarely used. However, the only reliable way to confirm regeneration is histology, which is possible solely in animal models (124).

The majority of periodontal regenerative surgeries have been almost exclusively used in infrabony pockets with angular bone loss, where the anatomy of a well contained bone defect particularly increases the success rate of these procedures. A meta-analysis excluding studies on furcation involvement and non self-contained infrabony defects concluded that GTR and EMD achieved better improvements in probing depth and CAL compared to mere open flap debridement (OFD) surgery in long term follow-ups (up to 5-10 years) (125). Still, infrabony defects represent a fraction of encountered periodontal lesions compared to suprabony defects which pose a greater challenge clinically with rather unpredictable treatment outcomes due to the horizontal pattern of bone loss (126). In fact, a review published in 2010 reported that horizontal bone loss involved around 92.2% of radiographically examined periodontal lesions, yet paradoxically, only 3.7% of published papers on regenerative periodontal therapy addressed this overwhelming majority (127).

Many factors are in play for the paucity of regenerative periodontal surgeries in suprabony defects. The horizontal bone loss associated with suprabony defects

means there are hardly any remaining bony walls to support the mucoperiosteal flap or to provide the vascular and cellular resources needed for healing (128). Moreover, most membranes used currently in GTR do not have the required mechanical properties to withstand forces transmitted through the flap with possible membrane collapse, loss of healing space and minimal to no osseous regeneration (129). To overcome these limitations, regeneration in suprabony defects in most instances relied on OFD in combination with growth factors, most notably EMD, which resulted in further clinical and radiographic improvement compared to OFD alone (130). This means that while the benefits of regenerative periodontal surgeries seem evident in infrabony pockets, further research is needed to make these techniques applicable in suprabony pockets. Furthermore, diabetic patients are at a higher risk of postsurgical complications (131), including poor wound healing (132).

### **1.6.3 Regenerative periodontal therapy in diabetic animal models**

Studies discussed in this section used single intraperitoneal injection of streptozotocin (STZ) to induce diabetes followed by measuring of blood glucose levels, usually 1 week later, to confirm diabetes onset. Additionally, control of diabetes was achieved using a subcutaneous sustained-release insulin implant which was aseptically placed in the dorsal side of the animals' neck where controlled diabetic animals were used. All studies used male Wistar rats, except the work by Lee et al. (133), where female Sprague-Dawley rats were used.

GTR formed new bone at similar rates in healthy, controlled diabetic and uncontrolled diabetic rats, with the later showing higher rate of infections and outcome variation (134). Diabetic rats treated by applying EMD (EMDOGAIN®) into surgically created bone defects showed less bone fill and density with more osteoclasts. EMD enhanced only bone fill in diabetic rats, but stimulated bone fill, density and new cementum formation in non-diabetic rats (135).

In a different study, where EMD application was preceded by root surface planing and conditioning, diabetic rats had higher rates of bacterial invasion, bone fracture, inflammatory infiltrate, apical migration of attachment epithelium and gingival recession. New bone, but not new cementum, was detectable in both diabetic and non-diabetic rats, and EMD had no influence on both (136). On the contrary, EMD showed better bone healing compared to control sites in diabetic and non-diabetic rats. Still, diabetic rats had slower bone regeneration and sparse

fibres between the root surface and the newly formed bone, compared to non-diabetic controls (137).

Bone graft and GTR in diabetic animal models were tested in skeletal and skull bones with varied results. In one study, commercial porcine cortical-lamellar bone graft, collagen gel and a collagen membrane were applied in tibial defects in diabetic and non-diabetic rats. Histologic examination of graft area revealed more graft resorption and new bone formation in healthy animals, but the significance of these results was not clearly evaluated (138). When GTR was tested in calvarial bones of rats using titanium domes, there was no difference in new bone formation between healthy, controlled and uncontrolled diabetic animals (139). In the same model, osseous healing following titanium disc placement was associated with higher levels of proinflammatory cytokines in diabetic animals, although this did not equate with difference in bone formation (133).

These findings could indicate the response of diabetics to regenerative periodontal surgeries could be unpredictable and in need of enhancement, especially considering the very few clinical studies as shown in the next section.

#### **1.6.4 Clinical trials in regenerative periodontal therapy in diabetic patients**

Clinical trials of regenerative periodontal surgeries in T2DM patients are not very abundant. One study reported EMD being successfully used in combination with autogenous bone graft in a case-report of a 66 years old T2DM patient (140). Minimally invasive periodontal surgery, with or without EMD, was tested in well controlled T2DM (n=10) and age matched non-diabetic patients (n=18) with infrabony pockets. The diabetic group included 3 well controlled (mean HbA1c 5.9%) and 7 poorly controlled (mean HbA1c 7.2%) patients. However, a larger sample and a cohort of diabetic patients with similar HbA1c levels would have been statistically advantageous. Nevertheless, there was no significant difference in bone fill or attachment gain between diabetic and non-diabetic patients after 3 years of follow-up. Importantly, there was no association between HbA1c, or duration of diabetes, and the attachment gain (141).

Only recently, a study used split mouth technique in well controlled T2DM patients (n=13) with bilateral infrabony pockets to test flap surgery, with and without EMD application. Both sides showed clinical improvement after 6 months of follow up,

with the EMD side showing enhanced reduction in probing depth and attachment gain. However, the study did not include non-diabetic controls, and longer follow-ups would have ascertained the long term outcomes of these treatment modalities in patients with T2DM (142). Taken altogether, more clinical trials with larger samples are necessary to establish evidence based guidelines regarding regenerative periodontal surgery in T2DM patients.

### **1.6.5 Clinical trials in dental implant therapy in diabetic patients**

Investigations of outcomes of dental implant placement in diabetics are more frequent. T2DM patients with HbA1c 6.1-8% showed no difference to non-diabetic controls (n = 30 for each group) in peri-implant probing depth, BOP or marginal bone loss for a follow-up of 24 months (143). Similarly, a retrospective study of 121 well-controlled diabetic and 136 healthy subjects receiving dental implants and followed-up for 3 years concluded there was no significant difference of failure rate among both groups (144). Another retrospective analysis of dental implants placed in posterior maxilla, with and without sinus lift, also concluded that well controlled diabetes was not a risk factor of implant failure. However, well controlled diabetics represented only 5.1% of the included patients (145). Another study evaluated GTR of edentulous maxilla anterior/premolar region, prior to implant placement in T2DM patients and non-diabetics. There was no difference in wound healing, radiographic bone gain, implant stability or marginal bone loss between both groups (n=12 for each). The follow-up was for 12 months, and both groups were age and gender matched with preoperative HbA1c of diabetic patients ranging between 6% and 7.5%, indicating an overall good glycaemic control (146).

A number of systemic review confirmed these data. Naujokat et al. (147) stated that well controlled diabetics can receive dental implant safely with predictable outcomes and failure rates similar to non-diabetics. Moraschini et al. (148) reached the same conclusion but they added that both T1DM and T2DM showed similar implant failure rates, and that marginal bone loss was encountered more in diabetics. Although the outcomes of implants placement or ridge augmentation in T2DM patients could serve as an indication of oral bone healing in these patients, the results of these studies should be interpreted with caution. Implant stability relies mainly on osseointegration, whereas periodontal regeneration is a

much more complex process that ideally entails soft and hard tissues regeneration with insertion of PDL fibres into both root surface and alveolar bone.

The scarcity of reports on surgical regenerative periodontal therapy in diabetic patients, despite some opinion indicating that diabetic patients can receive this kind of treatment safely and comparably to non-diabetics if they were well controlled (117), raises questions about the feasibility of this approach in the real clinical settings and the need for clinical guidelines regarding periodontal surgery in diabetic patients. Taken all together, periodontal tissue engineering can provide a more promising alternative therapy for diabetics.

## **1.7 Tissue engineering and periodontal regeneration**

The concept of tissue engineering was first introduced in 1993 and involves the interaction between 3 main elements: cells, signalling molecules including growth factors and matrices or scaffolds (that support cells and/or release signalling molecules) for tissue regeneration (149). This approach for regenerating periodontal tissues is both multifaceted and challenging with the complex soft and hard tissue architecture of periodontium, the precise alignment of PDL fibres and the exceptionally limited vicinity around teeth (150), and DM can further complicate this task. The next sections will discuss how these 3 elements are used for periodontal regeneration.

### **1.7.1 Scaffolds in regenerative periodontal therapy**

Biocompatible materials are used as scaffolds in regenerative medicine to carry and guide cells and growth factors (151). Acellular scaffolds can be implanted to be populated by host tissue cells or, alternatively, cells cultured and expanded *in vitro* can be loaded onto cellular scaffolds. Either way, scaffolds should be able to support attachment, proliferation and differentiation of cells (152). In addition, scaffolds should be biodegradable in a tailorable rate, allow for revascularization, and with mechanical properties matching these of the host tissue (153).

A number of factors have to be considered when designing or selecting a scaffold for periodontal regeneration. These include scaffold composition, mechanical properties and method of application. Given the complex architecture of periodontal tissues and the fact that scaffolds should simulate the ECM of native tissues, inorganic hard scaffolds, such as HA, tricalcium phosphate (TCP), biphasic calcium phosphate (BCP) and bioactive glass, would be ideal for bone

and cementum regeneration, while polymeric materials (natural polymers, such as gelatin, collagen, chitosan and synthetic polymers such as poly lactic acid, PLA, and poly lactic-co-glycolic acid, PGLA), better suit the PDL (154).

This has led to the development of 2 concepts: the first is hybrid or composite scaffolds where inorganic and polymeric components are combined to offer the benefits of both. For example, collagen/polycaprolactone (PCL) scaffold with amorphous calcium phosphate were used to induce cementum regeneration (155). The second concept is layered scaffolds with different compartments for each periodontal tissue. For instance, bilayered scaffolds with bone compartment (a composite scaffold of PCL and TCP) and PDL compartment (flexible PCL electrospun membrane), were proposed. The bone compartment was seeded with induced osteoblasts, which displayed consistent proliferation and colonization of polymers struts; and the PDL compartment was successfully seeded with PDL cell (156). Later, this model was refined with bone compartment manufactured by melt electrospinning and containing macroscopic pores and the animal studies demonstrated evidence of regeneration of all periodontal structures with cellular constructs superior to acellular ones (157).

Trilayered scaffolds with an additional compartment for cementum regeneration were introduced as well. A scaffold of tri-layered nanocomposite hydrogel scaffold is composed of chitin-PLGA/nanobioactive glass ceramics/CEMP-1 as the cementum layer, chitin-PLGA/fibroblast growth factor 2 (FGF-2) as the PDL layer, and chitin-PLGA/nanobioactive glass ceramics/platelet rich plasma (PRP) derived growth factors as the alveolar bone layer. Rabbit models indicated that triphasic scaffolds enhanced periodontal healing with formation of new cementum, PDL fibres and alveolar bone compared to controls (158).

Scaffolds manufacturing techniques have evolved through time. The 3D printing or additive manufacturing utilizes medical imaging, computer aided design (CAD) and additive manufacture techniques (layer-by-layer printing using inkjet printing, laser-assisted printing or extrusion-based printing) to fabricate automated, personalized and reproducible 3D scaffolds (159). The clinical application of 3D scaffolds in periodontal defects was first tested in 2015, with a case report of PCL/HA scaffold designed using cone beam computed tomography (CBCT) scans. The scaffold was then sterilised, immersed in recombinant human platelet derived growth factor (rh-PDGF) and stabilized over the defect. Although the first

year of follow up showed promising healing, the scaffold became exposed after 13 months, followed by a number of adverse events leading to wound failure and scaffold removal. These results were attributed by the authors to the bulk and rate of degradation of PCL (160).

Scaffolds role in periodontal regeneration was expanded further by incorporation of functional molecules, such as drugs and growth factors. This offers the benefits of temporal and spatial controlled release of such molecules, maximum retaining at wound site, minimum side effects related to systemic absorption and the possibility of combining several molecules into scaffold structure (161). For instance, zinc and calcium bioactive ions were added to matrix polymers to enhance their mechanical, antimicrobial and osteoinductive properties (162). Ibuprofen, a non-steroidal anti-inflammatory drugs (NSAIDs), has been loaded onto PCL scaffolds and applied in experimental model of periodontitis. Although these modified scaffolds lead to increased attachment gain, they had no effect on bone level (163).

Scaffolds loaded with single and multiple bioactive molecules have been experimented as well. Chitosan/HA scaffolds with recombinant human amelogenin displayed antibacterial effects against *P. gingivalis* and upregulated expression of osteogenic markers in PDLSCs (164). The aforementioned study of trilayered scaffold included 3 different bioactive molecules (CEMP-1, FGF-2 and PRP derived growth factors), one into each section (158).

### **1.7.2 Stem cells in regenerative periodontal therapy**

Stem cells are defined as cells capable of self-renewal and differentiating into multiple cell lineages (at least 3 different ones) (165). There is a plethora of stem cells that are currently being investigated for the purpose of tissue regeneration and cell therapies. They can be broadly classified into: embryonic stem cells (ESCs), induced pluripotent stem cells (iPSCs) and adult or postnatal stem cells (Figure 1-2).

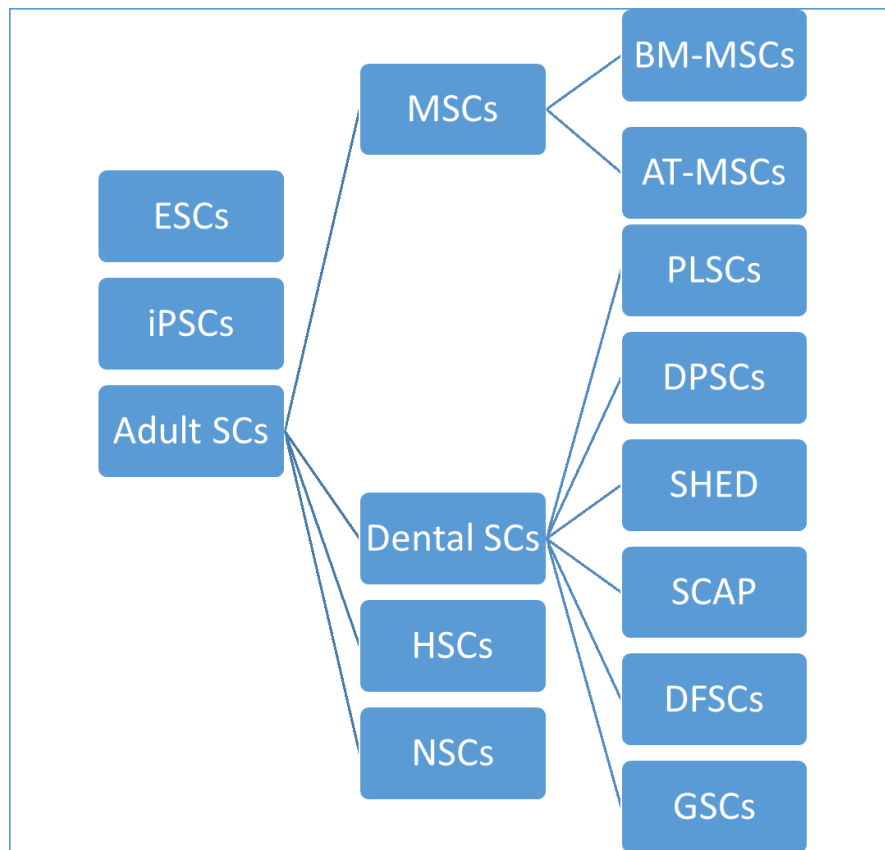


**Figure 1-2: Different types of stem cells used for tissue engineering**

ESC's: embryonic stem cells, iPSC's: induced pluripotent stem cells, MSC's: mesenchymal stem cells, HSC's: hematopoietic stem cells, NSC's: neural stem cells, BM-MSC's: bone marrow mesenchymal stem cells, AT-MSC's: adipose tissue mesenchymal stem cells, PDLSC's: periodontal ligament stem cells, DPSC's: dental pulp stem cells, SHED: stem cells of human exfoliated deciduous teeth, SCAP: stem cells of apical papilla, DFSC's: dental follicle stem cells, GSC's: gingival stem cells.

ESC's are found in the inner cell mass of blastocysts and can differentiate into cell lineages originating from all the 3 germ layers: ectoderm, mesoderm and endoderm. However, their use remains controversial due to ethical considerations, demanding culturing techniques and the risk of tumorigenicity (166), which explains the relative paucity of studies using human ESC's in periodontal regeneration. Porcine ESC's loaded onto collagen matrix were transplanted into surgically created bony defects involving the furcation area in minipigs, with the unloaded matrix serving as a control. The transplanted cells were associated with more cementum formation and more organized PDL fibres (167). Murine ESC's that were allowed to differentiate into dental epithelium and subsequently combined with mouse dental mesenchyme were capable of regenerating all dental structures, including cementum, alveolar bone and PDL

(168), while human ESCs osteogenic differentiation was augmented by co-culture with human PDL fibroblasts (169).

iPSCs were developed in 2006 by introducing 4 genes *Oct3/4*, *Sox2*, *c-Myc*, and *Klf4* through transfection with retroviral vectors into adult mice fibroblasts. iPSCs formed tumours with all germ layers when transplanted into nude mice (170). Since then, iPSCs have been developed using numerous cell types, most notably fibroblasts, from different species including human and reprogrammed into several lineages including MSCs (171). To decrease risk of genetic instability and tumour formation of iPSCs, transfection using non-viral vectors (plasmid, proteins and mRNA among others) (172); and inducing their differentiation into one of their downstream lineages, such as MSCs, before clinical use were proposed (173).

iPSCs have been derived from human gingival and PDL fibroblasts, dental pulp stem cells (DPSCs), stem cells of apical papilla (SCAP) and stem cells of human exfoliated deciduous teeth (SHED), with iPSCs from PDL cells showing superior osteogenic capacities in animal models compared to iPSCs from gingival cells (172). Mouse iPSCs loaded on silk scaffolds with EMD have successfully induced regeneration of periodontal tissues (more alveolar bone and cementum with PDL fibres in-between compared to acellular scaffolds with EMD) in animal models (174). Moreover, mouse ESCs and iPSCs were shown to differentiate into osteoblasts with similar upregulation of osteogenic markers (175).

Adult or postnatal stem cells are the stem cells found in postnatal tissues and they also show self-renewal and multilineage differentiation capabilities, albeit less than ESCs. Adult stem cells include hematopoietic stem cell (HSCs), MSCs and neural stem cells (NSCs) (176). The International Society for Cell & Gene Therapy (ISCT) proposed that for stem cells to be considered MSCs, they should fulfil the following criteria: firstly they must adhere to plastic under standard culture conditions, secondly they must positively express CD73, CD90 and CD105 and lack expression of CD14 or CD11b, CD19 or CD79 $\alpha$ , CD34, CD45 and Human Leukocyte Antigen – DR isotype (HLA-DR); and thirdly MSCs must have the capability of multilineage differentiation (osteogenic, chondrogenic and adipogenic) (177).

Stem cells have been isolated from various adult tissues, such as BM (BM-MSCs), adipose tissue (AT-MSCs) and different dental tissues, and the later includes PDLSCs, DPSCs, SHED, SCAP, dental follicle stem cells (DFSCs) (178)

and gingival stem cells (GSCs) (179). Dental stem cells gained a well-earned interest because they are relatively accessible. Freshly extracted teeth, that are normally discarded in dental clinics, are a source of a different types of dental MSCs (180). In particular, sound third molars and premolars extracted due to impaction or orthodontic reasons, respectively, are valuable sources of 'healthy' stem cells (181). Most of these cells have been investigated as possible candidates for periodontal regeneration.

DPSCs are found in dental pulp tissue and can differentiate into odontoblasts to form reparative dentine under influence of exogenous stimuli. When cultured under osteogenic conditions (dexamethasone, ascorbic acid and  $\beta$ -glycerophosphate), DPSCs differentiate into odontoblast like cells (182). DPSCs were used to regenerate periodontal tissues in canine models of periodontitis induced by both surgical removal of periodontal tissues and ligature applied around teeth to increase accumulation of dental plaque. DPSCs combined with Bio-Oss<sup>®</sup> bone graft prompted more new bone, cementum and PDL formation compared to Bio-Oss<sup>®</sup> alone (183).

Comparing DPSCs and PDLSCs cultured under osteogenic conditions revealed that they formed comparable number of calcium deposits, although PDLSCs cultures had larger granules. Moreover, ALP activity was higher in PDLSCs than DPSCs after 14 days of induction (184). When DPSCs were transplanted into animal models of periodontal bone defects, they reduced probing depth and CAL and enhanced bone regeneration, with cell sheets producing superior results compared to cell injection (185). A clinical trial testing collagen sponges with and without autologous DPSCs in deep intrabony defects concluded that cellular sponges significantly produced more bone fill and attachment gain after 12 months of follow-up (186). Additionally, DPSCs from inflamed pulp tissue were used in conjunction with TCP in 2 patients and improved periodontal clinical outcomes were observed on the course of 9 months. There was, however, no comparison to controls (187).

SHED are derived from the pulp of exfoliated deciduous teeth with properties generally resembling those of DPSCs (188). Their isolation causes no host morbidity as shedding is a natural event for deciduous teeth (deciduous dentition consists of 20 primary teeth per individual); and thus they provide a uniquely accessible source of stem cells (189). SHED were first isolated in 2003 where

they differentiated into odontoblasts and formed dentine, but not dentine-pulp complex. They also induced bone formation in animal models but did not actively participate in bone formation. SHED proliferation rates were higher than those of DPSCs, and all these observations suggest that SHED may not fully replicate the distinct characteristics of DPSCs (190).

SHED were also found to differentiate into osteoblast when transplanted into mice calvarial defects (191); and when injected into periodontal lesions in mice, they provoked further bone deposition and reduced osteoclasts and expression of TNF- $\alpha$  and IFN- $\gamma$  (192). Nevertheless, osteogenic capacities of PDLSCs seem to be superior to SHED, as they formed more mineral deposits after 3 weeks of osteogenic culture (193).

DFSCs are derived from the dental sac that contains developing teeth and are isolated from third molars extracted due to impaction. DFSCs undergo osteogenic differentiation with higher activity of ALP and upregulation of *RUNX2* and *COL1*(194) and when transplanted into animal models, DFSCs could form woven bone with cementocytes and osteocyte like cells, but without distinctive periodontal tissues (195). SCAP are derived from the apical papilla, the soft tissue located at apices of immature permanent teeth (teeth with roots not fully formed and apical foramina not fully closed) (196). SCAP were first isolated in 2006 and were shown to be clonogenic, express MSCs surface markers and undergo osteo/odontogenic differentiation (197). Allogenic SCAP cells that were injected into minipig models of periodontitis, induced by both surgery and ligature, were shown to promote regeneration of all periodontal tissues (198). GSCs have been successfully isolated from gingival connective tissue with the advantages of being abundant and reachable with minimum invasive approaches (199). GSCs loaded onto collagen scaffolds and transplanted into experimental periodontal defects improved CAL and probing depth (200). However, the potentials of human GSCs to differentiate into cementoblasts are yet to be fully established (201).

Out of these different stem cells populations, BM-MSCs and PDLSCs represent the best candidates for stem cell based periodontal regeneration for different reasons. PDLSCs are the native stem cells of PDL tissues and can differentiate into osteoblasts, fibroblasts and cementoblasts, with subsequent regeneration of periodontal tissue complex (11). Periodontal tissue regeneration achieved through stimulating endogenous stem cells using scaffolds, growth factors and

drugs, would overcome the costs and risks associated with stem cells isolation, expansion and transplantation (202). BM-MSCs, on the other hand, are considered the gold standard for cellular regenerative therapy (203), and can be harvested from multiple donor sites in relatively large numbers. This means minimum need for expansion and versatility of applications including banking for future use (204). Thus, both cell types will be covered in the next sections.

#### **1.7.2.1 Bone marrow mesenchymal stromal cells (BM-MSCs)**

BM-MSCs were first observed in guinea pig BM monolayer cultures in 1970 (205), and were later proven to have the criteria required for MSCs definition proposed by the ISCT mentioned earlier in section 1.7.2 (206). Indeed, positive expression of surface markers, CD73, CD90, CD105 and CD40, generally define BM-MSCs with variable colony forming and multilineage differentiation potentials, with surface markers CD271 and CD146 selecting cells known to possess higher levels of these potentials (207). BM-MSCs represent ideal candidates for autologous stem cell transplantation/therapy especially for bone and periodontal tissue engineering, due to the relative ease of harvesting and the high cell yield obtained (204). Moreover, BM-MSCs could differentiate into cementoblasts with proper induction. BM-MSCs cultured in osteogenic media and treated with Wnt3a showed upregulation of *CEMP-1*, *CAP*, *ALP* and *OCN* (208), confirming their cementogenic differentiation.

Multiple clinical trials using BM-MSCs for bone regeneration with and without scaffolds have been carried out (209). In a feasibility and safety trial, autologous iliac crest BM-MSCs were expanded and mixed with bioceramics, before being surgically applied to non-union skeletal fractures in 28 patients. One year follow-up found that all participants did not show any adverse events and 26 of them showed radiographic signs of bone healing (210). In a pilot trial, autologous alveolar bone BM-MSCs were expanded and then seeded on serum cross linked scaffolds (cross linked serum proteins); and finally subjected to osteogenic differentiation. The seeded scaffolds were applied into maxillary cystic cavity in 9 patients, who were followed-up for 7 months. None of the participants had adverse effects and follow-up CT scans displayed increased bone density of treated areas (211).

Periodontal regenerative capacities of BM-MSCs have been investigated at both the experimental and clinical levels. In the recently published review by Iwasaki

et al. (212), they cited 13 studies where autologous BM-MSCs were transplanted into animal models of periodontal defects either on their own or seeded on scaffolds. The majority of these investigations reported regeneration of cementum, alveolar bone and PDL within observation periods ranging from 3 to 24 months (212). For instance, green fluorescent protein (GFP) labelled BM-MSCs transplanted into class III furcation defects in dogs differentiated into cementoblasts, osteoblasts, osteocytes and fibroblasts (213). Interestingly, some of these studies observed more favourable results when BM-MSCs had been pre-treated prior to their transplantation, such as transfection with OPG (214). In another study, chondrogenic induction of rat BM-MSCs preceding their transplantation favoured regeneration of both alveolar bone and PDL, while osteogenic induction supported only alveolar bone formation and retaining multilineage potentials induced only formation of PDL fibres (215).

Clinical trials using BM-MSCs for periodontal regeneration are not very abundant. A recent review included a total of 18 studies using stem cells for clinical periodontal regeneration, with 5 clinical trials using autologous stem cells: 3 using PDLSCs, 1 using DPSCs and 1 trial using BM-MSCs. All the 5 clinical trials reported improved CAL, probing depth and bone fill. Nonetheless, one trial using PDLSCs and another using DPSCs described increased gingival recession compared to controls (216). In particular, the phase I/II clinical trial of autologous BM-MSCs, PRP and 3D woven fabric composite scaffold showed improved CAL, probing depth and bone growth over 36 months of follow up in 10 periodontitis patients not showing signs of systemic disease. The included teeth had probing depth  $\geq 4$  mm with radiographic evidence of vertical ABL. The authors stated that '2 healthy teeth per patient were used as control' and BM-MSCs were isolated from iliac bone marrow aspirate (BMA) (217). Another randomized clinical study compared autologous alveolar bone BM-MSCs seeded into collagen scaffolds supplemented with autologous fibrin/platelet lysate to acellular scaffolds and plain flap surgery for periodontal regeneration. While all approaches improved CAL and probing depth comparably after 12 months of follow up, less bone formation was observed with the acellular scaffolds. No adverse events were recorded in any subjects, indicating that BM-MSCs-loaded scaffolds could be safely and reliably used for periodontal regeneration (218). Taken together, BM-MSCs transplantation for treating periodontal defects is demonstrated to be a safe

procedure, however larger clinical trials with longer follow up durations would confirm its effectiveness (212).

Transplantation of BMA into periodontal defects has been proposed as an alternative to culture expanded BM-MSCs. In a rat model, BMA concentrate was associated with higher bone volumes, but cultured BM-MSCs induced higher rates of early bone maturation. Additionally, cementum deposition and newly formed Sharpey's fibres were observed only in rats receiving BM-MSCs (219). The authors suggest that BMA content of growth factors, cytokines and platelets could have favoured osteogenic differentiation at the expense of cementum and PDL reconstruction (219). However, it is also possible that the culture expanded BM-MSCs were naturally 'enriched' for stem cells with higher differentiation potentials compared to BMA.

While alveolar bone BM-MSCs are derived from NCCs or ectomesenchyme as mentioned earlier and do not express Hox genes, skeletal BM-MSCs which are mesodermal in origin do express Hox. This difference in embryonic origins and expression profile could mean that skeletal BM-MSCs may not be optimum for regeneration of craniofacial bone (220). Skeletal mesoderm-derived bone progenitor cells transplanted into mandibular defects differentiated into chondrocytes and remained Hox positive, while mandibular progenitor cells transplanted into tibial defects became Hox positive, differentiated into osteoblasts and formed bone (221). Furthermore, patient matched orofacial BM-MSCs proliferated more rapidly, had higher levels of ALP and formed more bone compared to iliac crest BM-MSCs. However, the relative scarcity of orofacial BM-MSCs, compared to the relatively higher yield of skeletal BM-MSCs, should be taken into consideration (222).

#### **1.7.2.2 Periodontal ligament stem cells (PDLSCs)**

PDLSCs represent one of the ideal cell candidates for periodontal regeneration, since they can differentiate into osteoblasts, fibroblasts and cementoblasts with subsequent regeneration of periodontal tissue complex (11). PDLSCs were first isolated in 2004 through their clonogenic potentials and positive immunohistochemical expression of 2 early MSCs markers, STRO-1 and CD146. The STRO-1 positive cells were enriched using magnetic activated cell sorting (MACS) and the STRO-1 positive population contained most of the colony forming cells. The expanded PDLSCs displayed *in vitro* multilineage

differentiation into osteoblasts and adipocytes and when transplanted into animal models, they produced PDL like tissue with dense collagen I bundles that were nested into newly formed cementum resembling Sharpey's fibres (223). In addition, PDLSCs were shown to differentiate into chondrocytes, cardiac myocytes, Schwann cells, astrocytes and retinal ganglion cells and pancreatic cells (224).

PDLSCs sustain the morphology (fibroblast like cells with oval nuclei) (225) and the surface markers expression profile of MSCs mentioned earlier (226). They also contain colony forming cell population (227) and express *Nanog* and *Oct-4*, which are embryonic stem cell markers that control self-renewal and pluripotency (228). In addition to multilineage differentiation, PDLSCs could undergo self-renewal more than 100 population doublings, with mechanical loading as a possible contributor to these relatively high proliferative capacities (229).

Under osteogenic culture conditions, PDLSCs form calcified nodules, upregulate early osteogenic markers responsible for osteoblast differentiation (*RUNX2* and *OSX*), bone matrix proteins (*OCN* and Osteopontin, *OPN*), *ALPL* and *BSP* (227,230–233). Osteogenic induction also changes PDLSCs morphology into polygonal cells with extended cytoplasmic processes as intercellular bridges, which is consistent with osteogenic lineages (234).

The nature of PDL tissue as a highly organized collagenous tissue with well oriented and dense fibres bundles acting as a shock absorbent of physiologic mechanical stresses is reflected in PDLSCs expression profile. PDLSCs express scleraxis, a tendon cells specific transcription factor, more than BM-MSCs or DPSCs (223). PDLSCs also express a specific isoform of periostin (*POSTN*), a major ECM protein involved in periodontal homeostasis, that was shown to be upregulated under osteogenic conditions (235).

A subset of PDL cells express *CEMP-1* with strong *CEMP-1* expression detected by immunohistochemistry in ALP-positive PDL cells (236). Osteogenic cultures of PDLSCs could show upregulation of both osteogenic and cementoblastic markers (237) and in another study upregulation of osteogenic markers, *BSP* and *OCN*, along with inhibition of cementoblastic marker *CEMP-1* (236). Additionally, PDL cells subset overexpressing *CEMP-1* following viral transfection exhibited lower mRNA levels of *RUNX2*, *OCN* and *POSTN* (236).

### **1.7.2.3 BM-MSCs versus PDLSCs for periodontal regeneration**

Studies comparing BM-MSCs and PDLSCs in the context of periodontal regeneration are fairly few and show variable results. PDLSCs formed more colonies, but took longer time to differentiate into osteocytes and chondrocytes when compared to BM-MSCs (6). A similar conclusion regarding colony forming efficiency was reached using patient matched jaw bone BM-MSCs and PDLSCs. Both cell types had similar proliferation rates initially, but PDLSCs outpaced BM-MSCs later (238). While PDL cells have shown lower adipogenic and chondrogenic potentials compared to BM-MSCs, their osteogenic potentials and expression levels of *POSTN* were comparable (239).

A pioneer study used composite cell sheets that combined both cell types and showed higher expression of bone markers and well aligned Sharpey's fibres upon transplantation in animal models compared to either cell type alone (240). Comparing cell sheets of autologous BM-MSCs and PDLSCs transplanted to canine periodontal defects, more cementum, well oriented PDL fibres and alveolar bone were observed with PDLSCs sheets (241). Autologous BM-MSCs formed more bone on both short and long terms compared to PDLSCs in a canine peri-implant defect model (242).

BM-MSCs potential for periodontal regeneration in an inflammatory microenvironment using TNF- $\alpha$  was compared to that of PDLSCs. One study showed that TNF- $\alpha$  reduced proliferative potential of BM-MSCs and mineralization of PDLSCs (243). A second study concluded that both cell types had similar proliferation rates and colony formation efficiencies. However, PDLSCs displayed weaker osteogenic potentials that were further inhibited by TNF- $\alpha$  (231).

### **1.7.2.4 BM-MSCs isolated from diabetic patients and/or cultured under diabetic conditions**

A review on the characterisation of MSCs from diabetic patients revealed most of this work focused on AT-MSCs with little consensus regarding the proliferation efficiency, viability, immunophenotyping, multipotency and homing of diabetic MSCs. The authors concluded that molecular basis and signalling molecules regulating diabetic MSCs still need to be fully understood (7).

The isolation and characterization of BM-MSCs from T2DM patients in the majority of published studies was performed in the context of evaluating their potentials to differentiate into insulin producing cells to reverse diabetes (7,244,245). One of the earliest of these studies was conducted in 2009 on BM-MSCs isolated from T2DM patients undergoing cardiac bypass surgery (n = 95), with a relatively wide age range of 15 to 80 years. The study concluded that diabetic BM-MSCs had multilineage differentiation potentials and expressed MSCs markers with cells from uncontrolled, long standing or elderly diabetics showing weaker proliferation. There was, however, no 'healthy' BM-MSCs included in the study as controls (244).

In another study, diabetic donors (n=3) were insulin dependent T2DM patients with mean HbA1c of 11%, indicating relatively poor glycaemic control. Their age range was 43-55 years while non-diabetic controls (n=3) had an age range of 38-55 years. BMA samples were not isolated from the same anatomical source for both groups (iliac crest of diabetic donors and the hip joint of non-diabetic donors). No data on other comorbidities were available and both cell populations had similar proliferation rates (245). In a study comparing healthy, ischemic and ischemic diabetic BM-MSCs cells from patients with critical limb ischemia (CLI) (n=4 for each group), no difference in clonogenic, osteogenic, adipogenic or angiogenic potentials was reported. CLI cells showed lower proliferation rates irrespective of patients' diabetic status when compared to healthy controls. Nevertheless, the study did not indicate the level of glycaemic control of diabetic donors. Moreover, all CLI patients had a history of CVD and were relatively older compared to controls, which could have influenced their BM-MSCs (the age range of healthy donors, ischemic patients and ischemic diabetic patients was 22-34, 46-85 and 67-85 years respectively) (246).

Recently, more studies have extensively compared diabetic and non-diabetic BM-MSCs through larger sample size. One of these concluded that multilineage differentiation (including osteogenic), immunomodulatory properties, transcriptomic data, surface markers expression and number of BM-MSCs in the isolated BM biopsies (of hip joints) were comparable in diabetic and non-diabetic BM-MSCs. These parameters, however, were reduced in both cell populations by passaging cells *in vitro*. Although the majority of diabetic donors were non-insulin dependent, their levels of glycaemic control were not highlighted (247).

Another investigation reached similar conclusions, in addition to diabetic BM samples containing fewer colony forming MSCs specifically those with osteogenic capacities, as measured by colony forming unit fibroblasts (CFU-Fs) and colony forming unit osteoblasts (CFU-Os) assays respectively. The non-diabetic controls were age matched and the diabetic donors had an overall good glycaemic control (248).

The combined results of both studies resonated well with a clinical trial that used autologous BM concentrate in treatment of tibial non unions in 54 diabetic patients (n=42 for T2DM and n=12 for T1DM); and equal number of non-diabetic matched control patients. BMA of both cohorts had similar number of MSCs as evident by the CFU-Fs assay, but this did not equate to having similar treatment outcomes as diabetic patients needed more time for healing and had smaller callus. Treatment failure in diabetics was rationalized to having more comorbidities and lower number of MSCs compared to diabetics who showed successful treatment outcomes. Consequently, the study recommended the use of larger volumes of BMA and higher number of transplanted cells in diabetic patients (249). Moreover, BM-MSCs from hip joints of T2DM patients showed similar content of CD73<sup>+</sup> CD90<sup>+</sup> cells and osteogenic differentiation potentials, but higher tendency for adipogenic differentiation compared to controls (250). On the other hand, alveolar bone BM-MSCs from T2DM patients were reported to form less mineral deposits (251,252).

So far from the aforementioned studies, it seems that in general T2DM influence on BM-MSCs may not be very drastic. Nonetheless, the results of studies investigating BM-MSCs under *in vitro* diabetic culture conditions using high glucose (HG), AGEs (which would better reflect the chronicity of changes in diabetic microenvironment compared to HG) and serum of diabetic patients show different findings. In general, HG induced lower proliferation rates, while HG combined with LPS and serum of T2DM patients had the opposite effect. AGEs were used only in 2 studies, with one reporting increased expression of *OPG*, *RANKL* and *RAGEs* and the other concluding reduced proliferation of BM-MSCs (Table 1-2).

However, T2DM microenvironment is more complicated than plain short term exposure to HG or AGEs, as it also entails ROS, hyperlipidaemia, hyperinsulinemia, as well as inflammatory cytokines (253) and some of diabetes

induced complications could be attributed to one or more of these factors. For instance, macrophages isolated from rats with short term diabetes and normal serum levels of lipids completely recovered to normal levels of cytokines production after 5 days of normoglycemic culture, while cells from rats with long term diabetes showed only partial recovery. Because both groups had higher levels of serum glucose, this differential recovery could be attributed to the fact that only the long term diabetic rats had higher serum lipids (254).

Furthermore, the HG concentrations used in these studies are far higher than the ones found biologically, even in severely uncontrolled diabetics. Where glucose concentration of 5.5 mM in culture media represent normoglycaemia or plasma glucose level of 100 mg/dL, 24 mM glucose in culture media denote hyperglycaemia or plasma glucose level of 432 mg/dL (for comparison uncontrolled diabetic patients have BGL of 200 mg/dL or above) (255), which poses questions about their physiologic relevance (256).

Data from studies on BM-MSCs from diabetic animal models are rather inconclusive. In one study BM-MSCs isolated from diabetic rats were similar to non-diabetic cells in morphology, growth rate and osteogenic potentials but diabetic cells formed more colonies (257). Conversely, another study reported that diabetic rats BM-MSCs showed similar morphology, telomere length, proportion of senescent cells and expression of stem cells surface markers. On the other hand, diabetic BM-MSCs displayed lower growth rates, weaker clonogenic and osteogenic capacities, larger proportion of apoptotic cells and higher *RANKL/OPG* expression levels denoting increased osteoclastogenic activity compared to BM-MSCs from non-diabetic rats (258). When diabetic rats BM-MSCs were cultured under HG, they showed higher proliferation rates and expression of inflammatory marker IL-6 along with weaker osteogenic differentiation compared to normoglycemic cultures (259). BM-MSCs from diabetic rat models displayed weaker mineralization and expression of osteogenic markers compared to non-diabetic cells (260); and BM-MSCs from non-diabetic rats cultured under HG showed similar deterioration (261).

In another study, HG had no effect on the proliferation, but inhibited the osteogenic differentiation of rats endosteal BM-MSCs (262). Moreover, HG induced senescence of rats BM-MSCs (263,264), while AGEs were associated with poor proliferation and migration in addition to high ROS production and

chemokines expression (265). Similar to human BM-MSCs, rats BM-MSCs osteogenic differentiation was attenuated by AGEs, and the differentiated cells had lower viability, higher apoptosis and RAGEs expression (266).

**Table 1-2: Summary of studies of BM-MSCs cultured under simulated diabetic conditions**

#	Study	Diabetic cond.	Ca nodules (AR staining)	ALPL expression	ALP activity	Osteogenic transcription factors		Osteogenic markers		Others
						<i>RUNX2</i>	<i>OSX</i>	<i>OCN</i>	<i>OPN</i>	
1	Ying et al. (267)	HG	↓	↓	↓	↓	↓	↓	<b>NR</b>	↓ <i>COL1</i> and <i>BMP-2</i> expression ↓ <i>PI3k</i> and <i>Akt</i> expression ↑ <i>ROS</i>
2	Chang et al. (268)	HG	<b>NR</b>	<b>NR</b>	<b>NR</b>	<b>NR</b>	<b>NR</b>	<b>NR</b>	<b>NR</b>	↓ PD time ↑ Senescence ↑ Autophagy
3	Li et al. (269)	HG	↑	<b>NR</b>	<b>NR</b>	<b>NR</b>	<b>NR</b>	<b>NR</b>	<b>NR</b>	↓ Proliferation (25mM HG, long term exposure) ↓ Apoptosis (40 mM HG, short term exposure)
4	Dhanasekaran et al (270). (late vs early P)	HG	<b>NC</b>	<b>NR</b>	<b>NR</b>	<b>NR</b>	<b>NR</b>	<b>NR</b>	<b>NR</b>	↓ Proliferation Cell morphology, karyotyping and BM-MSCs surface markers: <b>NC</b>
5	Shiomi et al. (271) (purchased BM-MSCs)	HG + LPS	↓(24 mM, 3 wks.)	<b>NR</b>	↓ (12 and 24 mM, 2 wks.)	↑ (8 and 12 mM, 3wks) ↓ (24 mM, 3 wks.)	<b>NR</b>	↓ (12 and 24 mM, 3 wks.)	<b>NR</b>	↑ Proliferation ↓ <i>IL-1<math>\beta</math></i> , <i>IL-6</i> , <i>IL-8</i> (8 and 12 mM, 1 and 2 wks.) ↑ <i>IL-1<math>\beta</math></i> , <i>IL-6</i> , <i>IL-8</i> (24 mM, 1 and 2 wks.)

#	Study	Diabetic cond.	Ca nodules (AR staining)	ALPL expression	ALP activity	Osteogenic transcription factors		Osteogenic markers		Others
						<i>RUNX2</i>	<i>OSX</i>	<i>OCN</i>	<i>OPN</i>	
6	Qu et al. (272)	HG + free fatty acid	↓	NR	↓	NR	NR	NR	NR	↑miR-449
7	Bian et al. (273) (BM-MSCs cell line)	HG + palmitic acid	↓	NR	↓	↓	NR	↓	NR	↓ Proliferation ↓p38 expression ↑ ROS
8	Wang et al. (274)	HG + palmitic acid	NR	↓	↓	NR	NR	NR	NR	↓ Cell viability and proliferation
9	Miranda et al. (88) (primary osteoblast like cells from T2DM patients)	HG + AGEs (vs HG)	NR	NR	NR	↓	↓	NR	NR	↑ <i>OPG</i> and <i>RANKL</i> expression
10	Lu et al. (275)	AGEs	NR	NR	NR	NR	NR	NR	NR	↓ Proliferation
11	Deng et al. (276)	T2DM serum	NR	NR	NR	↓	NR	↓	↓	↑ Proliferation
12	Rezabakhsh et al. (277)	T2DM serum	NR	NR	NR	NR	NR	NR	NR	↑ Apoptosis ↑ Autophagy ↓ Chemotaxis ↓ Angiogenesis

(↓): reduced compared to control culture media. (↑): increased compared to control culture media. AGEs: advanced glycation endproducts. ALP: alkaline phosphatase. *ALPL*: alkaline phosphatase (gene). AR: Alizarin Red. *BMP-2*: bone morphogenic protein-2. *COL1*: collagen 1. HG: high glucose. *IL*: interleukin. LPS: lipopolysaccharides. NC: no change. NR: not reported. *OCN*: osteonectin. *OPG*: osteoprotegerin. *OPN*: osteopontin. *OSX*: osterix. PD: population doubling. *RANKL*: receptor activator NF- $\kappa$ B ligand. ROS: reactive oxygen species. *RUNX2*: Runt related transcription factor 2. T2DM: type 2 diabetes mellitus.

### **1.7.2.5 PDLSCs isolated from diabetic patients and/or cultured under diabetic conditions**

There is limited literature on characterization of PDLSCs isolated from diabetic patients. PDLSCs and GSCs were harvested from impacted third molars extracted from healthy and controlled T2DM patients (HbA1c below 7% at time of study entry); and compared for their proliferation rates and expression of CD45, CD90 and CD105. Both PDLSCs and GSCs from healthy donors showed higher proliferation rates compared to diabetic counterparts. Moreover, PDLSCs had more proliferative potentials compared to GSCs in both healthy and diabetic conditions. All isolated cell populations showed positive expression of CD90 and CD105 and negative expression of CD45 (278).

Another study compared PDLSCs from teeth with periodontitis from diabetic patients to those both sound and with periodontitis extracted from non-diabetics. The diabetic cohort was well controlled with HbA1c levels range 6.5 – 7.5%. The authors concluded that periodontitis and diabetes PDLSCs group had the lowest osteogenic (calcium deposition and *RUNX2* expression) and adipogenic potentials (oil globules formation and peroxisome proliferator-activated receptor gamma (*PPAR* $\gamma$ ) expression), followed by periodontitis only and the best potentials were observed in PDLSCs isolated from sound teeth of non-diabetics (279).

The third study isolated PDL cells from extracted teeth of long standing insulin dependent diabetic mellitus patients, with age range 38–45 years. Diabetic teeth donors were well controlled at time of extraction although history of episodes of poor control was reported. Extracted teeth and subsequently isolated cells in both diabetic and healthy groups were a mix of sound and periodontally involved third molars, but the authors confirmed that this had no statistical influence on the results. This investigation concluded that diabetic PDL cells grew at similar rates compared to cells from healthy donors. However, they had lower ALP activity and lesser rate of mineralised nodules formation than healthy cells (280). Thus, it seems that in general PDLSCs from diabetics have a trend of lower proliferation rate and osteogenic potentials, but because of the small number of studies it would be hard to draw firm conclusions.

The 3 studies on PDLSCs from diabetics reviewed above report lower proliferation rate and osteogenic potentials, which comes in agreement with studies on PDLSCs from healthy subjects and cultured under induced diabetic conditions. This suggests that this experimental approach could mirror pathological changes seen in diabetic PDLSCs. Although several 3D and multi-layered models were developed to simulate and investigate PDL regeneration (281–285), none of them examined this under diabetic conditions.

Similar to BM-MSCs, several studies have cultured PDLSCs under diabetic conditions and their results are summarized in Table 1-3. Most of these studies used HG, while some used AGEs as well. PDLSCs were also cultured under inflammatory conditions with TNF- $\alpha$  with the intention of investigating periodontitis pathology. However, because diabetes induces systemic production of inflammatory cytokines, including TNF- $\alpha$ ; and thus is considered a low grade inflammatory disease, these studies could be relevant and were included as well. This assumption is underlined by the comparable results of studies culturing PDLSCs under HG and inflammatory conditions, as both reported reduced viability and osteogenic differentiation, as well as stimulated expression of IL-6 and IL-8. In some of these studies, the authors referred to the isolated cells as PDL cells or fibroblasts where their stem cells status was not completely verified using multilineage differentiation or expression of stem cells surface markers.

**Table 1-3: Summary of studies of PDLSCs cultured under simulated diabetic conditions**

#	Study	Diabetic cond.	Ca nodules (AR staining)	ALPL expression	ALP activity	Osteogenic transcription factors		Osteogenic markers		NF- $\kappa$ B expression	Others
						<i>RUNX2</i>	<i>OSX</i>	<i>OCN</i>	<i>OPN</i>		
1	Zhen et al. (286)	HG	↓	NR	NR	↓	↓	↓	NR	NR	↑miR-31
2	Liu et al. (287)	HG	NR	NR	↓	NR	↓	↓	↓	NR	↑DNA methylation
3	Kato et al. (255)	HG	↓	NR	↓	↑	NR	↓	NR	↑	↓ Proliferation ↓ Viability ↑ <i>IL-6</i> and <i>IL-8</i> expression Cell morphology: NC
4	Guo et al. (288)	HG	↓	↓	NR	↓	↓	NR	NR	NR	↓ Proliferation
5	Zheng et al. (289)	HG	NR	NR	↓	↓	↓	NR	NR	NR	↓ Proliferation
6	Zhan et al. (290)*	HG	NR	NR	NR	NR	NR	NR	NR	NR	↑ RAGEs expression ↓ Proliferation
7	Kim et al. (291)	HG	NR	↓	↓	↓	↓	NR	↓ **	NR	↓ COL1**
8	Yan et al. (292)	HG	↓	NR	↓	NR	NR	NR	NR	NR	↓ Migration ↑ ROS
9	Deng et al. (293)	HG	↓	↓	NR	↓	NR	NR	↓	NR	↑ Adipogenic differentiation

#	Study	Diabetic cond.	Ca nodules (AR staining)	ALPL expression	ALP activity	Osteogenic transcription factors		Osteogenic markers		NF- $\kappa$ B expression	Others
						<i>RUNX2</i>	<i>OSX</i>	<i>OCN</i>	<i>OPN</i>		
10	Bhattarai et al. (294)*	HG	↓	NR	NR	NR	NR	NR	NR	NR	↓ Proliferation ↑ ROS
11	Kim et al. (295)*	HG	↓	NR	NR	NR	NR	NR	NR	NR	↓ Proliferation ↓ Viability
12	Liu et al. (296)*	HG	NR	NR	NR	NR	NR	NR	NR	NR	↑ Apoptotic cells ↑ Caspase 3 activity
13	Luo et al. (297)	HG	NR	NR	NR	NR	NR	NR	NR	NR	↓ Proliferation ↑ <i>TNFR-1</i> expression
14	Wu at al. (298)	HG	NR	NR	NR	NR	NR	NR	NR	NR	↑ <i>IL-1<math>\beta</math></i> , <i>IL-6</i> , <i>TNF-<math>\alpha</math></i> and <i>RANKL</i>
15	Seubbuck et al. (299)*	HG	↑	NR	↑	NR	NR	NR	NR	NR	↑ Proliferation ↑ Expression of <i>Nanog</i> , <i>Oct4</i> , <i>Sox2</i> , <i>CD166</i> and <i>POSTN</i>
16	Xu et al. (87)*	AGEs	NR	NR	NR	NR	NR	NR	NR	↑	↓ Viability ↑ <i>IL-6</i> and <i>IL-8</i> expression ↑ ERS
17	Guo et al. (300)	AGEs	↓	NR	NR	NR	NR	NR	NR	NR	↑ RAGEs ↑ ROS

#	Study	Diabetic cond.	Ca nodules (AR staining)	ALPL expression	ALP activity	Osteogenic transcription factors		Osteogenic markers		NF- $\kappa$ B expression	Others
						<i>RUNX2</i>	<i>OSX</i>	<i>OCN</i>	<i>OPN</i>		
18	Mei et al. (301)*	AGEs	NR	NR	NR	NR	NR	NR	NR	NR	↓ Viability ↑ Apoptosis ↑ Autophagy ↑ ROS
19	Wang et al. (302)	AGEs	↓	NR	↓	↓	NR	NR	↓	NR	↓ Proliferation
20	Zhang et al. (303)	AGEs	↓	↓	↓	↓	↓	↓	↓	NR	↓ <i>COL1</i> expression ↓ <i>BSP</i> expression
21	Fang et al. (304)	AGEs	↓	↓	↓	↓	NR	↓	NR	NR	↓ Proliferation ↑ ROS ↑ Apoptosis ↑ Mitochondrial damage
22	Yang et al. (305)	TNF- $\alpha$	↓	NR	NR	↓	↓	NR	NR	NR	--
23	Yuan et al. (306)	TNF- $\alpha$	↓	↓	↓ (only at 10 ng/ml)	↓	NR	NR	NR	NR	↑ <i>IL-6</i> and <i>IL-8</i> expression
24	Jiang et al. (307)	TNF- $\alpha$	↓	NR	↓	↓**	NR	NR	NR	+	↓ Viability ↓ <i>Oct4</i> and <i>Sox2</i> expression ↑ <i>IL-6</i> and <i>IL-8</i> expression
25	Zheng et al. (41)*	HG+TNF- $\alpha$	NR	NR	NR	NR	NR	NR	NR	↑	↑ <i>RANKL</i> expression

#	Study	Diabetic cond.	Ca nodules (AR staining)	ALPL expression	ALP activity	Osteogenic transcription factors		Osteogenic markers		NF-κβ expression	Others
						<i>RUNX2</i>	<i>OSX</i>	<i>OCN</i>	<i>OPN</i>		
26	Yang et al. (308)	TNF-α +IL-1β	↓	<b>NR</b>	↓	↓	<b>NR</b>	↓	<b>NR</b>	<b>NR</b>	↓ <i>COL1</i> expression ↓ Bone formation in animal models

(↓): reduced compared to control culture media. (↑): increased compared to control culture media. \* PDL cells/fibroblasts. \*\*Protein level only. AGEs: advanced glycation endproducts. ALP: alkaline phosphatase. *ALPL*: alkaline phosphatase (gene). AR: Alizarin red. BSP: bone sialoprotein. *COL1*: collagen 1. ERS: endoplasmic reticulum stress. HG: high glucose. IL: interleukin. NC: no change. NR: not reported. *OSX*: Osterix. *OCN*: Osteonectin. *OPN*: Osteopontin. *POSTN*: Periostin. RAGEs: receptors of advanced glycated endproducts. RANKL: receptor activator NF-κβ ligand. ROS: reactive oxygen species. *RUNX2*: Runt related transcription factor 2. TNF-α: tumour necrosis factor-α. *TNFR-1*: tumour necrosis factor-alpha receptor-1.

### **1.7.3 Growth factors in regenerative periodontal therapy**

Growth factors (GFs) are natural proteins controlling fundamental cell activities such as mitotic division (proliferation), migration, metabolism and differentiation, consequently influencing tissue repair and regeneration following injury (309). A number of GFs are expressed in periodontal tissues, including insulin-like growth factors (IGF), PDGF and bone morphogenic proteins (BMPs) (310). They exert their actions through binding to specific cell surface tyrosine kinase receptors present on cementoblast, osteoblast and PDL fibroblasts (311). GFs expression closely correlates with osteogenic differentiation stages of bone cells, with vascular endothelial growth factor (VEGF) and IGF-1 upregulated early in cell proliferation stages, fibroblasts growth factor 2 (FGF-2) and BMP-2 upregulated later in cell differentiation and maturation stages; and PDGF and TGF- $\beta$  upregulated in both phases (312).

GFs have been successfully used to promote periodontal regeneration through a conductive or directly inductive effect of new tissue formation (313). The following GFs have been approved by the United States Food and Drug Administration for periodontal regeneration: Amelogenins/EMD, PDGF, BMPs, FGF-2 and platelet concentrate (314). However, there are no robust data on the use of these factors in diabetic patients and some studies reported failure of osteogenic differentiation of BM-MSCs stimulated with BMPs (315). In addition, lower serum levels of IGF axis proteins were reported even in well-controlled T2DM patients and were associated with a higher risk of CVD (316); and were also reported in patients with both impaired glucose tolerance and T2DM as a marker of reduced insulin sensitivity (317). Systemic administration of members of the IGF axis was reported to improve glycaemic control in T2DM patients (318), as well as insulin sensitivity and pancreatic  $\beta$ -cell functions (319), making IGF proteins promising candidates as therapeutic modalities for obesity, insulin resistance and diabetes (320,321). Taken altogether, utilizing IGF axis proteins in periodontal regeneration in diabetics could have the extra benefit of improving insulin sensitivity in periodontal tissue compared to other GFs. Although BMPs, for instance, were proposed as potential insulin sensitizers (322), it would be fair to assume IGFs would exert such effects more efficiently, due to their structural and functional similarity to insulin (323,324).

### 1.7.3.1 IGF axis

The insulin-like growth factor (IGF) axis consists of two ligands (IGF-1 and IGF-2), their corresponding receptors (IGF-1R and IGF-2R), as well as six circulating binding proteins (IGFBP-1 to IGFBP-6) (Figure 1-3). This axis plays a major role in development and maintenance of mineralized tissues (325).

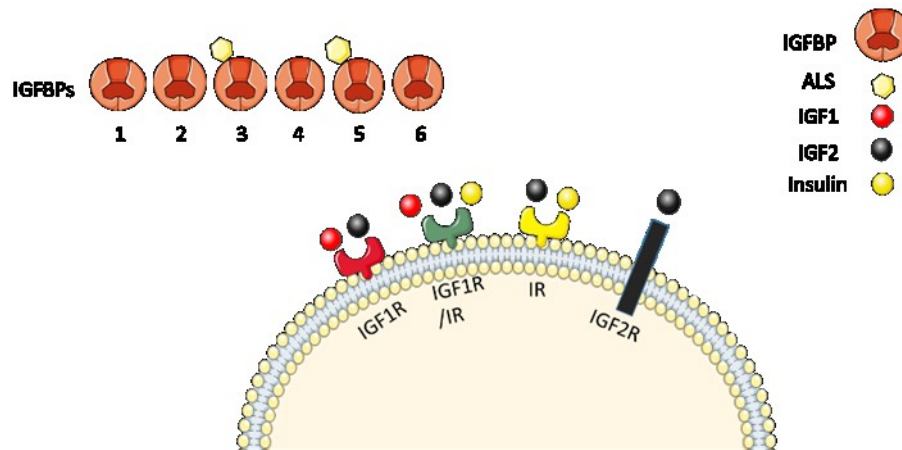


**Figure 1-3: Components of the IGF axis**

The IGF axis consists of IGF-1 (red circle), IGF-2 (black circle), IGF1-R (red receptor), IGF2-R (black receptor) and 6 binding proteins IGFBP-1 to -6. IGF-1 and IGF-2 bind IGF1-R with IGF-1 having higher affinity. Both ligands can bind hybrid receptor IGF1-R/IR (green receptor). However, only IGF-2 can bind IR and IGF2-R and insulin (yellow circle) can bind IR and hybrid receptor IGF1-R/IR. IGFBP-3 and -5 bind to acid labile subunit (ALS, yellow hexagon) to form tertiary complexes. This figure is designed using schematic art pieces provided by Servier Medical art (<http://servier.com/Powerpoint-image-bank>). Servier Medical Art by Servier is licensed under a Creative Commons Attribution 3.0 Unported License.

IGF axis is regulated by growth hormone (GH), which is secreted from the anterior pituitary gland under control of growth hormone-releasing hormone (GHRH) and somatostatin, and binds to its widely distributed receptors. Upon GH binding to hepatocytes, they secrete around 75% of circulatory IGF-1, while the locally produced IGF-1 by other tissues constitute around 25% of serum levels (326).

The IGFBPs are peptides of approximately 260 amino acids that bind IGFs with both IGF dependant functions (transportation in serum, control of vascular efflux and clearance, prolonging half-life, serving as reservoirs, tissue specific directing and regulation of receptor interaction); and independent functions (327). The later include regulating gene transcription, angiogenesis, autophagy and cell senescence (328). Expression of IGF and IGFBPs in calcified tissues is under regulation of factors classically known for prompting bone formation, such as

vitamin D3, GH, parathyroid hormone and IGF-1. This expression profile is complex depending on stage of differentiation and matrix mineralization (329).

### **Insulin-like growth factors -1 and -2**

IGF-1 serum concentrations are relatively high (150-400 ng/mL) and more than 99% of this is binding to IGF-BPs. It functions as both as hormone and a growth factor, promoting both autocrine and paracrine actions (330). IGF-1 is the most abundant growth factor in bone microenvironment, through local production by bone cells or remotely by hepatocytes and subsequent transportation to bone tissues (331).

IGF-1 binding to IGF-1R activates receptor autophosphorylation of the intracellular kinase domain, leading to activation of protein substrates, such as insulin receptor substrate 1 (IRS-1) and Src homolog and collagen protein (SHC). Ultimately, PI3K/PDK-1/Akt and Ras/Raf-1/MAPK (MAPK/ERK) signalling pathway are activated, with the first including activation of PI3K, increased levels of PIP3 and activation of PDK-1 and Akt. The activation of Ras/Raf-1/MAPK pathway depends on the SHC-Grb2-SOC complex (332).

IGF-1 is structurally similar to insulin and can act independently of it to enhance its hypoglycaemic effect. When insulin resistance starts to develop, IGF-1 serum level initially increases, then reaches a plateau at impaired fasting blood glucose levels and decrease afterwards with hyperglycaemia and established T2DM diagnosis (321). rhIGF-1 has been shown to reduce insulin resistance and ameliorate glycaemic control in both types of DM, with effects in T2DM propagated through binding to IGF-1R in skeletal muscles (333).

IGF-1 serum levels are also indicative of bone mineral density (334). IGF-1 increases RANKL production by osteoblasts, leading to osteoclasts activation and bone resorption. However, this is part of the overall role of IGF-1 in bone remodelling where bone resorption precedes deposition, with a net anabolic effect on bone (335).

IGF-2 has a high degree of homology to IGF-1, but with higher binding affinity to IGF2-R and subsequent internalization and degradation. It plays a major role in foetal development and its epigenetic regulation is linked to growth related abnormalities (321). Still, serum levels of IGF-2 in healthy adults exceed those of

IGF-1 by more than 3-fold. This excess is suppressed through binding to IGF-2R and IGFBPs (336).

### **Insulin-like growth factor receptors -1 and -2**

The IGF-1R is produced as a 1367 amino acid pre-pro-peptide single chain, with a 30 amino acid single peptide that is cleaved after translation. The mature molecule has 2 extracellular  $\alpha$ -subunits that are responsible for ligand binding and 2 transmembrane  $\beta$ -subunits that are responsible for signal transduction through the cytoplasmic tyrosine kinase domains (337). Ligand binding induces conformational changes of the receptor leading to activation of tyrosine kinase activity, which in turn activates downstream signalling molecules through protein phosphorylation (338). IGF-1R is structurally similar to IR and both can bind insulin, IGF-1 and IGF-2 with variable affinity and the mechanism of IGFs binding to IGF1-R is assumed comparable to insulin binding IR (339). IRS molecules mediate both IR and IGF1-R signalling, possibly leading to crosstalk of these signalling pathways in osteoblasts (340)

The IGF-2R/mannose 6 phosphate (M6P) receptor is a type 1 transmembrane glycoprotein, with the main action of suppressing IGF1-R signalling through binding to excess extracellular IGF-2. IGF-2/IGF2-R interaction is key for normal development and is involved in carcinogenesis as well, with IGF2-R reported as an oncogene in some cancers and as tumour suppressor gene in others (341).

### **Insulin-like growth factor binding proteins**

IGFBP-1 is a secretory protein of ~30 kDa present mainly in the liver and kidneys, with minor concentration in other tissues. Its serum levels were lower in patients with glucose intolerance and positively correlated with insulin sensitivity (342,343). IGFBP-1 phosphorylated form has more affinity to IGF-1 than the non-phosphorylated one and it was shown to have both stimulating and inhibitory effects on IGF-1(344).

IGFBP-2 is a plasma protein of 34 kDa produced mainly in the liver, as well as muscles and adipose tissue (345). IGFBP-2 effects on IGFs action are mainly inhibitory and serum levels of IGFBP-2 increased with aging in both men and women; and were associated with lower bone mineral density (BMD) (346) and with expression of bone resorption markers (347). IGFBP-2 in gingival crevicular fluid was higher in periodontitis patients and correlated positively with CAL and

BOP (348). However, on the cellular level, IGFBP-2 along with IGF-1 constitute key factors for osteoblasts differentiation (349). IGFBP-2 was upregulated during osteogenic differentiation of DPSCs and also enhanced IGF-1 induced matrix mineralisation of these cells (350).

IGFBP-3 is 40–45 kDa glycoprotein and represents by far the main IGFBP in serum (351). Around 75-80% of IGFs in serum form ternary complexes with IGFBP-3 (and less commonly IGFBP-5) and acid labile subunit (ALS) (352). Serum levels of IGFBP-3 were linked with higher BMD in healthy men (353), but also with vertebral fractures in postmenopausal women (354) and higher CAL and more teeth loss in patients with periodontitis (355). IGFBP-3 is produced mainly by hepatic tissues in addition to the kidneys, GIT and uterus under influence of GH, nutrition and age. IGFBP-3 was shown to have a number of IGF independent functions, such as regulating gene expression by binding to retinoid acid X receptor alpha (327).

IGFBP-4 is 237 residue protein with mostly inhibitory effects on IGF-1 and IGF-2 and its overexpression in bone tissue lead to impaired bone formation and growth. However, some studies have shown anabolic effect of IGFBP-4, where its systemic administration increased expression of *ALP* and *OCN* in mice bone and serum (356). IGFBP-4 has a cleavage site for pregnancy associated plasma protein A (PAPP-A), which upon binding, leads to IGFBP-4 proteolysis and IGF-1 release (357).

IGFBP-5 is a 29 kDa glycosylated protein with high affinity for IGF-1, leading to reduced IGF-1 receptor binding (358). It is found in multiple tissues and is the most ample IGFBP in bone. IGFBP-5 can bind ECM which offers protection against IGF-1 degradation, represent a reservoir for IGF-1 and potentiates its effects. IGFBP-5 stimulatory and inhibitory action on IGF have been reported (359). IGFBP-5 was shown to bind to a number of ECM proteins, including OPN and collagen, possibly to provide a reservoir of IGF-1 close to IGF-1R or sequester and inhibit IGF-1 or a combination of both (360).

*IGFBP-6* is expressed in numerous tissues particularly the lungs, liver, GIT and CNS and it is the only IGFBP that has higher affinity for binding IGF-2 than IGF-1. IGFBP-6 expression is regulated by vitamin D, retinoic acid, IGFs, glucocorticoids, Wnt and Hedgehog pathways (361). IGFBP-6 functions include inhibition of IGF-2 dependant cell division, migration, differentiation and survival,

in addition to inhibiting cell proliferation and stimulating apoptosis independently of IGF-2 (362). IGFBP-6 also holds intracellular function through binding to nuclear and possibly mitochondrial receptors (363).

With exception of IGF-2R, all IGF axis members are expressed in cementum and PDL tissue in variable degrees. Immunohistochemical analysis showed that cementum Sharpey's fibres show strong expression of IGF-1, IGF-2 and IGFBP-5, while PDL tissue ECM (not cells) displayed high immunoreactivity of IGF-1 and IGFBP-6. Interestingly, PDL cells showed immunoreactivity only to IGF-1R and cementum cells stained positive only with IGFBP-2 (364). This is consistent to some extent with the work of Reckenbeil et al. (365), that investigated IGF axis expression in PDL cells excluding IGF-2 and IGF2-R. PDL cells cultured under basal conditions barely expressed mRNA of *IGF-1* and *IGFBP-1*. However, IGF-1R was clearly expressed at both gene and protein levels.

Nevertheless, different expression profiles were concluded in other studies. Compared to gingival fibroblasts, PDL cells overexpressed *IGF-1R* and *IGFBP-5* on gene level (366). PDL cells were also found to express mRNA of *IGF-2* and *IGFBP-6* and both show time dependent increase at gene level and decrease at protein level, but this study did not examine other IGF axis genes and thus, no firm conclusions can be drawn about their relative expression patterns (367). Whether these expression patterns would be different in PDL cells from T2DM patients or under osteogenic conditions is still to be explored.

### **1.7.3.2 IGF axis in periodontal regeneration**

Members of IGF axis have been used for treatment of periodontal and bone defects in animal models since late 1980s. IGF-1 combined with PDGF was applied to roots surfaces of teeth with periodontitis in beagle dogs following OFD. This procedure prompted formation of new cementum and bone with the later lined with a continuous layer of osteoblasts, while control sites healed with formation of LJE (368). Similar results were also reported in monkeys (369). However, when PDGF and IGF-1 were tested individually, PDGF solely could provoke the periodontal regeneration, unlike IGF-1. Adding IGF-1 to PDGF significantly stimulated the positive effect of PDGF (370). Consistent with the above studies, PDGF and PDGF/IGF-1 combination, but not IGF-1 on its own, enhanced PDL cells attachment to dentine chips from human extracted teeth with periodontitis (371).

One study using collagen sponges loaded with a combination of IGF-2, FGF and TGF- $\beta$  and applied on alveolar bone defects recorded higher bone formation in contralateral control sites that received collagen sponges with vehicle only. The authors propose that the collagen sponge could have interfered with the wound healing process (372). Another possible explanation is unknown interactions of the 3 GFs applied simultaneously with little spatial or temporal control of release. In another study, IGF-1 surgically applied to experimental class II furcation defects in beagle dogs improved bone, cementum and PDL regeneration. However, the results were drastically improved when IGF-1 was incorporated into a local drug delivery system of dextran-co-gelatine microspheres, which could help sustain IGF-1 levels in the periodontal defect for longer periods without repeated administrations (237). Systemic IGF-1 improved glycaemic control and increased rate and height of bone formation in diabetic rats following teeth extraction. Although alveolar bone remodelling after dental extraction is not a periodontal bone defect, these results can still be a plausible cue for periodontal regeneration in diabetics (373). In swine models of periodontitis, locally applied IGFBP-5 improved probing depth, CAL and new bone formation (374).

Clinically, a phase I/II clinical trial showed that 150  $\mu\text{g/mL}$  of both rh-IGF-1 and rh-PDGF produced significant bone fill in angular bone loss including class II furcation involvement (375). rh-IGF-1 used with TCP bone graft and PLGA membranes in clinical surgical treatment of two wall intraosseous defects improved probing depth, CAL and bone levels, while combining rh-IGF-1 with rh-VEGF produced even better results (376).

### **1.7.3.3 Effects of IGF axis on BM-MSCs**

FGF-2, but not IGF-1, increased number and size of colonies formed by BM-MSCs although the majority of these cells expressed IGF1-R, possibly due to high concentrations of IGFBPs in the cultures (377). IGF-1 stimulation of BM-MSCs in osteogenic cultures lead to a significant increase in ALP activity, while BMP-7 lead to a non-significant decrease in ALP activity (378). Another study found that IGF-1 induced both ALP activity and minerals formation in BM-MSCs superior to BMP-7, even if the difference was not statistically significant, suggesting that IGF-1 represents a more promising candidate for clinical application in bone fractures (379). IGF-1 mediated osteogenesis was linked to activation of MAPK and PKD signalling pathways and subsequent upregulation

of *OSX* (380), as well as other osteogenic markers, such as *ALP*, *RUNX2* and *OCN* (381). IGF-1 pro-osteogenic effects extended to aging BM-MSCs as well (382).

On the other hand, IGF-1 induced proliferation, adipogenic differentiation and lipid accumulation in BM-MSCs and these effects were inhibited by IGF1-R blockers (383), suggesting a more complex role of IGF-1 in regulating multilineage differentiation potentials of BM-MSCs. Indeed, IGF-1 signalling axis has shown pro-adipogenic potentials, in addition to its well documented pro-osteogenic effects (384). IGF-2 also induced ALP activity, Alizarin Red (AR) staining and expression of *RUNX2* and *COL-1* in BM-MSCs (385) and could contribute to regulation of IGF-1 bioavailability in BM-MSCs (386). IGF-2 was necessary for IGFBP-4 proteolysis and subsequent release and higher bioavailability of IGF-1. This was increased by pre-treating human osteoblasts with TGF- $\beta$ , which stimulated PAPP-A and suppressed PAPP-A inhibitor (386).

Relatively ample literature about IGF axis in rodent BM-MSCs exists. IGF-1 enhanced osteogenic differentiation (ALP activity and AR staining) of rats BM-MSCs in a dose dependant pattern with maximum effect at 100-200 ng/mL. This was manifested by increased *RUNX2* and *OCN* expression at both mRNA and protein levels at a dose of 100 ng/mL (387). IGF-1 was also found to enhance the osteogenic effect of BMP-6 more than BMP-2 in mouse preosteoblasts (388). Subcutaneous administration of IGF-1 and BM-MSCs in mice with a stabilized tibial fracture enhanced soft and hard tissue healing with increased force and stiffness of the newly formed tissues (389). Moreover, pre-treatment of BM-MSCs from diabetic rats with a combination of IGF-1 and FGF-2 enhanced their proliferation rates (390).

Both IGF-1 and IGFBP-2 were crucial for early differentiation of mice osteoblasts through activation of AMP-activated protein kinase (AMPK) (391,392). IGFBP-2 binding to receptor tyrosine phosphatase  $\beta$  (RTP $\beta$ ), and not its binding to IGF-1, enhanced IGF-1-stimulated activation of the protein kinase B (AKT) pathway and subsequent osteoblasts differentiation. Conversely, blocking IGFBP-2 binding to RTP $\beta$  has led to inhibition of both phenomena (393). IGFBP-3 showed a variable range of effects ranging from inhibition of pro-osteogenic influence of BMP-6 on mice osteoblasts (394), to increasing IGF-1 concentration in bone matrix and

enhancing its bone forming effect in terms of bone mass, density and microarchitecture in rats (395).

#### **1.7.3.4 Effect of IGF axis on PDL cells**

Controversial findings were reported about PDL cells response to IGF-1. PDL fibroblasts, and to a lesser extent gingival fibroblasts, showed higher proliferation in response to IGF-1, but not GH, possibly due to lack of immediate effect of GH on these cells. This exposure to IGF-1 also influenced expression of proteoglycans, with down regulation of decorin and upregulation of versican and biglycan, indicating potential role of IGF-1 in ECM homeostasis of PDL tissues (396). On the contrary, PDL cells have shown enhanced proliferation in response to EMD alone and in combination of IGF-1, but not IGF-1 on its own. Both factors and their combination had no effect on cells migration, adhesion or expression of COL-1 (397).

Okubo et al. (398) reported rh-IGF-1 stimulated proliferation of PDL cells, and EMD treatment enhanced PDL cells proliferation and upregulated IGF-1 on both gene and protein levels. Anti-IGF-1 antibodies reversed the EMD-mediated growth of PDL cells and thus, these EMD effects could be conveyed in part through endogenous production of IGF-1 by these cells. This is different from the results of cDNA array analysis by Parkar et al. (399), where EMD upregulated a number of GFs in PDL cells, including *PDGF*, *BMP-1* and *-4* but not *IGF-1* (399). One possible explanation is the difference in concentration and duration of EMD treatment, where Okubo et al. (398) used 50 µg/mL EMD for a max of 2 days, while Parkar et al. (399) used 100 µg/mL EMD for 4 days.

Additionally, *IGF-1* was upregulated in PDL cells under hypoxic conditions, possibly to decrease apoptosis and promote ROS scavenging through PI3K/Akt/mTOR signalling pathway (400). *IGF-1* was also upregulated by intermittent compressive stress simulating occlusal load via TGF-β pathway. Interestingly, hypoxia attenuated this upregulation, suggesting that *IGF-1* upregulation in response to occlusal forces could be inhibited in hypoxic deep periodontal pockets, which may contribute to progression of periodontitis (401). Single exposure to TGF-β upregulated *IGF-1* and promoted osteogenesis in PDL cells, while the opposite was observed after repeated exposures to TGF-β. In the later situation, IGF-1 induction rescued the deteriorating osteogenic

differentiation of PDL cells, suggesting it could be a valuable tool for promoting bone regeneration under chronic inflammatory conditions (402).

*IGF-1* was expressed at higher levels in PDLSCs than DPSCs. However, when both cell types underwent osteogenic/odontogenic induction, *IGF-1* was upregulated in DPSCs, but downregulated in PDLSCs. With the overall changes in gene expression in PDLSCs being more complex (including higher number of altered genes mostly downregulated), this possibly reflects the distinctive nature of both cell populations. DPSCs primarily differentiate into odontoblasts for pulp maintenance, while PDLSCs differentiate into 3 different cell population for homeostasis of both soft and hard tissues forming periodontium (184).

IGF-1 at a concentration of range 20-200 ng/mL could promote PDLSCs proliferation. With an optimum concentration of 100 ng/mL, IGF-1 increased cellular organelles, Alizarin red staining and ALP activity. Moreover, IGF-1 induced the upregulation of *RUNX2*, *OCN* and *OSX* expression at both mRNA and protein levels under osteogenic media (403). Similar results were obtained by combining IGF-1 with platelet rich fibrin (PRF) (404). IGF-1 also reduced apoptosis and caspase-3 expression in PDL cells (405).

Exogenous IGF-1 and IGF-2 induced proliferation of both preconfluent and confluent PDL cells under basal conditions. However, IGF-1 treatment was associated with higher expression of OCN in both preconfluent and confluent cells and higher ALP activity only in preconfluent PDL cells. These effects were not matched by IGF-2 (IGF-2 induced only ALP activity in confluent cells). This is consistent with IGF-2 acting as a promitogenic agent maintaining a pool of undifferentiated cells, while IGF-1 is more committed to PDL cells differentiation (406). Opposing results were reported for PDL cells cultured under osteogenic media, with adding rh-IGF-1 increasing mineral deposition, despite decreasing ALP activity and having no significant influence on OCN expression in PDL cells (365). Interestingly, osteogenic media suppressed *IGF-1* and upregulated *IGF-2* mRNA expression, which may indicate that their roles change in different contexts or culture conditions (407).

These effects of IGF-1 on PDLSCs were most likely mediated through IGF-1R, as silencing this receptor inhibited the IGF-1 induced proliferation and migration of PDLSCs. IGFR-1 silencing also decreased *IGF-1* expression by PDLSCs (408)

and selective blockers of IGF-1R kinase reduced calcium deposits of PDL cells, confirming its role in regulating IGF-1 mediated osteogenesis (407).

## **Chapter 2 Aim and Objectives**

The main aim of this project was to characterise BM-MSCs isolated from T2DM patients compared to cells from non-diabetics and investigating their osteogenic potentials and expression of IGF axis genes for use in autologous stem cell based bone and periodontal regeneration.

This aim was addressed through multiple experimental objectives as follows:

1. Characterisation and enumeration of BM-MSCs from diabetic and non-diabetic donors, using colony forming unit fibroblasts (CFU-Fs) assay, population doubling time (PDT) assay and flow cytometric analysis.
2. Evaluation of osteogenic potentials of both cell populations, using alkaline phosphatase (ALP) and Alizarin Red (AR) stains, as well as expression of osteogenic and periodontal markers genes under basal and osteogenic conditions using qPCR.
3. Evaluation of IGF axis expression in both cell populations at gene and protein levels under basal and osteogenic conditions.

## Chapter 3 Materials and Methods

### 3.1 Materials

#### 3.1.1 Cell isolation, culture and staining

**Table 3-1: Materials used in cell isolation, culture and staining**

Product	Product number	Manufacturer
0.25% (w/v) trypsin-EDTA solution	T4049	Sigma-Aldrich
0.4% (w/v) Trypan blue solution	T8154	Sigma-Aldrich
15 mL centrifuge tubes	430790	Corning®
50 mL centrifuge tubes	430828	Corning®
6 well cell culture plate	18341	Corning®
70 µm cell strainer	352350	Falcon
Acetone	20066423	VWR International
Alizarin Red Staining Quantification Assay kit	SC-8678	ScienCell™ Research Laboratories
α-Modified Minimum Essential Medium (α-MEM)	BE12-169F	Lonza BioWhittaker
Citrate concentrate solution	854C-20ML	Sigma-Aldrich
Collagenase type I, powder	17100-017	GIBCO™
Corning® Primaria™ 100 mm Standard Cell Culture Dish	353803	Corning®
Dexamethasone, powder	31375	Sigma-Aldrich

Product	Product number	Manufacturer
Dimethyl sulfoxide (DMSO)	276855	Sigma-Aldrich
Dispase II (neutral protease, grade II), powder	4942078001	Roche
Fast Blue RR salt, capsules	FBS25-10CAP	Sigma-Aldrich
Foetal bovine serum (FBS)	F9665	Sigma-Aldrich
Formaldehyde	BP531-500	Fisher Bioreagents
Glycerol phosphate disodium salt hydrate powder	G6501-25G	Sigma-Aldrich
L-ascorbic acid powder	A4403	Sigma-Aldrich
L-glutamine (L-G) solution 200 mM	G7513	Sigma-Aldrich
Methylene blue powder	66719-100G	Sigma-Aldrich
Mr Frostie™	5100-0036	Thermo Scientific Nalgene
Naphthol AS-MX phosphate alkaline solution	855-20ML	Sigma-Aldrich
Nunc Cryovials 1.8 mL	368632	ThermoFisher Scientific
Penicillin/Streptomycin (P/S) solution	P4333	Sigma-Aldrich
Phosphate buffered saline (PBS)	BE17-516F	Lonza BioWhittaker
Pipette tips (10, 20, 200 and 1000 µL)	--	Starlab, Tip One
Stripettes (5, 10, 25 and 50 mLs)	--	Corning®

Product	Product number	Manufacturer
Tissue culture flasks (T25 cm <sup>2</sup> , T75 cm <sup>2</sup> and T175 cm <sup>2</sup> )	--	Corning®
ViewPlate-96 Black, Optically Clear Bottom with lid	6005182	PerkinElmer

### 3.1.2 Flow cytometry

**Table 3-2: Materials used in flow cytometry**

Product	Product number	Manufacturer
Antibodies	(Table 3-3)	BD Biosciences
Brilliant stain buffer	563794	BD Biosciences
Compensation Beads	552843	BD Biosciences
Falcon Round Bottom Polystyrene Tube 5 mL Without Cap (12 x 75 mm)	352052	Falcon
Fixable viability stain (FVS) 780	565388	BD Biosciences
Fixation buffer	554655	BD Biosciences
Human Fc Block Pure	564220	BD Biosciences

**Table 3-3: Antibodies used in flow cytometry analysis**

Antibody against	Fluorophore	Clone	Product number	Manufacturer
CD73	Phycoerythrin (PE)	AD2	561014	BD Biosciences
CD90	Fluorescein Isothiocyanate (FITC)	5E10	561969	
CD105	Brilliant Violet 421 (BV421)	266	566265	
CD14	Brilliant Violet 510 (BV510)	MPHIP9	563079	
CD19	Allophycocyanine (APC)	HIB19	561742	
CD34	Brilliant Blue 700 (BB700)	581	745835	
CD45	Brilliant Violet 650 (BV650)	HI30	563717	
HLA-DR	Brilliant Ultraviolet 395 (BUV395)	G46-6	565972	

### 3.1.3 Quantitative polymerase chain reaction (qPCR)

**Table 3-4: Materials used in qPCR**

Product	Product number	Manufacturer
0.2 mL PCR Tubes with Flat Caps	TF10201	Applied Biosystems
96-Well Semi-Skirted PCR Plate, White	11402-9909	Bio-Rad Laboratories Ltd
Ethanol molecular biology grade	108543-0250	VWR International
High capacity RNA to cDNA kit	4387406	Applied Biosystems
Invitrogen™ UltraPure™ DNase/RNase-Free distilled water	10977035	ThermoFisher Scientific
Nonstick, RNase-free Microfuge Tubes, 1.5 mL	AM12450	Applied Biosystems
PCR plate cover seal	PCR0516	4titude
RNase-Free DNase Set	79254	Qiagen
RNase-free microfuge tubes 2 mL	AM12425	ThermoFisher Scientific
RNeasy® Mini Kit	74104	Qiagen
TaqMan® Gene Expression Assays	( Table 3-5)	Applied Biosystems
TaqMan® Gene Expression Master Mix-1 x 5 ml	4369016	Applied Biosystems
B-Mercaptoethanol Molecular Biology Grade	A1108-0100	PanReac AppliChem

**Table 3-5: TaqMan® gene expression assays used in qPCR**

#	Gene	Description (reference)	TaqMan® Gene Expression Assay number
1	Glyceraldehyde-3-phosphate dehydrogenase ( <i>GAPDH</i> )	Housekeeping gene (409)	Hs99999905-m1
2	Hypoxanthine-guanine phosphoribosyl transferase 1 ( <i>HPRT1</i> )	Housekeeping gene (410)	Hs99999909_m1
3	Alkaline phosphatase ( <i>ALPL</i> )	Osteogenic marker (411)	Hs01029144-m1
4	Runt-related transcription factor-2 ( <i>RUNX2</i> )	Transcription factor - Early marker of osteogenic differentiation (411)	Hs00231692-m1
5	Osteocalcin ( <i>OCN</i> )	Calcium binding ECM protein - Late marker of osteogenic differentiation (412)	Hs00609452-g1
6	Collagen1 A1 ( <i>COL1A1</i> )	Marker of fibroblasts and osteoblasts differentiation (413)	Hs00164004_m1
7	Periostin ( <i>POSTN</i> )	Marker of PDL fibroblasts differentiation (414)	Hs01566750_m1
8	Cementum protein-1 ( <i>CEMP-1</i> )	Marker of cementoblasts differentiation (415)	Hs04185363_s1
9	Osteoprotegerin ( <i>OPG-TNFRSF11B</i> )	Receptor for TNF and decoy receptor for RANKL (416)	Hs00900360_m1
10	Receptor activator NF- $\kappa$ B ligand ( <i>RANKL</i> )	Marker of osteoclasts differentiation and bone resorption (416)	Hs01092186_m1

#	Gene	Description (reference)	TaqMan® Gene Expression Assay number
11	Insulin like growth factor-1 ( <i>IGF-1</i> )	Natural growth factor (GF) (417)	Hs01547656-m1
12	Insulin like growth factor-2 ( <i>IGF-2</i> )	Natural GF (417)	Hs04188276-m1
13	Insulin like growth factor-1 receptor ( <i>IGF1-R</i> )	Natural GF receptor (417)	Hs00609566-m1
14	Insulin like growth factor-2 receptor ( <i>IGF2-R</i> )	Natural GF receptor (417)	Hs00974474-m1
15	Insulin like growth factor binding protein-1 ( <i>IGFBP-1</i> )	Carrier protein for IGFs (418)	Hs00236877-m1
16	Insulin like growth factor binding protein-2 ( <i>IGFBP-2</i> )	Carrier protein for IGFs (418)	Hs01040719-m1
17	Insulin like growth factor binding protein-3 ( <i>IGFBP-3</i> )	Carrier protein for IGFs (418)	Hs00426289-m1
18	Insulin like growth factor binding protein-4 ( <i>IGFBP-4</i> )	Carrier protein for IGFs (418)	Hs01057900-m1
19	Insulin like growth factor binding protein-5 ( <i>IGFBP-5</i> )	Carrier protein for IGFs (418)	Hs00181213-m1
20	Insulin like growth factor binding protein-6 ( <i>IGFBP-6</i> )	Carrier protein for IGFs (418)	Hs00181853-m1

### 3.1.4 Enzyme linked immunosorbent assay (ELISA)

**Table 3-6: Kits used for the ELISA assays**

Product	Product number	Manufacturer
Human IGFBP-2 Quantikine® ELISA kit	DGB200	R&D Systems
Human IGFBP-3 Quantikine® ELISA kit	DGB300	
Human IGFBP-4 DuoSet® ELISA kit	DY804	
DuoSet® ELISA Ancillary Reagent Kit 3	DY009	

### 3.1.5 Prepared buffers, fixatives and stains

**Table 3-7: List of buffers, fixatives and stains**

Buffer	Preparation
1% Methylene blue in borate buffer	1 g methylene blue powder dissolved in 100 mL of 10 mM borate buffer
3.7% Formaldehyde buffer	1 mL of 37% formaldehyde solution added to 9 mL PBS
Borate buffer	1.91 g disodium tetraborate decahydrate dissolved in 500 mL H <sub>2</sub> O and pH adjusted at 8.8 using 1 M boric acid
Citrate working solution	1 mL citrate concentrate added to 49 mL of distilled (d) H <sub>2</sub> O.
FACS buffer	PBS supplied with 0.5% v/v bovine serum albumin (BSA) and 0.05% v/v sodium azide
Fast-Blue solution	1 capsule of Fast Blue RR salt into 48 mL of d H <sub>2</sub> O at room temperature (RT). The solution was wrapped in foil for light protection and warmed in 37°C water bath. When dissolved, 2 mL of Naphthol As-MX phosphate alkaline solution was added.

### 3.1.6 Equipment

**Table 3-8: Equipments used in different experiments**

Equipment	Manufacturer
Applied Biosystems™ Veriti™ 96-Well Thermal Cycler	ThermoFisher Scientific
Centrifuges	eppendorf
Cytation 5 Plate Reader	Biotek
CytExpert software	Beckman Coulter
CytoFLEX LX Flow Cytometer	Beckman Coulter
NanoDrop ND-1000 Spectrophotometer	NanoDrop Technologies, Inc.
The LightCycler® 480 (PTC-100 Peltier - version 9)	Roche
Varioskan LUX 1.00.38 Plate Reader	ThermoFisher Scientific

## 3.2 Methods

### 3.2.1 Isolation of human bone marrow mesenchymal stem cells

Human bone samples of knee joints from T2DM and non-diabetic patients (n=3 for each), undergoing knee joint replacement surgeries at Chapel Allerton Hospital were used for isolation of human BM-MSCs. The samples were collected under ethical approval from Yorkshire and Humberside National Research Ethics Committee (reference number 14/YH/0087 – Appendix A) and with patients' informed written consent. Demographic data of the donors and preoperative HbA1c of diabetic donors are listed in Table 3-9.

**Table 3-9: Demographic data of BM-MSCs donors.**

Donor	Age (yrs)	Gender	Diabetic (HbA1c mmol/mol)	Other comorbidities
D1	81	F	Yes (45)	OA, HT
D2	82	M	Yes (NA)	OA
D3	85	F	Yes (47)	OA
ND1	76	F	No	OA
ND2	64	M	No	OA
ND3	86	M	No	OA

D: diabetic, HT: hypertension, NA: not available, ND: non-diabetic, OA: osteoarthritis

Bony chips (approximate size of 25 – 30 mm<sup>2</sup>) were generated from the cancellous bone parts of the knee joints using sterile bone rongeurs, dental chisel and mallet. These chips were incubated in a mixture of equal volumes of 3 mg/mL collagenase type I and 4 mg/mL dispase for 4 hrs at 37°C, with gentle agitation every 30 mins until the chips looked pale and fragile, as described previously (419–421).

Digestion was arrested using 3 mLs of complete media ( $\alpha$ -Modified Minimum Essential Medium ( $\alpha$ -MEM), supplemented with 20% foetal bovine serum (FBS), 1% penicillin/streptomycin (P/S) and 1% L-glutamine (L-G)). The cell suspension

was aspirated away from the bony chips and centrifuged at 148 x g for 5 mins. The supernatant was removed and the cell pellet was resuspended in complete media and passed through a 70 µm cell strainer to generate single cell suspension for optimum expansion. Cells were cultured in 3 x T175 tissue culture flasks, labelled as passage (P) 0 and kept in an incubator at 37° C and 5% CO<sub>2</sub>. After 2 days, media was fully discarded and adherent cells were washed twice with 10 mL PBS, to remove hematopoietic cells present in suspension. Fresh media was added (40 mL/T175 flask), and after this media was fully changed every 5 days.

### **3.2.2 Cell culture, passaging, expansion and freezing**

When P0 cells reached 80% confluence, they were washed twice with 10 mL PBS and detached using 5 mL trypsin-EDTA 0.25% (w/v) solution for 10 mins. When the cells were completely detached as observed under a light microscope, 2 mL of complete basal media was added to halt the action of trypsin; and the cell mix was transferred to a 15 mL centrifuge tube and centrifuged at 148 x g for 5 mins. The supernatant was discarded and the cell pellet was resuspended in 5 mL fresh media and live cells were counted using a haemocytometer and 0.01% (w/v) Trypan blue stain to distinguish dead cells.

To expand cells for further experiments (flow cytometry analysis and osteogenic differentiation assay), cells were subcultured at density of 4000 cells/cm<sup>2</sup> in T75 and T175 flasks in 20 mL and 40 mL of media respectively. When confluent, cells were passaged as described above. Excess cells at each passage were frozen by resuspension in expansion media supplemented with 10% dimethyl sulfoxide (DMSO) at a density of ~1.5 x 10<sup>6</sup> cells per 1.8 mL cryovial. Cells were chilled at a speed of 1°C/ min in Mr Frostie containers and stored at -80°C freezers for short term or liquid nitrogen for long term storage (Figure 3-1).

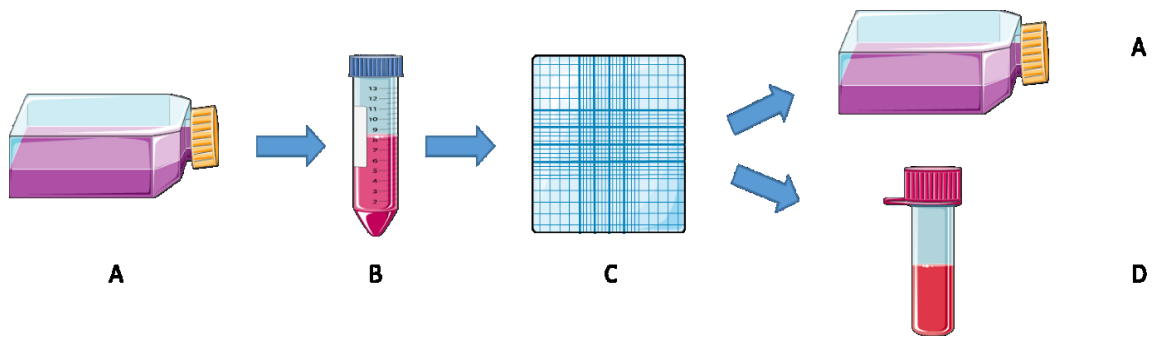


**Figure 3-1: Cells passaging, counting and expansion**

A: Tissue culture flask, B: Centrifuge tube, C: Neubauer counting chamber, D: Cryovial. This figure is designed using schematic art pieces provided by Servier Medical art (<http://servier.com/Powerpoint-image-bank>). Servier Medical Art by Servier is licensed under a Creative Commons Attribution 3.0 Unported License

### 3.2.3 Colony forming unit fibroblasts (CFU-Fs) assay

Colony forming unit-fibroblasts (CFU-Fs) assay was performed in order to evaluate the proportions of highly-proliferative cells in early-passage cultures as described before (422). BM-MSCs at P1/2 were counted and seeded at a density of 1000 cells (following optimization) in 15 mL of complete media in 100 mm tissue culture dish in duplicates. Media was fully changed every 5 days, and at day 14 media was removed. Cells were then washed twice with 10 mL PBS, fixed using 10 mL of 3.7% formaldehyde solution for 20 mins; and then stained using 10 mL of 1% methylene blue in borate buffer solution for 45 mins. The cells were gently washed with d H<sub>2</sub>O and colonies of 50 or more cells were counted and averaged for each donor. The percentage of colony forming MSCs was calculated using the equation as described before (423):

$$\% \text{ MSCs} = \text{number of colonies} / \text{number of seeded cells} \times 100.$$

### 3.2.4 Population doubling time assay

To assess the population doubling time of diabetic versus non-diabetic cells, BM-MSCs at P1 were seeded in T25 flasks at a density of  $1 \times 10^5$  cells per flask. Cells were passaged and counted, as described in Section 3.2.2. Counts of seeded and trypsinized cells, P numbers and passaging dates were recorded to generate a curve of accumulative population doublings versus accumulative culture days, as previously described (424). For each passage, population doubling (PD), accumulative population doubling (APD) and population doubling time (PDT) were calculated using the following formulas:

PD =  $\text{Log}_2$  (Count of trypsinized cells/count of seeded cells)

APD = Sum of PDs

PDT = Accumulative days (duration) of culture / APD

### **3.2.5 Flow cytometry analysis**

Flow cytometric analysis allows for robust multiparametric analysis of thousands of cells within the sample preparation on an individual cells basis, depending on 2 physical light scattering parameters (forward and side scatter) and multiple fluorescent signals emitted from antibody-conjugated fluorophores. This allows for analysis of phenotypically distinct cell subpopulations (425). A flow cytometer contains 3 components: fluidics (that direct the liquid containing the sample to the light), optics (excitation lasers and detectors collecting scattered light and fluorescent signals); and electronics (converting the collected signals to digital data) (426). In addition to forward and side scatter, dyes or fluorochrome that can be conjugated to monoclonal antibodies and get excited by lasers in the flow cytometer are used to identify markers expressed by the cells (427).

As outlined in chapter 1 of this thesis, the ISCT suggested a panel of markers for identification of MSCs populations. This includes positive (CD73, CD90, CD105) and negative (CD14, CD19, CD34, CD45 and HLA-DR) markers (Table 3-10). These negative markers are normally expressed by hematopoietic cells and therefore, are used to eliminate the possibility of MSCs contamination by such cells (177).

**Table 3-10: Surface markers used for MSCs identification through flow cytometric analysis**

Marker	Biological role	Reference
CD73 (ecto-5'-NT)	Cell surface glycoprotein, expressed on different cell types	(428)
CD90 (Thy-1)	Cell surface glycoprotein expressed by MSCs, fibroblasts and myofibroblasts	(429)
CD105 (Endoglin)	Cell surface glycoprotein, important for angiogenesis	(430)
CD14	Expressed by monocytes and macrophages	(177,431,432)
CD19	Expressed by B cells	(177,431)
CD34	Expressed by hematopoietic stem and progenitors cells as well as endothelial cells	(177,431)
CD45	Leukocyte common antigen	(177,432)
HLA-DR	MHC class II cell surface receptor	(424)

### 3.2.5.1 Setting up compensation matrix

Compensation is the process integral to multicolour flow cytometry to correct spectral overlap or spillover, which happens with fluorophores that are measurable in more than one detector/channel. This is achieved by minimizing the spillover of other fluorophores into one particular channel so that each channel contains information from one fluorophore only (433).

For compensation matrix setup, single stained tubes of each fluorophore were run and analysed on the cytometer using either cells or compensation beads (Table 3-11). CompBeads are polystyrene particles of two populations: the CompBeads anti-Mouse Ig,  $\kappa$  particles which bind any mouse  $\kappa$  light chain-bearing immunoglobulin, and the CompBeads negative control, which has no binding capacity. When mixed together with a single antibody-conjugated fluorophore, they provide 2 populations of beads with distinctive fluorescence that is used to setup the compensation while preserving the cells populations. BM-MSCs were used for compensation for the fixable viability stain (FVS), as this

stain excludes dead cells by positively staining them, as dead cells have 'leaky' cell membranes unlike living ones.

**Table 3-11: Tubes used for compensation matrix setup**

#	Tube	Purpose
1	Unstained cells	Control
2	BM-MSCs stained with FVS 780	Compensating for FVS 780
3	Negative beads only	Control
4	Beads stained with anti CD73-PE	Compensating for PE
5	Beads stained with anti CD90-FITC	Compensating for FITC
6	Beads stained with anti CD105-BV421	Compensating for BV421
7	Beads stained with anti CD14-BV510	Compensating for BV510
8	Beads stained with anti CD19-APC	Compensating for APC
9	Beads stained with anti CD34-BB700	Compensating for BB700
10	Beads stained with anti CD45-BV650	Compensating for BV650
11	Beads stained with anti-HLA-DR-BUV395	Compensating for BUV395

### 3.2.5.2 Fluorescence minus one (FMOs) control

FMOs controls are based on staining cells with all antibody-fluorophore conjugates used in the panel, except one, for which the threshold to be set to best determine the negative cell population. Thresholds or gates can be drawn based on FMOs and applied to the fully stained sample to identify positive events, with data from FMO and fully stained tubes displayed and compensated similarly (433,434). Compared to isotype controls, gates based on FMO controls are more sensitive to dully fluorescent cells and also take into account potential interactions between antibody reagents and are therefore, considered of greater value in complex multi-colour staining panels (434).

For each analysis, a total of 9 FMO tubes were prepared, in addition to the unstained cells and all stained cells (the sample stained with the full panel of all antibodies and the live dead stain). These FMOs served as the negative controls to which the all stained tube was compared for the expression of the corresponding antibody/fluorophore (Table 3-12).

**Table 3-12: FMO controls used in flow cytometry analysis**

	Anti-CD73	Anti-CD90	Anti-CD105	Anti-CD14	Anti-CD19	Anti-CD34	Anti-CD45	Anti-HLA-DR	FVS 780
Tube 1 CD73 FMO	-	+	+	+	+	+	+	+	+
Tube 2 CD90 FMO	+	-	+	+	+	+	+	+	+
Tube 3 CD105 FMO	+	+	-	+	+	+	+	+	+
Tube 4 CD14 FMO	+	+	+	-	+	+	+	+	+
Tube 5 CD19 FMO	+	+	+	+	-	+	+	+	+
Tube 6 CD34 FMO	+	+	+	+	+	-	+	+	+
Tube 7 CD45 FMO	+	+	+	+	+	+	-	+	+
Tube 8 HLA-DR FMO	+	+	+	+	+	+	+	-	+
Tube 9 FVS 780 FMO	+	+	+	+	+	+	+	+	-

### 3.2.5.3 Samples preparation and analysis

Flow cytometric analysis of surface markers was used to characterize the different stem cell populations examined in this study. Cells at P3-5 were cultured as above, and harvested at 80% confluency.

Cells were centrifuged at 148 x *g* for 5 mins, washed twice with PBS and strained with 70 µL cell strainer to ensure single cell suspension and eliminate any cell 'clumps'. Cells were then counted and resuspended in PBS at density of 2 x 10<sup>7</sup> cells/mL. Two aliquots of 50 µL each were put aside for the unstained cells and FMO – FVS cells.

The remaining cells were incubated with FVS at concentration of 1:1000 (1 µL for each 1 mL of cells suspension) at room temperature (RT), for 10-15 mins in the dark. Cells were then washed twice and resuspended in FACS buffer. Cells were aliquoted into the remaining FMO tubes and the all-stained tube in equal volumes. Every sample/tube contained approximately 1x10<sup>6</sup> cells.

Five (5) µL of Fc block reagent was added each tube and incubated for 10 mins at RT to reduce nonspecific binding of the Fc region of the antibody reagents due to the Fc receptors that are present on the surface of some cell types. Fifty (50) µL of Brilliant stain buffer was added to each of the stained tubes, to reduce the dye-dye interaction.

The appropriate fluorochrome-conjugated antibodies were then added to each tube and incubated for 45 mins on ice sealed from light. Cells were then washed twice with 1 mL FACS buffer, centrifuged at 148 x *g* for 5 mins at a temperature of 5°C and supernatant was removed.

Fixation buffer (250 µL) were added to each cell pellet and cells were resuspended by pipetting and incubated for 15-30 mins at 4°C. Fixed cells were then washed twice and resuspended in 500 µL of FACS buffer. Fixed cells were kept at 4°C protected from light until read within 1 week.

The analysis was performed using the CytoFLEX Flow Cytometer. For each donor/experiment, the following tubes were analysed: Unstained tube, FMO tubes and fully stained tube. The samples preparation steps are outlined in Figure 3-2 . Data was then compensated and analysed using CytExpert software.

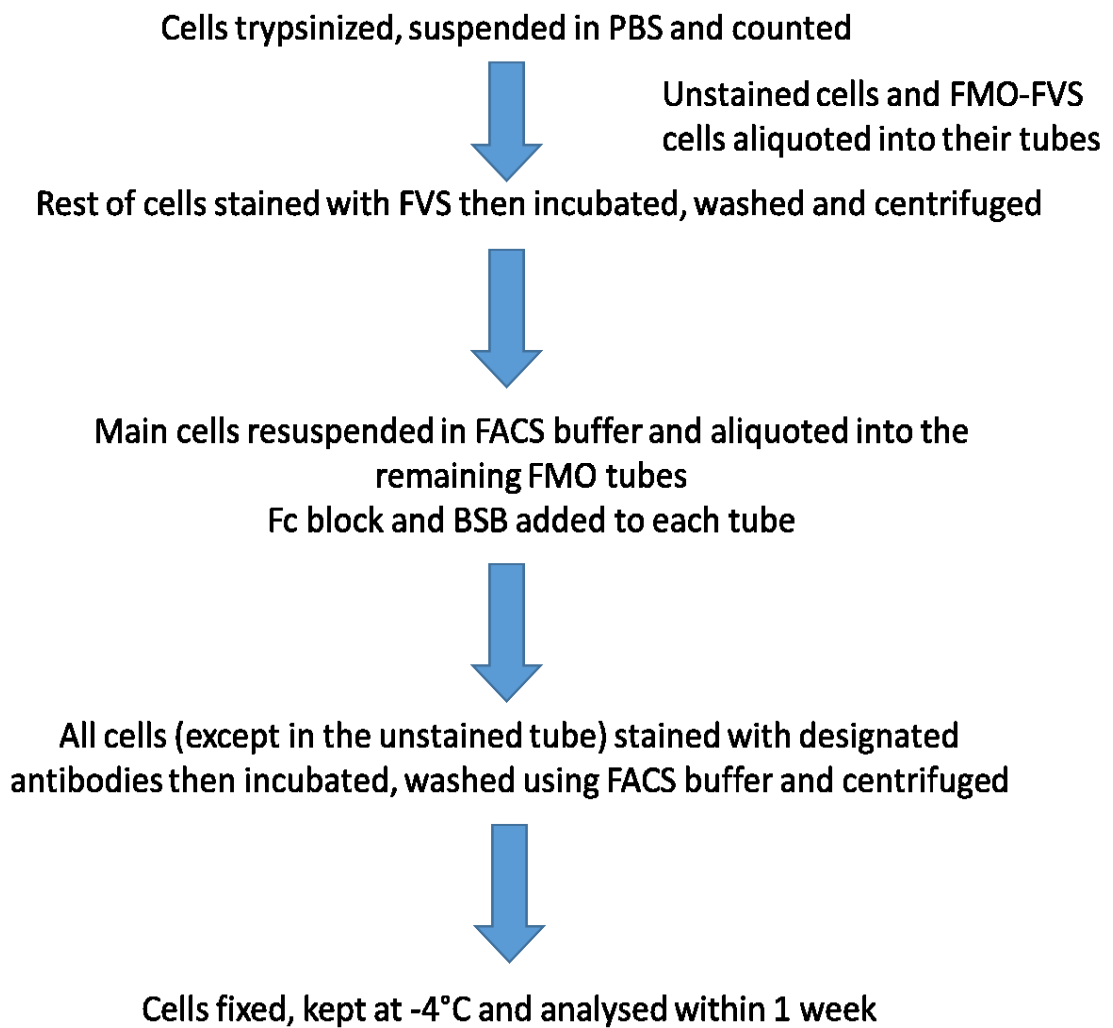


**Figure 3-2: Samples preparation for flow cytometry analysis**

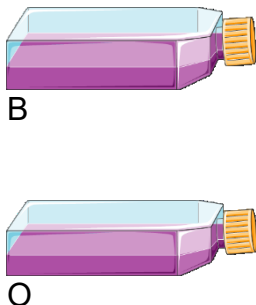
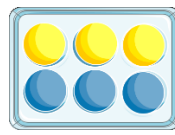
### **3.2.6 Osteogenic differentiation of BM-MSCs**

To assess the osteogenic potentials of BM-MSCs, cells isolated from each donor at P 2-4 were cultured under basal conditions (complete media, Section 3.2.2) and osteogenic conditions (basal media supplied with 10nM dexamethasone, 50 µg/mL L-ascorbic acid and 5mM β-glycerophosphate, as described in other reports (435)), for 3 different durations: 1, 2 and 3 weeks. The experimental design is outlined in Table 3-13.

For alkaline phosphatase (ALP) and Alizarin Red (AR) stains, cells were seeded in 6 well plates at a density of  $3 \times 10^4$  cells/well. Media was changed weekly and at each time-point cell cultures were terminated as cells were washed, fixed and stained, as described in the following sections.

For qPCR gene expression analysis, cells were seeded in T25 flasks at a density of  $1 \times 10^5$  cells in 10 mL media. Additionally,  $1 \times 10^5$  of trypsinized cells were mixed with RLT lysis buffer and frozen at  $-80^\circ\text{C}$ , to serve as baseline (T0) controls as described earlier (436). Similar to cultures planned for staining, media was changed weekly. At each time-point media was collected for ELISA analysis, centrifuged at  $148 \times g$  to remove any debris, aliquoted into eppendorfs of 1.5 mL each and stored at  $-80^\circ\text{C}$ . Cells were then trypsinized as described earlier; and lysed for RNA extraction and subsequent cDNA synthesis and qPCR analysis.

**Table 3-13: Experimental design for assessment of osteogenic potentials of isolated BM-MSCs**

Time-point (wks)	qPCR	ALP staining	AR staining	ELISA
0	Placing $1 \times 10^5$ trypsinized cells into RLT buffer, freezing at $-80^\circ\text{C}$  Seeding 2 x T25 flask (one basal, B and one osteogenic, O) each with $1 \times 10^5$ cells for each time-point (1, 2 and 3) – total 6 flasks	Seeding 2 wells for each time-point (1 B and 1 O, no replicates) each with $3 \times 10^4$ cells.	Seeding 6 wells for each time-point (3 B and 3 O, duplicates) each with $3 \times 10^4$ cells.	---
1	Trypsinizing Wk1 flasks (1 B and 1 O), add RLT buffer, freeze at $-80^\circ\text{C}$  	Staining Wk 1 wells (1 B and 1 O)  	Staining Wk1 wells (3 B and 3 O)*  	Collecting media from qPCR flask, aliquoting and storing at $-80^\circ\text{C}$
Full media change of all Wk2 and Wk3 cultures				
2	Same as Wk1 + Full media change of all Wk3 cultures			
3	Same as Wk1			

\* Wells stained with AR stain were also used for stain extraction and quantification, B: basal, O: osteogenic. This figure is designed using schematic art pieces provided by Servier Medical art (<http://servier.com/Powerpoint-image-bank>). Servier Medical Art by Servier is licensed under a Creative Commons Attribution 3.0 Unported License.

### **3.2.6.1 Alkaline phosphatase (ALP) staining assay**

This assay uses a chemical substrate of ALP enzyme (naphthol) and the products of the ALP-substrate reaction or their derivatives produce the characteristic blue stain, which allows detection of ALP activity (437). First media was aspirated from each well and cells were gently washed twice with 1 mL PBS per well. Next PBS was removed, 2 mLs of fixative (2 parts of citrate working solution mixed with 3 parts of acetone) were added to each well for 30 secs and then washed twice in d H<sub>2</sub>O, as previously described (438). Fast Blue stain mixture (section 3.1.5) was added (2 mL per well) and incubated for 30 mins at RT in the dark. Stained cells were washed twice with d H<sub>2</sub>O, examined under light microscope and imaged.

### **3.2.6.2 Alizarin red (AR) staining and quantification of calcium nodules**

The AR staining and quantification of deposited calcium nodules were assessed after 1, 2, and 3 weeks of culture under basal and osteogenic conditions as described earlier (439).

#### **AR staining**

The staining was performed according to manufacturer's recommendations. First, culture media was removed from all wells and cells were gently washed 3 times with PBS (2 mL/well). Cells were then fixed using 4% formaldehyde (2 mL/well) for 15 mins at RT. Formaldehyde was removed and cells were washed gently 3 times with d H<sub>2</sub>O (2 mL/well) and then water was discarded. One mL of 40 mM AR dye was added to each well and incubated at RT for 20–30 mins, with gentle shaking. AR dye was removed and cells were washed 5 times with d H<sub>2</sub>O (2 mL/well). Stained cells were examined and images were taken using a light microscope and plates were stored at -20°C until quantification.

#### **Quantification of AR stain**

The AR stain quantification assay was performed according to manufacturer's recommendations. First, 800 µL of 10% acetic acid was added to each well and incubated at RT for 30 mins, with gentle shaking. Next, cells were detached from the bottom of the wells using a cell scraper and the acetic acid containing the cells was transferred to 1.5 mL microfuge tubes, which were vortexed for 30 secs. The tubes were then sealed with parafilm, heated at 85°C for 10 mins and then incubated on ice for 5 mins. Tubes were centrifuged at 20,000 x g for 15 mins;

and 500  $\mu\text{L}$  of the supernatant was transferred to a new tube. Next, 200  $\mu\text{L}$  of 10% ammonium hydroxide was added to each tube to neutralize the acetic acid. Standards were prepared by adding and mixing 100  $\mu\text{L}$  of 40 mM AR standard solution with 900  $\mu\text{L}$  of standard dilution solution to make 1 mL of 4 mM AR standard solution. Next, 500  $\mu\text{L}$  of standard dilution solution were added into 8 microfuge tubes (1.5 mL) labelled #1 to #8 and 500  $\mu\text{L}$  of the 4 mM AR stain solution were added and well mixed into tube #1 to get the 2 mM AR stain standard. This first standard was serially diluted to get a total of 7 standards with the concentrations of 2 mM, 1 mM, 0.5 mM, 0.25 mM, 0.125 mM, 0.0625 and 0.0313 mM. No AR standard was added to tube #8, which served as the blank. Finally, 150  $\mu\text{L}$ /well of each AR stain standard, the blank and each tube/sample were aliquoted in triplicates in an opaque-walled, transparent-bottomed 96-well plates.

The absorbance of each well was read at 405 nm (known as optical density or OD) using Cytation 5 Plate Reader. The OD readings of triplicate wells were averaged and the OD of the blank well was subtracted from the OD of the samples to get the calibrated OD. The calibrated OD values of the standard wells were plotted on the y axis versus the AR stain concentration on the x axis to produce the standard curve. The equation of the standard curve was calculated and used to extrapolate the AR concentration of samples.

### **3.2.7 Analysis of gene expression using quantitative polymerase chain reaction (qPCR)**

qPCR is a sensitive and efficient assay that can amplify a specific segment of DNA from a wide pool of DNA, using the following basic components:

- Template cDNA that contains the target DNA sequence to be amplified.
- Primers which are short DNA fragments with a specific sequence of DNA bases complementary to target DNA and thus, specify which part of template DNA is amplified.
- Nucleotides, the building blocks of amplified DNA.
- DNA polymerase, the enzyme responsible for building up DNA target.

The qPCR allows for repeated cycles of DNA amplification (each cycle consists of 3 phases: denaturation, annealing and extension); and with each cycle the amount of target DNA doubles (440).

One of the main applications of qPCR is measuring gene expression (mRNA) in a cell. This is usually done by extraction of RNA from cells, using this RNA as a template to construct single stranded complementary DNA (cDNA), through reverse transcription and then cDNA is used as a template for PCR (441).

### **3.2.7.1 mRNA extraction and quantification (including elimination of genomic DNA) from BM-MSCs cultured under basal and osteogenic conditions**

Cells were detached using trypsin–EDTA solution as described above and RNA extraction was done using RNeasy Mini Kit, according to manufacturer's instructions. First, RLT buffer was added to the cell pellet (350  $\mu$ L for cells  $\leq 5 \times 10^6$ ) and mixed well. The mix was transferred to nuclease free 2 mL Eppendorf tubes and stored at  $-80^\circ\text{C}$ . Cell lysate was removed from  $-80^\circ\text{C}$  and allowed to thaw on ice. Equal volume of 70% ethanol was added to the lysate (1:1 v/v with RLT buffer) and well mixed by pipetting. Next, 700  $\mu$ L of the solution was transferred to the RNeasy Mini spin column placed in 2mL collection tube. Samples were centrifuged for 15 secs at 8000 x *g* and flow-through was discarded. Then, 350  $\mu$ L of RW1 buffer was added and samples were centrifuged for 15 secs at 8000 x *g*, flow-through was discarded and 80  $\mu$ L of DNase enzyme (10  $\mu$ L of DNase stock solution and 70  $\mu$ L of RDD buffer) was added directly to the RNeasy spin column membrane and incubated for 15 mins at RT.

Next, 350  $\mu$ L of RW1 buffer was added and samples were centrifuged for 15 secs at 8000 x *g* and flow-through was discarded. Then, 500  $\mu$ L of RPE buffer was added and samples were centrifuged for 15 secs at 8000 x *g* and flow-through was discarded. Finally, 500  $\mu$ L of RPE buffer was added and samples were centrifuged for 2 mins at 8000 x *g*. The spin column was placed in a new 1.5 mL collection tube and 30  $\mu$ L of nuclease free water was added. Finally, the tubes were centrifuged for 1 min at 8000 x *g* and RNA eluate was collected.

RNA quantification was performed using NanoDrop Spectrophotometer. Two  $\mu$ L of each RNA sample was used and the resultant quantities were recorded as ng/ $\mu$ L. The 260/280 ratio was also recorded to assess purity of RNA yield and these were typically between 1.8 and 2.

### **3.2.7.2 Reverse transcription**

Single stranded DNA was generated from RNA using High-Capacity RNA-to-cDNA Kit according to manufacturer's instructions. Kit components were allowed to thaw on ice and the reagents were mixed so that each reaction had a total volume of 20  $\mu$ L:

- 10  $\mu$ L RT buffer
- 1  $\mu$ L enzyme mix
- Up to 9  $\mu$ L RNA sample with a max of 2  $\mu$ g RNA per reaction.
- Nuclease free H<sub>2</sub>O sufficient to make the total reaction volume 20  $\mu$ L

Reactions were incubated in a thermal cycler for 60 mins at 37°C, then for 5 mins at 95°C and held at 4°C. The resultant cDNA was stored at -20°C until qPCR amplification.

### **3.2.7.3 qPCR**

qPCR reactions were carried out to measure the relative changes in gene expression using Taqman<sup>®</sup> gene expression assays (Table 3-5). Each reaction was conducted into the 96 well plate in duplicates, with each of a volume of 20  $\mu$ L consisting of:

- 10  $\mu$ L Master Mix.
- 8  $\mu$ L nuclease free water.
- 1  $\mu$ L cDNA sample.
- 1  $\mu$ L of Taqman<sup>®</sup> gene expression assay.

Each plate also included non template negative controls (Master Mix, nuclease free water and TaqMan<sup>®</sup> assay) to exclude any cDNA contamination of the reagents. The plates were well sealed and centrifuged for 10 secs using a plate centrifuge and then put into thermal cycler machine (Roche LC480 Light Cycler). Amplification was carried out according to manufacturers' recommendations. The reaction composed of 3 phases:

- Preincubation cycle at 95°C for 10 mins.
- 45 Amplification cycles, each at 95°C for 5 secs, then at 65°C for 1 min.
- Final cooling at 4°C for 30 secs.

### **3.2.7.4 Data analysis**

For each gene, the relative change of gene expression was assessed using the  $\Delta C_t$  method. For each sample at each time-point, the threshold cycle ( $C_t$ ) value for each gene was generated in duplicate using the thermal cycler, indicating the cycle at which the amplicon fluorescence was above the threshold. The average  $C_t$  of each gene of interest (GOI) was calculated and normalized to the average  $C_t$  of the housekeeping gene (HKG) GAPDH, HPRT1 and the average  $C_t$  of both genes (normalization to multiple HKGs). This normalization was calculated for each time-point separately using the equation:

$$\Delta C_t = C_t_{\text{gene of interest (GOI)}} - C_t_{\text{HKG}}$$

### **3.2.8 ELISA assay for assessing protein levels of IGFBPs in conditioned media**

Cells were cultured under basal and osteogenic conditions for 1, 2 and 3 weeks and at each time-point, conditioned media was collected, centrifuged at  $148 \times g$  for 5 mins at RT and aliquoted to prelabelled 1.5 mL Eppendorf tubes. Conditioned media aliquots were stored at  $-80^\circ\text{C}$  till ELISA analysis was carried out; and unconditioned basal and osteogenic media were used as controls. Concentrations of IGFBP-2, IGFBP-3 and IGFBP-4 in conditioned media were measured using human IGFBP-2 and IGFBP-3 Quantikine<sup>®</sup> ELISA kits and IGFBP-4 DuoSet<sup>®</sup> ELISA kit, respectively, according to manufacturer's instructions.

#### **3.2.8.1 IGFBP-2 concentrations measurement using IGFBP-2 Quantikine<sup>®</sup> ELISA kit**

##### **Reagents preparation**

All reagents except the conjugate antibody were first brought to RT. Wash Buffer Concentrate was gently mixed to dissolve any crystals, before mixing 20 mL with 480 mL of d H<sub>2</sub>O to prepare 500 mL of Wash Buffer. IGFBP-2 standard was reconstituted using d H<sub>2</sub>O to make a stock solution of 200 ng/mL, which was well mixed and allowed to sit for 15 mins. Serial dilutions of IGFBP-2 standard were made by first mixing 100  $\mu\text{L}$  of standard and 900  $\mu\text{L}$  of Calibrator Diluent RD5-20 into a tube labelled with the concentration 20 ng/mL. Then, 500  $\mu\text{L}$  of this tube were mixed with 500  $\mu\text{L}$  of the diluent to prepare a dilution of 10 ng/mL. A total of

7 serial dilutions were made ending with a solution of concentration of 0.313 ng/mL. The diluent was used as the zero standard or blank (0 ng/mL).

### **Assay procedure**

Samples were removed from -80°C freezer and allowed to thaw on ice. Assay Diluent RD1X (100 µL) was added to each well. Samples, controls (basal and osteogenic media) and standards (50 µL), were added to wells in duplicates. The plate was covered with the adhesive strip and incubated for 2 hrs at RT. Each well was aspirated and thoroughly washed with 400 µL of Wash Buffer for 4 times. After the last wash, any remaining Wash Buffer was aspirated and the plate was inverted and plotted against clean paper towels.

Human IGFBP-2 Conjugate (200 µL) was added to each well and the plate was covered with a new adhesive strip and incubated for 1 hr at RT. Towards the end of the incubation time, Substrate Solution was prepared by mixing equal volumes of Colour Reagent A and B and the mixture was protected from light. The wells were washed as described above; and Substrate Solution (200 µL) was added to each well. Next, the plate was sealed from light and incubated for 30 mins at RT. Finally, Stop Solution (50 µL) was added to each well and colour change was observed.

OD was determined for each well within 30 mins using a microplate reader at 450 and 540 nm; and the average of duplicates of each standard, sample and control was calculated. Readings at 540 nm were subtracted from readings at 450 nm to correct for optical imperfections in the plate. A standard curve was made by plotting the average OD for standards on the y-axis and their concentrations on the x-axis and IGFBP-2 concentrations in samples were extrapolated.

### **3.2.8.2 IGFBP-3 concentrations measurement using IGFBP-3 Quantikine®**

#### **ELISA kit**

#### **Reagents preparation**

Wash Buffer Concentrate was warmed and well mixed to remove any crystals; and 20 mL of the Concentrate were mixed with 480 mL of d H<sub>2</sub>O to prepare 500 mL of Wash Buffer. Calibrator Diluent RD5P (20 mL) was added to d H<sub>2</sub>O (80 mL) to prepare 100 mL of Calibrator Diluent RD5P (diluted 1:5). Human IGFBP-3 standard was reconstituted using Calibrator Diluent RD5P to prepare a stock

solution of 50 ng/mL. The reconstituted solution was well mixed and allowed to sit for 15 mins.

Reconstituted IGFBP-3 standard was serially diluted by first mixing Calibrator Diluent RD5P (300 µL) with the standard (300 µL) to prepare a dilution of 25 ng/mL. Then, a total of 6 standard dilutions (1:1) were prepared ending with the one of 0.781 ng/mL. The undiluted IGFBP-3 standard (50 ng/mL) served as the high standard and Calibrator Diluent RD5P (diluted 1:5) served as the zero standard or blank (0 ng/mL).

### **Assay procedure**

Samples were removed from freezer and thawed on ice. Assay Diluent RD1-62 (100 µL) was added to each well. Samples, controls and standards (100 µL) were added to wells as planned in duplicates and the plate was covered with the adhesive strip and incubated for 2 hrs at 2-8°C.

Each well was aspirated and thoroughly washed with 400 µL of Wash Buffer for 4 times. After the last wash, any remaining Wash Buffer was aspirated and the plate was inverted and plotted against clean paper towels. Cold Human IGFBP-3 Conjugate (200 µL) was added to each well. The plate was covered with a new adhesive strip and incubated for 2 hrs at 2-8° C. Towards the end of the incubation time, Substrate Solution was prepared by mixing equal volumes of Colour Reagent A and B. The mixture was protected from light.

The washing procedure described above was repeated and Substrate Solution (200 µL) was added to each well. The plate was sealed from light and incubated for 30 minutes at RT. Stop Solution (50 µL) was added to each well and colour changes were observed. OD was determined as described before, a standard curve was plotted and IGFBP-3 concentrations in samples were extrapolated as mentioned above.

### **3.2.8.3 IGFBP-4 concentrations measurement using IGFBP-4 DuoSet® ELISA kit**

#### **Reagents preparation**

1x PBS (60 mL) was prepared by mixing 20x PBS (3 mL) with d H<sub>2</sub>O (57 mL). Reagent Diluent 3 (diluted 1:5, 60 mL) was prepared by mixing Reagent Diluent Concentrate 3 (12 mL) with 1x PBS (48 mL) and then 2% heat inactivated goat

serum was added. 1x Wash Buffer (600 mL) was prepared by mixing Wash Buffer Concentrate (24 mL) with d H<sub>2</sub>O (576 mL).

Mouse Anti-Human IGFBP-4 Capture Antibody was reconstituted with 1 mL of PBS without carrier protein, to the working concentration of 4 µg/mL, as indicated in the kit Certificate of Analysis. Biotinylated Goat Anti-Human IGFBP-4 Detection Antibody was reconstituted with 1 mL of Reagent Diluent with 2% heat inactivated normal goat serum, to the working concentration of 100 ng/mL, as indicated in the kit Certificate of Analysis. Streptavidin conjugated to horseradish-peroxidase (Streptavidin-HRP, 1 mL) was diluted 200-fold using Reagent Diluent.

One vial of recombinant Human IGFBP-4 Standard was reconstituted with 0.5 mL of Reagent Diluent, to prepare a stock standard solution (460 ng/mL). A total of seven 2-fold serial dilutions were prepared with concentrations ranging from 32 ng/mL to 0.5 ng/mL. The Reagent diluent served as the zero standard or blank.

### **Assay procedure**

Immediately after preparation of diluted Capture Antibody, the 96-well microplate was coated with the diluted Capture Antibody, by adding 100 µL per well. The plate was then sealed and incubated overnight at RT. The next day, each well was aspirated and thoroughly washed 3 times as described earlier.

The plate was blocked by adding 300 µL of Reagent Diluent to each well and incubated for at least 1 hr at RT and then the washing procedure was repeated. Samples, controls, and standards (100 µL per well) were added in duplicates. The plate was covered with an adhesive strip and incubated for 2 hrs at RT; and the washing procedure was repeated.

Detection Antibody (100 µL, diluted in Reagent Diluent with the inactivated normal goat serum) was added to each well. The plate was covered with a new adhesive strip and incubated for 2 hrs at RT and the washing procedure was repeated. The working dilution of Streptavidin-HRP A (100 µL) was added to each well. The plate was covered, wrapped in aluminium foil for light protection and incubated for 20 mins at RT. Within 15 mins of its use, Substrate Solution was prepared by mixing equal volumes of Colour Reagent A and Colour Reagent B and protected from light. The washing procedure described above was repeated. Substrate Solution (100 µL) was added to each well. The plate was wrapped in aluminium foil for light protection and incubated for 20 mins at RT. Stop Solution

(50  $\mu$ L) was added to each well and colour changes were observed. The OD of each well was measured and IGFBP-4 concentrations were extrapolated as described before.

### **3.2.9 Statistical analysis**

Data were analysed using GraphPad Prism software (v 9.2.0). The results of CFU-Fs, PDT, flow cytometry and AR stain quantification analyses are presented as mean  $\pm$  standard deviation (SD). The results of qPCR and ELISA assays are presented as mean  $\pm$  standard error of mean (SEM). Paired t test was used to compare matching groups (basal and osteogenic cultures of the same cells population at each time-point) while unpaired t test was used to compare non matching groups (non-diabetic and diabetic cells cultures at each culture condition and time-point). Repeated measures one way ANOVA (RM-ANOVA) was used to compare different time-points of each cell population under the same culture condition for AR stain quantification, qPCR and ELISA assays. P values were determined and differences were considered statistically significant if  $p < 0.05$ .

## **Chapter 4 Results**

### **Characterisation of diabetic BM-MSCs in comparison to non-diabetic controls**

#### **4.1 Introduction**

BM-MSCs are the most investigated MSCs for bone regeneration due to their superior osteogenic capabilities (442). Autologous stem cells transplantation offers multiple advantages over other approaches for bone regeneration. For instance, it carries no risk of immunologic reaction which could be associated with allogenic cell transplantation (217). Therefore, characterisation of BM-MSCs isolated from patients with systemic diseases is of utmost importance for successful clinical translation of this regenerative therapeutic approach. This is especially true for diabetes, which is projected to affect more than 10% of world population by 2045 and is associated with multiple macro- and micro-vascular complications (443).

Basic identification and characterisation of MSCs is a cornerstone for any subsequent investigation. The International Society for Cellular Therapy (ISCT) proposes that MSCs are defined by their ability to adhere to plastic, positive expression of CD73, CD90 and CD105 in the absence of CD45, CD34, CD14 or CD11b, CD79a or CD19 and HLA-DR expression and finally their multilineage differentiation potentials (177). The CFU-Fs assay is considered one of the longest standing and simplest methods for MSCs enumeration, based on their capability to adhere to plastic and to proliferate forming colonies (422). The expression of the above mentioned MSCs markers have been investigated using multi-parameter flow cytometric immunophenotyping of BM-MSCs and their MSCs expression profile has been confirmed (423,444), including in BM-MSCs from diabetics (245,248). Yet the number of studies investigating diabetic BM-MSCs is relatively limited compared to 'healthy' BM-MSCs. Moreover, as elaborated later in this chapter, there is considerable variation in these studies regarding anatomical origin of BM-MSCs, their method of isolation and the overall experimental design.

The present study was designed to compare diabetic and non-diabetic BM-MSCs, in terms of their clonogenic potentials, growth kinetics and expression of stem cells surface markers using flow cytometry. This would highlight whether diabetes has an influence on BM-MSCs and whether these cells are competent for regenerative periodontal applications. Three donors from each group were included and their demographic data are shown in chapter 3 of this thesis.

## 4.2 Results

### 4.2.1 Colony forming unit fibroblasts (CFU-Fs) assay of diabetic and non-diabetic BM-MSCs

BM-MSCs from non-diabetic (n=3) and diabetic (n=3) donors at P1/2 were counted and seeded at density of 1000 cells in 100 mm tissue culture dishes in duplicate. After 14 days, cells were fixed, stained and colonies of 50 or more cells were counted and averaged. The percentage of colony forming MSCs for each donor was calculated and compared. Figure 4-1 shows a representative image of stained CFU-Fs from a diabetic and a non-diabetic donor. Non-diabetic BM-MSCs had an average of  $9.58 \pm 2.42\%$  CFU-Fs, while the mean CFU-Fs from diabetic cells was  $10.07 \pm 6.41\%$ , and this difference was not statistically significant (Figure 4-2).

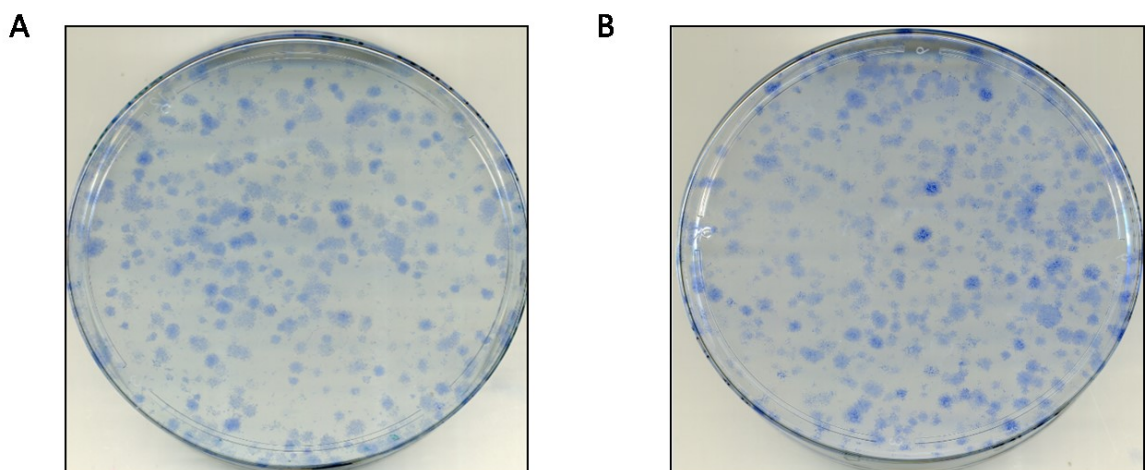


**Figure 4-1: Representative CFU-Fs of early passage BM-MSCs isolated from a non-diabetic (A) and a diabetic donor (B).**

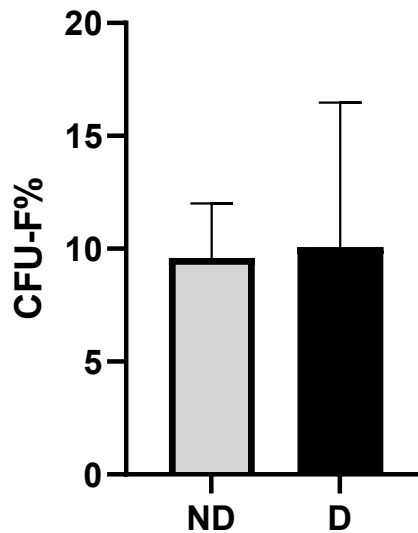


**Figure 4-2: CFU-Fs in non-diabetic (ND) and diabetic (D) early passage BM-MSCs.**

The data are presented as the mean of biological replicates (n=3) ± SD and was analysed using unpaired t test. p=0.91.

#### **4.2.2 Population doubling time (PDT) assay of diabetic and non-diabetic BM-MSCs**

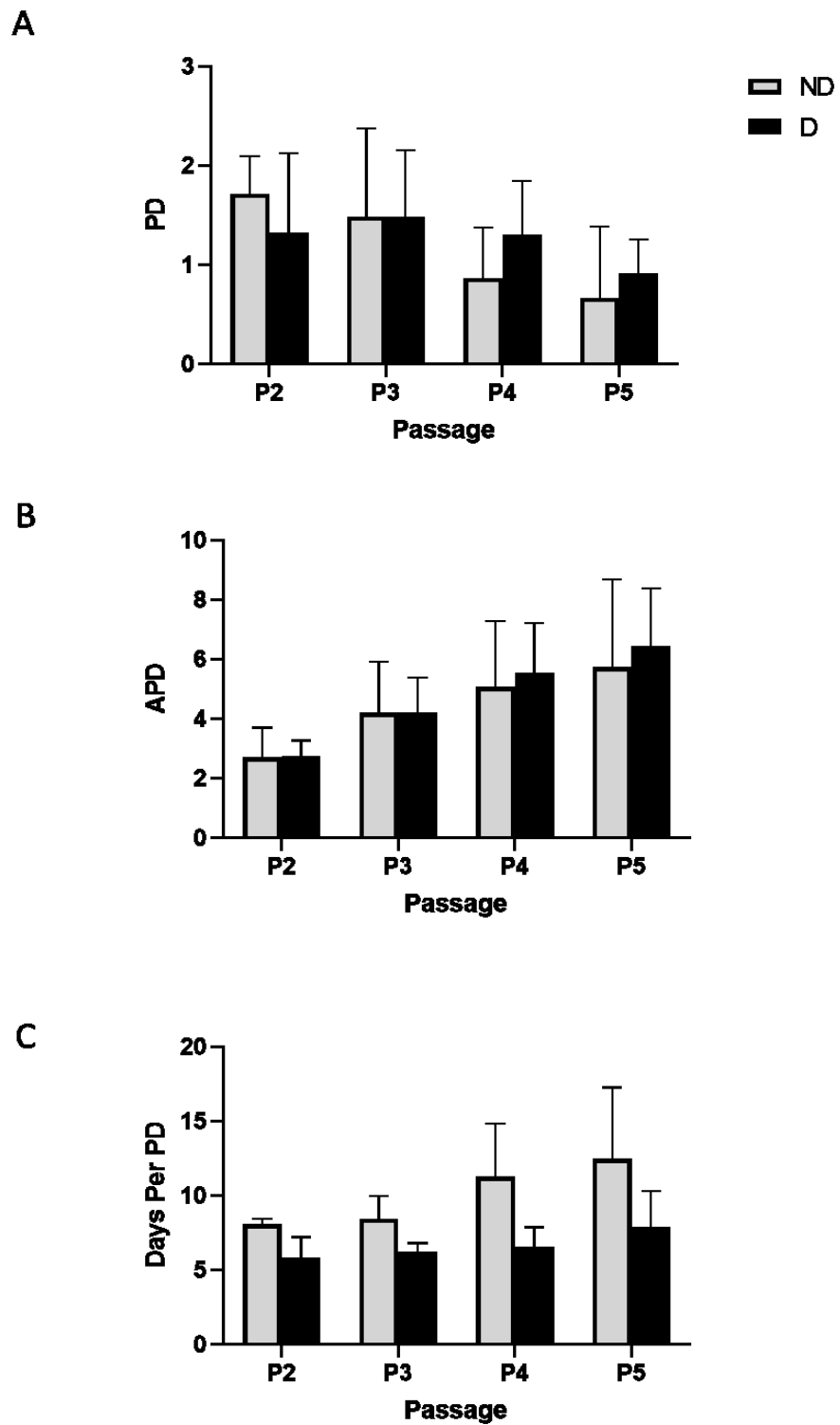
To assess the proliferative capacities and potential impact of passaging on BM-MSCs growth kinetics, cells from diabetic and non-diabetic donors at P1 were seeded in T25 flasks at a density of  $1 \times 10^5$  per flask. Cells were passaged and counted and at each passage, population doubling (PD), accumulative population doubling (APD) and population doubling time (PDT) were calculated, as described in chapter 3 of this thesis.

Table 4-1 shows the means and SDs of PD, APD and PDT at P2:5 for non-diabetic and diabetic BM-MSCs. Figure 4-3 shows PD (A), APD (B) and PDT of non-diabetic and diabetic cells at P 2-5 (C) and none of these differences were statistically significant. Unsurprisingly, there was a trend of reduced PD and increased PDT in P5 versus P2 in both cell populations, indicating relatively lower proliferation rates at later passages.

**Table 4-1: PD, APD and PDT of non-diabetic and diabetic BM-MSCs**

Passage	PD		p value	APD		p value	PDT		p value
	ND (mean $\pm$ SD)	D (mean $\pm$ SD)		ND (mean $\pm$ SD)	D (mean $\pm$ SD)		ND (mean $\pm$ SD)	D (mean $\pm$ SD)	
P2	1.72 $\pm$ 0.38	1.33 $\pm$ 0.79	0.5	2.72 $\pm$ 0.99	2.74 $\pm$ 0.54	0.97	8.1 $\pm$ 0.34	5.82 $\pm$ 1.4	0.1
P3	1.49 $\pm$ 0.89	1.49 $\pm$ 0.66	0.99	4.21 $\pm$ 1.73	4.23 $\pm$ 1.18	0.99	8.45 $\pm$ 1.56	6.24 $\pm$ 0.58	0.12
P4	0.87 $\pm$ 0.51	1.31 $\pm$ 0.54	0.37	5.08 $\pm$ 2.22	5.54 $\pm$ 1.69	0.79	11.28 $\pm$ 3.56	6.58 $\pm$ 1.31	0.14
P5	0.67 $\pm$ 0.72	0.92 $\pm$ 0.34	0.63	5.76 $\pm$ 2.93	6.46 $\pm$ 1.93	0.75	12.48 $\pm$ 4.79	7.91 $\pm$ 2.4	0.24

APD: Accumulative population doubling, D: Diabetic, ND: Non-diabetic, PD: Population doubling, PDT: Population doubling time.



**Figure 4-3: PDT assay of non-diabetic (ND) and diabetic (D) BM-MSCs**

A: Population doubling (PD). B: Accumulative population doubling (APD). C: Population doubling time (PDT). Data presented as mean  $\pm$  SD and was analysed using unpaired t test.

### **4.2.3 Flow cytometric analysis of stem cells surface markers of diabetic and non-diabetic BM-MSCs**

#### **4.2.3.1 Stem cell surface markers expression on non-diabetic and diabetic BM-MSCs**

BM-MSCs from non-diabetic and diabetic donors at P3-5 were cultured under basal conditions until 80% confluent. They were then detached and stained with the antibody panel as described in the chapter 3 of this thesis, to assess the expression pattern of ISCT MSCs surface markers (positive MSCs markers were CD73, CD90 and CD105 and the negative markers were CD14, CD19, CD34, CD45 and HLA-DR). An appropriate compensation matrix was set up using cells and CompBeads and FMOs tubes were used as negative controls to determine the negative population of each antibody used. Cells were analysed using CytoFLEX Lx Flow Cytometer and data was compensated and analysed using CytExpert software.

The dot plot showing FSC versus SSC was used to set up the first gate (P1), whose purpose is to exclude dead cells and debris which typically have lower values of both. Next, viable cells were further gated based on their negative uptake of the FVS (this dye binds to cell surface and intracellular amines, the latter will only be stained where a cellular membrane is permeable, as occurs in dead or dying cells. This increases the fluorescence of non-viable cells). The signal of FVS in the corresponding channel was plotted versus FSC and cells with FVS fluorescence below  $10^5$  were gated as likely viable cells and carried forward in the following analyses (Figure 4-4).

Following the gating described above, the FMO for each antibody was used as the negative control, where gates were placed to include 98% of the FMO cells. Histogram overlays of FMO and the all stained sample were constructed and the proportion of cells falling beyond the FMO gate in the all stained sample was determined as the proportion of cells positively stained with the antibody/fluorophore conjugate (Figure 4-4). This approach was used on cells from all donors, and representative plots are shown from a non-diabetic donor (ND1, Figure 4-5) and a diabetic donor (D2, Figure 4-6). CD73 is shown as an example of a positive marker and CD14 is shown as an example of a negative marker.

Both diabetic and non-diabetic cultures contained substantial populations that expressed the positive markers, CD73, CD90 and CD105, but only contained minimal levels of expression of negative markers CD14, CD19, CD34, CD45 and HLA-DR. Table 4-2 show the proportion of cells expressing each marker in non-diabetic and diabetic BM-MSCs and none of these differences was statistically significant. Figure 4-7 show the percentage of cells expressing each marker in BM-MSCs from non-diabetic and diabetic donors.

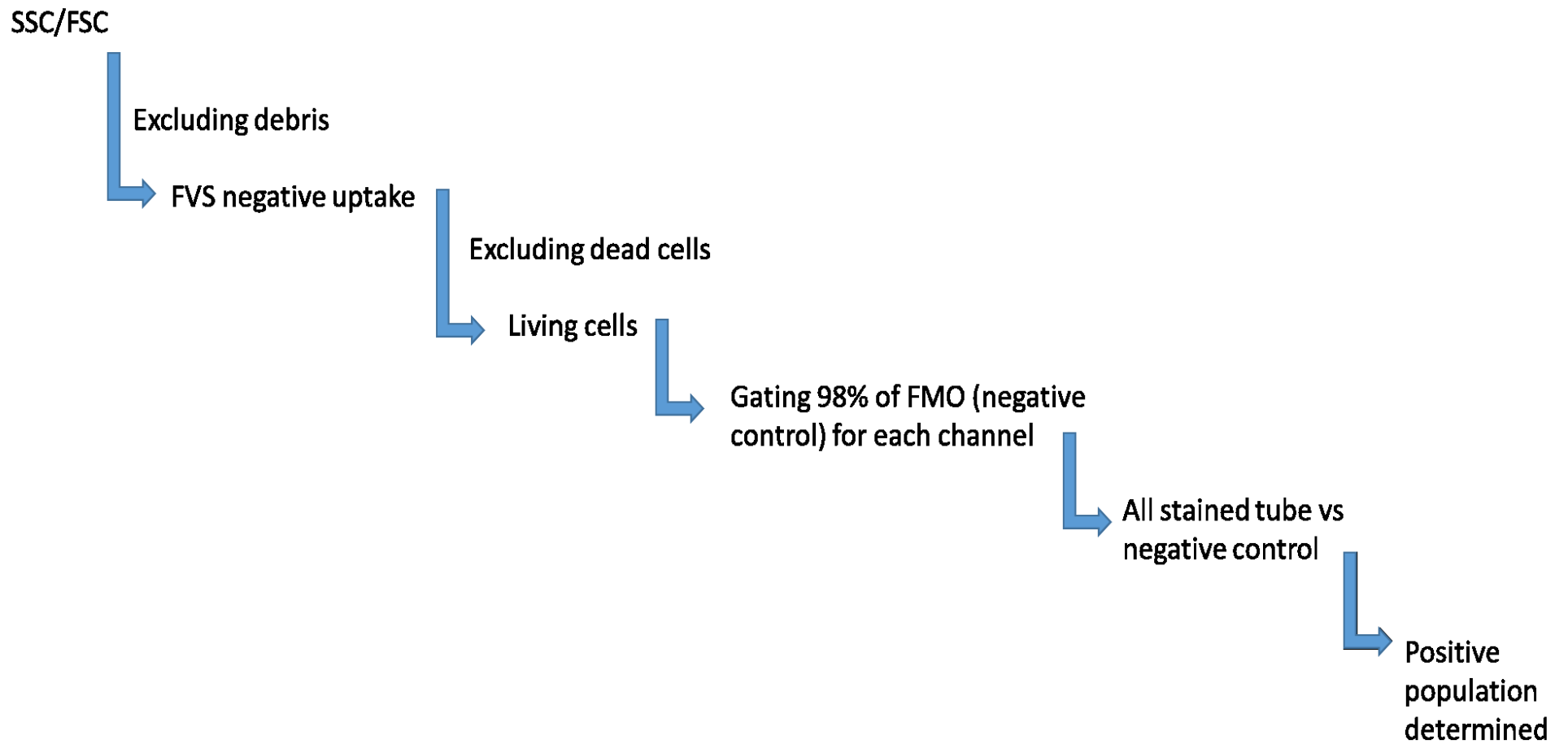


**Figure 4-4: Flow chart showing sequential gating strategy for evaluation of MSCs surface markers expression on BM-MSCs**

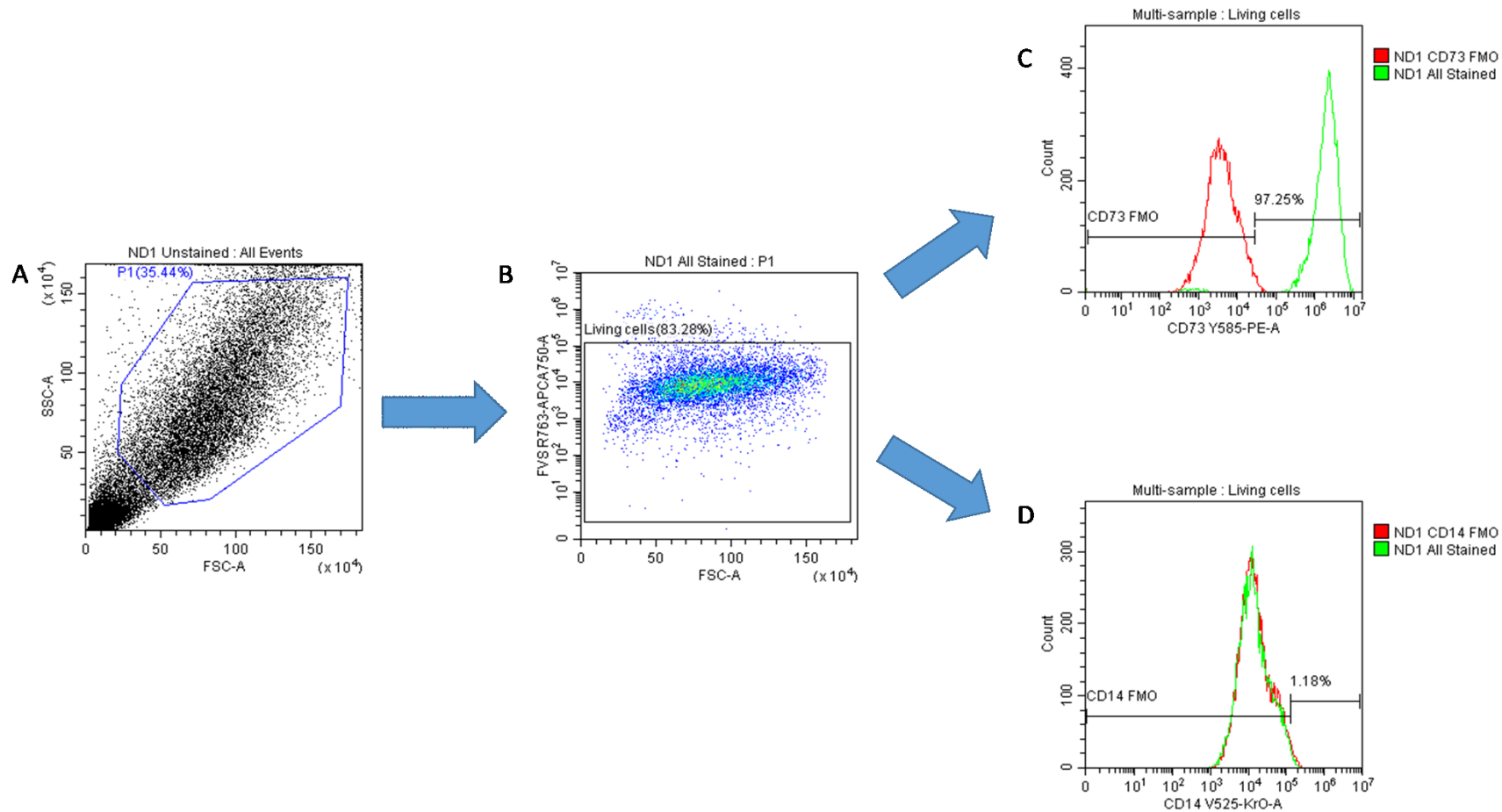


**Figure 4-5: Expression of MSCs surface markers on non-diabetic BM-MSCs**

A: Gating to exclude dead cells and debris based on their forward and side scatter. B: Gating of living cells based on their negative uptake of FVS. C: Expression of CD73 (as an example of a positive MSCs marker) in sample stained with all panel antibodies (all stained cells) relative to FMO control (minus CD73 antibody). The gates were set to include 98% of the FMO control cells. D: Lack of CD14 expression (as an example of a negative MSCs marker) in all stained cells relative to FMO control missing CD14 antibody. The gates were set to include 98% of the FMO control.

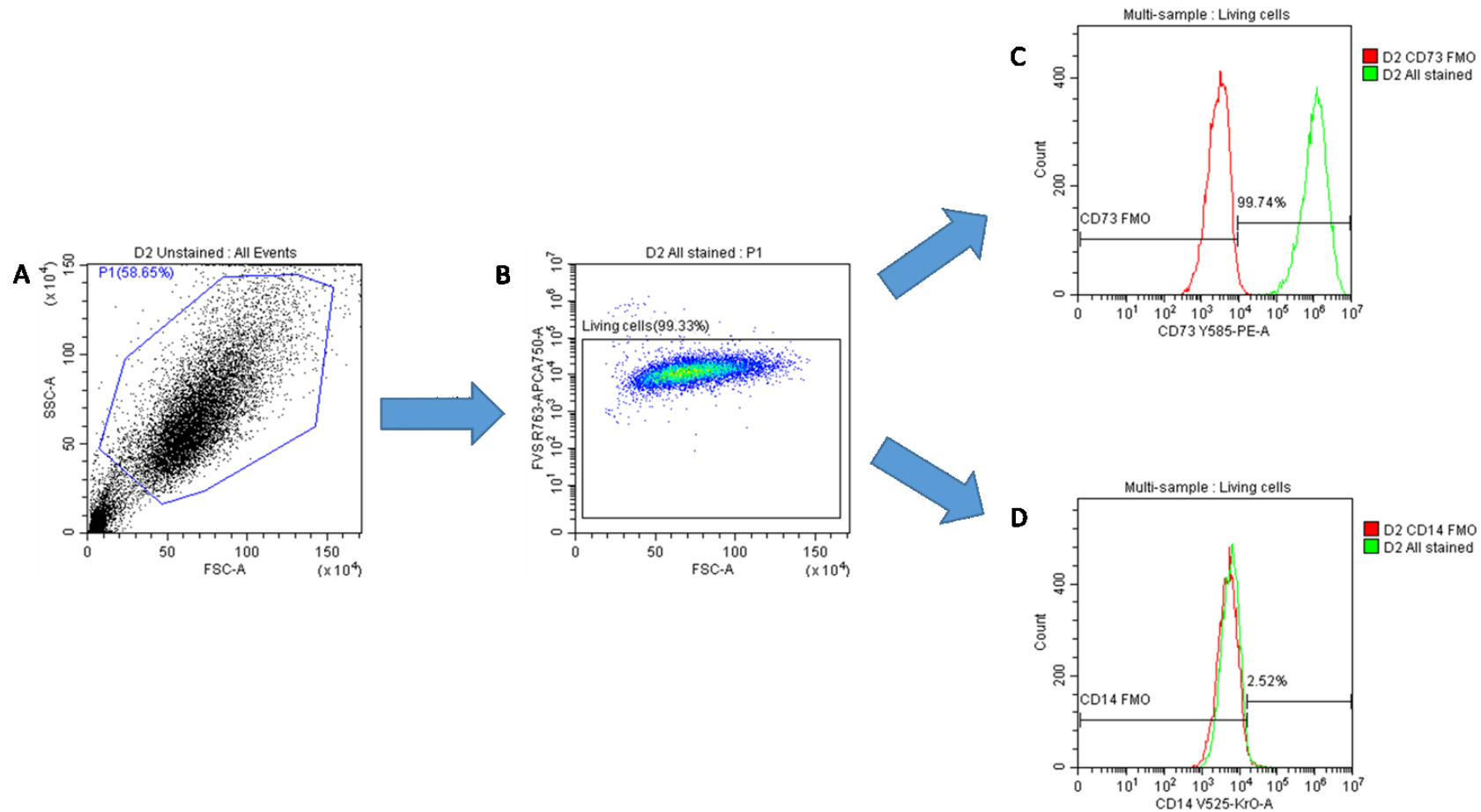


**Figure 4-6: Expression of MSCs surface markers on diabetic BM-MSCs**

A: Gating to exclude dead cells and debris based on their forward and side scatter. B: Gating of living cells based on their negative uptake of FVS. C: Expression of CD73 (as an example of a positive MSCs marker) in all stained cells relative to FMO control missing CD73 antibody. The gates were set to include 98% of the FMO control cells. D: Lack of CD14 expression (as an example of a negative MSCs marker) in all stained cells relative to FMO control missing CD14 antibody. The gates were set to include 98% of the FMO control.

**Table 4-2: Proportions of cells expressing MSCs markers in non-diabetic and diabetic BM-MSCs**

Marker	Non-diabetic (mean $\pm$ SD %)	Diabetic (mean $\pm$ SD %)	p value
CD73	96.58 $\pm$ 3.49	99.22 $\pm$ 0.71	0.32
CD90	95.42 $\pm$ 3.7	98.11 $\pm$ 1.08	0.33
CD105	90.2 $\pm$ 9.58	97.05 $\pm$ 4.18	0.34
CD14	3.09 $\pm$ 2.32	2.07 $\pm$ 0.51	0.53
CD19	4.03 $\pm$ 2.52	3.65 $\pm$ 2.72	0.87
CD34	3.54 $\pm$ 2.38	5.2 $\pm$ 4.61	0.62
CD45	1.42 $\pm$ 0.3	2.27 $\pm$ 1.08	0.3
HLA-DR	1.28 $\pm$ 0.32	2.42 $\pm$ 0.87	0.14

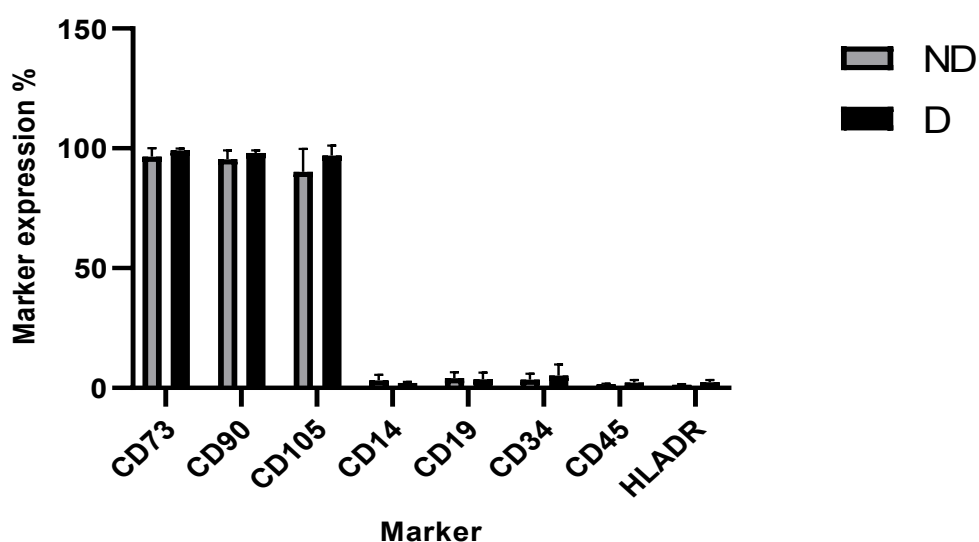


**Figure 4-7: Expression of MSCs surface markers on non-diabetic (ND) and diabetic (D) BM-MSCs.**

Data presented as mean  $\pm$  SD (n=3) and was analysed using unpaired t test.

#### **4.2.3.2 Identification and enumeration of MSCs populations in non-diabetic and diabetic BM-MSCs based on their phenotype**

BM-MSCs cultures from non-diabetic and diabetic donors were compared regarding the population of cells that fulfil the ISCT criteria for MSCs identification (177). Since MSCs would typically express all of the positive markers and none of the negative markers, a hierarchical gating strategy using dot plots was used as shown in Figure 4-8. Cells positive for both CD73 and CD90 were gated and carried forward to be analysed and further gated based on expression of CD105, in the absence of CD14 expression. This analytical approach was performed sequentially where cells were then subjected to further gating set up to select cells that were negative for CD19, CD34, CD45 and HLA-DR and ultimately the proportion of MSCs population relative to living cells was calculated. This scheme was used with both non-diabetic cells (donor ND1 as a representation is shown in Figure 4-9) and diabetic cells as well (donor D2 as a representation is shown in Figure 4-10). Non-diabetic cells included  $82.88 \pm 7.28\%$  MSCs while diabetic cells included  $94.02 \pm 1.5 \%$  MSCs and this difference was not statistically significant (Figure 4-11).

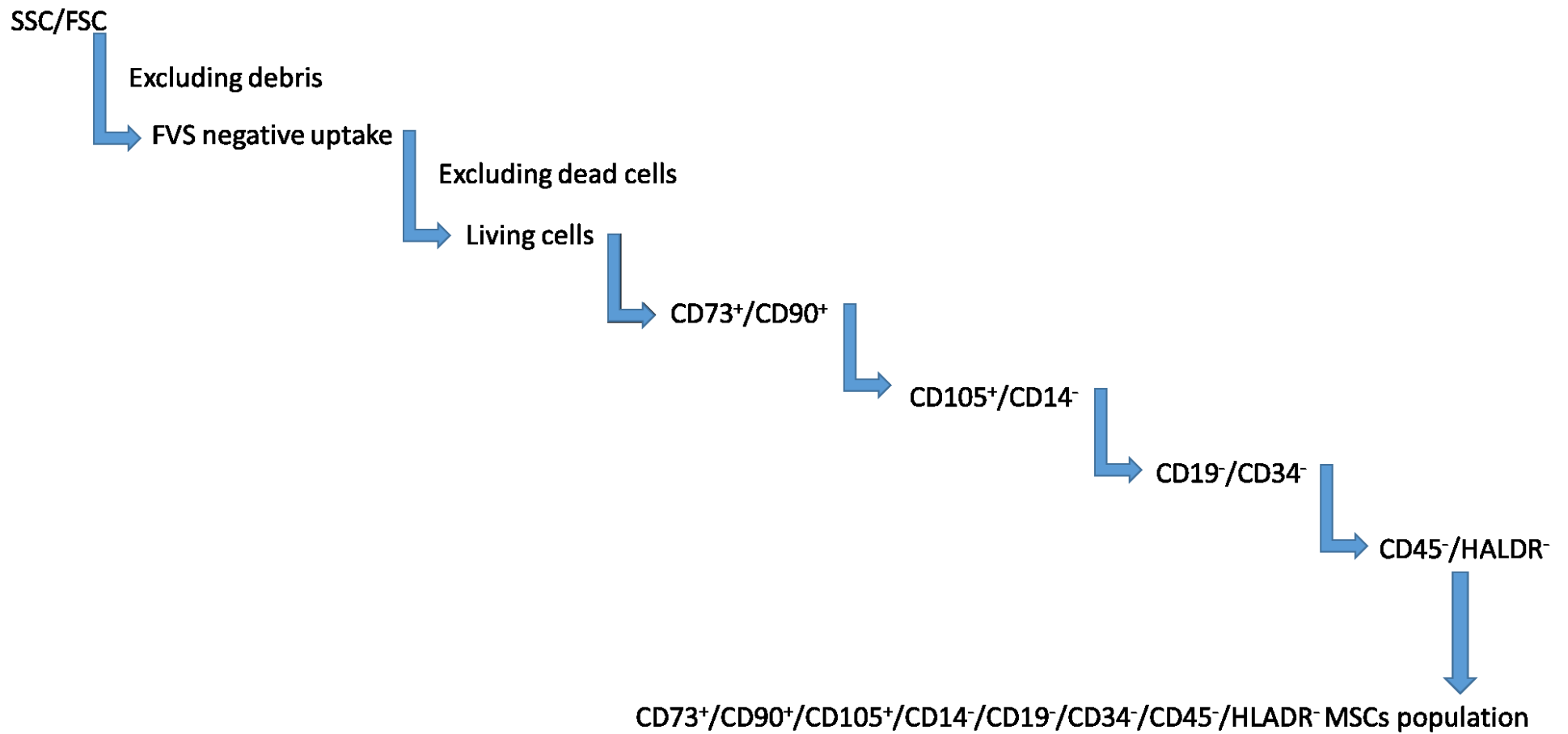
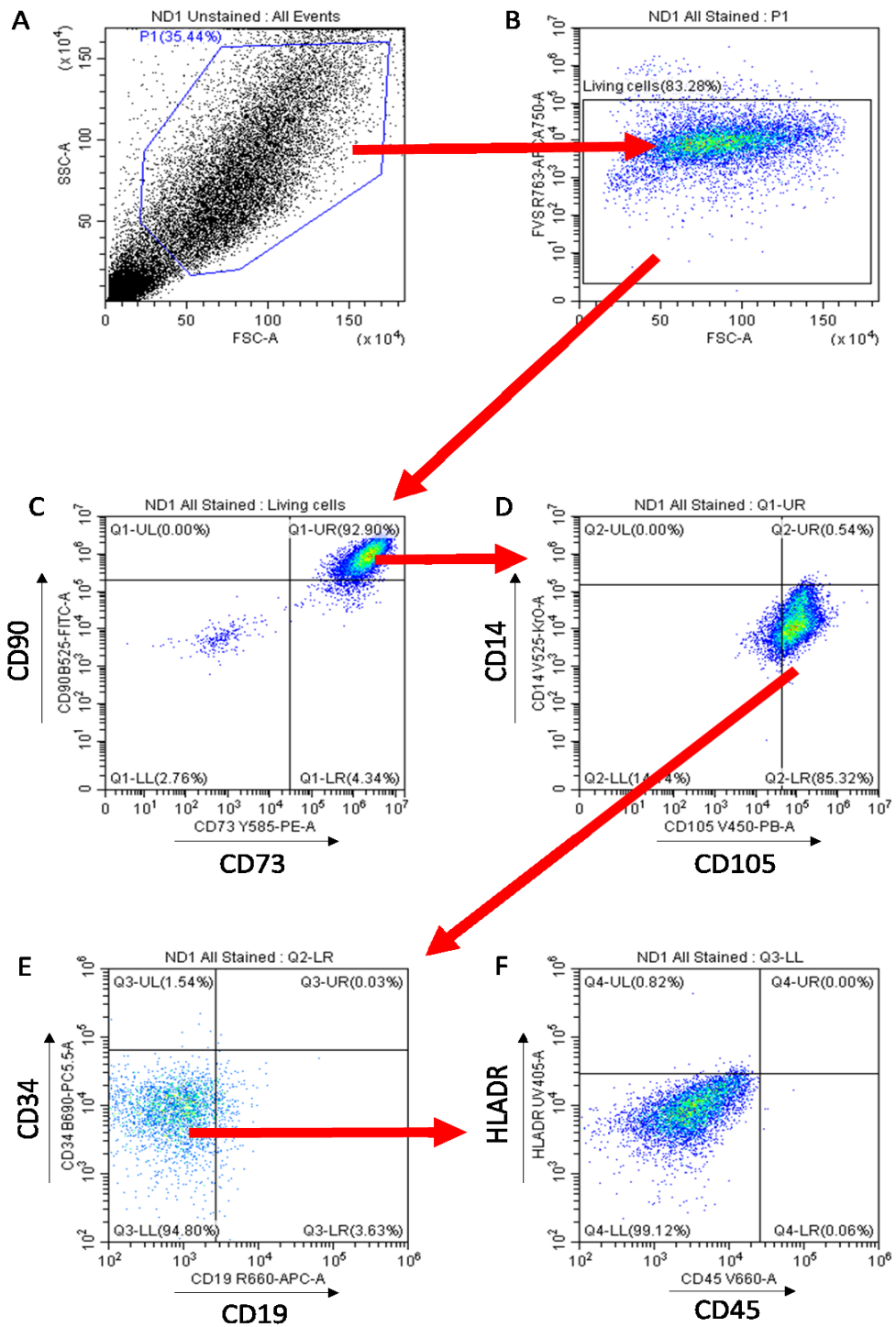
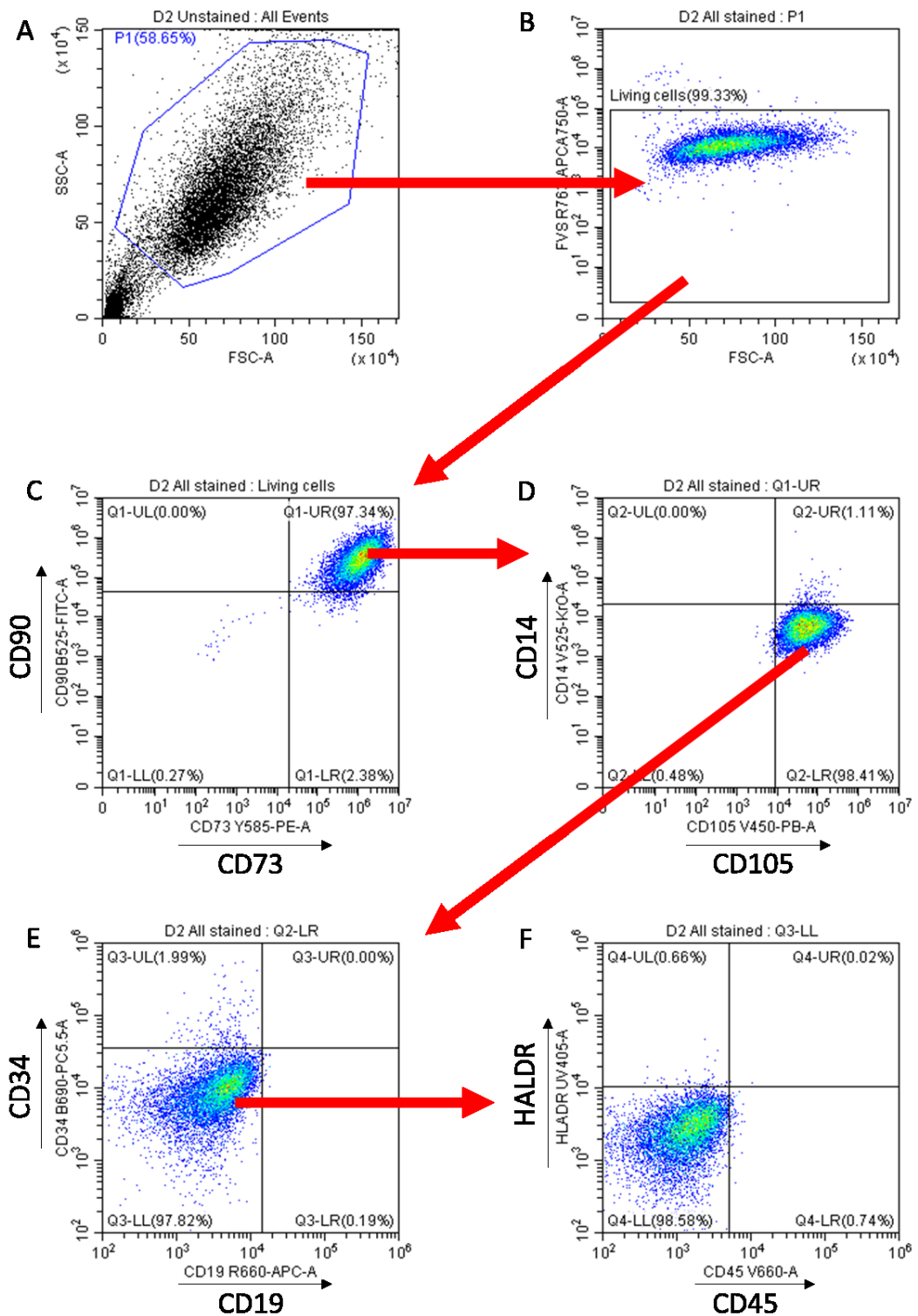


Figure 4-8: Flow chart showing gating strategy for MSCs enumeration in non-diabetic and diabetic BM-MSC.



**Figure 4-9: Sequential gating for enumeration of MSCs population in non-diabetic BM-MSCs**

A: Gating to exclude dead cells and debris based on their forward and side scatter. B: Gating to include living cells based on their negative uptake of FVS. C: Gating to include CD73<sup>+</sup>CD90<sup>+</sup> cells in quadrant Q1-UR. D: gating to include CD73<sup>+</sup>CD90<sup>+</sup>CD105<sup>+</sup>CD14<sup>-</sup> cells in quadrant Q2-LR. E: Gating to include CD73<sup>+</sup>CD90<sup>+</sup>CD105<sup>+</sup>CD14<sup>-</sup>CD19<sup>-</sup>CD34<sup>-</sup> cells in quadrant Q3-LL. F: Gating to include CD73<sup>+</sup>CD90<sup>+</sup>CD105<sup>+</sup>CD14<sup>-</sup>CD19<sup>-</sup>CD34<sup>-</sup>CD45<sup>-</sup>HLA-DR<sup>-</sup> cells in quadrant Q4-LL.



**Figure 4-10: Sequential gating for enumeration of MSCs population in diabetic BM-MSCs**

A: Gating to exclude dead cells and debris based on their forward and side scatter. B: Gating to include living cells based on their negative uptake of FVS. C: Gating to include CD73<sup>+</sup>CD90<sup>+</sup> cells in quadrant Q1-UR. D: gating to include CD73<sup>+</sup>CD90<sup>+</sup>CD105<sup>+</sup>CD14<sup>-</sup> cells in quadrant Q2-LR. E: Gating to include CD73<sup>+</sup>CD90<sup>+</sup>CD105<sup>+</sup>CD14<sup>-</sup>CD19<sup>-</sup>CD34<sup>-</sup> cells in quadrant Q3-LL. F: Gating to include CD73<sup>+</sup>CD90<sup>+</sup>CD105<sup>+</sup>CD14<sup>-</sup>CD19<sup>-</sup>CD34<sup>-</sup>CD45<sup>-</sup>HLA-DR<sup>-</sup> cells in quadrant Q4-LL.

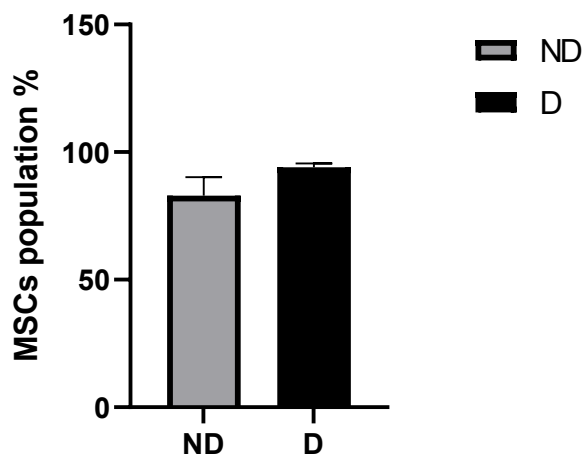


**Figure 4-11: MSCs enumeration in non-diabetic (ND) and diabetic (D) BM-MSCs**

Data presented as mean  $\pm$  SD (n=3) and was analysed using unpaired t test,  $p = 0.11$ .

### 4.3 Discussion

The results presented in this chapter show that both diabetic and non-diabetic BM-MSCs have similar clonogenic and proliferative capacities. CFU-Fs assay have been used for decades to quantify MSCs from different tissue sources, including bone marrow aspirates (BMA) (445) and early passage cultured BM-MSCs (446), with the latter approach reporting higher counts of CFU-Fs compared to uncultured fresh tissue digests. The presented data showed there was no significant difference in number of CFU-Fs in both cell types (Figure 4-2), which agrees with previous reports (246,249). In one report, BM-MSCs count in BMA, following density gradient centrifugation, from diabetics and non-diabetics was comparable (247) which is also in harmony with the presented findings.

Nonetheless, reduced CFU-Fs and CFU-Os in diabetic BM-MSCs compared to non-diabetics has been reported by Cassidy et al. (248). A possible explanation for this discrepancy is BM-MSCs source and isolation technique. While BM-MSCs in this thesis were isolated from OA knee joints using enzymatic digestion, BM-MSCs in the aforementioned study were isolated from BM of femoral necks of patients undergoing hip replacement surgery. Moreover, in our study diabetic patients had age range of 81-85 yrs and non-diabetics of 64-86 yrs. Cassidy et al (248) recruited diabetic donors with age range of 57-91 yrs and non-diabetics of 51-89 yrs. It is possible that the cohort included in the present study experienced age dependant decline in CFU-Fs due to their relatively older age as reported

elsewhere (446,447). This decline could have 'masked' any changes potentially attributed to the donors' diabetic status.

Moreover, the CFU-Fs in this thesis used early passage BM-MSCs which were cultured for 14 days as reported earlier (424,448), and the results were reported as a percentage of seeded cells. Cassidy et al. (248) cultured their CFU-Fs and CFU-Os using fresh BM aliquots for 8-10 days and reported their results per 100,000 mononuclear cells (MNCs). It is possible that this relatively shorter duration of both assays and the use of fresh BM rather than passaged cells allowed Cassidy et al. (248) to 'pick up' minor differences between diabetic and non-diabetic cells.

The presented results indicated no difference in PD, APD or PDT in diabetic versus non-diabetic BM-MSCs (Figure 4-3), and these findings were supported by literature showing similar outcomes (245,247,248). Brewster et al. (246) reported reduced proliferation of ischemic and ischemic/diabetic BM-MSCs compared to healthy controls, but no differences in APD between ischemic and ischemic/diabetic cells, which is also comparable to our results. Thus, consensus opinion seems to support that T2DM is unlikely to influence BM-MSCs growth kinetics.

In contrast, BM-MSCs cultured under HG or other diabetic simulation conditions showed significantly lower proliferation capacities (268,273,275). This could indicate that such changes are related to MSCs environment rather than inherent alterations in diabetic cells. HG culture conditions possibly use excessive levels of glucose that may be much higher than those present physiologically in diabetics (256) and do not fully or accurately replicate the complicated type 2 diabetic microenvironment that entails hyperglycaemia, hyperlipidaemia, hyperinsulinemia, inflammatory cytokines, hypoxia, AGES and ROS (253) as detailed in chapter 1 of this thesis.

Nevertheless, one study has shown initial higher proliferation rates of BM-MSCs cultured under simulated diabetes/periodontitis conditions (HG and LPS), followed by sustained reduced proliferation as a result of the cytotoxic effects of LPS (271). Another study showed that serum of T2DM patients with 8-10% HbA1c concentrations boosted BM-MSCs proliferation compared to non-diabetic serum with <6.5% HbA1c with authors suggesting that a certain degree of hyperglycaemia could induce BM-MSCs proliferation. On the other hand, serum

with >10% HbA1c concentrations typically seen in poorly controlled diabetics considerably reduced BM-MSCs proliferation rates (276).

Both diabetic and non-diabetic cells in this study showed steady decline in proliferation over passaging and this also is consistent with previous reports (247). Indeed, BM-MSCs extensive culture and passaging can be considered *in vitro* aging, possibly leading to cells senescence and reduced proliferation due to decline of fast dividing cells (449). Zhang et al. (450) noted increased senescent phenotype in diabetic BM-MSCs using senescence-associated  $\beta$ -galactosidase (SA- $\beta$ -Gal) staining, and a similar conclusion was made using BM-MSCs cultured under HG (268). Yin et al. (451) in a recent review discussed possible mechanisms through which hyperglycaemia can induce senescence in MSCs, including mitochondrial dysfunction, oxidative stress and telomere attrition (451).

The expression of MSCs surface markers was assessed using multi-parameter flow cytometric immunophenotyping and the presented data show that both diabetic and non-diabetic viable BM-MSCs included similar and relatively high proportions of MSCs, which expressed positive and negative markers at comparable levels. This set of experiments used a multi-parameter flow cytometry panel consisting of 8 antibody/fluorophore conjugates and a FVS as described in chapter 3 of this thesis. These conjugates were selected to minimize the risks of spectral overlap and the need for subsequent compensation. Factors considered in this process included fluorophores brightness and excitation and emission spectra and whether they were conjugated to antibody detecting a positive (abundantly expressed on MSCs) or negative marker (scarcely expressed) was also considered. The FVS used in this panel is an amine binding dye that would be taken up by dead cells because of their permeable plasma membranes as described earlier in this chapter. This type of dyes can be advantageous over DNA binding dyes which could 'leak' of stained cells leading to some signal loss (452).

CD73, CD90 and CD14 expression patterns in diabetic BM-MSCs in this study were similar to those reported by Phadnis et al. (244). However, their study reported lower levels of CD105 expression ( $\sim 37.6 \pm 15.56\%$ ) and higher levels of CD34 ( $< 17.4 \pm 8.14\%$ ) and CD45 ( $< 26.9 \pm 12.92\%$ ) expression, possibly indicating an overall lower proportion of cells that fulfilled the MSC criteria in their samples. This could be due to differences of recruited donors of BM-MSCs in

both studies: Phadnis et al. (244) isolated BM-MSCs from the sternum of T2DM patients undergoing cardiac bypass surgery, with age range 15-85 yrs old. The BM-MSCs in the current study were isolated from OA knee joints of T2DM patients undergoing joint replacement surgery, with age range of 81-85 yrs. Moreover, the sternal BM-MSCs were isolated using mechanical disruption of BMA, followed by density gradient separation, as opposed to here, where BM-MSCs were isolated using enzymatic digestion of cancellous bone chips from the excised knee joints. Although BM-MSCs from iliac crest and vertebral body of the same donor have shown variable osteogenic potentials, still they expressed similar levels of CD34, CD90 and CD105 (453). This means that anatomical site may not influence MSCs expression profiles dramatically.

Another explanation that could be considered but unlikely to be influential is the above mentioned difference in age range of BM-MSCs donors in this thesis compared to Phadnis et al. (244). Although ageing is known to negatively influence BM-MSCs numbers and proliferation rates (454), BM-MSCs from elderly and younger donors showed no difference in their phenotypes (247). Indeed, the MSCs surface markers assessed in this thesis are known to be relatively stable, with no apparent influence of aging on their expression patterns unlike other markers, such as CD106 or CD146, which can show variable expression patterns (454).

The presented results are also similar to those reported by Gabr et al. (245), who reported similar expression levels of MSCs markers in diabetic and non-diabetic BM-MSCs. Although they did not isolate their cells from knee joints as was performed in this study (the diabetic BM-MSCs were from BMA of iliac crest, while the non-diabetic cells were harvested from BMA during hip replacement surgery), it seems that in this instance the variable isolation site and method did not influence the expression patterns of isolated cells. The presented results also fall within the same range as those reported by Andrzejewska et al. (247), where both diabetic and non-diabetic BM-MSCs expressed similar levels of MSCs markers. The authors isolated the cells from metaphyseal BM biopsies of patients undergoing hip replacement surgery, and it was passaging (*in vitro* aging) that lead to a weak decrease in CD105 expression in both diabetic and non-diabetic cells with no impact attributed to the diabetic status. The current findings also agree with those of Cassidy et al. (248), where both diabetic and non-diabetic

BM-MSCs fit the aforementioned MSCs phenotype with no significant differences.

Brewster et al. (246) compared the MSCs markers expression in healthy, ischemic and ischemic diabetic BM-MSCs, cultured in media with FBS and platelet lysate. The authors reported their results as mean fluorescent intensity, which makes it challenging and inconsistent to make comparisons to the current findings described as proportion of positive markers expression relative to FMO controls. There were no identifiable differences between both media types and differences between the 3 cells populations investigated were not reported, although they all fitted the expected MSCs expression patterns (246).

It could be argued that osteoarthritic status of the knee joints used in the present study could have influenced the BM-MSCs expression pattern of MSCs surface markers. Although OA influences all components of the joint, including subchondral bone (455), its impact on expression of MSCs markers on BM-MSCs from OA joints is not fully established. One report comparing BM-MSCs from healthy and osteoarthritic hip joints found that all MSCs surface markers were similarly expressed except for increased CD90 and reduced CD166 expression in OA cells. Other markers had comparable expression levels in OA and healthy cells, indicating similar MSCs phenotype (456). Another study on BM-MSCs from talus and distal tibia of OA ankle joints as well as BM-MSCs from 'healthy' iliac crest, were all 95% or more positive for MSCs positive markers and 3% or less positive for MSCs negative markers (444).

It is worth mentioning that while Phadnis et al. (244), Gabr et al. (245) and Brewster et al. (246) used isotype controls to gate the negative populations, this thesis used FMO controls. FMO controls account for background staining resulting from spillover and control for interactions between multiple antibodies used simultaneously, thus is more relevant and increasingly used in complex multi-parameter flow cytometric immunophenotyping. While isotype controls on the other hand has been extensively used to address background staining attributed to non-specific binding to Fc receptors (457), the staining protocol followed in this thesis used Fc block which would act to minimise non-specific binding via interaction with Fc receptors. Because of the number of antibody/fluorophores conjugates used in the present study, FMO controls were judged to be more appropriate compared to isotype controls. Additionally,

including the all stained sample in this thesis allowed for true multi-parameter phenotyping where cells were stained for all the markers within one sample to confirm concurrent expression of all the markers in the same cell preparation.

Different studies cultured BM-MSCs under normoglycemic and simulated diabetic conditions, as detailed in chapter 1 of this thesis with some of these studies running flow cytometric analysis only on cells grown under normoglycemic media for confirmation of MSCs phenotype prior to further experiments (275). However, none of these evaluated the expression patterns following exposure to diabetic culture conditions. Interestingly, one study compared early versus late passage BM-MSCs, subcutaneous and omentum AT-MSCs under HG conditions. For all included cell types, there was no significant change in expression patterns in later passages compared to early ones, with positive MSCs markers generally expressed at + 90% and negative MSCs markers expressed generally at – 20%. The fact that the 3 cell types maintained their phenotype even under extensive culture in HG was interesting, but the lack of normoglycemic cultures as controls does not give the full picture (270).

In general, MSCs of different sources including BM-MSCs and AT-MSCs have shown no difference between diabetic and non-diabetic cells regarding their phenotype, as Mahmoud et al. (7) have elaborated in their extensive review on diabetic MSCs. Nevertheless, there are some isolated reports of altered expression patterns attributed to diabetes. For instance, diabetic AT-MSCs showed higher expression levels of CD90 and CD105, coupled with upregulation of Nanog and Oct-4 compared to non-diabetic cells. Because the MSCs niche is under strict control of different factors striking a fine balance between self-renewal and differentiation, the authors suggest that the diabetic microenvironment could have 'skewed' the MSCs into a self-renewal or a 'de-differentiated' status, leading to this overexpression of stemness markers (458).

All the above mentioned studies compared expression of MSCs surface markers in diabetic and non-diabetic BM-MSCs. However, they did not include MSCs enumeration based on the hierarchical expression of these markers as described in this chapter. This approach uses the data already collected in flow cytometric analysis of MSCs surface markers expression, but with a few extra steps of analysis. Such methodology was described in the work by Alkharobi et al. (459), who compared DPSCs from sound and carious teeth using 3 positive (CD90,

CD105 and CD146) and 2 negative (CD31, CD45) MSCs markers. Herein, a total of 8 markers (3 positive and 5 negative markers) were used as recommended by the ISCT as minimal criteria to define MSCs. This is particularly important for BM-MSCs identification to exclude blood cells and hematopoietic stem cells that the bone marrow normally harbours (177). While this thesis concluded that non-diabetic BM-MSCs contained  $82.88 \pm 7.28\%$  MSCs population compared to  $94.02 \pm 1.5\%$  in diabetic cells, Alkharobi et al. (459) reported much lower proportions with DPSCs from carious teeth expressed including  $34 \pm 16.6\%$  MSCs population compared with  $18.5 \pm 19.3\%$  in 'healthy' DPSCs. As mentioned above, Alkharobi et al. (459) used DPSCs with a different panel to the one employed in this thesis and encountered considerable variation in CD146 expression.

Flow cytometry based MSCs enumeration and sorting has been repeatedly reported in the literature using a variety of antibody/fluorophore conjugates. For instance, BM-MSCs were enriched based on their positive expression of D7-FIB (a fibroblast marker) and then  $CD45^{low}$  D7-FIB<sup>+</sup> LNGFR<sup>+</sup> (LNGFR or CD271 is low affinity nerve growth factor receptor) population was enumerated within the enriched cells (447). Moreover, BM-MSCs were purified as  $CD45^{low}/CD271^{+}$  cells using FACS (419,421,460,461). Both procedures are used to enrich uncultured BM-MSCs, which is different to the approach utilized in this thesis. However, to the best of my knowledge, the work described in this thesis should be the first attempt to use flow cytometry based MSCs enumeration with passaged human diabetic BM-MSCs. It would be interesting to employ the  $CD45^{low}/CD271^{+}$  cells sorting and enumeration with uncultured diabetic BM-MSCs and further examine their regenerative potentials as outlined later in the General Discussion chapter of this thesis.

## Chapter 5 Results

### Osteogenic differentiation of diabetic and non-diabetic BM- MSCs with a vision for periodontal regeneration

#### 5.1 Introduction

BM-MSCs have been the subject of several clinical trials for bone regeneration (209). A phase I/II study where autologous BM-MSCs were transplanted to infrabony periodontal defects has shown that they improved probing depth, tooth mobility and linear bone growth without safety issues (217). Autologous BM-MSCs could be a promising approach for periodontal regeneration in T2DM patients as well, but evidence relating to possible impact of T2DM on the osteogenic potentials of these cells is still inconclusive (7).

The aim of this chapter is to evaluate the osteogenic differentiation potentials and expression of periodontal markers in diabetic and non-diabetic BM-MSCs under osteogenic and basal culture conditions. This was assessed at 3 different time-points (1, 2 and 3 weeks) using ALP stain and AR stain and quantification. Moreover, qPCR analysis was carried out for evaluation of relative changes of gene expression of osteogenic markers (*ALPL*, *RUNX2* and *OCN*), periodontal fibroblasts differentiation markers (*COL1* and *POSTN*) and cementoblasts differentiation markers (*CEMP-1*). In addition, expression of *OPG*, *RANKL* and *OPG/RANKL* ratios were investigated to evaluate bone deposition/resorption homeostasis in the isolated cells.

## **5.2 Results**

### **5.2.1 Alkaline phosphatase (ALP) staining of diabetic and non-diabetic BM-MSCs cultured under basal and osteogenic conditions**

ALP is an enzyme converting organic phosphates to inorganic phosphates and serves as a fairly early marker of osteogenic differentiation (462). Diabetic and non-diabetic BM-MSCs (n=3 for each group) were cultured under basal and osteogenic conditions for 3 different durations, fixed and stained with ALP stain as described in chapter 3 of this thesis. ALP staining intensity of both diabetic and non-diabetic BM-MSCs cultured under basal conditions showed a subtle increase as culture duration increased from 1 to 3 weeks. At each time-point, the staining of diabetic BM-MSCs was weaker than that of non-diabetic BM-MSCs (One donor from each group is represented in Figure 5-1). Under osteogenic conditions, a similar pattern was observed albeit with an accentuated overall staining intensity compared to basal cultures (One donor from each group is represented in Figure 5-2). There was also increased cell density/confluence in osteogenic versus basal cultures, most notably at the Wk3 time-point.

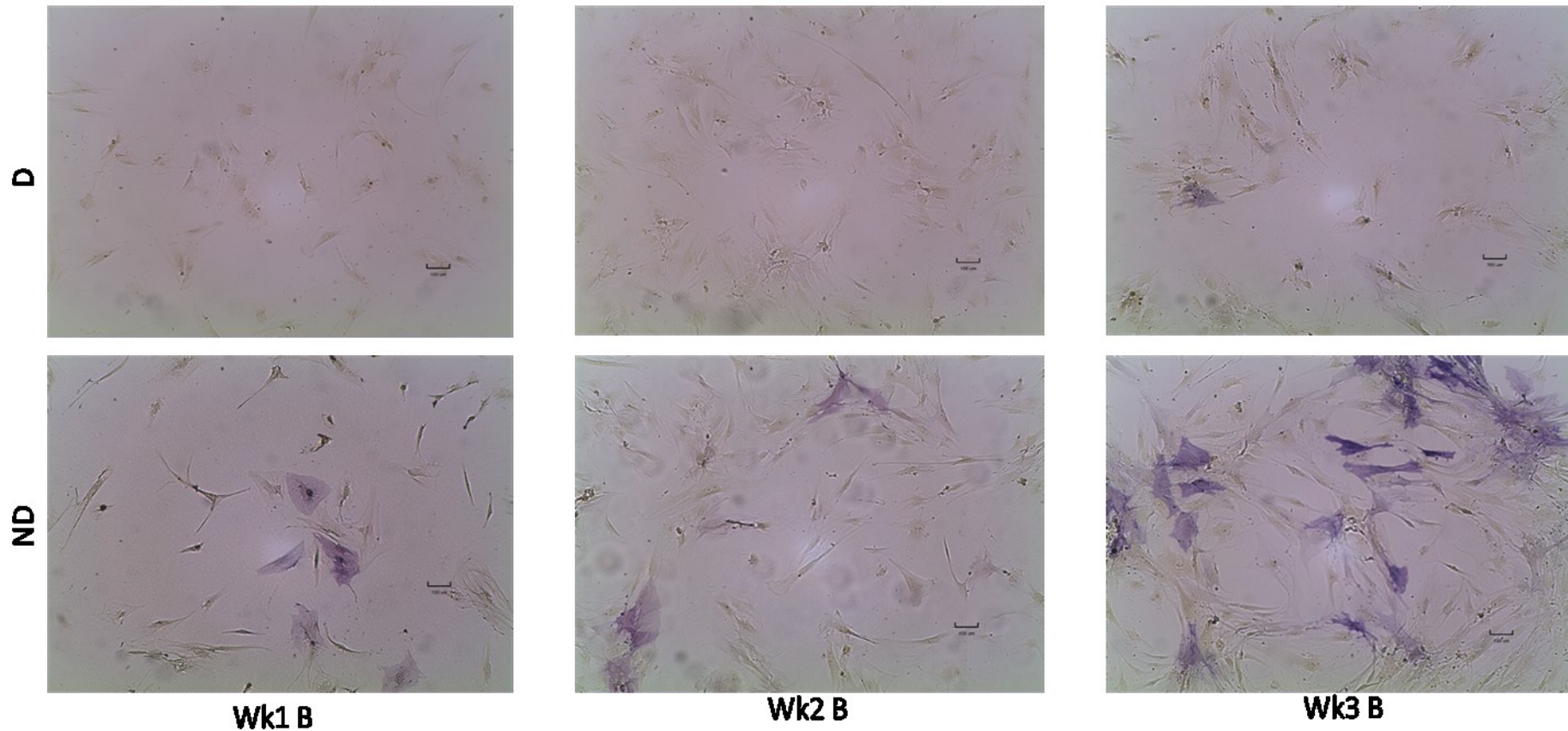


**Figure 5-1: BM-MSCs from diabetic (D) and non-diabetic (ND) donors cultured under basal (B) conditions and stained with alkaline phosphatase stain at Wk1, Wk2 and Wk3 time-points**

Scale bar = 100  $\mu$ m. One donor from each group is represented.

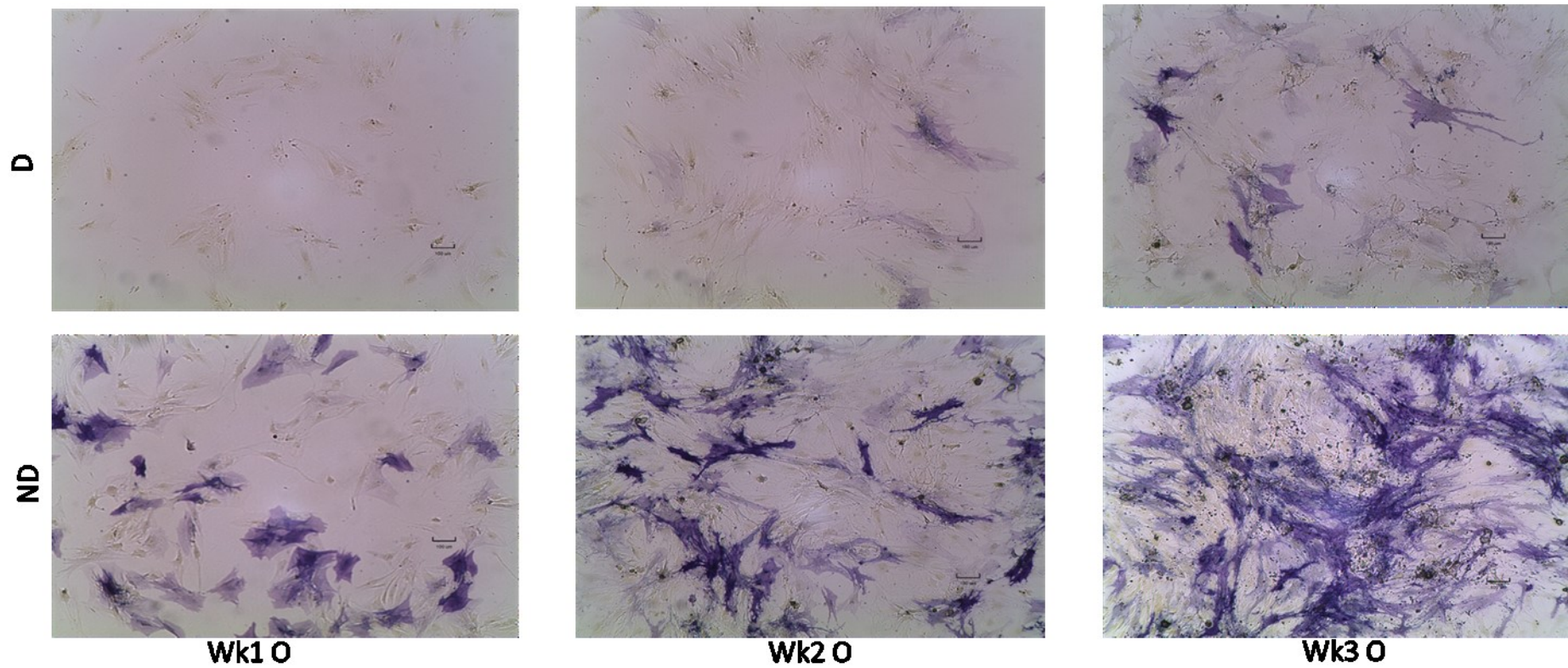


**Figure 5-2: BM-MSCs from diabetic (D) and non-diabetic (ND) donors cultured under osteogenic (O) conditions and stained with alkaline phosphatase stain at Wk1, Wk2 and Wk3 time-points**

Scale bar = 100  $\mu$ m. One donor from each group is represented.

### **5.2.2 Alizarin Red (AR) staining and quantification of calcified nodules in diabetic and non-diabetic BM-MSCs cultured under basal and osteogenic conditions**

Diabetic and non-diabetic BM-MSCs (n=3 for each group) cultured under basal and osteogenic conditions in technical triplicates were stained with AR stain at time-points 1, 2 and 3 weeks as described in chapter 3 (Figure 5-3 and Figure 5-4, each with representative images of one donor from each group). The results show higher staining intensity in osteogenic versus basal media which is subtle in Wk1 but tends to be more distinguishable in Wk2 and Wk3 cultures.

AR stain quantification showed a statistically significant higher mineralization in basal cultures of diabetic BM-MSCs at Wk3 versus Wk1 ( $p=0.0009$ ) and at Wk3 versus Wk2 ( $p=0.0039$ ). Diabetic cells also showed a statistically significant higher calcification in osteogenic cultures versus basal cultures at Wk1 ( $p=0.0042$ ) and at Wk2 ( $p=0.0052$ ). A similar pattern was observed in non-diabetic cells at Wk3 ( $p=0.0373$ ). There was, however, no significant differences between non-diabetic and diabetic cells at the different time-points/culture conditions (Figure 5-5).

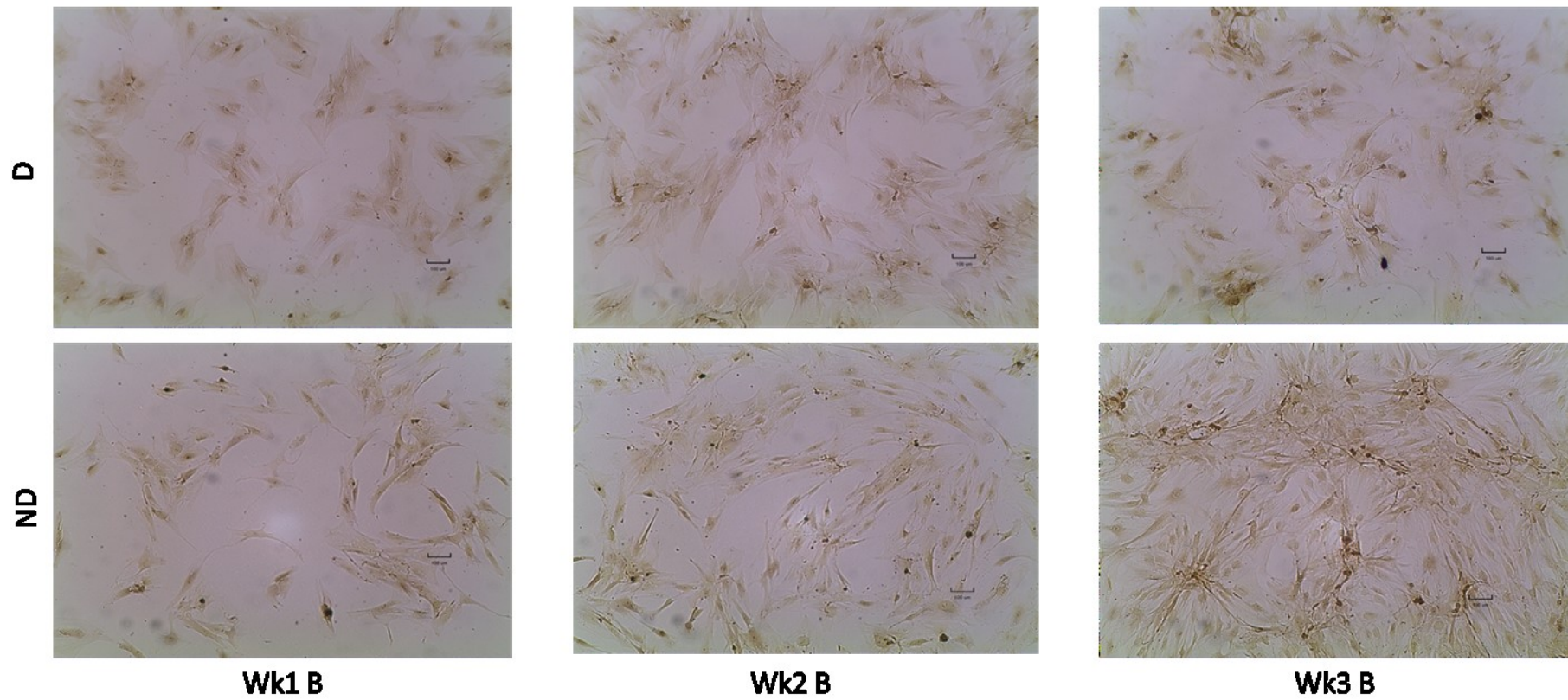


**Figure 5-3: BM-MSCs from diabetic (D) and non-diabetic (ND) donors cultured under basal (B) conditions and stained with Alizarin Red stain at Wk1, Wk2 and Wk3 time-points**

Scale bar = 100  $\mu$ m. One donor from each group is represented.

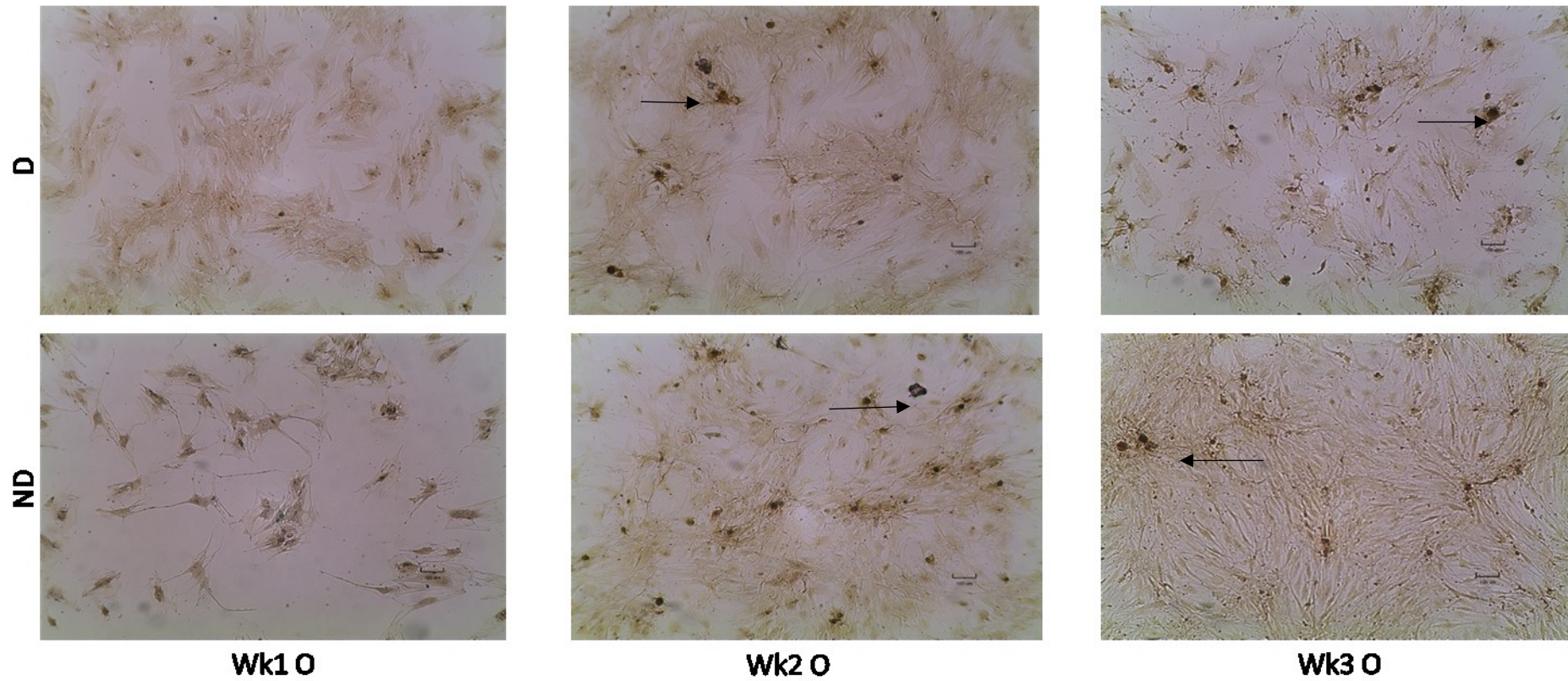


**Figure 5-4: BM-MSCs from diabetic (D) and non-diabetic (ND) donors cultured under osteogenic (O) conditions and stained with Alizarin Red stain at Wk1, Wk2 and Wk3 time-points**

Scale bar = 100  $\mu$ m. Black arrows point to calcified nodules. One donor from each group is represented.

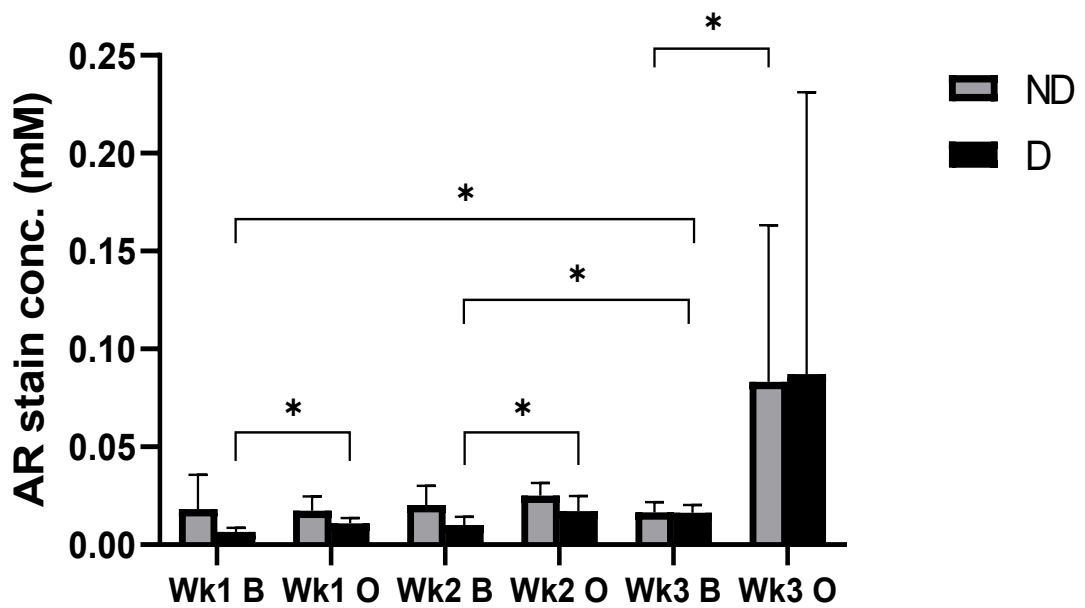


**Figure 5-5: Quantification of Alizarin Red stain in cultures of non-diabetic (ND) and diabetic (D) BM-MSCs**

Cells were cultured for 1, 2 and 3 weeks under basal (B) and osteogenic (O) conditions. Data are presented as mean  $\pm$  SD (n=3). \*p < 0.05.

### 5.2.3 Relative changes in the expression of osteogenic and periodontal markers genes in diabetic and non-diabetic BM-MSCs using qPCR

The relative changes of gene expression of osteogenic, periodontal and bone homeostasis markers in non-diabetic and diabetic BM-MSCs under basal and osteogenic conditions after 1, 2 and 3 weeks of culture were assessed using qPCR as described earlier in chapter 3.

#### 5.2.3.1 Optimization and selection of housekeeping gene (HKG)

As described earlier, qPCR data in this study were reported as relative changes of expression of genes of interest (GOIs) normalised to HKG in 7 samples for each donor: baseline expression (T0) of freshly trypsinized untreated cells and cells cultured under basal and osteogenic conditions for 1, 2 and 3 weeks (Wk1B, Wk1O, Wk2B, Wk2O, Wk3B and Wk3O). In each sample, the relative change of gene expression was calculated using the formula  $2^{-\Delta Ct}$  where:

$$\Delta Ct = Ct_{GOI} - Ct_{HKG}.$$

Two different HKGs were assessed: Glyceraldehyde-3-Phosphate Dehydrogenase (*GAPDH*) and Hypoxanthine-Guanine Phosphoribosyl transferase 1 (*HPRT1*). *GAPDH* represents a 'classical' choice of HKG and has been used in multiple studies on BM-MSCs (463–465), while some investigations opted for using *HPRT1* instead (421,466). Studies on optimising reference genes in BM-MSCs concluded *HPRT1* could be a more reliable HKG in this cell type (410,467).

The expression levels of both *GAPDH* and *HPRT1* were assessed in all samples and 3 different normalization strategies were tested: Normalization to *GAPDH*, normalization to *HPRT1* and normalization to the average Ct of both genes. This approach of normalising Ct of GOIs to the average Ct of multiple HKGs has been proposed to increase robustness, validity and reproducibility of relative gene expression results using qPCR (468). Gene expression using the 3 approaches was assessed for *ALPL* (Figure 5-6) and *COL1A1* (Figure 5-7) as a representative of a relatively rare and an abundant gene respectively as shown by the scale of the y axes in both figures. In general *GAPDH* had higher expression levels as evident by its lower Ct values compared to *HPRT1*. This could mean that some GOIs with relatively higher Ct values/lower expression levels would not be detectable creating false data gaps if normalization to *GAPDH* was utilised. As discussed later in this chapter, the majority of GOIs investigated in the present study had relatively lower expression levels and thus normalization to *HPRT1* was selected and used for all GOIs for more consistent and balanced results. The overall analysis of diabetic and non-diabetic BM-MSCs (n=3 for each group) was presented as mean  $\pm$  standard error of mean (SEM). Paired t test was used to compare matching groups (basal and osteogenic cultures of the same cells population at each time-point) while unpaired t test was used to compare non matching groups (diabetic and non-diabetic cells cultures at each culture condition and time-point). RM-ANOVA was used to compare different time-points of each cell population under the same culture condition and showed no statistically significant time dependant differences in all genes. For all comparisons,  $p < 0.05$  was considered statistically significant.

*ALPL*

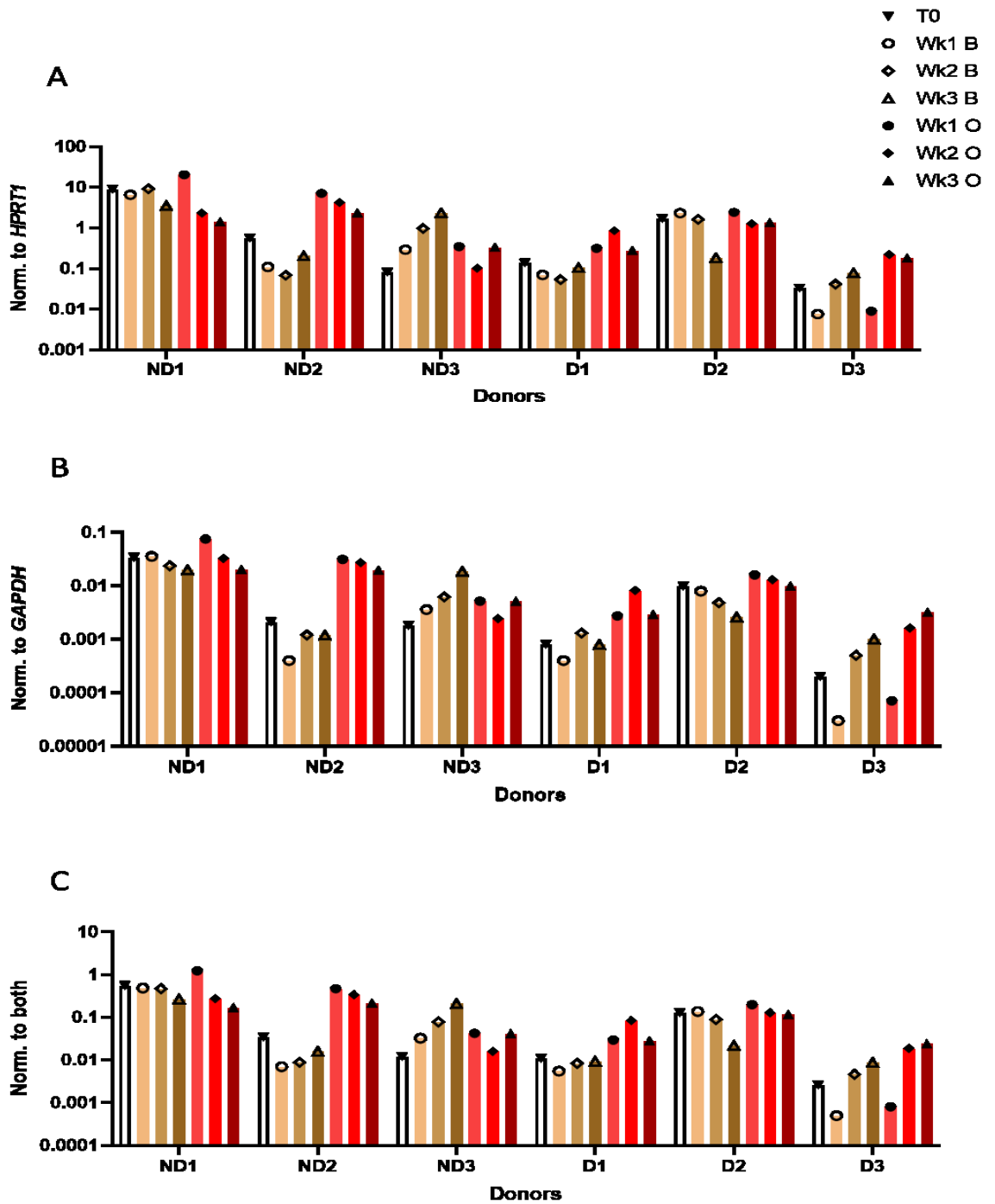


Figure 5-6: *ALPL* relative expression in BM-MSCs from non-diabetic (ND) and diabetic (D) donors normalized to *HPRT1* (A), *GAPDH* (B) and the average of both genes (C).

T0: time-point 0 (untreated cells)

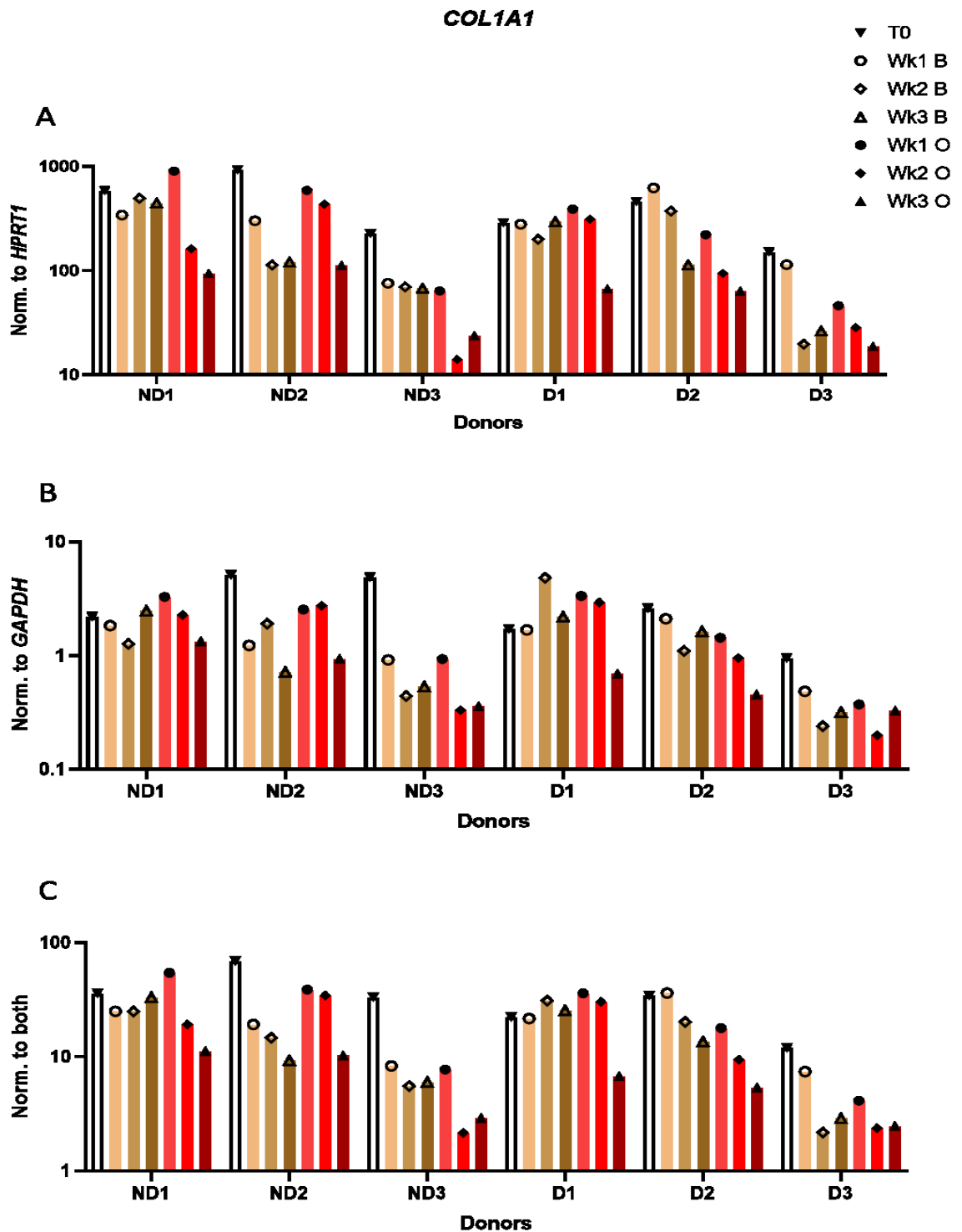


Figure 5-7: *COL1A1* relative expression in BM-MSCs from non-diabetic (ND) and diabetic (D) donors normalized to *HPRT1* (A), *GAPDH* (B) and the average of both genes (C).

T0: time-point 0 (untreated cells)

### **5.2.3.2 Relative changes in the expression of *ALPL* gene in non-diabetic and diabetic BM-MSCs**

Figure 5-8 (A) again reproduces data shown in Figure 5-6, and shows the expression levels of *ALPL* in BM-MSCs from individual non-diabetic and diabetic donors at T0, basal and osteogenic cultures at 3 different time-points. Cells from all donors showed expression of *ALPL* albeit at different levels.

Figure 5-8 (B) shows the overall analysis of *ALPL* expression levels in non-diabetic versus diabetic BM-MSCs. There were no significant differences between non-diabetic and diabetic cells at the different time-points/culture conditions, or between basal and osteogenic cultures of either cell population. However, there was a trend of lower *ALPL* expression in diabetic versus non-diabetic BM-MSCs at Wk3 basal cultures. There was also a trend of *ALPL* upregulation in osteogenic versus basal cultures of non-diabetic BM-MSCs at Wk1, and diabetic BM-MSCs at both Wk1 and Wk3.

### ALPL

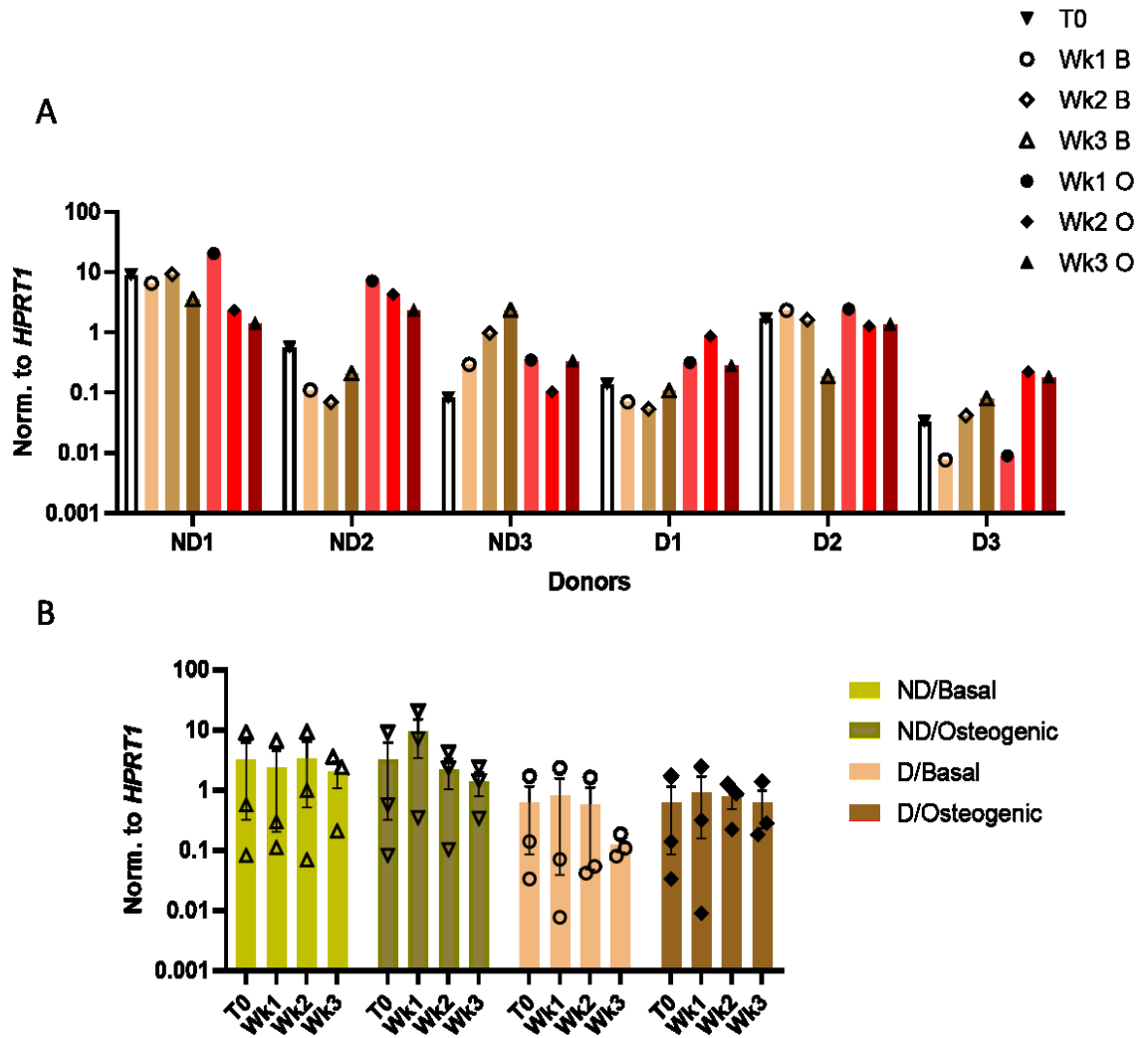


**Figure 5-8: Relative changes in gene expression of *ALPL* in non-diabetic and diabetic BM-MSCs**

A: Gene expression of *ALPL* in individual non-diabetic (ND) and diabetic (D) donors at T0, basal and osteogenic conditions at Wk1, Wk2 and Wk3 time-points.

B: Overall analysis of relative changes in *ALPL* gene expression in ND and D BM-MSCs. Data are presented as mean  $\pm$  SEM (n=3 for each group).

### **5.2.3.3 Relative changes in the expression of *RUNX2* gene in non-diabetic and diabetic BM-MSCs**

Figure 5-9 (A) shows expression levels of *RUNX2* in BM-MSCs from individual non-diabetic and diabetic donors at the different time-points/culture conditions. *RUNX2* is an early osteogenic marker typically upregulated in the first phase of osteoblasts differentiation (469). *RUNX2* was upregulated at Wk1 in osteogenic versus basal cultures of all non-diabetic cells. On the other hand, *RUNX2* was upregulated in BM-MSCs from all 3 diabetic donors at WK3 in osteogenic versus basal cultures.

Figure 5-9 (B) shows the overall analysis of *RUNX2* expression levels in diabetic versus non-diabetic BM-MSCs. There were no statistically significant differences between non-diabetic and diabetic cells at the different time-points/culture conditions. Moreover, there was no statistically significant differences between basal and osteogenic cultures of either cell population. Nonetheless, there was a trend of lower *RUNX2* expression in basal cultures of diabetic versus non-diabetic cells at Wk3. Moreover, there was also a trend of *RUNX2* upregulation in osteogenic versus basal cultures in both diabetic and non-diabetic BM-MSCs albeit at different time-points. For non-diabetic cells, this upregulation was observed at Wk1, whereas for diabetic cells, it was detected at Wk3.

## RUNX2

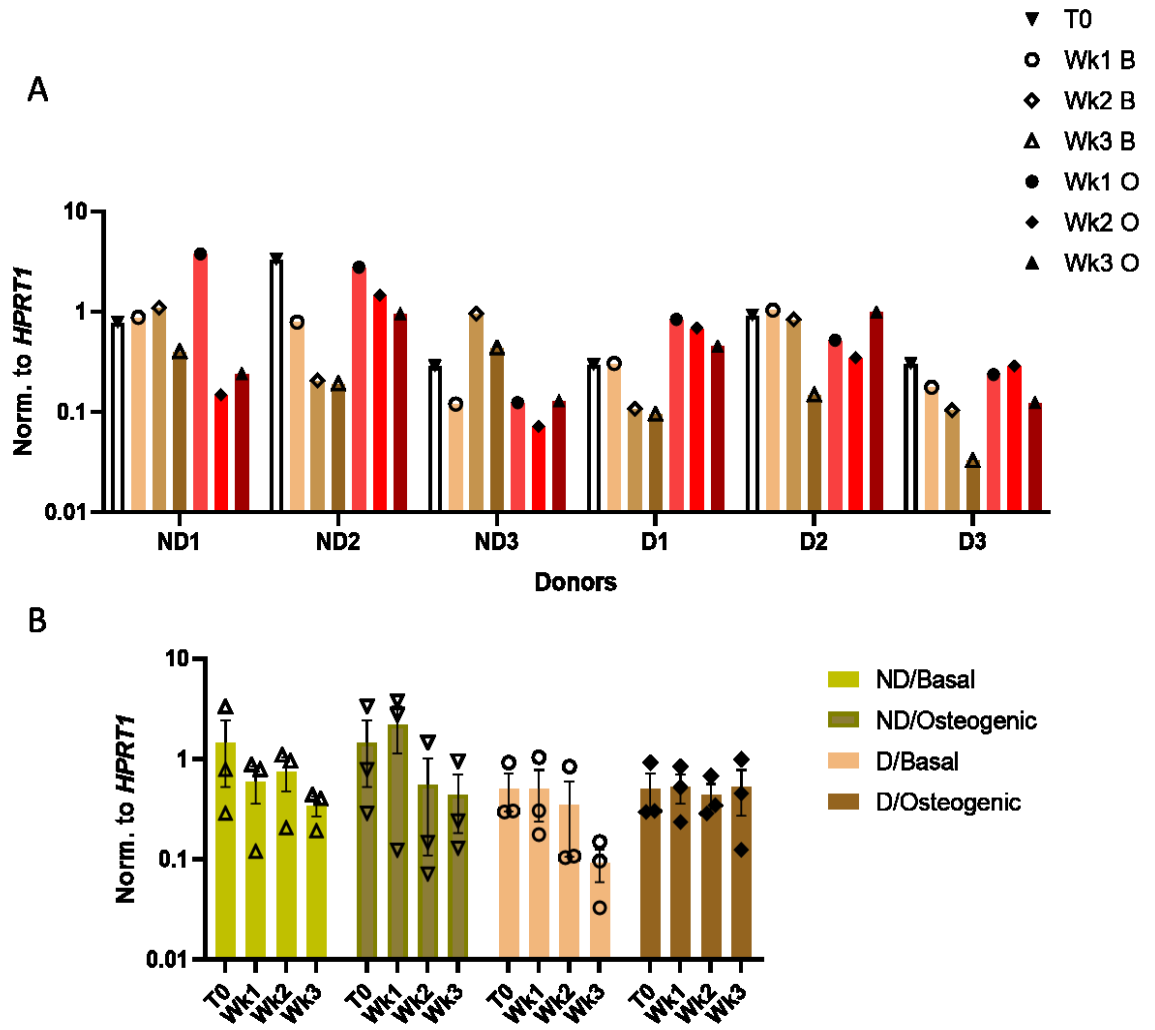


**Figure 5-9: Relative changes in gene expression of *RUNX2* in non-diabetic and diabetic BM-MSCs**

A: Gene expression of *RUNX2* in individual non-diabetic (ND) and diabetic (D) donors at T0, basal and osteogenic conditions at Wk1, Wk2 and Wk3 time-points.

B: Overall analysis of relative changes of *RUNX2* gene expression in ND and D BM-MSCs. Data are presented as mean  $\pm$  SEM (n=3 for each group).

#### **5.2.3.4 Relative changes in the expression of *OCN* gene in non-diabetic and diabetic BM-MSCs**

Figure 5-10 (A) shows expression levels of *OCN*, a late osteogenic marker (470), in BM-MSCs isolated from individual non-diabetic and diabetic donors at the different time-points/culture conditions.

Figure 5-10 (B) shows the overall analysis of *OCN* expression levels in non-diabetic versus diabetic BM-MSCs. There were no trends or statistically significant differences between non-diabetic and diabetic cells at the different time-points/culture conditions, or between basal and osteogenic cultures of either cell population.

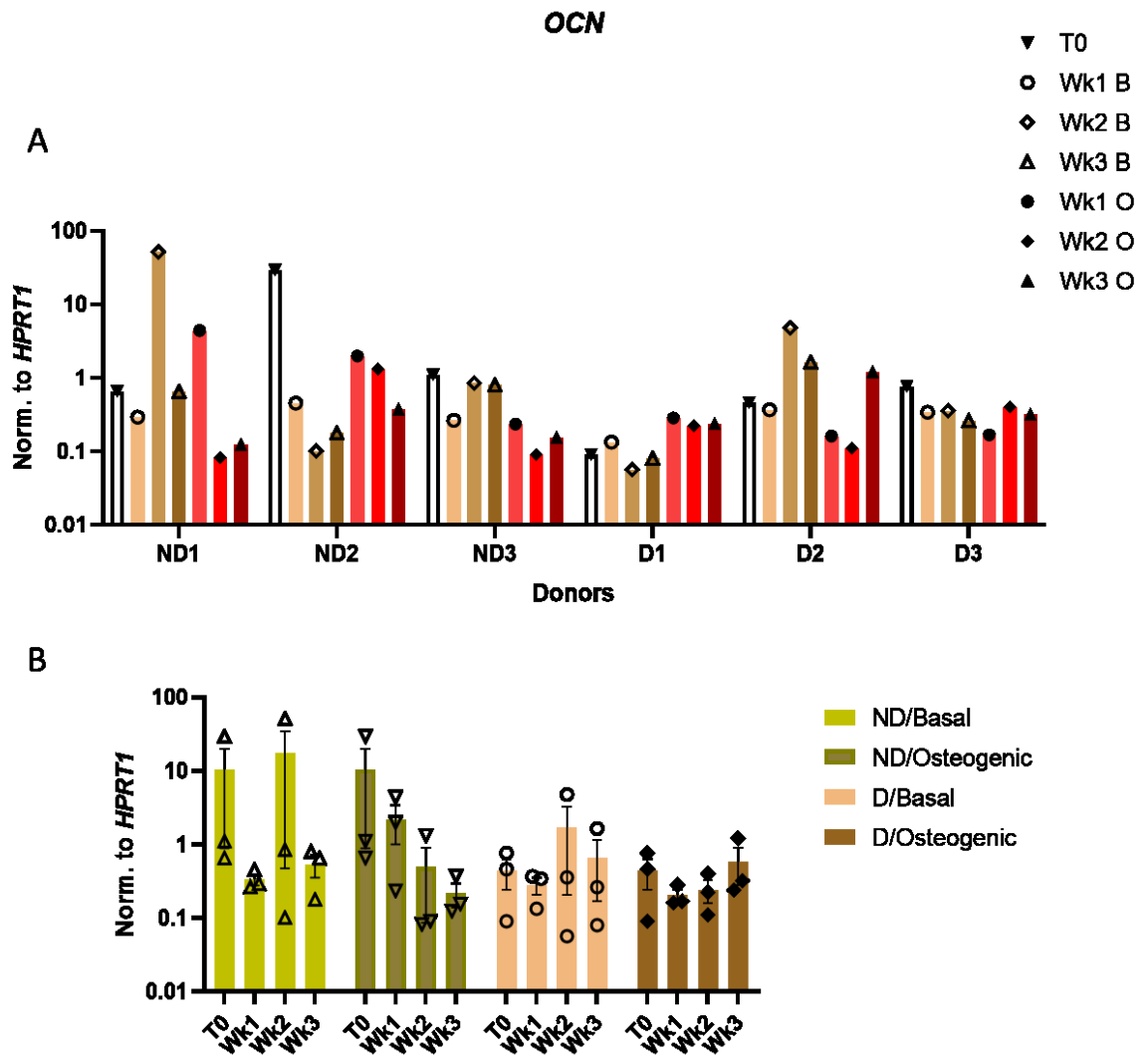


**Figure 5-10: Relative changes in gene expression of *OCN* in non-diabetic and diabetic BM-MSCs**

A: Gene expression of *OCN* in individual non-diabetic (ND) and diabetic (D) donors at T0, basal and osteogenic conditions at Wk1, Wk2 and Wk3 time-points.

B: Overall analysis of relative changes in *OCN* gene expression in ND and D BM-MSCs. Data are presented as mean  $\pm$  SEM (n=3 for each group).

### **5.2.3.5 Relative changes in the expression of *COL1A1* gene in non-diabetic and diabetic BM-MSCs**

Figure 5-11 (A) again reproduces data shown in Figure 5-6, and shows expression levels of *COL1A1* in BM-MSCs derived from individual non-diabetic and diabetic donors at the different time-points/culture conditions. *COL1* is a marker of both osteogenic (471) and fibroblastic (472) differentiation of stem cells. The scale of y axis indicates higher levels of expression compared to *RUNX2* and *OCN*. *COL1A1* was downregulated at Wk3 in osteogenic versus basal cultures of BM-MSCs from all non-diabetic and diabetic donors.

Figure 5-11 (B) shows the overall analysis of *COL1A1* expression in non-diabetic and diabetic BM-MSCs. There were no statistically significant differences in *COL1A1* expression levels in non-diabetic versus diabetic cells at the different time-points/culture conditions. Both non-diabetic and diabetic BM-MSCs showed a trend of *COL1A1* downregulation in osteogenic versus basal cultures at Wk3 time-point.

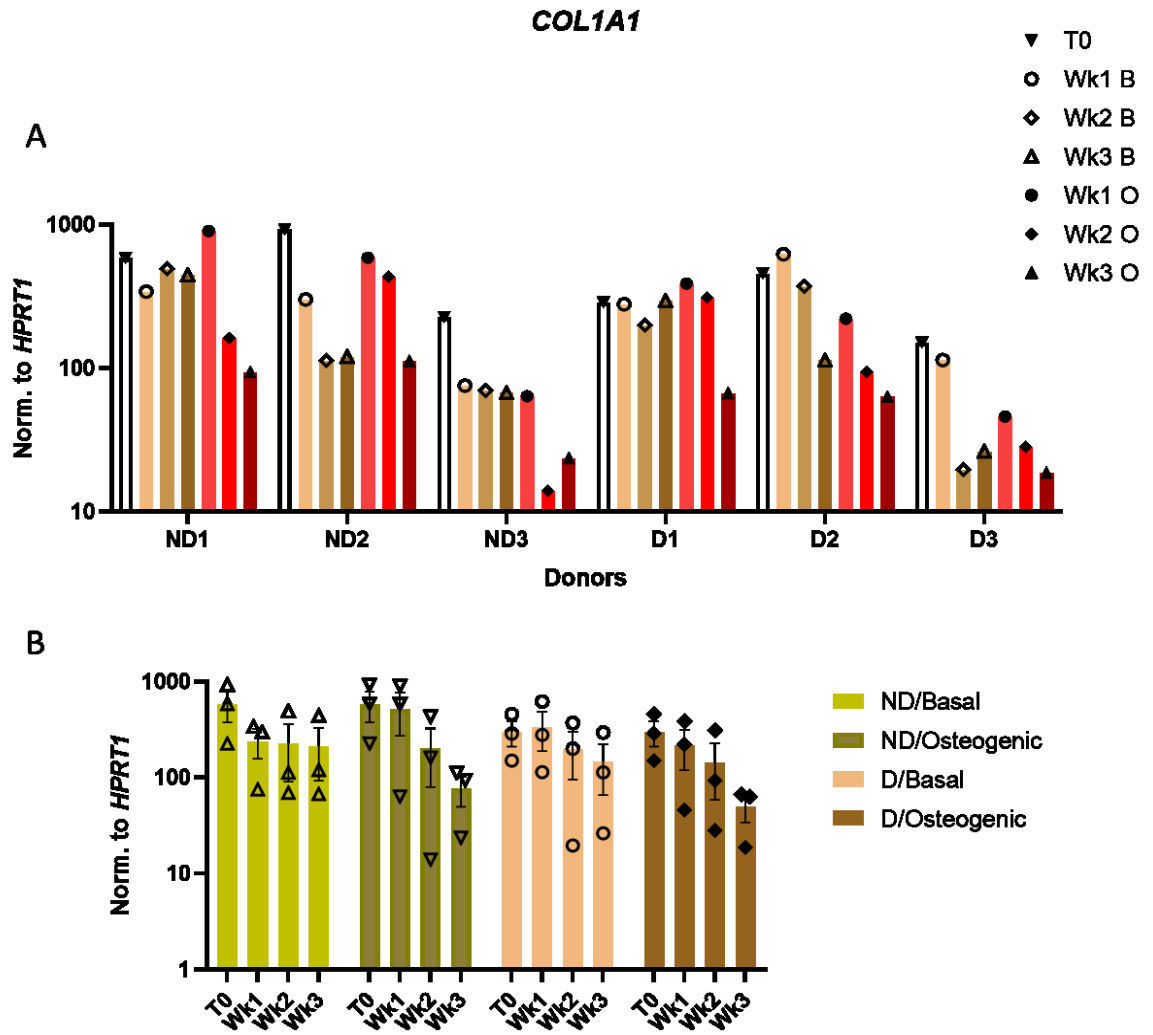


**Figure 5-11: Relative changes in gene expression of *COL1A1* in non-diabetic and diabetic BM-MSCs**

A: Gene expression of *COL1A1* in individual non-diabetic (ND) and diabetic (D) donors at T0, basal and osteogenic conditions at Wk1, Wk2 and Wk3 time-points.

B: Overall analysis of relative changes in *COL1A1* expression in ND and D BM-MSCs. Data are presented as mean  $\pm$  SEM (n=3 for each group).

### **5.2.3.6 Relative changes in the expression of *POSTN* gene in non-diabetic and diabetic BM-MSCs**

Figure 5-12(A) shows expression of *POSTN* in BM-MSCs derived from individual non-diabetic and diabetic donors. *POSTN*, a marker of PDL fibroblasts (473) as well as osteoblasts (474) differentiation, was expressed in all cultures although at variable levels. All diabetic donors showed lower levels of *POSTN* expression at T0 and Wk3 basal cultures compared to non-diabetic controls.

Figure 5-12(B) shows the overall analysis of *POSTN* expression in non-diabetic and diabetic BM-MSCs. *POSTN* had statistically significant lower levels of expression in diabetic versus non-diabetic cells in Wk3 osteogenic cultures ( $p < 0.05$ ), with a similar trend of lower *POSTN* at T0 and Wk3 basal cultures. There was no statistically significant differences between basal and osteogenic cultures of both non-diabetic and diabetic BM-MSCs. However, there was a trend of *POSTN* downregulation in Wk2 osteogenic versus basal cultures of non-diabetic BM-MSCs.

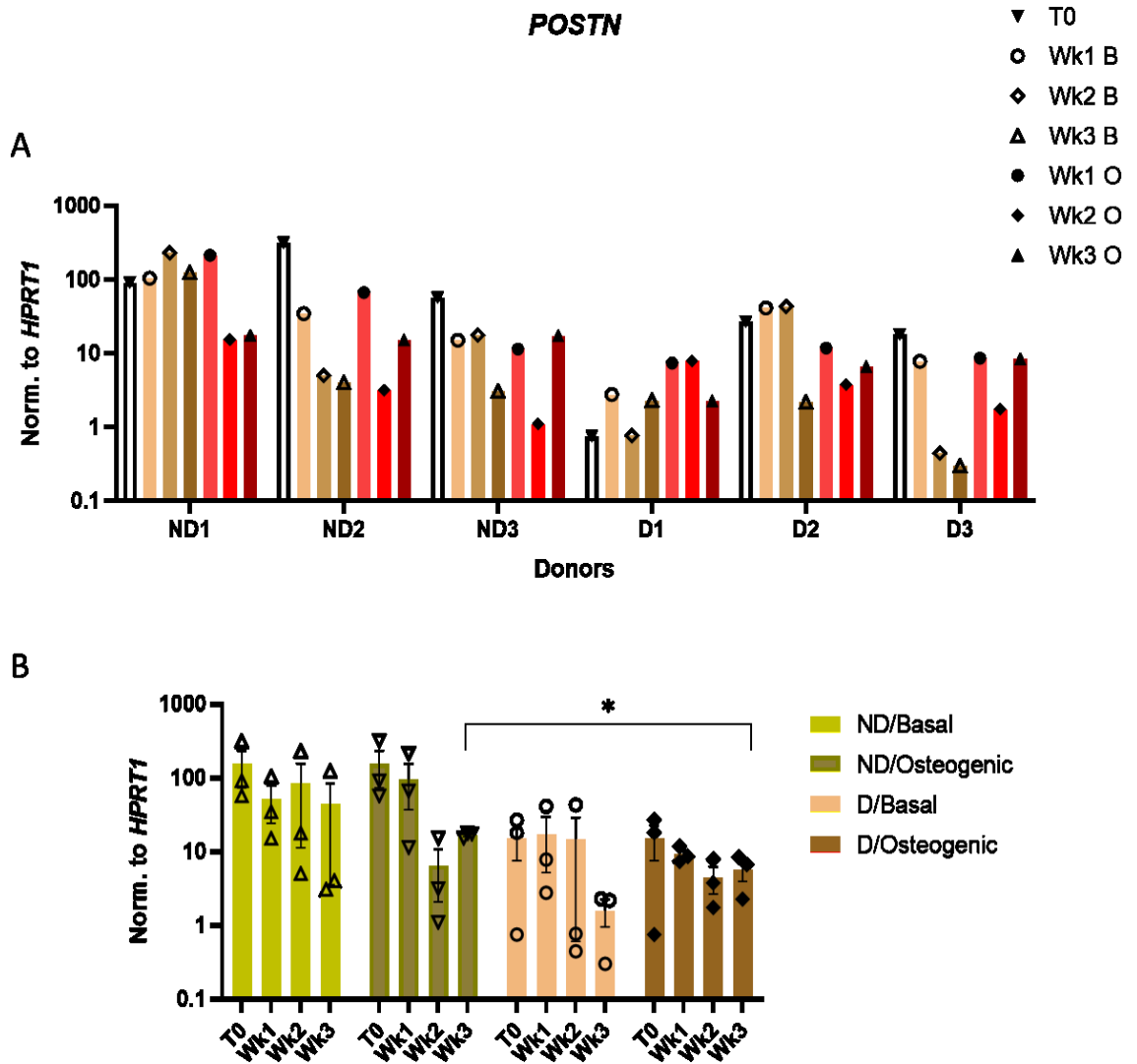


**Figure 5-12: Relative changes in gene expression of *POSTN* in non-diabetic and diabetic BM-MSCs**

A: Gene expression of *POSTN* in individual non-diabetic (ND) and diabetic (D) donors at T0, basal and osteogenic conditions at Wk1, Wk2 and Wk3 time-points.

B: Overall analysis of relative changes in *POSTN* gene expression in ND and D BM-MSCs. Data are presented as mean  $\pm$  SEM (n=3 for each group). \*p < 0.05.

### **5.2.3.7 Relative changes in the expression of *CEMP-1* gene in non-diabetic and diabetic BM-MSCs**

Figure 5-13(A) shows expression of *CEMP-1*, a cementoblasts marker (475), in BM-MSCs derived from individual non-diabetic and diabetic donors. *CEMP-1* was expressed in all cultures albeit at variable levels.

Figure 5-13(B) shows the overall analysis of *CEMP-1* expression in diabetic versus non-diabetic cells. *CEMP-1* expression levels were significantly lower in diabetic versus non-diabetic cells in Wk1 basal cultures ( $p < 0.05$ ) with a similar trend in Wk1 osteogenic cultures as well. There was no statically significant differences between basal and osteogenic cultures of both non-diabetic and diabetic BM-MSCs. Nonetheless, there was a trend of *CEMP-1* upregulation in Wk3 osteogenic versus basal cultures of diabetic cells.

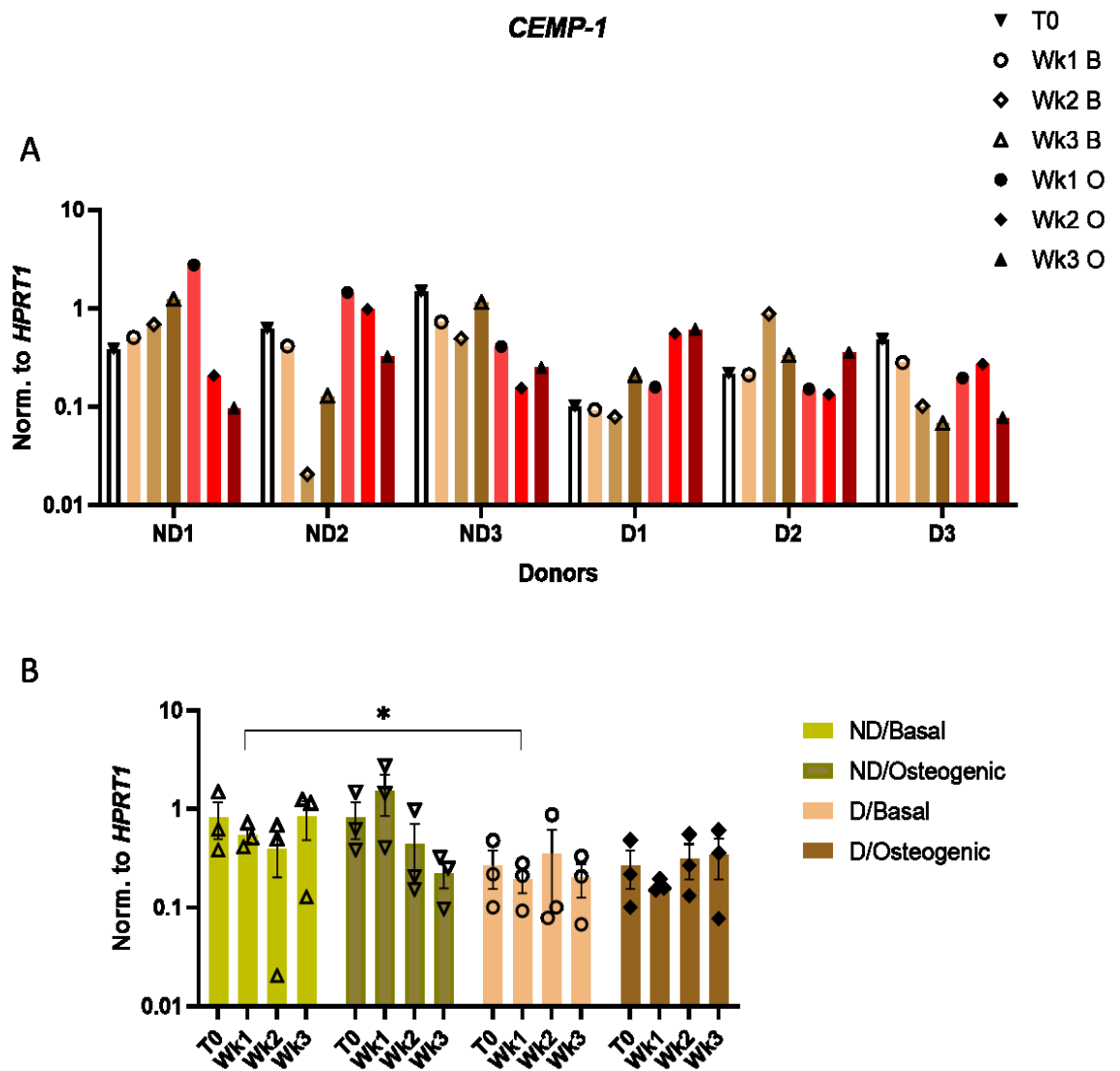


**Figure 5-13: Relative changes in gene expression of *CEMP-1* in non-diabetic and diabetic BM-MSCs**

A: Gene expression of *CEMP-1* in individual non-diabetic (ND) and diabetic (D) donors at T0, basal and osteogenic conditions at Wk1, Wk2 and Wk3 time-points.

B: Overall analysis of relative changes in *CEMP-1* gene expression in ND and D BM-MSCs. Data are presented as mean  $\pm$  SEM (n=3 for each group). \* p<0.05.

#### **5.2.3.8 Relative changes in the expression of *OPG* gene in non-diabetic and diabetic BM-MSCs**

Figure 5-14(A) shows expression of *OPG* in BM-MSCs derived from individual non-diabetic and diabetic donors. All cultures expressed *OPG* though at variable levels. All non-diabetic donors displayed *OPG* upregulation in osteogenic versus basal cultures at Wk1.

Figure 5-14(B) shows the overall expression of *OPG* in non-diabetic and diabetic BM-MSCs. There were no statistically significant differences between non-diabetic and diabetic cells at the different time-point/culture conditions, or between basal and osteogenic cultures of either cell population.

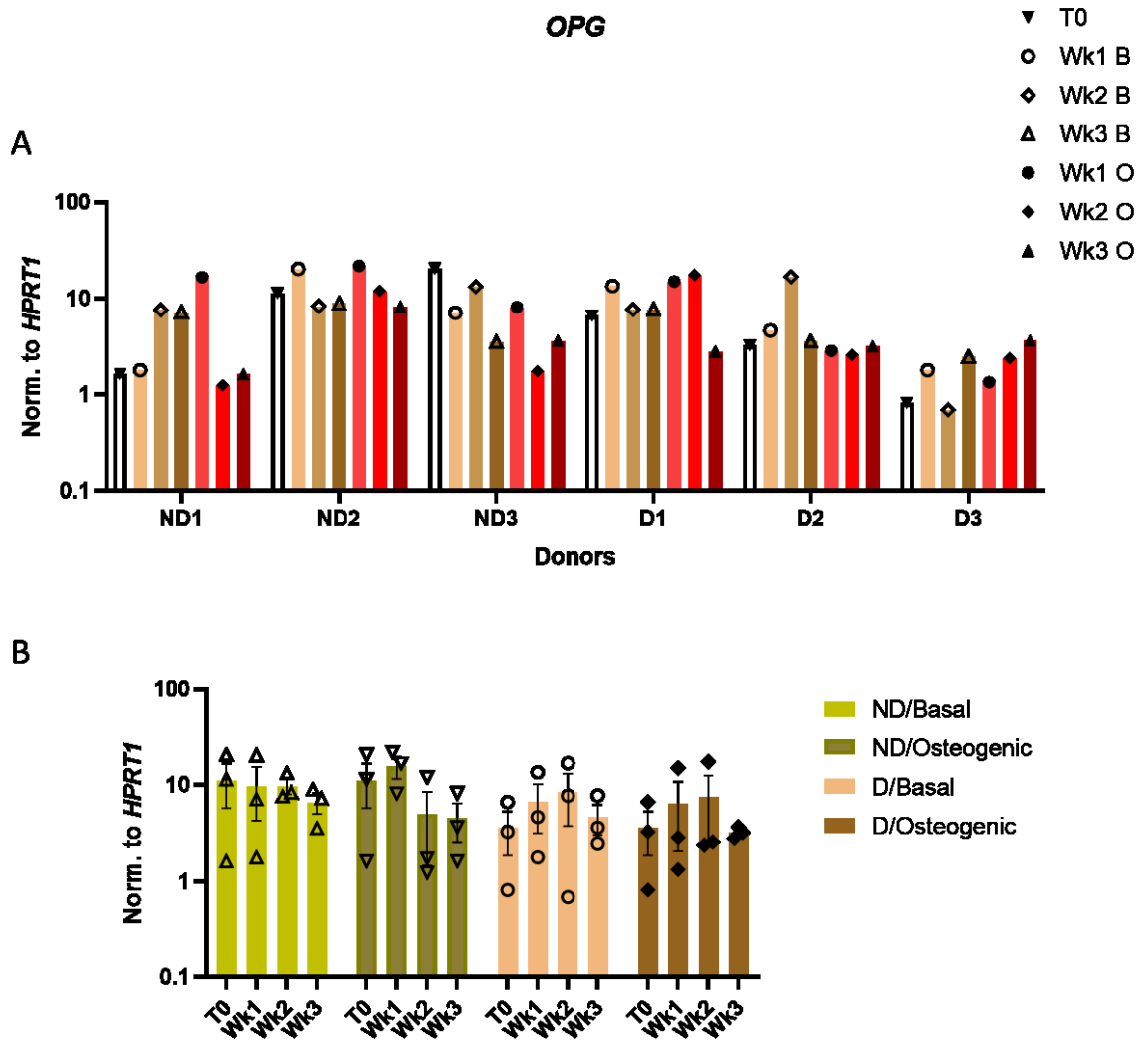


**Figure 5-14: Relative changes in gene expression of *OPG* in non-diabetic and diabetic BM-MSCs**

A: Gene expression of *OPG* in individual non-diabetic (ND) and diabetic (D) donors at T0, basal and osteogenic conditions at Wk1, Wk2 and Wk3 time-points.

B: Overall analysis of relative changes in *OPG* gene expression in ND and D BM-MSCs. Data are presented as mean  $\pm$  SEM (n=3 for each group).

#### **5.2.3.9 Relative changes in the expression of *RANKL* gene in non-diabetic and diabetic BM-MSCs**

Figure 5-15(A) shows the expression of *RANKL* in BM-MSCs derived from individual non-diabetic and diabetic donors. *RANKL* was expressed in all cultures, but at variable levels.

Figure 5-15(B) shows the overall expression of *RANKL* in non-diabetic and diabetic BM-MSCs. There were no significant differences between diabetic and non-diabetic cells at the different time-points/culture conditions, or between basal and osteogenic cultures of either cell population.

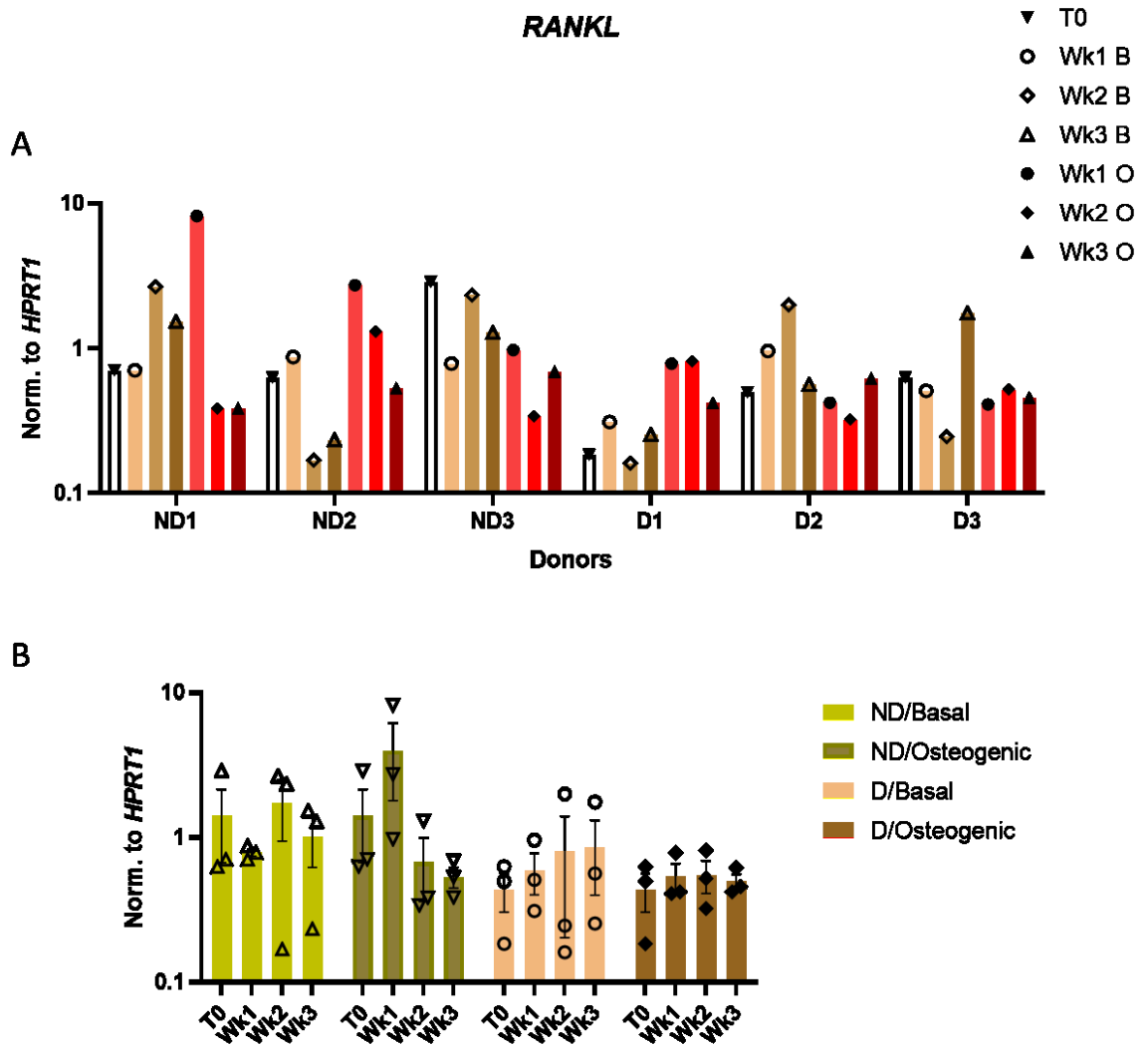


**Figure 5-15: Relative changes in gene expression of *RANKL* in non-diabetic and diabetic BM-MSCs**

A: Gene expression of *RANKL* in individual non-diabetic (ND) and diabetic (D) donors at T0, basal and osteogenic conditions at Wk1, Wk2 and Wk3 time-points.

B: Overall analysis of relative changes in *RANKL* gene expression in ND and D BM-MSCs. Data are presented as mean  $\pm$  SEM (n=3 for each group).

#### **5.2.3.10 Relative changes in the *OPG/RANKL* ratio in non-diabetic and diabetic BM-MSCs**

Figure 5-16(A) shows the *OPG/RANKL* ratio in BM-MSCs from individual non-diabetic and diabetic donors at the different time-points/culture conditions. All non-diabetic and diabetic cells showed a ratio  $>1$ , indicating relatively higher osteoblastic activity.

Figure 5-16(B) shows the overall analysis of *OPG/RANKL* ratio in non-diabetic and diabetic BM-MSCs. There were no statistically significant differences between non-diabetic and diabetic cells at the different time-points/culture conditions, or between basal and osteogenic cultures of either cell population.

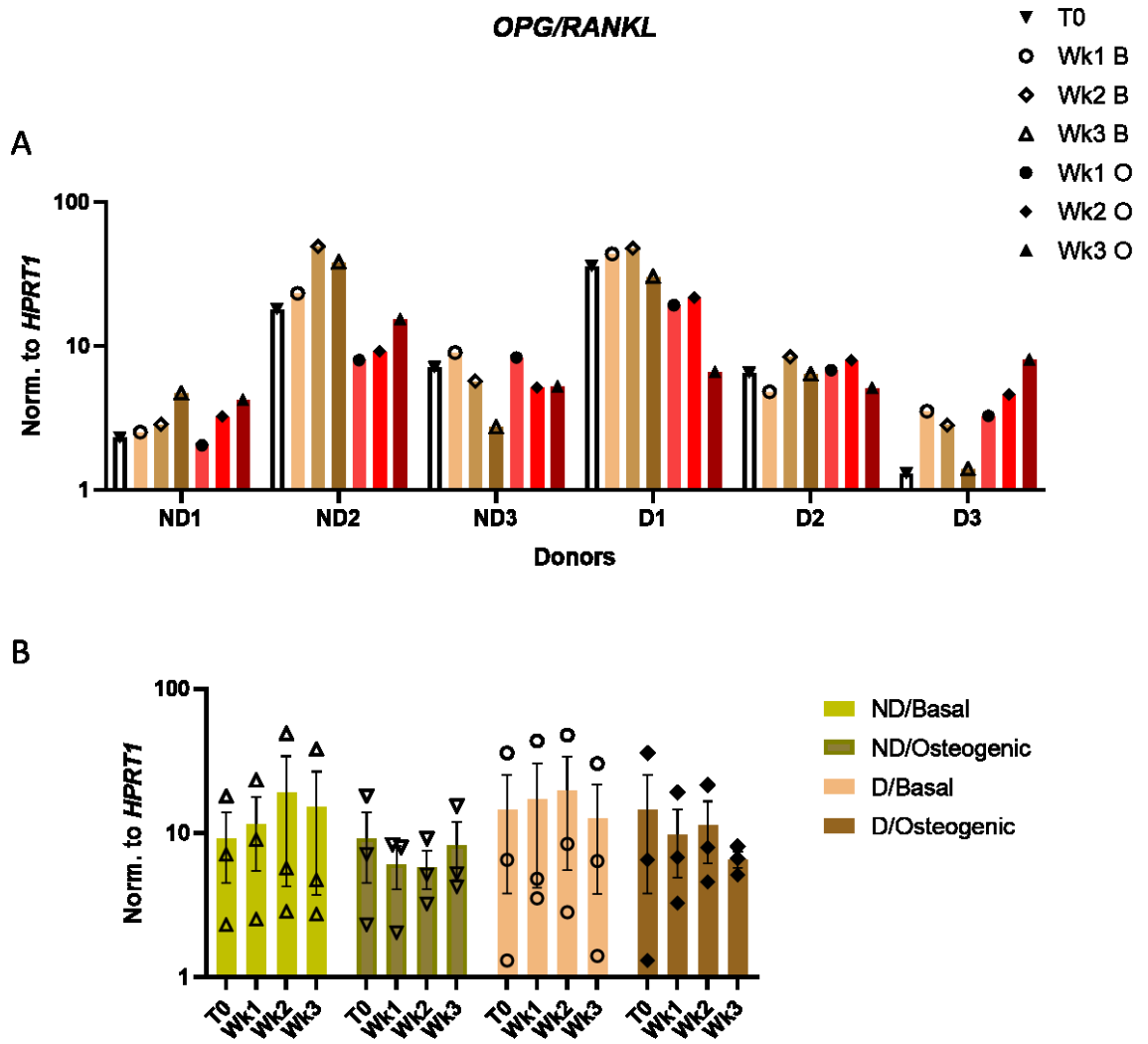


**Figure 5-16: *OPG/RANKL* ratio in non-diabetic and diabetic BM-MSCs**

A: *OPG/RANKL* ratio in individual non-diabetic (ND) and diabetic (D) donors at T0, basal and osteogenic conditions at Wk1, Wk2 and Wk3 time-points.

B: Overall analysis of *OPG/RANKL* ratio in ND and D BM-MSCs. Data are presented as mean  $\pm$  SEM (n=3 for each group).

### 5.3 Discussion

The results presented in this chapter relate to the osteogenic differentiation of diabetic and non-diabetic BM-MSCs. Both cell types have been cultured under basal and osteogenic conditions for 3 different durations: 1, 2, and 3 weeks and at each time-point the cultures were terminated and various assays were utilised to assess osteogenic potentials of both cell populations. These time-points were selected as they represent the 3 different phases of mineralisation as described elsewhere: The first phase is cell proliferation, followed by osteogenic differentiation and finally matrix mineralisation (476). Thus, changes of expression of osteogenic markers at each stage can be picked up and compared in diabetic and non-diabetic BM-MSCs.

The results of the present study showed, as expected, a general trend of increased ALP staining intensity in osteogenic media compared to basal media. This difference was more accentuated as the duration of culture increased with Wk3 osteogenic cultures usually displaying the highest staining intensity (Figure 5-1 and Figure 5-2), with generally higher staining intensity in cultures of BM-MSCs from non-diabetic donors compared to diabetic donors. In general, this supports the qPCR findings showing a trend of higher *ALPL* expression in non-diabetic versus diabetic cells at Wk3 basal cultures.

The above results also agree with those of Sun et al. (251), who reported lower ALP staining and activity in cultures of alveolar BM-MSCs isolated from type 2 diabetic versus non-diabetic donors, despite the variation in the tissue source of BM-MSCs (alveolar bone versus knee joints in the present study) and the composition of the osteogenic media (only glycerophosphate and ascorbic acid but not dexamethasone, while in this thesis all 3 supplements were used). In addition, ALP staining was assessed after 7 days of culture and the ALP activity was measured at days 3, 5 and 7 (251), whereas in the present study the staining was evaluated at days 7, 14 and 21. Liang et al. (252) also observed weaker ALP staining in cultures of diabetic alveolar BM-MSCs compared to non-diabetic controls.

AR staining was employed to evaluate the formation of calcified nodules in cultures of diabetic and non-diabetic BM-MSCs (Figure 5-3 and Figure 5-4). This stain forms Alizarin Red S–calcium complex and has been used extensively for detection of mineral deposits (477). Although cetylpyridinium chloride based

techniques could be more time and work efficient, AR staining and quantification is more sensitive with consistent measurements in weakly stained monolayer cultures. Moreover, this approach allows for both direct visualisation of calcium deposits under light microscope, followed by colorimetric quantification within the same cultures (439).

Unsurprisingly, the AR staining intensity increased with the culture duration, however there were no notable differences between diabetic and non-diabetic cells, whether under basal or osteogenic conditions. This was followed by stain quantification to detect differences in calcification content. The present results showed significantly higher mineralisation when comparing time-points or culture conditions, confirming the positive effect of culture duration and the use of osteogenic supplementation to boost mineralisation of BM-MSCs (Figure 5-5). Still, all these changes were detected within the same cell type without any statistically significant differences between diabetic and non-diabetic cells. Such findings are in agreement with other studies that reported similar calcium depositions by diabetic and non-diabetic BM-MSCs (247,248). Moreover, Andrzejewska et al. (247) also reported time dependant increase in calcium deposition in both diabetic and non-diabetic BM-MSCs, while in the present study this was observed only in basal cultures of diabetic cells (Figure 5-5).

In contrast, other investigations concluded that cultures of alveolar bone BM-MSCs from diabetic donors had lower AR staining compared to non-diabetics (251,252,450), suggesting that alveolar bone BM-MSCs could be more prone to be affected by diabetes compared to knee joint BM-MSCs that were used in the present study. Additionally, the osteogenic media in one study (251) did not include dexamethasone, and the second study (450) used double the glycerophosphate and 10 times the dexamethasone concentrations used in this thesis, which could have contributed to these different findings and the third study (252) used readymade osteogenic media.

Studies of BM-MSCs cultured under simulated diabetic conditions showed variable results. In one study, BM-MSCs cultured under HG (25 mM glucose) formed more calcium nodules compared to control media after 14 and 28 days in culture (269). Such a rarely reported pro-osteogenic effect of HG could be due to variation in BM-MSCs anatomical source or isolation technique which were not clearly stated in the study. Other studies reported reduced mineralisation under

HG conditions (267), HG and LPS (271), HG and free fatty acids (272), as well as HG and palmitic acid (273). Similar conclusion can be drawn from literature on PDLSCs, where HG (255,288,293,478) and AGEs (300,302–304) induced weaker mineralisation. However, one study (299) described opposing results, where HG induced mineralisation, ALP activity and *POSTN* expression in PDL cells. This rationale behind this discrepancy was highlighted in chapters 1 and 3 of this thesis.

This thesis investigated multiple osteogenic markers (*ALPL*, *RUNX2* and *OCN*) and bone homeostasis markers (*OPG*, *RANKL* and *OPG/RANKL* ratio) across 3 different time-points: 1, 2 and 3 weeks. The expression of this range of markers was chosen because osteogenic differentiation is a complex process, involving differential expression of multiple genes over time. Some of these changes include upregulation of early osteogenic markers (transcription factors, such as *RUNX2*) (479). This is followed by upregulation of late osteogenic markers, mainly matrix proteins involved in the mineralisation process, such as *OCN* (262). Moreover, *OPG* and *RANKL* are well known for their role in regulating bone homeostasis (acquisition/loss balance) through fine ‘tuning’ osteoblasts and osteoclasts differentiation (480). Since periodontal regeneration would entail cementum and periodontal ligament restoration as well, markers of cementoblasts differentiation (*CEMP-1*) (178,481) and PDL fibroblasts (*COL1* (472,482,483) and *POSTN* (239,484–487)) were also included in the present study. Taken altogether, the findings of this chapter would give a comprehensive analysis of gene expression changes related to osteogenic and periodontal differentiation of diabetic versus non-diabetic BM-MSCs in monolayer cultures.

The presented results showed a trend of lower *ALPL* expression levels in Wk3 basal cultures of diabetic versus non-diabetic cells (Figure 5-8), suggesting diabetic cells cannot sustain *ALPL* expression in prolonged basal cultures compared to their non-diabetic counterparts. This agrees with the findings of Ying et al. (267), who cultured BM-MSCs under osteogenic and osteogenic HG conditions; and found that HG cultures showed *ALPL* downregulation. Osteoblasts from osteoarthritic knee joints also demonstrated *ALPL* downregulation in cultures supplied with AGE-modified BSA (AGE-BSA) (488). On the other hand, AT-MSCs from diabetic and non-diabetic donors displayed

similar *ALPL* expression levels (489), possibly indicating weaker influence of diabetes on *ALPL* expression in AT-MSCs.

The present data showed that *ALPL* had a trend of upregulation in osteogenic versus basal media at Wk1 in both diabetic and non-diabetic cells (Figure 5-8). This is parallel to the differences observed in ALP staining intensity described earlier in this chapter, and is consistent with ALP being an essential and early marker of active osteogenesis that is usually upregulated during the initial phases of osteogenic differentiation (490). ALP enzyme induces hydrolysis of ATP and pyrophosphate and thus is necessary for phosphate production and hydroxyapatite crystallization (464). The ALP staining intensity on the other hand peaked at Wk3 osteogenic cultures (Figure 5-1 and Figure 5-2), as it takes time for the ALP protein/enzyme to be produced and active relative to mRNA.

*RUNX2* belongs to the gene family *RUNX* that also includes *RUNX1*, which regulates hematopoietic cell development and *RUNX3*, which regulates neurogenesis and GIT development (491). The Runt domain in *RUNX2* is responsible for its binding to DNA and subsequently acting as a master transcriptional factor, regulating expression of multiple genes involved in osteoblastic commitment of MSCs (along with its downstream target *OSX*) (492). *RUNX2* guides MSCs to the osteoblastic lineage and inhibits their adipogenic differentiation. Furthermore, *RUNX2* along with *OSX* and the canonical Wnt pathway control the transition of osteoblasts progenitors into immature osteoblasts expressing osteogenic markers, such *COL1* (493).

The presented results showed no statistically significant difference in *RUNX2* expression when comparing non-diabetic and diabetic BM-MSCs (Figure 5-9). Such findings are in accord with the work of Koci et al. (489) on AT-MSCs from diabetic and non-diabetic donors where similar *RUNX2* expression levels were reported. Still, alveolar bone BM-MSCs from diabetic patients showed lower *RUNX2* expression, as well as lower AR staining, as previously mentioned (251), which could indicate that MSCs may be influenced by diabetes differentially depending on their tissue of origin with alveolar bone BM-MSCs showing more vulnerability to diabetes induced changes.

On the other hand, downregulation of *RUNX2* in BM-MSCs cultured under diabetic stimulatory conditions have been reported in a number of studies: one using HG (30 mM) (267), a second study using HG (30 mM) combined with

palmitic acid (100  $\mu$ M) as a possibly more accurate representation of hyperglycaemia and hyperlipidaemia associated with diabetes by combining HG and fatty acids (273), and a third using serum of diabetic patients (276). Conversely, Shiomi et al. (271) reported *RUNX2* upregulation at moderate HG concentrations (8 and 12 mM) and its downregulation at higher HG concentrations (24 mM), and both concentrations were combined with LPS (1 mg/mL) as a simulation of periodontitis. The authors suggest the initial upregulation of *RUNX2* could aim at increasing glucose uptake by the differentiating osteoblasts, especially that *OCN*, a downstream gene of *RUNX2*, acts on pancreatic  $\beta$  cells to induce insulin secretion (271). Indeed, *OCN*, as described later in this chapter, has been linked with higher insulin production by  $\beta$  cells and higher insulin sensitivity in animal models, although human studies were inconclusive (494).

*OCN* is also known as bone  $\gamma$ -carboxyglutamic acid (Gla) protein or BGP, and is encoded by the human osteocalcin gene, *BGLAP*. *OCN* is mainly produced by osteoblasts and odontoblasts (495). Following protein synthesis, *OCN* is either carboxylated with high affinity to calcium ions in ECM of bony tissues or uncarboxylated and released into systemic circulation with several endocrinal functions (496). The present study showed no trends or statistically significant differences of *OCN* expression levels when comparing non-diabetic and diabetic cells at the different culture conditions/time-points (Figure 5-10). This differs from the work of Sun et al. (251), where diabetic alveolar BM-MSCs displayed lower *OCN* levels. The differences between their methodologies and those used in this thesis have been highlighted earlier in this chapter. *OCN* downregulation was also reported in BM-MSCs cultured under a number of diabetic culture conditions: HG (267), HG and LPS (271), HG and palmitic acid (273), and serum of T2DM patients (276) as well as osteoblasts cultured under AGE-BSA (488). *OCN* was also downregulated in PDLSCs cultured under HG (286,287,497) and AGEs (303,304). Additionally, *OCN* serum levels are lower in diabetic patients and are inversely associated with fasting blood glucose levels and glycated haemoglobins, suggesting a protective effect against diabetes. This is further supported by animal studies showing uncarboxylated *OCN* improving insulin sensitivity and glucose tolerance (498).

No statistically significant differences in *OCN* expression osteogenic versus basal cultures of both non-diabetic and diabetic BM-MSCs were detected in the present study (Figure 5-10). Evidence on the exact role of *OCN* in bone mineralisation is somewhat contentious, with reports of both pro-osteoblasts and pro-osteoclasts effects. Multiple studies also reported *OCN* both inhibiting and promoting bone mineralisation. Additionally, serum levels of *OCN* are a sensitive marker of bone formation in humans, but can also indicate bone turnover since *OCN* is released into blood during bone resorption (412). These inconclusive data on *OCN* as an osteogenic marker could explain the *OCN* expression levels observed in the present study. Although *OCN* expression is used as an osteogenic marker, with its upregulation indicating osteogenic differentiation of MSCs in a considerable body of literature (238,459,499), another study reported *OCN* downregulation, coupled with upregulation of the adipogenic marker *PPAR- $\gamma$* , in osteogenic cultures of human BM-MSCs (500). The authors suggested that these expression patterns were possible due to using dexamethasone as an osteogenic supplement (500), however they used similar concentrations of dexamethasone and ascorbic acid and double the glycerophosphate concentrations used in this thesis. Interestingly, their results showed that ALP and parathyroid hormone were more sustainably upregulated in osteogenic cultures and thus, they could be more reliable osteogenic markers (500).

*COL1* has been used as a marker for both osteoblasts (415) and PDL fibroblasts (472,482) differentiating from MSCs, since collagen fibres are an integral part of ECM of all connective tissues, including bone and periodontal ligament (501). Such 'overlap' in its expression could have caused the relatively higher levels of *COL1* expression detected in the present study, since it could be expressed by BM-MSCs differentiating into both osteoblasts and fibroblasts (*COL1* expression levels were around 10-fold higher compared to *ALPL* or *OCN*) (Figure 5-11). *COL1* produced by osteoblasts constitute the major part of ECM of bone and in return promotes osteoblast adhesion and differentiation (502), both facts are the rationale behind using collagen as a scaffold for bone tissue engineering in multiple studies (186,503,504).

There was no difference in *COL1* expression between diabetic and non-diabetic BM-MSCs at any time-point (Figure 5-11), possibly indicating no influence of diabetes on *COL1* expression in BM-MSCs. Conversely, diabetic BM-MSCs

isolated from alveolar bone showed lower *COL1* expression (as well as lower *RUNX2* and *OCN* expression as detailed earlier in this chapter) (251); and this could be attributed to the difference in tissue origin of the BM-MSCs. Osteoblasts cultured under AGE-BSA also displayed *COL1A1* downregulation in the study mentioned above by Franke et al. (488).

However, both diabetic and non-diabetic BM-MSCs showed a trend of *COL1* downregulation at Wk3 in osteogenic versus basal cultures. A possible explanation is that *COL1A1* being an early marker of osteoblasts/odontoblasts differentiation (usually peaking at day 4-7 of culture) and an essential constituent of the initial organic phase of calcified tissues ECM (505). Egusa et al. (506) described osteogenic differentiation of BM-MSCs using a commercial osteogenic media and AT-MSCs using media supplemented with 0.1 mM of dexamethasone, 10mM of  $\beta$ -glycerophosphate and 50 mM of ascorbate-2-phosphate. After 21 days, both cell populations formed calcified nodules but with *COL1A1* downregulation in AT-MSCs and unchanged expression levels in BM-MSCs. The authors commented that MSCs from different sources undergo differentiation to the same endpoint through different pathways and that possible epigenetic mechanisms, such as gene silencing could be an integral part of this process. *COL1* downregulation was also demonstrated in another study of osteogenic cultures of AT-MSCs at day 10 and 18 (507); and in DPSCs cultured for 3 weeks on dentine substitute biomaterial (Biodentine™) (505).

POSTN was first identified in the mouse calvarial osteoblastic cell line MC3T3-E1 (508) and later was shown to be expressed in human PDL tissues and in ECM of the periosteum, following its secretion by osteoblast precursors (484). POSTN is a matricellular protein, which are a group of extracellular proteins not serving directly as a component of the ECM but rather regulating cell-matrix interactions through binding to cell surfaces, ECM and growth factors (509). POSTN has been shown to bind to osteoblasts with subsequent activation of multiple signalling pathways. POSTN also binds to BMP-1 and COL1, prompting collagen crosslinking and connective tissue stability (510). These roles of *POSTN* could mean it is upregulated in MSCs differentiating into osteoblasts as well as PDL fibroblasts (239,484–487) similar to *COL1*. Again this could be behind the relative higher expression levels of this marker compared to other osteogenic markers or the cementogenic marker *CEMP-1* (Figure 5-12, the scale of y axis indicates

*POSTN* was expressed at approximately 10-fold compared to the expression levels of *OCN* and *CEMP-1*).

The present data show *POSTN* expression levels in diabetic cells were significantly lower than non-diabetic cells in Wk3 osteogenic cultures ( $p < 0.05$ ). *POSTN* is upregulated in healing bone following fracture (511) and could be involved in periodontal healing as well through regulation of survival, proliferation, migration and adhesion of PDL cells and osteoblasts (512), including periodontal defects post periodontal surgeries (513). Thus, these lower *POSTN* expression levels in the present study could possibly contribute to less than optimal periodontal regeneration in diabetics, if these cells were to be used as an autogenous regenerative therapeutic modality to treat periodontal defects. Indeed, 'tweaking' of BM-MSCs functional deficiencies prior to their transplantation to enhance their success rate has been proposed (514) as will be outlined later in this thesis.

In contrast to the presented results, Seubbick et al. (299) reported *POSTN* upregulation in PDL cells cultured under HG conditions. Interestingly, this paper is one of a very few reporting pro-proliferation and pro-osteogenic effects of HG. The authors proposed that glucose as a source of energy boosted the metabolism of PDL cells, increasing their proliferation rates and also inducing calcium influx into cells with subsequent higher osteogenic differentiation potentials. The authors also suggested that pathological changes seen in diabetics could not be attributed to HG alone, but to a more complicated diabetic microenvironment as described earlier in this thesis (299). Indeed, PDL cells cultured under AGEs did show *POSTN* downregulation at both gene and protein levels (515).

*POSTN* also showed no statistically significant differences between osteogenic and basal cultures of both non-diabetic and diabetic BM-MSCs (Figure 5-12). Very few studies have investigated *POSTN* expression profile under osteogenic cultures. In one study, *POSTN* was downregulated in osteogenic cultures of BM-MSCs from steroid induced osteonecrotic femoral heads, while it was upregulated in the control group (516). It should be noted, however, that osteonecrosis and diabetes represent different pathologies: steroid induced osteonecrosis is a localized disease caused by excessive or prolonged steroids therapy for chronic inflammatory conditions, such as asthma and inflammatory bowel disease, leading to possibly insufficient blood supply and cell apoptosis

within the affected joints (516). Diabetes, on the other hand, is a systemic metabolic disease inducing a generalised low grade inflammatory state across multiple tissues (517–519), as discussed in the first chapter of this thesis.

*CEMP-1* was identified in 2006 as a protein expressed by cementoblasts covering the root surface, a subpopulation of PDL cells and perivascular cells in PDL tissues (520). *CEMP-1* showed statistically significant lower expression in diabetic versus non-diabetic cells in Wk1 basal cultures ( $p < 0.05$ ) (Figure 5-13). As this marker was not investigated in diabetic BM-MSCs or BM-MSCs cultured under diabetic conditions before, there are yet any close comparator. In fact, little is known about cementogenic differentiation of BM-MSCs (208) compared to PDLSCs or dental stem cells in general. Nevertheless, *CEMP-1* was downregulated at the protein level in PDL cells cultured under HG conditions (50mM) in a time dependant manner (521), which is in agreement with the results of this thesis. This is further supported by a report of reduced cementum thickness in extracted teeth of T2DM versus non-diabetic controls (522), however this study did not include immunohistochemical analysis of *CEMP-1* expression in cementum tissues, which would have shed more light on potential mechanisms behind the observed diminished thickness of cementum in diabetics.

The presented data showed no statistically significant differences in *CEMP-1* expression in osteogenic versus basal cultures of both non-diabetic and diabetic cells (Figure 5-13). *CEMP-1* was upregulated in PDL cells cultures supplied with ascorbic acid and glycerophosphate (523). Moreover, addition of Wnt (524), vitamin D and vitamin C (525) to osteogenic media (ascorbic acid, glycerophosphate, dexamethasone) caused a similar upregulation of *CEMP-1* in PDL cells. On the other hand, *CEMP-1* was downregulated in PDL cells cultures supplied with BMP-2 and a combination of ascorbic acid, glycerophosphate and dexamethasone (236). Nonetheless, expression of *CEMP-1* by BM-MSCs under osteogenic conditions remains to be fully established.

The RANK/RANKL/OPG system consists of RANK, its ligand RANKL, and the decoy receptor of RANKL, OPG. The role of this system as the chief regulator of bone homeostasis in health and disease has been extensively explored (526). RANKL is a type 2 transmembrane protein expressed mainly on osteoblasts, osteocytes and T lymphocytes, with a capacity to bind the functional receptor RANK and the decoy receptor OPG (527). RANK is a type I transmembrane

protein initially discovered on osteoclasts precursor and mature osteoclasts, but later identified on other cells including mammary cells and malignant cells (528). RANK/RANKL binding leads to expression of transcription factors essential for osteoclastogenesis and bone resorption most notably nuclear factor- $\kappa$ B (NF- $\kappa$ B) (529).

OPG, on the other hand, was identified as a member of the TNF receptor family, which inhibits osteoclasts differentiation and causes increased bone density in animal models (530). OPG is mainly secreted by osteoblasts (531) and it is not a transmembrane but a soluble protein exported to the extracellular space (532). By acting as a decoy receptor of RANKL, OPG inhibits activation of NF- $\kappa$ B and subsequent inflammatory and skeletal changes (533). While RANKL/RANK binding modulates osteoclasts differentiation and activation, OPG prevents excessive bone resorption by binding to RANKL and thus inhibiting its binding to RANK. This is why OPG/RANKL ratio can be used as a predictor of bone mass (534) where OPG/RANKL ratio above 1 indicates a relatively higher tendency of bone deposition (535) which was true for both diabetic and non-diabetic BM-MSCs in this thesis (Figure 5-16).

There was no statistically significant difference in *OPG* or *RANKL* expression (Figure 5-14 and Figure 5-15 respectively) or their ratio (Figure 5-16) when comparing diabetic and non-diabetic cells. This is different to the results reported by Miranda et al. (88) who isolated osteoblast like cells from osteoporotic and osteoporotic diabetic patients and these cells were cultured under 3 different experimental conditions: LG, HG in addition to HG and AGEs. For osteoporotic diabetic cells, the HG media caused downregulation of *OPG*, *RANKL* and higher *OPG/RANKL* ratio (or lower *RANKL/OPG* ratio) compared to low glucose media and all these changes were reversed in HG+AGEs media. Difference in cell type (BM-MSCs in this thesis versus osteoblasts like cells in the study by Miranda et al. (88)), donors' medical profile (OA and OA-diabetic versus OP and OP-diabetic); and the use of simulating diabetic cultures all could be possible reasons behind these discrepancies. The upregulation of *OPG* and *RANKL* in HG and AGEs versus HG cultures was justified by the authors as some alleviatory effect produced by the AGEs binding to their receptors. Moreover, the authors also argued that *OPG* upregulation could be linked to the vascular calcification and

damage seen in diabetics and causing a significant part of diabetic complications (88).

Zhang et al. (536) described both *OPG* downregulation and *RANKL* upregulation, while Wu et al. (298) and Feng et al. (537) reported unchanged *OPG* expression and *RANKL* upregulation in PDL cells cultured under HG. *RANKL* upregulation was also observed in PDL cells cultured under HG and TNF- $\alpha$  (41). Such difference from the present findings could be attributed to the different cell type investigated and the use of HG and TNF- $\alpha$  to simulate diabetes. Interestingly, higher *RANKL* expression and lower *OPG/RANKL* ratio were detected in bone specimens removed during implant placement in T2DM patients (499). This experimental design is possibly not directly addressing BM-MSCs differentiation or fully comparable to periodontal regeneration, as the bone removed during the implant placement was from the residual ridge at least 1 year following dental extractions (499), however it can at least partially reflect the levels of bone homeostasis in diabetics.

A recent study showed women with T2DM had lower serum levels of RANKL, lower number of osteoblast precursors but higher numbers of osteoclasts precursors in their peripheral blood mononuclear cells (PBMCs). Although this indicated lower bone turnover rate, their BMD was not different from age and BMI matched healthy controls. The authors commented that lower RANKL levels could be behind the reduced osteoclasts maturation (538). Furthermore, HG was shown to inhibit RANKL induced osteoclastogenesis in murine cells. Since osteoclastogenesis removes damaged bone, generates anabolic signals for osteoblasts and maintains optimum levels of bone mineralization, hardness and overall quality, this defective osteoclastogenesis could explain bone fragility seen in diabetics (529). On the other hand, AGE-BSA induced *RANKL* upregulation in osteoblasts possibly indicating a pro-osteoclastogenic effect of AGEs (488).

To conclude, although diabetic BM-MSCs displayed weaker ALP staining intensity and statistically significant lower expression of *POSTN* and *CEMP-1* at Wk3 osteogenic and Wk1 basal cultures respectively, their overall osteogenic potentials were comparable to their non-diabetic counterparts. The next chapter would shed more light on possible changes of IGF axis during osteogenic differentiation of diabetic BM-MSCs.

## Chapter 6 Results

### IGF axis expression in diabetic and non-diabetic BM-MSCs

#### 6.1 Introduction

The IGF axis plays an essential role in normal human growth and development by regulating cell proliferation and differentiation. It consists of 2 ligands (IGF-1 and IGF-2), 2 cell surface receptors (IGF1-R and IGF2-R) and 6 soluble binding proteins (IGFBP-1 to 6) (539). Strong evidence supports a central role for the GH/IGF-1 axis, along with the IGF receptors and binding proteins, in the development and repair of the dento-alveolar complex (418).

IGF-1 promoted proliferation and osteogenic differentiation (404), as well as expression of anti-apoptotic marker Caspase in PDL cells (405). Additionally, collagen sponges with conditioned media of BM-MSCs with high levels of IGF-1 (compared to VEGF, TGF- $\beta$ , HGF, FGF-2, PDGF-BB and BMP-2) enhanced alveolar bone regeneration in patients requiring alveolar bone augmentation (540) and rhIGF-1 improved bone deposition in diabetic rats during distraction osteogenesis (541). IGF-2 is vital for appositional and longitudinal bone growth in mice, including temporal regulation of chondrocytes maturation and survival. Moreover, *IGF-2* null mice showed disturbed bone growth and abnormal glucose metabolism suggesting a strong role of IGF-2 in regulating and linking these biological phenomena (542).

IGF-1 binding to IGF-1R and subsequent activation of the IGF-1/IGF1-R pathway is crucial for IGF-1 dependant MSCs proliferation and osteogenic differentiation (543). The role of IGF-2R in osteogenic differentiation is not yet fully explored. However it is possible that IGF-2 pro-osteogenic effects could be mediated through IGF-1R (329). IGFBPs bind IGFs with high affinity, thereby limiting IGFs bioavailability and subsequent binding to IGFRs, as well as preventing potential insulin-like side effects (544); and their decline in aging osteoblasts was proposed as a possible mechanism behind their reduced osteogenic potentials (545). Several IGFBPs were suggested to play important roles in the osteogenic

differentiation of several types of MSCs. For instance, *IGFBP-2* was upregulated during osteogenic differentiation of human dental follicle cells (546) and human dental pulp cells (350). In addition, *IGFBP-6* was downregulated during osteogenic differentiation of MC3T3 murine cell line and its overexpression inhibited ALP activity and mineralisation (547).

In this chapter, the expression of IGF axis genes in diabetic and non-diabetic BM-MSCs cultured under basal and osteogenic conditions was evaluated. This was carried out at gene level using qPCR at time-points T0 and also after 1, 2 and 3 weeks of culture. ELISA was then used to evaluate the changes in protein levels of IGFBPs that showed statistically significant differences in gene expression in diabetic versus non-diabetic cells. The aim was to test the hypothesis that diabetes had an influence on the expression of the IGF axis in BM-MSCs isolated from T2DM patients.

The overall analysis of qPCR and ELISA data of non-diabetic and diabetic BM-MSCs (n=3 for each group) are presented as mean  $\pm$  standard error of mean (SEM). Paired t test was used to compare matching groups (basal and osteogenic cultures of the same cells population at each time-point), while unpaired t test was used to compare non-matching groups (non-diabetic and diabetic cells cultures at each culture condition and time-point). RM-ANOVA was used to compare different time-points of each cell population under the same culture condition and showed no statistically significant time dependant changes in expression levels of all genes. However, there were some time dependant increases in levels of IGFBPs (as detailed in section 6.2.2). For all comparisons,  $p < 0.05$  was considered significant.

## 6.2 Results

### 6.2.1 Relative changes in the expression of IGF axis genes in diabetic and non-diabetic BM-MSCs

#### 6.2.1.1 Relative changes in the expression of *IGF-1* gene in non-diabetic and diabetic BM-MSCs

Figure 6-1(A) shows expression of *IGF-1* in BM-MSCs isolated from individual non-diabetic and diabetic donors. *IGF-1* was below detection levels at 2 instances (Wk2 osteogenic cultures of donor ND2 and Wk3 osteogenic cultures of donor D3).

Figure 6-1(B) shows the overall analysis of *IGF-1* expression in non-diabetic and diabetic BM-MSCs. There were no statistically significant differences between non-diabetic and diabetic cells at the different time-points/culture conditions. Nonetheless, both cell populations showed a trend of lower levels of *IGF-1* in osteogenic versus basal cultures at Wk1, 2 and 3, reaching statistical significance at Wk2 osteogenic versus basal cultures of non-diabetic BM-MSCs ( $p < 0.05$ ). Furthermore, non-diabetic and diabetic BM-MSCs showed relatively unchanged levels of *IGF-1* across the different time-points under basal conditions. Osteogenic cultures, however, showed a more distinctive pattern in both cell populations: initial downregulation of *IGF-1* at Wk1, followed by further downregulation at Wk2 and then upregulation at Wk3.

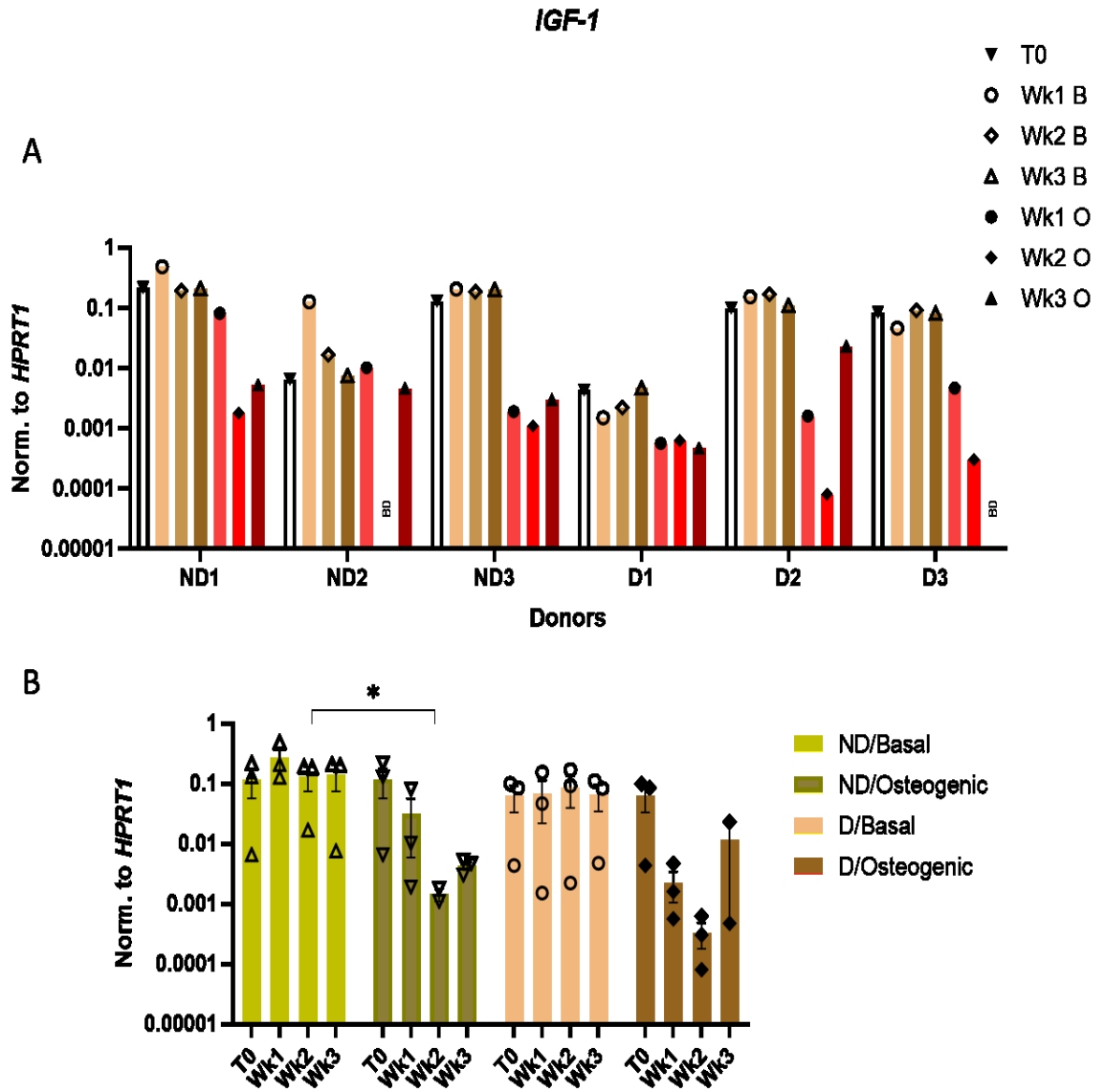


**Figure 6-1: Relative changes in gene expression of *IGF-1* in non-diabetic and diabetic BM-MSCs**

A: Gene expression of *IGF-1* in individual non-diabetic (ND) and diabetic (D) donors at T0, basal and osteogenic conditions at Wk1, Wk2 and Wk3 time-points.

B: Overall analysis of relative changes in *IGF-1* gene expression in ND and D BM-MSCs. Data are presented as mean  $\pm$  SEM (n=3 for each group). BD: below detection. \*p <0.05.

### **6.2.1.2 Relative changes in the expression of *IGF-2* gene in non-diabetic and diabetic BM-MSCs**

Figure 6-2(A) shows the expression of *IGF-2* in BM-MSCs isolated from individual non-diabetic and diabetic donors. *IGF-2* was below detection levels at 3 instances (Wk2 basal cultures of donor ND2, Wk1 and Wk2 basal cultures of donor D3).

Figure 6-2(B) shows the overall analysis of *IGF-2* expression in non-diabetic and diabetic BM-MSCs. There were no statistically significant differences between non-diabetic and diabetic cells at the different time-points/culture conditions. Nonetheless, there was a trend of *IGF-2* upregulation in Wk1 osteogenic cultures of non-diabetic BM-MSCs.

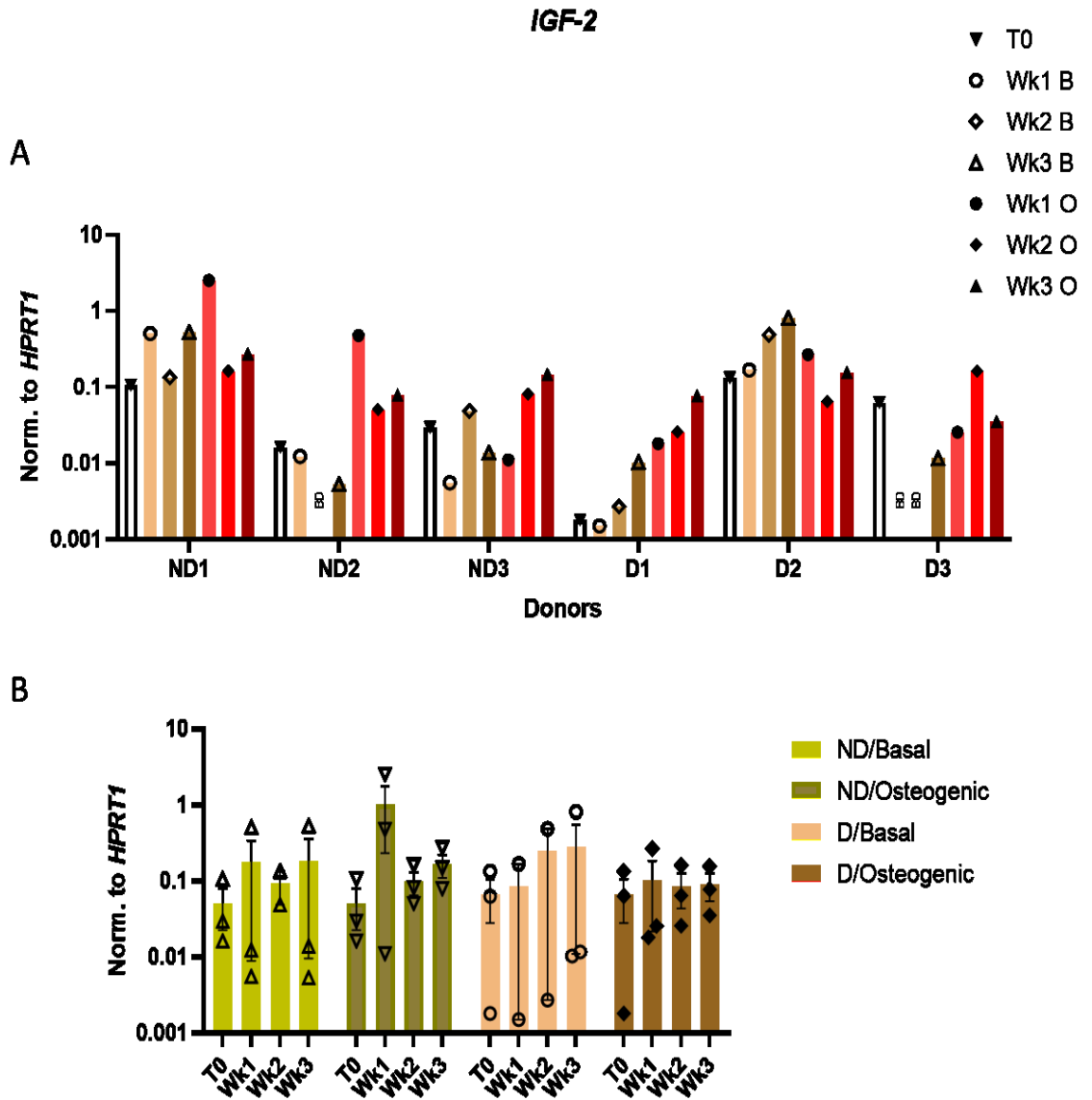


**Figure 6-2: Relative changes in gene expression of *IGF-2* in non-diabetic and diabetic BM-MSCs**

A: Expression of *IGF-2* in individual non-diabetic (ND) and diabetic (D) donors at T0, basal and osteogenic conditions at Wk1, Wk2 and Wk3 time-points.

B: Overall analysis of relative changes in *IGF-2* gene expression in ND and D BM-MSCs. Data are presented as mean  $\pm$  SEM (n=3 for each group). BD: below detection.

### **6.2.1.3 Relative changes in the expression of *IGF1-R* gene in non-diabetic and diabetic BM-MSCs**

Figure 6-3(A) shows the expression of *IGF-1R* in BM-MSCs isolated from individual non-diabetic and diabetic donors. All cells expressed *IGF-1R* at the different time-points/culture conditions with some variation.

Figure 6-3(B) shows the overall analysis of *IGF-1R* expression in non-diabetic and diabetic BM-MSCs. There were no trends or statistically significant differences between expression levels of *IGF1-R* in non-diabetic versus diabetic cells or in basal versus osteogenic cultures.

### IGF1-R

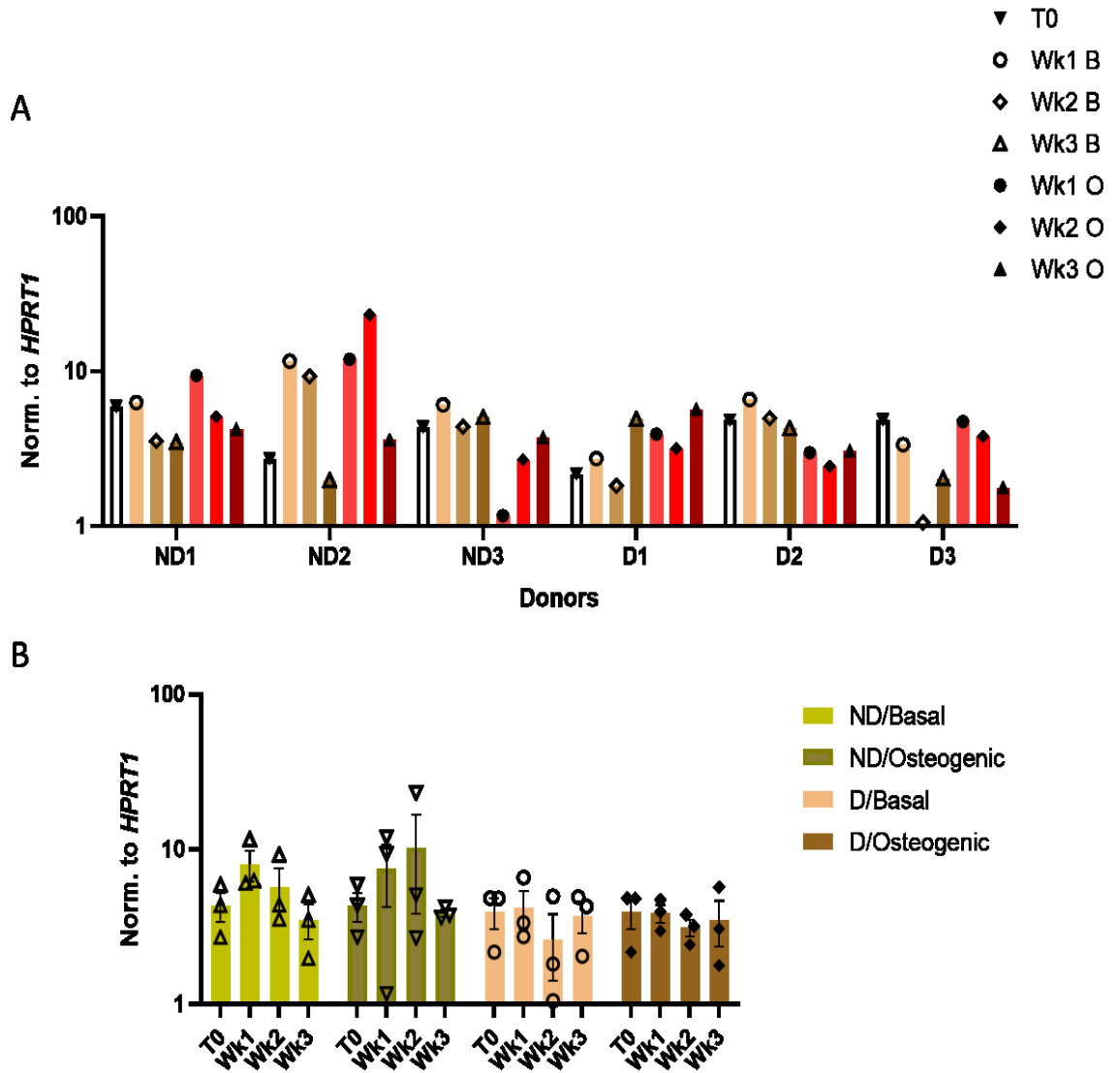


**Figure 6-3: Relative changes in gene expression of *IGF-1R* in non-diabetic and diabetic BM-MSCs**

A: Gene expression of *IGF1-R* in individual non-diabetic (ND) and diabetic (D) donors at T0, basal and osteogenic conditions at Wk1, Wk2 and Wk3 time-points.

B: Overall analysis of relative changes in *IGF1-R* gene expression in ND and D BM-MSCs. Data are presented as mean  $\pm$  SEM (n=3 for each group).

#### **6.2.1.4 Relative changes in the expression of *IGF2-R* gene in non-diabetic and diabetic BM-MSCs**

Figure 6-4(A) shows the expression of *IGF-2R* in BM-MSCs isolated from individual non-diabetic and diabetic donors. All cells expressed *IGF-2R* at the different time-points/culture conditions with little variation.

Figure 6-4(B) shows the overall analysis of *IGF-2R* expression in non-diabetic and diabetic BM-MSCs. Similar to *IGF1-R*, there were no trends or statistically significant differences between expression levels of *IGF2-R* in non-diabetic versus diabetic cells or in basal versus osteogenic cultures.

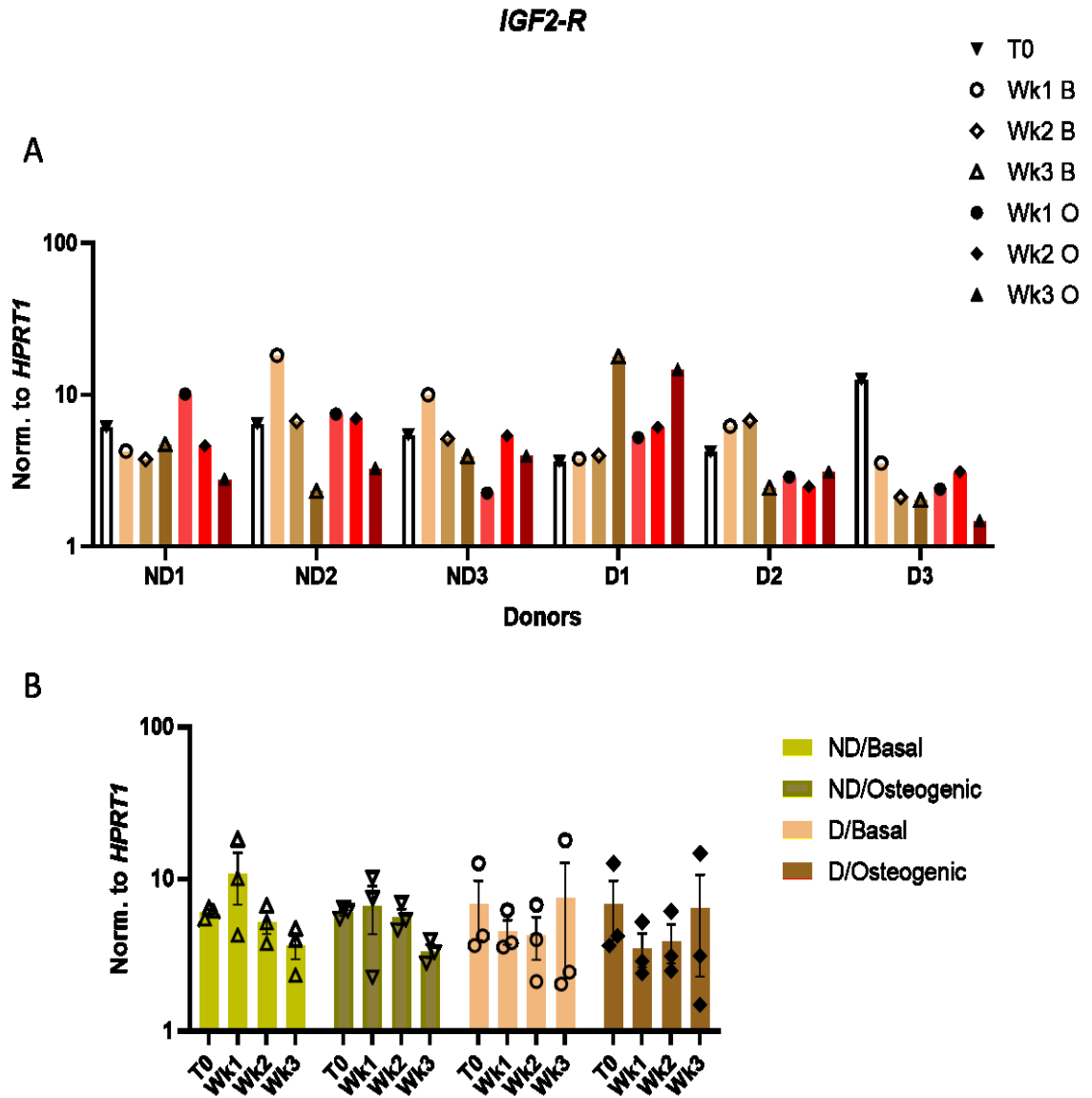


**Figure 6-4: Relative changes in gene expression of *IGF-2R* in non-diabetic and diabetic BM-MSCs**

A: Gene expression of *IGF2-R* in individual non-diabetic (ND) and diabetic (D) donors at T0, basal and osteogenic conditions at Wk1, Wk2 and Wk3 time-points.

B: Overall analysis of relative changes in *IGF2-R* gene expression in ND and D BM-MSCs. Data are presented as mean  $\pm$  SEM (n=3 for each group).

#### **6.2.1.5 Relative changes in the expression of *IGFBP-1* gene in non-diabetic and diabetic BM-MSCs**

Figure 6-5(A) shows *IGFBP-1* expression in BM-MSCs isolated from non-diabetic and diabetic individual donors. All cells expressed *IGFBP-1* under the different culture conditions/time-points but at generally low levels.

Figure 6-5(B) shows the overall analysis of *IGFBP-1* expression in non-diabetic and diabetic BM-MSCs. There were no statistically significant differences between expression levels of *IGFBP-1* in non-diabetic versus diabetic cells, but there was a trend of lower *IGFBP-1* expression in diabetic cells at T0, Wk1 basal and Wk2 osteogenic cultures compared to non-diabetic BM-MSCs. Moreover, *IGFBP-1* showed a trend of downregulation at Wk1 osteogenic versus basal cultures of non-diabetic cells and this change was not mirrored in diabetic BM-MSCs.

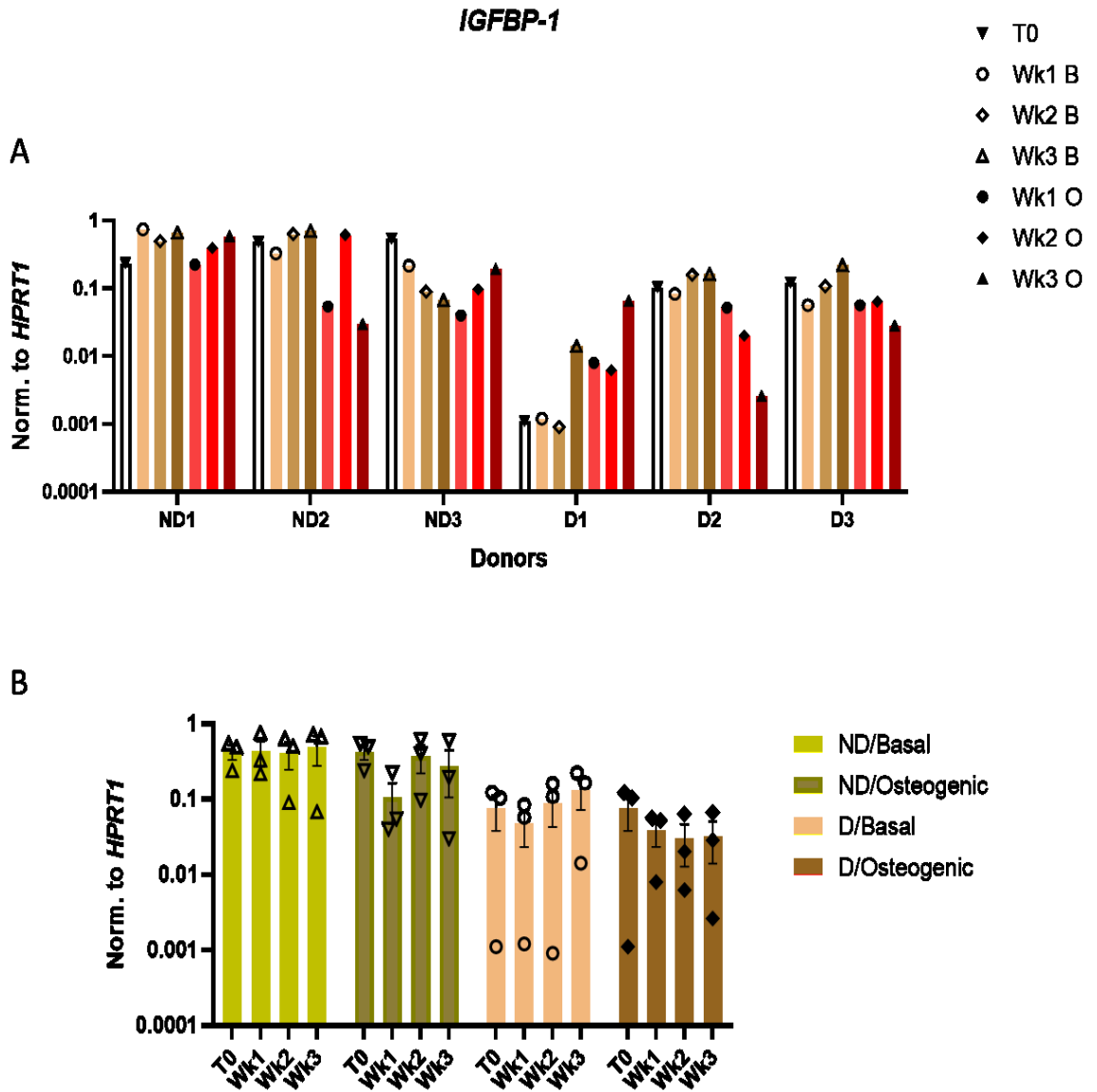


**Figure 6-5: Relative changes in gene expression of *IGFBP-1* in non-diabetic and diabetic BM-MSCs**

A: Gene expression of *IGFBP-1* in individual non-diabetic (ND) and diabetic (D) donors at T0, basal and osteogenic conditions at Wk1, Wk2 and Wk3 time-points.

B: Overall analysis of relative changes in *IGFBP-1* gene expression in ND and D BM-MSCs. Data are presented as mean  $\pm$  SEM (n=3 for each group).

#### **6.2.1.6 Relative changes in the expression of *IGFBP-2* gene in non-diabetic and diabetic BM-MSCs**

Figure 6-6(A) shows the expression of *IGFBP-2* in BM-MSCs isolated from individual non-diabetic and diabetic donors. All cells expressed *IGFBP-2* the different time-points/culture conditions.

Figure 6-6(B) shows the overall analysis of *IGFBP-2* expression in non-diabetic and diabetic BM-MSCs. *IGFBP-2* expression levels were significantly lower in diabetic versus non-diabetic BM-MSCs in Wk1 basal cultures ( $p < 0.05$ ). In addition, *IGFBP-2* had a trend of upregulation in osteogenic cultures of both diabetic and non-diabetic cells albeit at different time-points (Wk2 and Wk3 osteogenic cultures for non-diabetic BM-MSCs and Wk1 and Wk3 osteogenic cultures for diabetic BM-MSCs).

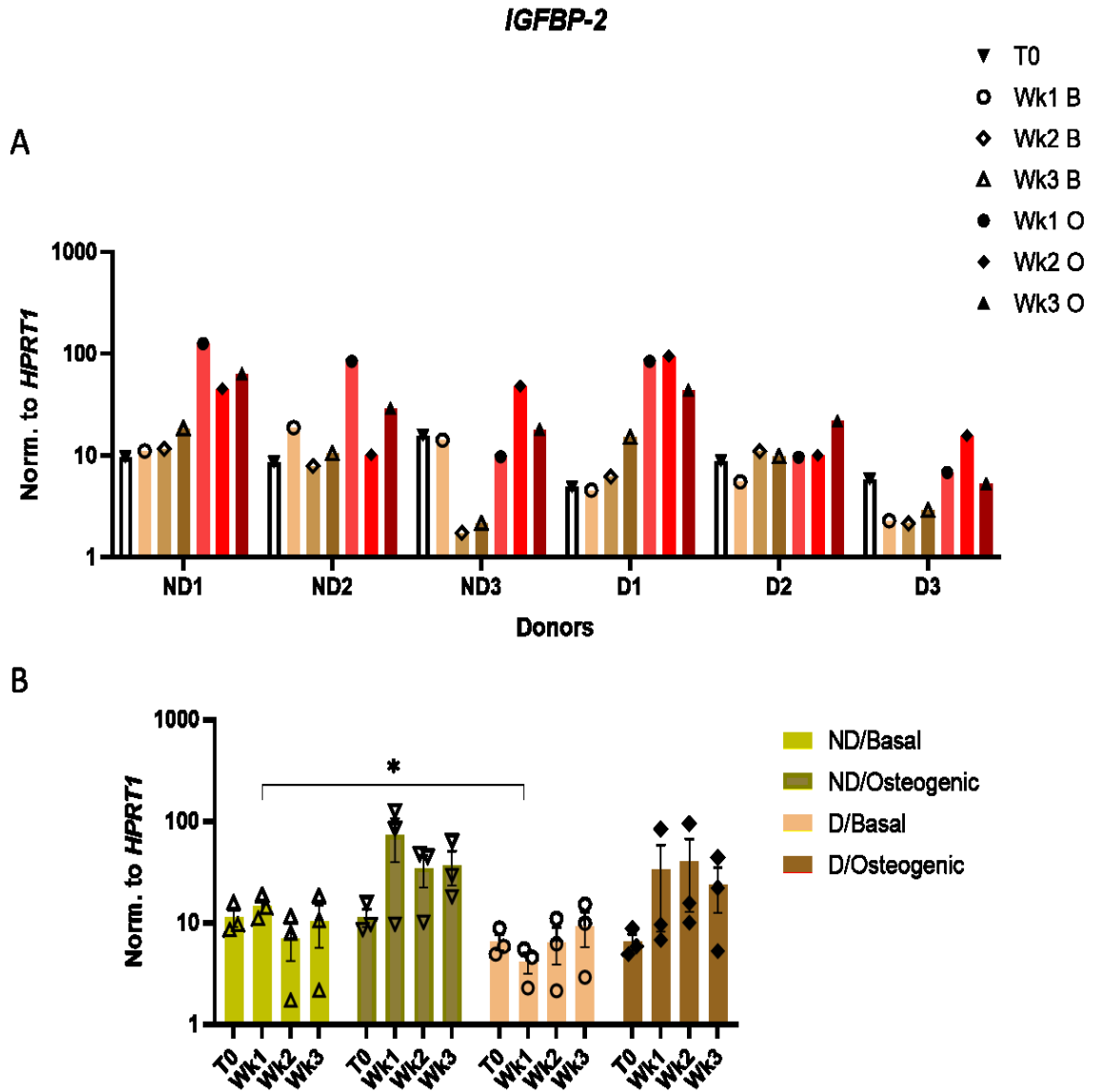


**Figure 6-6: Relative changes in gene expression of *IGFBP-2* in non-diabetic and diabetic BM-MSCs**

A: Gene expression of *IGFBP-2* in individual non-diabetic (ND) and diabetic (D) donors at T0, basal and osteogenic conditions at Wk1, Wk2 and Wk3 time-points.

B: Overall analysis of relative changes in *IGFBP-2* gene expression in ND and D BM-MSCs. Data are presented as mean  $\pm$  SEM (n=3 for each group).

### **6.2.1.7 Relative changes in the expression of *IGFBP-3* gene in non-diabetic and diabetic BM-MSCs**

Figure 6-7(A) shows the expression of *IGFBP-3* in BM-MSCs isolated from individual non-diabetic and diabetic donors. *IGFBP-3* was expressed at the different time-points/culture conditions at variable levels.

Figure 6-7(B) shows the overall analysis of *IGFBP-3* expression in non-diabetic and diabetic BM-MSCs. *IGFBP-3* expression levels were significantly lower in diabetic versus non-diabetic cells in Wk3 basal cultures ( $p < 0.05$ ); and a similar trend was also observed in Wk2 basal cultures. Furthermore, *IGFBP-3* was significantly downregulated in Wk3 osteogenic versus Wk3 basal cultures of non-diabetic BM-MSCs ( $p < 0.05$ ), with similar trends at Wk1 and Wk2 osteogenic cultures. Interestingly, none of these changes were reflected in diabetic BM-MSCs.

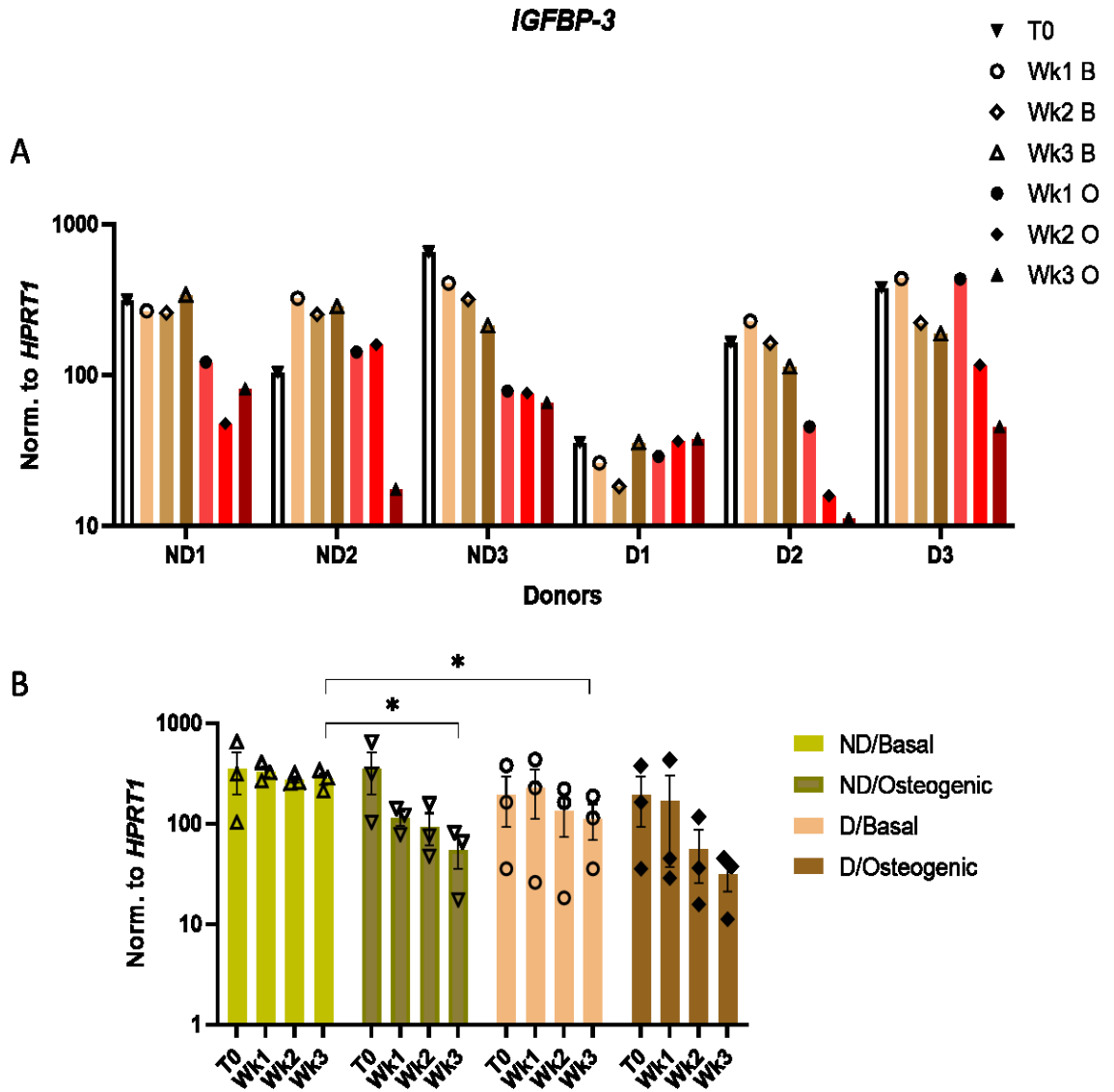


**Figure 6-7: Relative changes in gene expression of *IGFBP-3* in non-diabetic and diabetic BM-MSCs**

A: Gene expression of *IGFBP-3* in individual non-diabetic (ND) and diabetic (D) donors at T0, basal and osteogenic conditions at Wk1, Wk2 and Wk3 time-points.

B: Overall analysis of relative changes in *IGFBP-3* gene expression in ND and D BM-MSCs. Data are presented as mean  $\pm$  SEM (n=3 for each group).

#### **6.2.1.8 Relative changes in the expression of *IGFBP-4* gene in non-diabetic and diabetic BM-MSCs**

Figure 6-8(A) shows the expression of *IGFBP-4* in BM-MSCs isolated from individual non-diabetic and diabetic donors. *IGFBP-4* was expressed abundantly at the different time-points /culture conditions as indicated by the scale of the y axis.

Figure 6-8(B) shows the overall analysis of *IGFBP-4* expression in non-diabetic and diabetic BM-MSCs. *IGFBP-4* expression levels were significantly lower in diabetic versus non-diabetic cells at Wk3 under basal culture conditions ( $p < 0.05$ ). *IGFBP-4* also had a trend of downregulation in Wk2 osteogenic cultures of non-diabetic cells.

### IGFBP-4

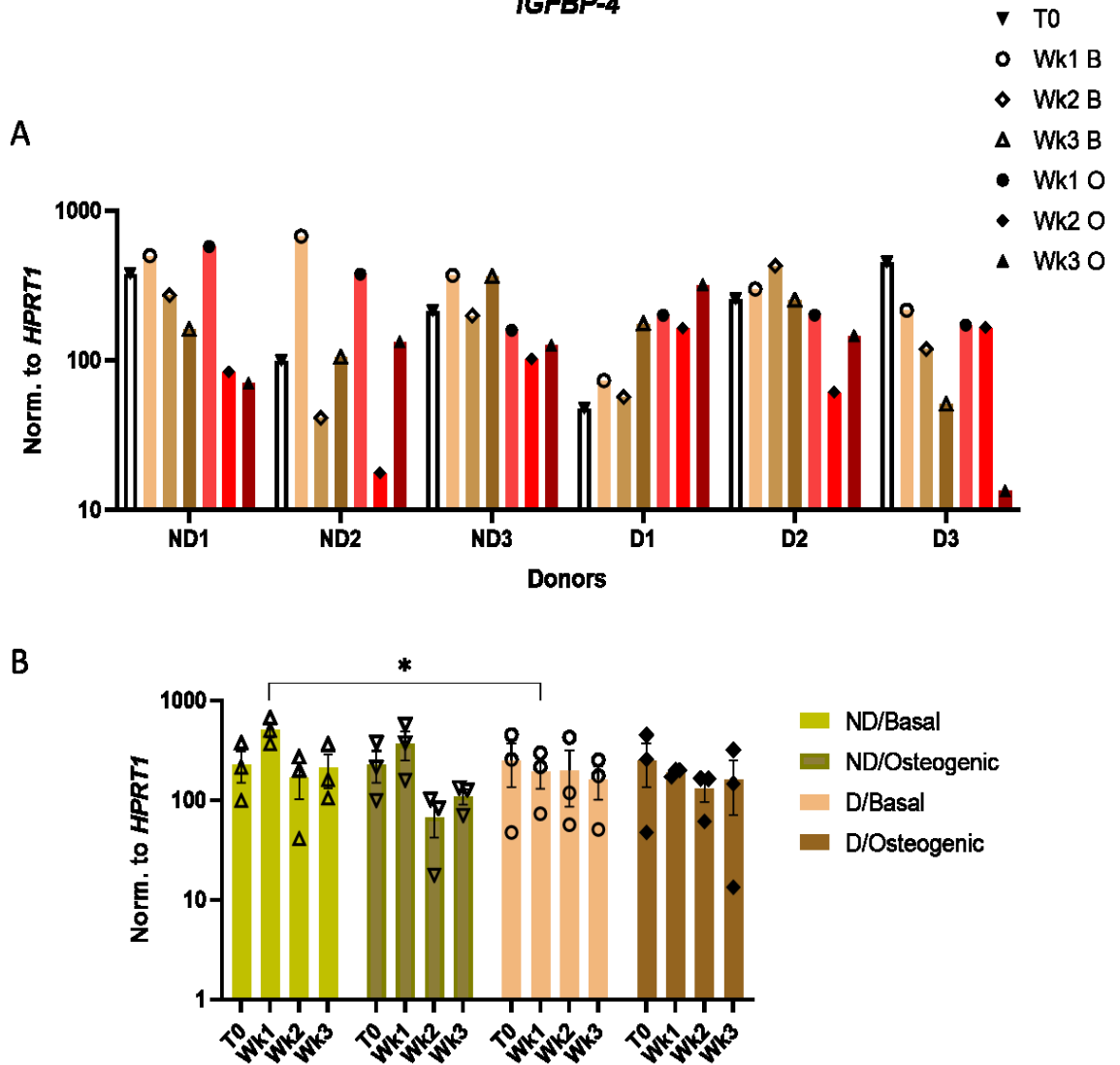


**Figure 6-8: Relative changes in gene expression of *IGFBP-4* in non-diabetic and diabetic BM-MSCs**

A: Gene expression of *IGFBP-4* in individual non-diabetic (ND) and diabetic (D) donors T0, basal and osteogenic conditions at Wk1, Wk2 and Wk3 time-points.

B: Overall analysis of relative changes in *IGFBP-4* gene expression in ND and D BM-MSCs. Data are presented as mean  $\pm$  SEM (n=3 for each group).

#### **6.2.1.9 Relative changes in the expression of *IGFBP-5* gene in non-diabetic and diabetic BM-MSCs**

Figure 6-9(A) shows the expression of *IGFBP-5* in BM-MSCs isolated from individual non-diabetic and diabetic donors. *IGFBP-5* was expressed at the different time-points/culture conditions.

Figure 6-9(B) shows the overall analysis of *IGFBP-5* expression in non-diabetic and diabetic BM-MSCs. There was no trends or significant differences between diabetic and non-diabetic cells. However, *IGFBP-5* showed a trend of downregulation in osteogenic cultures of diabetic and non-diabetic cells across the 3 time-points: Wk1, Wk2 and Wk3.

**IGFBP-5**

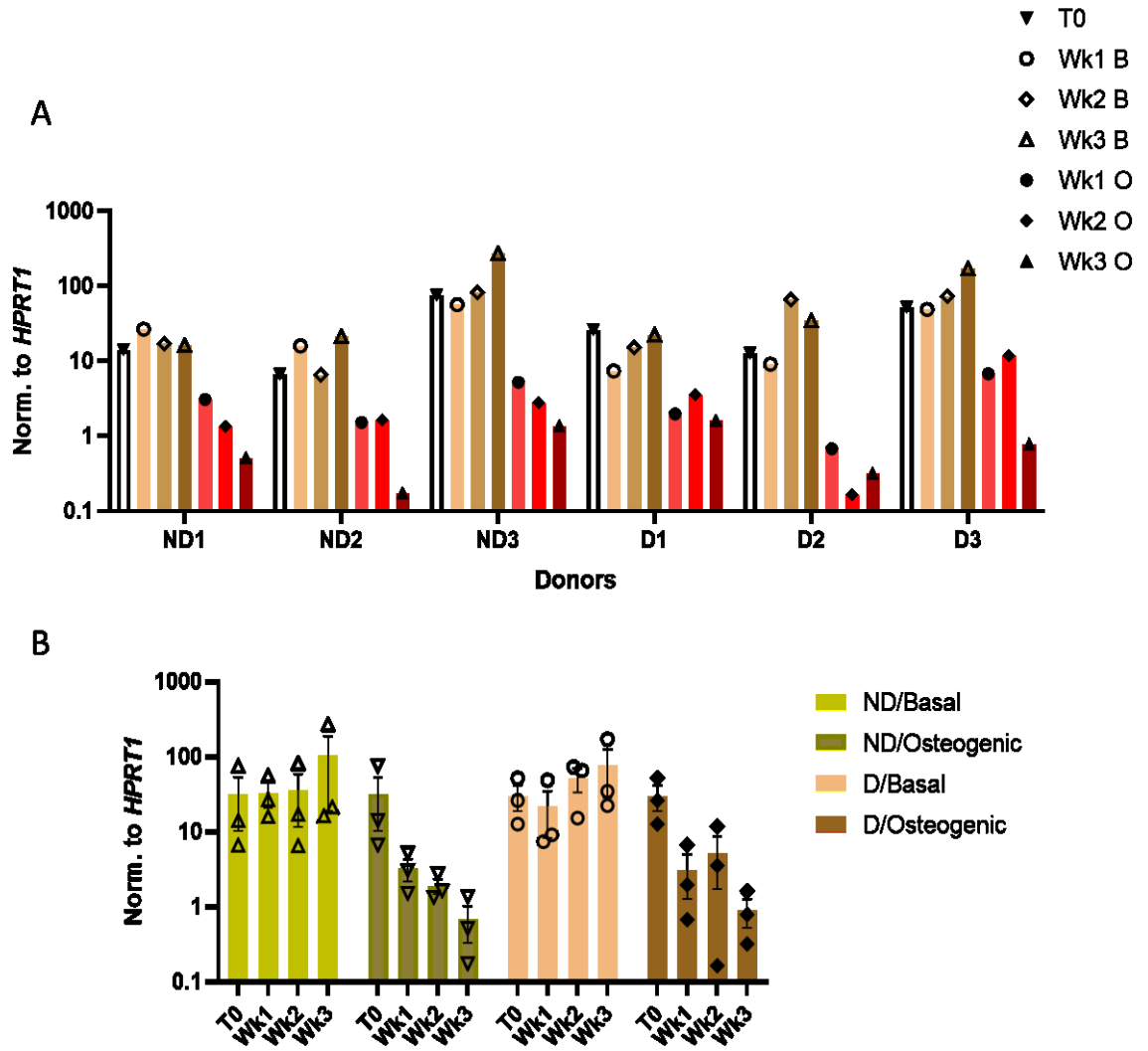


**Figure 6-9: Relative changes in gene expression of *IGFBP-5* in non-diabetic and diabetic BM-MSCs**

A: Gene expression of *IGFBP-5* in individual non-diabetic (ND) and diabetic (D) donors at T0, basal and osteogenic conditions at Wk1, Wk2 and Wk3 time-points.

B: Overall analysis of relative changes in *IGFBP-5* gene expression in ND and D BM-MSCs. Data are presented as mean  $\pm$  SEM (n=3 for each group).

#### **6.2.1.10 Relative changes in the expression of *IGFBP-6* gene in non-diabetic and diabetic BM-MSCs**

Figure 6-10(A) shows the expression of *IGFBP-6* in BM-MSCs from individual non-diabetic and diabetic donors. *IGFBP-6* was expressed at the different time-points/culture conditions, with minimal expression at T0 and Wk2 basal cultures of donor ND2.

Figure 6-10(B) shows the overall analysis of *IGFBP-6* expression in non-diabetic and diabetic BM-MSCs. There were no statistically significant differences in the expression levels of *IGFBP-6* in diabetic versus non-diabetic cells or in basal versus osteogenic cultures. Still, there was a trend of *IGFBP-6* downregulation in Wk3 osteogenic cultures of non-diabetic BM-MSCs without equivalent changes in the diabetic cells under the same culture conditions.

**IGFBP-6**

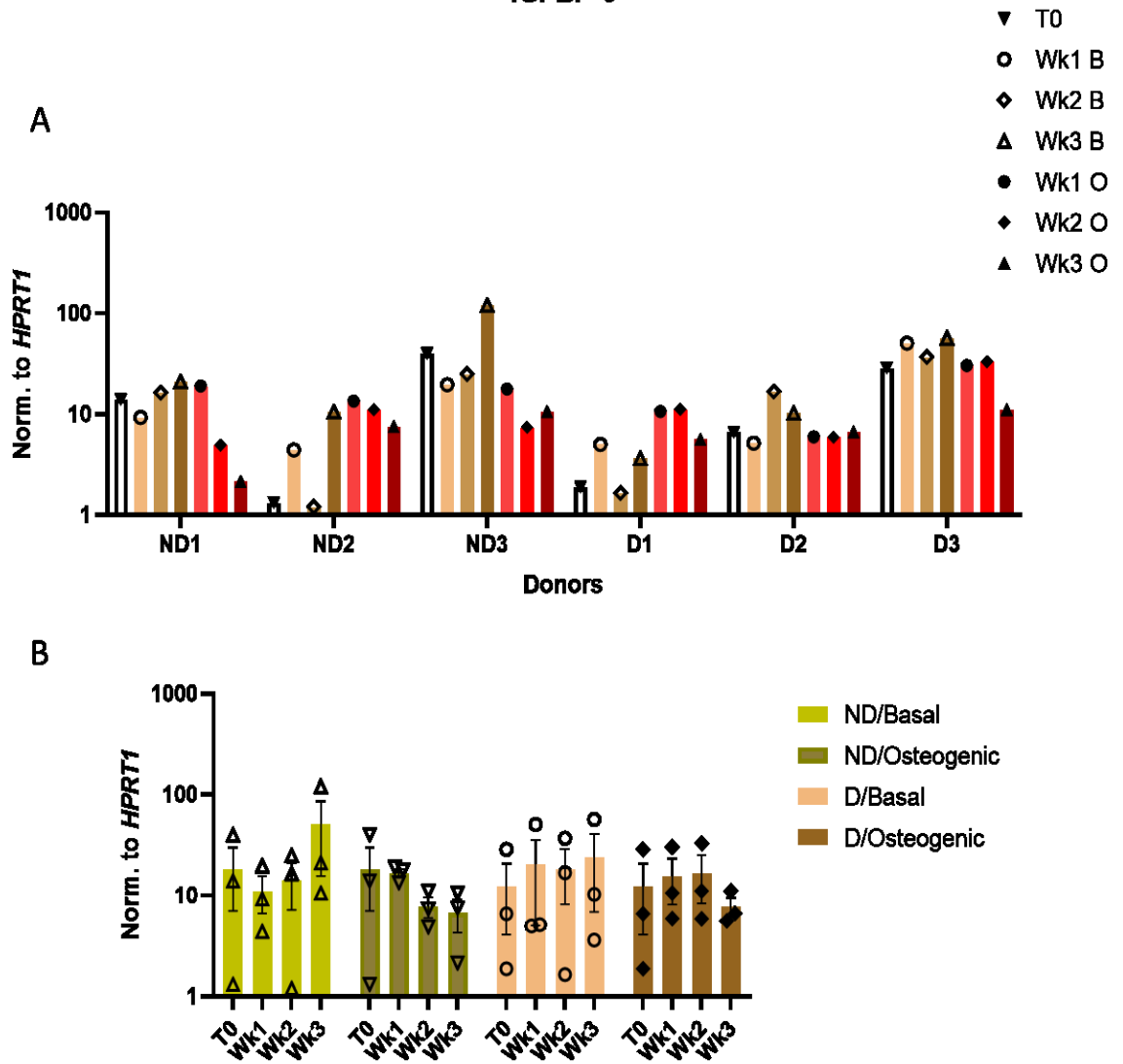


**Figure 6-10: Relative changes in gene expression of *IGFBP-6* in non-diabetic and diabetic BM-MSCs**

A: Gene expression of *IGFBP-6* in individual non-diabetic (ND) and diabetic (D) donors at T0, basal and osteogenic conditions at Wk1, Wk2 and Wk3 time-points.

B: Overall analysis of relative changes in *IGFBP-6* gene expression in ND and D BM-MSCs. Data are presented as mean  $\pm$  SEM (n=3 for each group).

### 6.2.1.11 Comparing the IGF axis gene expression in non-diabetic and diabetic BM-MSCs at baseline (T0)

Figure 6-11 shows relative levels of expression of IGF axis genes at T0 in untreated non-diabetic and diabetic BM-MSCs. Generally non-diabetic and diabetic cells showed similar levels of expression of the IGF axis genes. However, some genes have been expressed at very low levels, such as *IGF-1* and *2*. *IGF-1R* and *IGF-2R*, on the other hand, were also expressed similarly in both cell populations but at relatively higher levels compared to the *IGF-1* and *-2*. Looking at the *IGFBPs*, *IGFBP-1* showed the lowest expression levels, followed by *IGFBP-2*, *IGFBP-5* and *IGFBP-6*, which all showed roughly similar levels of expression. *IGFBP-3* and *IGFBP-4* showed the highest levels of expression among all IGF axis genes.

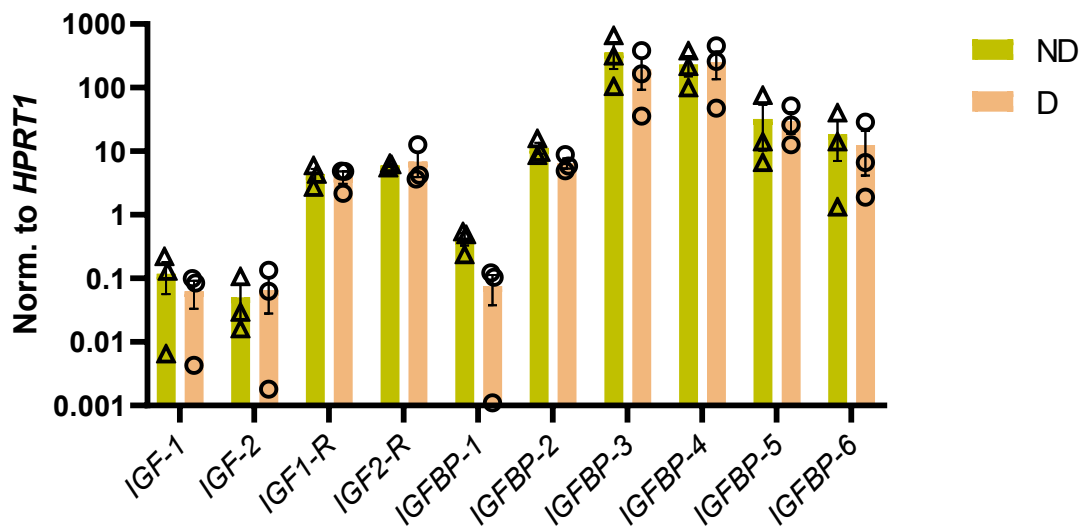


Figure 6-11: Comparing the levels of IGF axis genes expression in non-diabetic and diabetic BM-MSCs at baseline (T0)

## **6.2.2 Protein levels of IGFbps in conditioned media of diabetic and non-diabetic BM-MSCs**

Since qPCR results showed statistically significant changes in expression of *IGFBP-2*, *IGFBP-3* and *IGFBP-4* genes in diabetic versus non-diabetic BM-MSCs at some time-points, the level of these proteins was assessed in the conditioned media of basal and osteogenic cultures of both cell populations using ELISA as described in chapter 3 of this thesis. Conditioned media was collected at time-points week 1, 2 and 3 and samples were appropriately diluted to fall within the kit range following initial optimization. Wk2 and 3 cultures had full media change weekly, hence the concentrations of IGFbps in media collected at each of these 2 time-points are reflective of weekly not cumulative release of each protein. Samples of unconditioned basal and osteogenic media were assayed as controls in each ELISA assay and had negligible concentrations of IGFBP-2, -3 and -4 that were below the detection range of the corresponding ELISA kit.

### **6.2.2.1 IGFBP-2 levels in conditioned media of non-diabetic and diabetic BM-MSCs**

Figure 6-12 shows IGFBP-2 protein concentrations in conditioned media of non-diabetic and diabetic BM-MSCs. There were no statistically significant differences between both cell populations at the different time-points/culture conditions. There were also no statistically significant differences between time-points or between osteogenic versus basal cultures. However, IGFBP-2 had a trend of higher levels in osteogenic cultures compared to basal cultures, mirroring and supporting changes on gene expression level as evidenced by qPCR analysis (Figure 6-6).

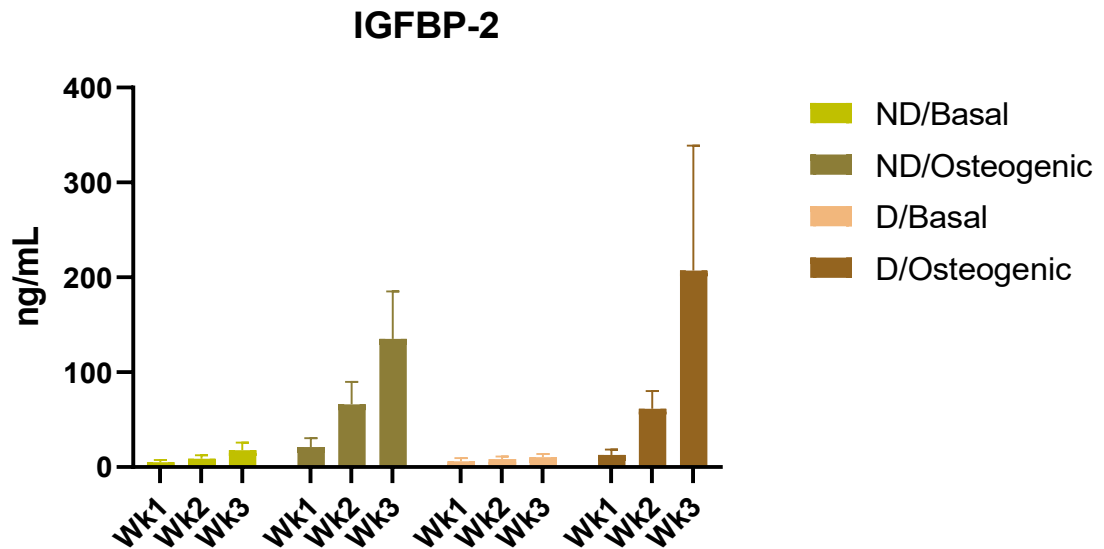


**Figure 6-12: IGFBP-2 levels in conditioned media of non-diabetic and diabetic BM-MSCs**

Data are presented as mean  $\pm$  SEM (n=3 for each group). D: diabetic, ND: non-diabetic.

#### **6.2.2.2 IGFBP-3 levels in conditioned media of non-diabetic and diabetic BM-MSCs**

Figure 6-13 shows IGFBP-3 protein concentrations in conditioned media of non-diabetic and diabetic BM-MSCs. There were no statistically significant differences between both cell populations at the different time-points/culture conditions. Different to qPCR results (Figure 6-7), basal cultures of non-diabetic cells showed statistically significant higher concentrations of IGFBP-3 at Wk3 versus Wk1 and Wk3 versus Wk2 ( $p < 0.05$ ) and a similar trend was observed for basal cultures of diabetic BM-MSCs, but without statistical significance.

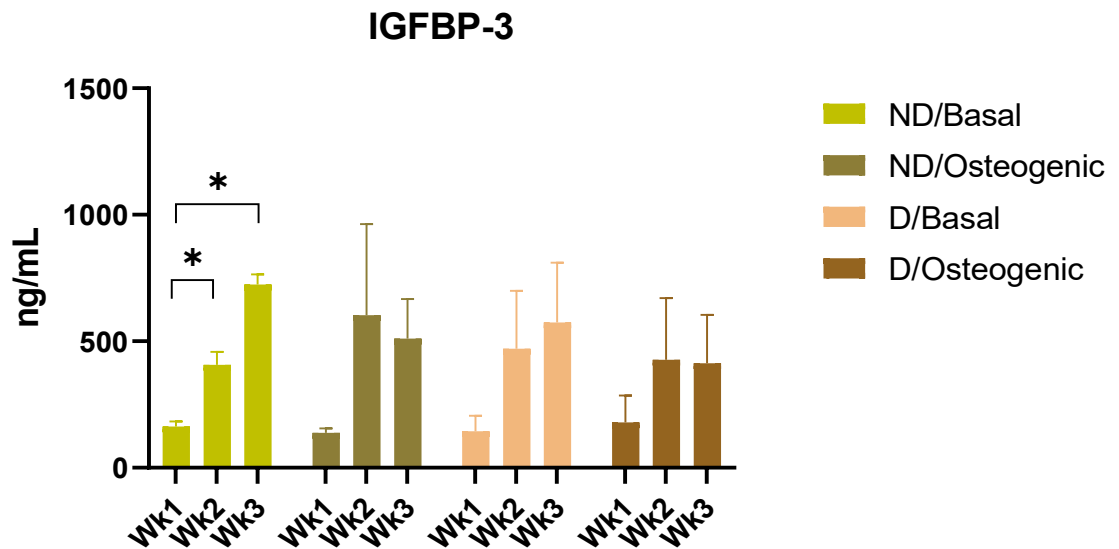


**Figure 6-13: IGFBP-3 levels in conditioned media of non-diabetic and diabetic BM-MSCs**

Data are presented as mean  $\pm$  SEM (n=3 for each group). D: diabetic, ND: non-diabetic. \* p < 0.05.

### 6.2.2.3 IGFBP-4 levels in conditioned media of non-diabetic and diabetic BM-MSCs

Figure 6-14 shows IGFBP-4 protein concentrations in conditioned media of non-diabetic and diabetic BM-MSCs. There were no statistically significant differences between both cell populations at the different time-points/culture conditions. Non-diabetic cells showed statistically significant higher levels of IGFBP-4 under basal conditions at Wk2 versus Wk1; and under osteogenic conditions at Wk3 versus Wk1 and Wk3 versus Wk2 (p < 0.05), indicating time dependant increase of IGFBP-4 concentrations under both culture conditions. Similar to non-diabetic cells, diabetic BM-MSCs showed a trend of time dependant increase of IGFBP-4 concentrations under basal cultures but without reaching statistical significance. Non-diabetic BM-MSCs also showed significantly higher IGFBP-4 concentrations in osteogenic versus basal cultures at Wk3 (p < 0.05); and diabetic cells showed a similar pattern (statistically significant higher IGFBP-4 concentrations in osteogenic versus basal cultures), but at Wk1 (p < 0.05).

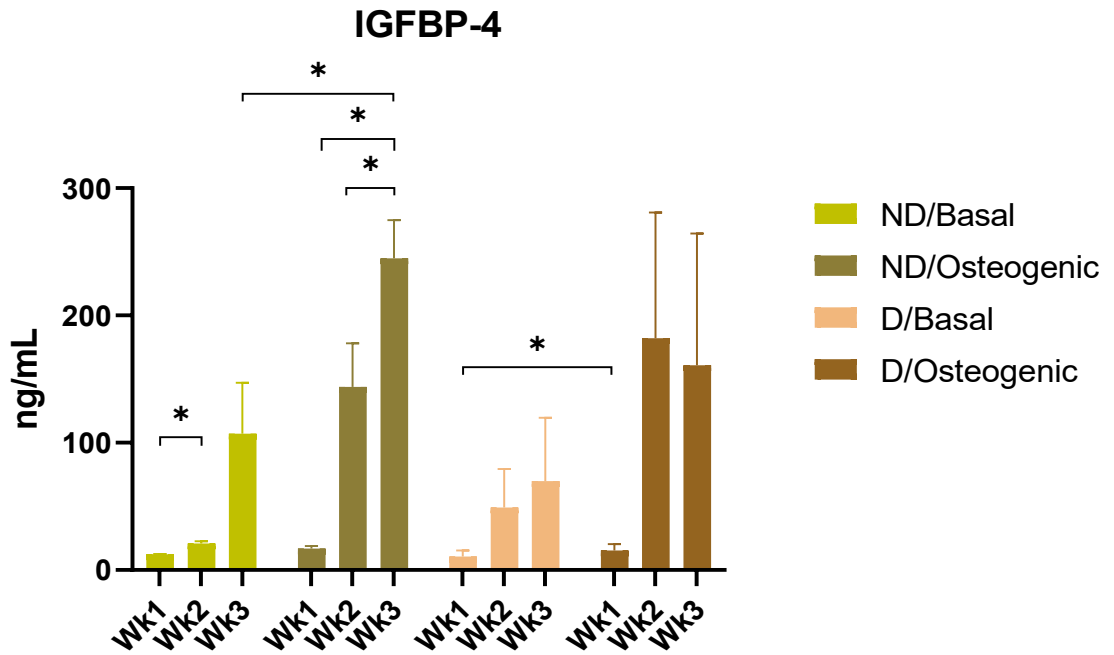


**Figure 6-14: IGFBP-4 levels in conditioned media of non-diabetic and diabetic BM-MSCs**

Data are presented as mean  $\pm$  SEM (n=3 for each group). D: diabetic, ND: non-diabetic. \*  $p < 0.05$ .

## 6.3 Discussion

### 6.3.1 Relative changes in the expression of IGF axis genes in diabetic and non-diabetic BM-MSCs

In this study, diabetic and non-diabetic BM-MSCs were cultured under basal and osteogenic conditions for 3 different durations: 1, 2 and 3 weeks. The capacity of both cells to differentiate into osteogenic lineages has been shown in the previous chapter. In the current chapter, the relative expression of IGF axis genes under these conditions and time-points is discussed.

In accordance with earlier studies reporting that *IGF-1* and *IGF-2* were expressed by human osteoblasts (548), both untreated non-diabetic and diabetic BM-MSCs in the present study expressed *IGF-1* and *IGF-2* at T0. As *IGF-1* was downregulated in osteogenic cultures, its levels of expression in some donors/cells were so low they dropped below the detection level in these conditions. The same observation was true for *IGF-2* but under basal conditions. Furthermore, *IGF-1* levels were generally comparable in non-diabetic and diabetic cells, whether at T0, in basal or osteogenic cultures, with no significant differences or trends observed. In contrast to the presented findings, *IGF-1* was shown to be downregulated in human DPSCs cultured under both basal and osteogenic media supplemented with HG (549), and the critique of diabetic simulating culture conditions was elaborated on in previous chapters of this thesis.

The presented results also disagree with the findings of Khan et al. (550), where BM-MSCs from diabetic mice showed lower levels of *IGF-1* expression. A very similar conclusion was reached by Zhao et al. (551), using BM-MSCs from diabetic rats. Such variable results can be attributed to both studies isolating BM-MSCs from animal models while this thesis investigated human BM-MSCs from patients with T2DM. Nonetheless, MC3T3E1 mouse calvarial cell line cultured in media supplemented with AGE-BSA had a notably different expression profile of *IGF-1*. Cells cultured under basal media and exposed to AGE-BSA had lower expression levels of *IGF-1*, whereas cells cultured in osteogenic media and exposed to AGE-BSA showed no changes of *IGF-1* expression at day 15 and upregulated *IGF-1* expression at day 25 compared to control cultures with BSA

alone. This could indicate a protective effect of osteogenic media against AGE-BSA influence on *IGF-1* expression (552).

*IGF-1* also had a trend of downregulation in osteogenic versus basal cultures of both diabetic and non-diabetic BM-MSCs at 3 time-points (Wk1, Wk2 and Wk3), reaching statistical significance at Wk2 osteogenic cultures of non-diabetic cells ( $p < 0.05$ ) (Figure 6-1). This is most likely due to the use of dexamethasone as a supplement in the osteogenic media in this thesis. Indeed, *IGF-1* downregulation was reported in cultures of rat osteoblasts supplemented with cortisol (553) and also in cultures of rat osteoprogenitor-containing bone cells supplemented with dexamethasone (476). In the second study, this decline was observed at 3 different time-points: 8, 14 and 20 days which are very close to the time-points used in this thesis. Interestingly, dexamethasone in the above mentioned study first induced osteoblast proliferation (up to day 8), followed by their differentiation (day 8-20) as evidenced by increased ALP staining intensity and area. The authors noted that no mineralisation was detected by day 20, probably because of lack of glycerophosphate in the media (476).

The presented results also agree, at least in part, with the work of Birnbaum et al. (554), where mouse calvarial osteoblasts showed initial high levels of *IGF-1* expression (day 10), followed by downregulation at days 20 and 30. The authors suggest that *IGF-1* was upregulated in the initial proliferative phase, reflecting its role as a pro-proliferation growth factor while such role may not be essential during the early and late mineralisation phases (intervals 10-20 and 20-30 days, respectively). Further endorsing dexamethasone potential role behind *IGF-1* downregulation, the fact that MC3T3 cells have shown a gradual (though not statistically significant) increase in *IGF-1* expression from day 5 to day 21 (555); and rats osteoblasts have also shown *IGF-1* upregulation at days 3 and 6 (556) and in both studies the culture media was supplemented only with glycerophosphate and ascorbic acid.

*IGF-1* induced osteogenic differentiation of rat BM-MSCs (387), rabbit PDLSCs (408), human PDLSCs (403), human SCAP (557), human BM-MSCs (378,381) and human DPSCs cultured under HG conditions (549). On the other hand, *IGF-1* stimulated differentiation and activation of rat osteoclasts and subsequent bone resorption *in vitro* (558), and rh-*IGF-1* was also reported to induce osteoclasts differentiation in rat models of orthodontic tooth movement (559). Moreover,

IGF-1 binding to IGF1-R on human osteoclast precursors induced their migration (560) and expression levels of *RANK* and *RANKL* were reduced in long bones of IGF-1 knockout mice, indicating its role in regulating osteoblasts-osteoclasts interaction (561). Taken altogether, IGF-1 most likely regulates bone remodelling through both pro-osteogenic and pro-osteoclastogenic effects (562).

Similar to *IGF-1*, the presented data indicate *IGF-2* levels were very alike in diabetic and non-diabetic BM-MSCs (Figure 6-2). To the best of my knowledge, the expression of *IGF-2* was not fully investigated in BM-MSCs isolated from diabetic patients or cultured under diabetic simulation conditions. The closest comparator in literature would be serum levels of IGF-2 in prediabetic patients. Such investigations were in the context of looking at whether IGF axis proteins could be used as markers of glycaemic control or the risk of developing CVD in patients with T2DM. One study showed that serum levels of IGF-2 did not show significant difference in patients with prediabetes compared to non-diabetic controls (563), which agrees with the presented findings. On the other hand, serum levels of IGF-2 were higher in STZ-induced diabetic rats compared to non-diabetic controls. As such increase was not reflected in rats' livers, the authors suggest this excess IGF-2 could have come from the kidneys as a part of diabetes effects on renal functions (564). Another study reported higher IGF-2 in diabetic rats sera along with its upregulation in the heart, but not renal or hepatic tissues (565) suggesting differential IGF-2 expression patterns in different tissues/organs of diabetic animal models.

*IGF-2* also showed a trend of upregulation in osteogenic versus basal cultures of non-diabetic BM-MSCs at Wk1 time-point. This agrees with the work of Al-Khafaji et al. (325), where *IGF-2* was also upregulated in osteogenic cultures of human DPSCs and the work of Fanganiello et al. (566) on osteogenic differentiation of SHED. IGF-2 was also upregulated during osteogenic differentiation of iliac crest BM-MSCs (466). This is consistent with IGF-2 and its transcription promoters regulating expression of hallmark osteogenic markers, *RUNX2* and *OSX*, and subsequent MSCs osteogenic differentiation (567). Indeed, IGF-2 null mice were around 60% smaller than their wild type counterparts (568) and Silver-Russell syndrome, a congenital disorder manifested by prenatal and postnatal growth retardation, abnormal facial features and body asymmetry, has been linked with epigenetic downregulation of *IGF-2* (569). Also supportive to the current study,

IGF-2 promoted cellular viability and osteogenic differentiation of BM-MSCs cultured on Bio-Oss® bone graft (570). On the other hand, *IGF-2* expression levels showed no changes in rats osteoblasts cultured with dexamethasone, which is not very surprising given the fact that IGF-2 is most active in embryonic bone development in rats but its expression levels drop after birth (476).

IGF-1, IGF-2 and insulin can all bind IGF-1R with IGF-1 having the highest affinity and the GH/IGF-1/IGF1-R axis activity is crucial for normal growth and development (571). This could possibly explain the relatively unchanged expression levels of IGF1-R in both non-diabetic and diabetic cells under basal and osteogenic conditions. Mice MSCs lacking IGF-1R could not differentiate into osteoblasts and mice with knocked out *IGF1-R* had lower bone mass compared to their wild type counterparts (395). The presented results indicate that *IGF1-R* did not show any differences between diabetic and non-diabetic BM-MSCs (Figure 6-3). This is in contrast with the findings of Jiang et al. (572), where IGF1-R on the protein level was higher in PDLSCs cultured under HG versus normoglycemic media, but such discrepancy can be attributed to the different MSCs used in their work and using simulating diabetic micro-environment rather than isolating cells from diabetics. On the other hand, *IGF1-R* was downregulated on both mRNA and protein levels in DPSCs cultured under both basal and osteogenic conditions supplied with HG, similar to IGF-1 as mentioned above (549).

Ferland-McCollough et al. (250) concluded that diabetic BM-MSCs expressed higher levels of adipogenic markers including IGF1-R and platelet-derived growth factor receptor  $\beta$  compared to non-diabetic cells. Other studies did report upregulation of *IGF-1* and *IGF1-R* during BM-MSCs adipogenesis (573). However, more research is needed to confirm how IGF-1/IGF-1R signalling can contribute to both osteogenic and adipogenic differentiation of BM-MSCs and which factors could favour one lineage over the other.

*IGF-1R* also showed no significant changes between basal and osteogenic culture of both diabetic and non-diabetic cells, despite a trend of both *IGF-1* downregulation and *IGF-2* upregulation under osteogenic conditions. This could signpost IGF axis regulating osteogenic differentiation of BM-MSCs through changes in IGFs, rather than IGF-Rs expression levels, which remained relatively stable. Nonetheless, *IGF1-R* overexpression in DPSCs was associated with

increased expression of osteogenic and odontogenic markers and the opposite was observed when *IGF-1R* was inhibited (574), indicating that IGFs axis could coordinate osteogenic differentiation of different MSCs in variable ways. On the other hand, *IGF-1R* was downregulated in dexamethasone treated cultures of rats osteoprogenitor-containing bone cell populations (476), and this disagreement compared to the presented findings could be attributed to the differences in cells source and osteogenic supplements as outlined earlier in this chapter.

*IGF2-R* as discussed earlier lacks a tyrosine kinase domain and thus, its main role is binding IGF-2 to limit its bioavailability and binding to IGF1-R or IR. However, some recent data indicate an active role of IGF-2/IGF2-R in homing of epithelial progenitor cells (575). The presented results show no change in *IGF-2R* expression whether in diabetic versus non-diabetic BM-MSCs or in osteogenic versus basal cultures of both cell populations, designating quite stable levels of expression of this molecule similar to *IGF1-R* (Figure 6-4). However, similar to *IGF1-R*, *IGF2-R* was downregulated in dexamethasone treated cultures of rats osteoprogenitor-containing bone cell populations (476).

*IGFBP-1* had a trend of lower expression in diabetic versus non-diabetic BM-MSCs at T0, Wk1 basal and Wk2 osteogenic cultures. Interestingly, although none were statistically significant, these trends were detectable in 3 different culture conditions: untreated, basal and osteogenic (Figure 6-5). This agrees with the work of Yan et al. (549), where *IGFBP-1* was downregulated in DPSCs cultured under basal and osteogenic media supplied with HG. Nevertheless, IGFBP-1 serum levels were higher in patients with T2DM compared to controls and displayed negative correlation with IGF-1 levels in both diabetics and controls, indicating IGFBP-1 potential inhibitory effects on IGF-1 activity (576). On the other hand, IGFBP-1 serum levels were lower in patients with impaired glucose tolerance and correlated positively with insulin sensitivity (342). Rajpathak et al. (577) proposed that insulin could induce *IGFBP-1* downregulation to allow for higher levels of free IGF-1 as a compensatory mechanism for the insulin resistance. To conclude, further studies could be needed to elucidate the relationship between IGFBP-1 and different stages of insulin resistance and T2DM.

The presented data indicate *IGFBP-1* had a trend of lower expression in Wk1 osteogenic versus basal cultures of diabetic cells. Since IGFBP-1 stimulated osteoclasts differentiation and ensuing bone resorption (578), this could mean BM-MSCs or differentiating osteoblasts in their normal niche would produce lower levels of IGFBP-1 to limit osteoclastogenesis during phases of active bone deposition. This is also consistent with studies showing higher serum levels of IGFBP-1 associated with lower BMD in adult males (579) and higher fracture risk in elderly females (580). Furthermore, osteoprogenitor-containing bone cell populations isolated from female rats also showed lower expression levels of *IGFBP-1* in dexamethasone cultures at day 14 and 20 (476).

*IGFBP-2* expression levels were significantly lower in Wk1 basal cultures of diabetic versus non-diabetic BM-MSCs ( $p < 0.05$ ) (Figure 6-6). Given the fact that IGFBP-2 was repeatedly shown to have pro-angiogenic roles (581,582), such lowered levels of expression in diabetic cells could reflect the well documented poor angiogenic capacities of different tissues in diabetics (583), which is behind a number of diabetic complications such as poor wound healing. Indeed, angiogenic potential of AT-MSCs from patients with T2DM and CVD (584) or even T2DM alone (448) were reduced, and the same was observed when BM-MSCs were cultured with serum of T2DM patients (277,585) or HG (586).

Interestingly, BM-MSCs from diabetic rats showed poor angiogenic potentials in *in vivo* models compared to non-diabetic cells despite the fact that diabetic cells cultured *in vitro* expressed higher levels of angiogenic and lower levels of anti-angiogenic markers genes (253). This discrepancy highlights the possibility of different characters of MSCs in *in vitro* culture settings, compared to their natural niches or upon transplantation where vasculature, immunity and generally the microenvironment could influence MSCs behaviour.

Here in the present study, data showed a trend of *IGFBP-2* upregulation in osteogenic cultures compared to basal ones in both diabetic (Wk1 and Wk3) and non-diabetic (Wk2 and Wk3) cells, possibly because IGFBP-2 could stimulate osteogenesis as shown earlier, where IGFBP-2 induced osteoblastic differentiation of murine MC-3T3 cells independently of IGF-1 through binding to receptor tyrosine phosphatase  $\beta$  (587). The presented data are also supported by the work of Cheng et al. (588), where *IGFBP-2* was upregulated in dexamethasone treated human BM-MSCs at days 5 and 7; and the work of Jia

et al. (476), where *IGFBP-2* was upregulated in dexamethasone treated murine osteoprogenitor-containing bone cell populations at days 8, 14 and 20 (roughly parallel to the time-points used in this thesis).

The above findings are also consistent with other studies reporting *IGFBP-2* upregulation in osteogenic cultures of MSCs. For instance, BM-MSCs cultured under exposure to  $10^{-7}$  M (100 nM) dexamethasone showed upregulation of both *IGF-2* and *IGFBP-2* compared to basal cultures (589). Despite Hamidouche et al. (589) using different osteogenic supplements (dexamethasone versus a combination of ascorbic acid, glycerophosphate and dexamethasone in the present study) at different concentrations (100 nM dexamethasone versus 10 nM here in this study) and different time-points (3, 7, and 14 days versus 1, 2 and 3 weeks) to this thesis, both studies observed upregulation of *IGFBP-2* in osteogenic cultures. The presented results here also agree with those of Alkharobi et al. (350), where IGF axis was investigated in DPSCs from healthy and carious teeth and *IGFBP-2* was upregulated in osteogenic cultures of both cell populations. Moreover, this upregulation was coupled with *IGFBP-3* downregulation and both phenomena enhanced IGF-1 pro-osteogenic effect when added to DPSCs cultures (350).

Experimental manipulation of *IGFBP-2* in animal models has shown controversial results. *IGFBP-2* overexpression leads to shortening of wing long bones in chick embryos through inhibition of chondrocytes proliferation in early phases of long bones development. Moreover, *IGFBP-2* overexpression blocked IGF-1 and -2 mediated stimulation of chondrocytes proliferation and matrix synthesis (590). In contrast, preosteoblasts isolated from *IGFBP-2* null mice showed weaker expression of OCN compared to cells from controls and their osteogenic potentials were improved by adding exogenous *IGFBP-2* to the culture media (587). Notwithstanding, *IGFBP-2* was shown to be essential for differentiation of mature and functioning osteoclasts (591). Taken altogether, this suggests a complex role of *IGFBP-2* fine tuning bone turnover rather than a simple one way pro-osteogenic impact.

*IGFBP-3* showed significantly lower expression levels in diabetic versus non-diabetic cells at Wk3B cultures ( $p < 0.05$ ) (Figure 6-7). This could be explained by the hyperinsulinemia usually associated with T2DM compensating for the insulin resistance (592), as *IGFBP-3* was shown to be suppressed by insulin (593).

These findings are consistent with earlier reports of reduced *IGFBP-3* expression in subcutaneous adipose tissue of diabetics, which may reflect impaired differentiation capacities of adipose cells favouring more fat accumulation in non adipose tissues and the ensuing insulin resistance (594). Indeed, *IGFBP-3* could regulate adipocytes differentiation upon binding to PAPP through TGF- $\beta$  pathway (595).

*IGFBP-3* was significantly downregulated in osteogenic versus basal cultures of non-diabetic BM-MSCs at Wk3 ( $p < 0.05$ ) with a trend of downregulation at Wk1 and Wk2 time-points. One possible explanation is that, similar to IGF-1, dexamethasone could be behind this observation, as it was reported earlier to reduce *IGFBP-3* expression in human BM-MSCs (588) and rats hepatocytes (596). A second plausible theory is related to *IGFBP-3* overexpression having anti-proliferative effect on mouse fibroblasts that was independent of IGF-1/IGF1-R pathway (597). As shown in chapter 5 of this thesis and reported earlier (598), BM-MSCs cultured under osteogenic media were generally more confluent compared to basal media controls and this, at least in part, could be attributed to *IGFBP-3* downregulation. Thirdly, since *IGFBP-3* is the major *IGFBP* in serum binding around 90% of IGFs and decreasing their availability to bind IGF-Rs (327), *IGFBP-3* downregulation in osteogenic media could allow for higher levels of free IGFs to bind their receptors and exert their pro-proliferation and pro-osteogenic effects. As mentioned earlier, Alkharobi et al. (350) reported not just *IGFBP-3* being downregulated in osteogenic cultures of DPSCs, but also that co-administration of *IGFBP-3* and IGF-1 inhibited IGF-1 pro-osteogenic effects, which is supported by earlier reports (599).

*IGFBP-3* was also downregulated in day 20 cultures of rat bone cells supplemented with dexamethasone, despite initial upregulation at days 8 and 14 (476), which agrees in part with the findings of the current study. The difference in *IGFBP-3* expression profile at the earlier time-points could be due the difference in cells source (human in this thesis versus rats), cell population (BM-MSCs versus osteoprogenitor-containing bone cells) and the culture conditions (3 osteogenic supplements including dexamethasone versus dexamethasone only). While inhibitory effects of *IGFBP-3* are well documented, *IGFBP-3* could potentiate IGF-1 signalling by binding to *IGFBP-3* putative transmembrane

receptors and subsequent production of sphingosine-1-phosphate (S1P) and increased IGF1-R tyrosine phosphorylation (600).

*IGFBP-4* showed significantly lower expression levels by diabetic versus non-diabetic BM-MSCs at Wk1B cultures ( $p < 0.05$ ) (Figure 6-8). To the best of my knowledge, there are as yet no other reports of *IGFBP-4* expression by BM-MSCs isolated from T2DM patients. However, porcine vascular smooth muscles cells cultured under HG conditions showed similar gene expression levels of *IGFBP-4*, but lower protein levels compared to controls. This coincided with increased *IGFBP-4* proteolysis and IGF-1 levels in HG cultures, which could mediate endothelial proliferation and contribute to CVD in diabetics (601). The presented results also agree with the work of Hjortebjerg et al. (316), where diabetic patients had lower serum levels of *IGFBP-4*, and the *IGFBP-4* fragments resulting from its proteolysis in serum could serve as a marker of CVD risk in diabetics (316).

Conversely, serum levels of *IGFBP-4* in diabetic patients were reported to be similar (576), as well as lower (316), compared to controls and diabetic animal models showed higher serum levels of *IGFBP-4* (602). Such contrasting findings should be considered given the fact that liver is the main source of serum *IGFBPs* with endocrine effects while almost every other tissue produces *IGFBPs*, albeit at variable levels, acting in autocrine/paracrine fashion (603). Therefore, serum levels of *IGFBPs* may not necessarily indicate or correlate with expression levels in other tissues/cells including BM-MSCs.

*IGFBP-4* showed a trend of downregulation in osteogenic versus basal cultures of non-diabetic BM-MSCs at Wk2. Since osteogenic cultures in this study were typically more confluent than their basal counterparts, such downregulation is possibly consistent with earlier reports of general anti-proliferative and anti-osteogenic effects of *IGFBP-4*. For instance, *IGFBP-4* treated cultures of rats BM-MSCs showed lower proliferation rates, while its immunodepletion had the reverse effect (604). Transgenic mice overexpressing *IGFBP-4* had lower bone volume and diminished postnatal bone growth (605). However, other studies reported pro-osteogenic effects of *IGFBP-4*, where its systemic administration amplified serum levels of OCN, ALP and free IGF-1 in mice combined with higher bone formation rates. The authors suggested *IGFBP-4* proteolysis and subsequent enhanced bioavailability of free IGF-1 contributed to these changes (606).

Furthermore, one study reported no significant change of *IGFBP-4* expression in dexamethasone treated cultures of rat osteoblasts at day 8, but this was followed by downregulation at day 14 and then upregulation at day 20. Such changes were possibly related to the different phases of osteogenic differentiation: early proliferation (where *IGFBP-4* downregulation could prevent its inhibitory effects on IGF-1) followed by active differentiation (*IGFBP-4* upregulation possibly suppresses proliferative effects of IGF-1) (476). Another interesting report concluded that *IGFBP-4* exhibited both negative and positive control of IGF-2 mediated growth and that *IGFBP-4* expression was essential for optimal *IGF-2* activity (607). Such complex and sometimes contradictory data on *IGFBP-4* role in osteogenesis indicates it might be worth of further investigation.

Diabetic and non-diabetic BM-MSCs expressed *IGFBP-5* at similar levels, without statistically significant differences or trends of differences (Figure 6-9). Again to the best of my knowledge, expression of *IGFBP-5* in diabetic BM-MSCs is yet to be fully investigated. However, serum levels of *IGFBP-5* were lower in T2DM patients compared to controls (576), but higher in female adolescents with T1DM (608). As mentioned earlier, such findings should be carefully interpreted because liver is the main source of circulating *IGFBPs* and therefore serum levels may not reflect *IGFBPs* expression patterns in individual tissues/organs (603).

*IGFBP-5* showed a trend of downregulation in osteogenic cultures versus basal cultures of both diabetic and non-diabetic cells at Wk1, 2 and 3 cultures. This is in contrast to previous reports of *IGFBP-5* upregulation in osteogenic cultures of BM-MSCs, PDLSCs, AT-MSCs and Wharton's Jelly MSCs (609) using a commercial osteogenic differentiation kit, which may not contain the same osteogenic supplements used in the current study. It is possible that, similar to other IGF axis genes, this downregulation of *IGFBP-5* in osteogenic media observed in the current study is possibly attributed to the use of dexamethasone. Indeed, *IGFBP-5* was downregulated in dexamethasone treated cultures of human BM pre-osteoblastic cells contributing to increased levels of IGF-2 and both changes supported the overall pro-osteogenic effect of dexamethasone in these cultures (588). In contrast, *IGFBP-5* was downregulated during osteogenic differentiation of the murine NIH3T3 fibroblast cell line using dexamethasone alone or a combination of dexamethasone and vitamin D, but not vitamin D alone (610). Although *IGFBP-5* expression did not change during

osteogenic differentiation of DPSCs using dexamethasone and ascorbic acid, exogenous IGFBP-5 inhibited the pro-osteogenic effects of IGF-1 in these cells (325). Nevertheless, *IGFBP-5* expression levels showed no change in response to dexamethasone in rat osteoprogenitor-containing bone cell populations (476). This supports the notion of the intricate regulation of *IGFBP-5* expression by dexamethasone. Moreover, these opposing effects of dexamethasone on *IGFBP-5* expression could be attributed to the different cells used in the above mentioned studies (325,476,610) compared to this thesis.

In contrast, exogenous IGFBP-5 has been shown to enhance osteogenic and odontogenic potentials of different types of MSCs, including BM-MSCs and PDLSCs (374), as well as DPSCs (611). IGFBP-5 transfection into Wharton's jelly MSCs also enhanced their osteogenic potentials in monolayer cultures and upon transplantation into *in vivo* periodontal defects (609). These paradoxical effects of IGFBP-5 have been described earlier, where exogenous IGFBP-5 is more likely to bind IGF-1 and regulate IGF-1/IGF1-R axis, while endogenous IGFBP-5 could bind to potential nuclear receptors (612). Indeed, IGFBP-5 could bind to nuclear vitamin D receptor in human osteosarcoma cells lines (613). On the other hand, *IGFBP-5* overexpression decreased expression of osteogenic markers in MC3T3 cells (614) and both exogenous addition and adenoviral transfection of IGFBP-5 inhibited BMP-2 induced osteogenic differentiation of murine MSCs (615).

*IGFBP-6* showed a trend of downregulation in Wk3 osteogenic versus basal cultures of non-diabetic cells only (Figure 6-10). Distinct from other IGFBPs, IGFBP-6 has higher affinity to bind IGF-2 compared to IGF-1. Thus, IGFBP-6 inhibits IGF-2 effects by limiting its binding to IGF-1R (616). As a result, *IGFBP-6* downregulation in osteogenic media could contribute to higher availability of IGF-2 under these conditions. Moreover, IGFBP-6 has been shown to promote apoptosis and inhibits the anti-apoptotic effects of IGFs in some cancer types (617), thus its downregulation in osteogenic media could have contributed to the increased cell density observed in these cultures. IGFBP-6 exerts these pro-apoptotic effects independently of IGFs as well through translocation to the nucleus and modulating DNA repair process (618). Likewise, IGF-2 weak immunoreactivity combined with IGFBP-6 positive immunostaining in human

epithelial cells of Malassez could explain the physiologic non-proliferative status of these cells (619).

Comprehensive analysis of IGF axis genes expression has been evaluated in different types of cancers, including osteosarcoma (620), prostate cancer (621) and ovarian cancer (622). However only a few studies explored IGF axis in stem cells, and the work of Al-Khafaji et al. (325) on DPSCs is a notable example. Looking at the overall expression patterns of different IGF axis genes at T0, the presented data shows that the differences between diabetic and non-diabetic BM-MSCs are not very dramatic (Figure 6-11). Both cell population showed relatively low expression levels of IGF-1 and IGF-2, which is in part consistent with the work of Al-Khafaji et al. (325), as they detected *IGF-2*, but not *IGF-1*, in DPSCs cultures. The presented data show that these relatively low levels of expression of *IGF-1* and *IGF-2* are coupled with relatively higher expression of their receptors in both diabetic and non-diabetic BM-MSCs. Al-Khafaji et al. (325) suggested IGFs could be sourced out from the rich vasculature of dental pulp or produced by neighbouring cells and bind to DPSCs in a paracrine manner. Such scenarios could be valid for BM-MSCs as well. It is possible that the OA status of BM-MSCs used in the current study or the donors' age could have contributed to these low expression levels of both IGFs.

*IGFBP-1* was the least expressed IGFBP in BM-MSCs cultures and this agrees with the findings of Al-Khafaji et al. (325). This was also the case with BM-MSCs isolated from rats vertebrae and femurs (623). Following *IGFBP-1*, the presented data shows the order of expression levels was *IGFBP-2* < *IGFBP-5* and -6 < *IGFBP-3* and 4, meaning that *IGFBP-3* and 4 were the most abundant IGFBPs in BM-MSCs conditioned media. This is slightly different from the findings of Al-Khafaji et al. (325), where *IGFBP-1* was followed by *IGFBP-3*, -6, -2 and then *IGFBP-5* and -4, which had the highest expression levels in DPSCs cultures. On the other hand, BM-MSCs of rats vertebrae expressed *IGFBP-2* to -6, with *IGFBP-2*, -4 and -6 showing the highest expression levels and BM-MSCs of rats femurs expressing only *IGFBP-4* and -6 (623).

### **6.3.2 Protein levels of IGFBPs in conditioned media of diabetic and non-diabetic BM-MSCs**

Although *IGFBP-2*, -3 and -4 showed statistically significant lower expression on gene level in diabetic versus non-diabetic BM-MSCs at certain time-points, the

protein levels of these IGFBPs in conditioned media showed no statistically significant differences in diabetic versus non-diabetic cultures at any time-point or culture condition. This means that lower mRNA levels did not eventually caused similar alteration of released protein levels and diabetic BM-MSCs would still have comparable levels of these proteins compared to their non-diabetic counterparts. Although mRNA abundances were thought to be the key determining factor of protein levels, this notion seemed to be too simplistic (624). Protein levels in fact are the result of complex interplay of post-transcriptional, translational and protein degradation processes (625), and such discrepancy between mRNA and protein levels have been described in large scale transcriptomic and proteomic analyses (626).

Some of the factors regulating the rate of mRNA translation into protein include mRNA secondary structure, regulatory small RNA (sRNA) that influence mRNA stability and its binding rate to ribosomes, ribosomal occupancy, mRNA sequestration and subsequent lack of translation (627). Following translation, protein levels are affected by post translational modification, including protein folding, interactions with other proteins, as well as degradation through the ubiquitin–proteasome system and autophagy (628).

Because IGFBPs can bind IGFs, as well as cell receptors and ECM proteins to exert their IGFs independent functions (629), it is possible some of the IGFBPs were bound to their receptors on cell membranes and consequently were not included in the ELISA assay, as it used cell culture supernatant as a substrate. Furthermore, the assays could have measured free rather than total IGFBPs, thus excluding IGFBPs molecules bound to IGFs.

These results are in agreement with those of Cassidy et al. (248), where levels of IGFBP-2 and -3 were similar in conditioned media of diabetic and non-diabetic BM-MSCs. Similarly, serum levels of IGFBP-2 and -3 were similar in obese diabetic females compared to controls (594). On the other hand, serum levels of IGFBP-2 were higher and IGFBP-3 were lower in obese diabetic patients versus controls (630). However, because IGFBPs are mainly synthesized in the liver (631), serum concentrations of IGFBPs are more likely to indicate their hepatic production rather than their secretion by other tissues.

Consistent with qPCR results, IGFBP-2 concentrations were higher in osteogenic versus basal conditioned media of both diabetic and non-diabetic BM-MSCs

(Figure 6-12). Nonetheless, ELISA results have revealed an interesting finding different to qPCR, which is a trend of time dependant increase of IGFBP-2 concentrations in osteogenic cultures of both non-diabetic and diabetic BM-MSCs. Because media was fully changed weekly for Wk2 and Wk3 cultures, this rise of concentrations is not cumulative, but expressive of weekly release. One possible explanation is the higher cell confluence or numbers as the culture duration increased. Another conceivable scenario is lower rates of IGFBP-2 degradation by proteolytic enzymes, such as pregnancy associated plasma protein A (PAPP-A), which was detected in cultures of DPSCs (325). Although PAPP-A has been described as the main proteinase of IGFBP-4, IGFBP-2 was reported as a potential substrate as well (356,632). This pattern of *IGFBP-2* upregulation and subsequent higher protein levels in osteogenic cultures is consistent with the work of Alkharobi et al. (350) on DPSCs; and suggests the possibility of similar expression profile of IGFBP-2 across different types of stem cells under osteogenic conditions.

Concentrations of IGFBP-3 also showed a trend of time dependant increase in basal cultures of both diabetic and non-diabetic cells, reaching statistical significance at Wk3 versus Wk2 and Wk3 versus Wk1 basal cultures of non-diabetic cells (Figure 6-13). This is different to qPCR results where IGFBP-3 expression levels remained relatively unchanged. Free IGFBP-3 has a half-life of around 30-90 mins (633), which means it could be degraded within a few hours and the observed higher concentrations in Wk2 and Wk3 basal cultures are more likely reflecting 'fresh' rather than cumulative production by BM-MSCs. This also indicates that the actual levels of produced IGFBP-3 could be higher than those measured using the ELISA assay.

Additionally, while osteogenic cultures showed *IGFBP-3* downregulation compared to basal cultures, this was not the case for protein levels that showed on differences between both culture conditions. In both cases it could be inhibition of IGFBP-3 proteinases, such as PAPP-A2 (634), that lead to these relatively higher concentrations. Similar to PAPP-A, PAPP-A2 is a metalloproteinase specific for cleavage of IGFBP-3 and -5, which are the main IGFBPs binding to IGFs in the circulation and thus, PAPP-A2 can play a significant role in controlling serum levels of the IGFs (634).

The same can be true for IGFBP-4 concentrations, which showed a trend of time dependant increases in basal and osteogenic cultures of diabetic and non-diabetic cells, with statistically significant differences at Wk2 versus Wk1 in basal cultures of non-diabetic cells, and Wk3 versus Wk2 and Wk3 versus Wk1 osteogenic cultures of non-diabetic cells ( $p < 0.05$ ) (Figure 6-14). IGFBP-4 levels were also higher in osteogenic versus basal cultures of diabetic cells at Wk1 and non-diabetic cells at Wk3. In both cases, such changes could be attributed to inhibition of IGFBP-4 proteinases, most notably PAPP-A, either in long term cultures or under osteogenic conditions. Nonetheless, Al-Khafaji et al. (325) reported the opposite, with *PAPP-A* upregulated and stanniocalcin-2 (*STC-2*, an inhibitor of PAPP-A) downregulated in osteogenic cultures of DPSCs. This could be attributed to the different cell origin or culture duration as DPSCs were cultured for 1 week and ELISA data showed minimal changes at Wk1 time-point in the present thesis. Measuring gene expression and protein concentrations of PAPP-A, -A2, and *STC-2* in future experiments would give more details about the regulation of IGFBPs protein levels in BM-MSCs cultures.

Other IGFBPs proteinases include MMPs, which were shown to degrade IGFBP-3 and -5, cathepsins, which could degrade IGFBPs in both intracellular and extracellular contexts, and complement protein 1s (635). While these proteinases could cleave different IGFBPs, cleavage of IGFBP-4 could be restricted to PAPP-A, a process which is stringently dependent upon IGFBP-4 binding to IGF-1 or -2 (636). Moreover, a number of inflammatory cytokines, such as IL-1 $\beta$  and TNF- $\alpha$ , induce *PAPP-A* expression, with its upregulation observed in a number of tissue injury models (636).

The time dependant rises in levels of IGFBP-2 and -4 (and to a lesser extent in IGFBP-3), could be attributed to higher cell numbers as culture duration extends, specially that gene expression levels of the 3 IGFBPs remained almost steady in basal cultures. Higher rates of cell proliferation could also explain the higher IGFBP-4 concentrations in osteogenic versus basal cultures, where qPCR data showed no evidence of *IGFBP-4* upregulation. Additionally, these higher concentrations could be due to release of stored IGFBPs, rather than active *de novo* synthesis by BM-MSCs, but such distinction can be made by adding protein synthesis inhibitors, such as cycloheximide, to the cultures as previously reported (105). For instance, higher IGFBP-3 levels in media of culture human fibroblasts

was attributed to 2 different sources: IGF-1 releasing IGFBP-3 bound to cell surface receptors and ECM, and TGF- $\beta$  stimulating *de novo* IGFBP-3 synthesis (106).

In conclusion, although *IGFBP-2*, *-3* and *-4* showed statistically significant lower gene expression levels in cultures of diabetic versus non-diabetic BM-MSCs, these differences were not detected on the protein level. On the other hand, *IGFBP-2* showed higher expression levels in osteogenic versus basal cultures of both diabetic and non-diabetic BM-MSCs on both gene and protein levels, while *IGFBP-3* showed lower expression levels in osteogenic versus basal cultures of diabetic and non-diabetic cells only on gene levels. Moreover, *IGF-1* was significantly downregulated in osteogenic versus basal cultures of non-diabetic cells at Wk2, while *IGFBP-5* showed a trend of downregulation in osteogenic versus basal cultures of both diabetic and non-diabetic BM-MSCs across Wk1, Wk2 and Wk3 time-points. Thus, these IGF axis molecules could be used to coordinate osteogenic potentials of BM-MSCs as discussed in the General Discussion chapter of this thesis.

## Chapter 7 General discussion

### 7.1 Discussion

T2DM has been shown to influence multiple health conditions, with the bidirectional relationship with periodontitis attracting a relatively larger scientific interest. Stem cell based periodontal regeneration could be a promising therapeutic approach in patients with periodontitis, including diabetics. BM-MSCs are multilineage stem cells offering a number of advantages, including pro-angiogenic and immunomodulatory potentials (637), and could be associated with lower risk of postoperative complications, both at donor and recipient sites compared to iliac crest autogenous bone graft (638). Another advantage of BM-MSCs is their relative abundance (639) and thus, their expansion for carrying out research or for therapeutic applications may not be critical, unlike dental stem cells which are harvested in limited number and would almost definitely need some form of expansion. Nonetheless, osteogenic and periodontal differentiation potentials, as well as expression of IGF axis in BM-MSCs isolated from diabetic patients, have not been fully investigated.

BM-MSCs from hip joints (247,248) and alveolar bone (252,450) of T2DM patients have been previously investigated. However, to the best of my knowledge, this thesis represents a first attempt to characterize BM-MSCs isolated from knee joints of T2DM patients. This included assessing their clonogenic, proliferative and osteogenic differentiation potentials compared to non-diabetic controls. Moreover, this study would also be the first to examine expression of periodontal markers genes, *POSTN* and *CEMP-1*, in diabetic BM-MSCs, as well as identification of possible changes in the expression of IGF axis genes. This would contribute to fully understanding how T2DM could influence BM-MSCs and whether they could be used for autologous stem cells based periodontal regeneration in diabetic patients (248).

In this thesis, BM-MSCs were first isolated from osteoarthritic knee joints of T2DM and non-diabetic patients undergoing knee replacement surgery. Both cell populations were initially characterized using CFU-Fs assay, PDT assay and flow cytometric analysis of stem cells surface markers. For these investigations, both cell populations were cultured and expanded using the same media (complete

basal media). Using 2 different media (for instance HG cultures for diabetic cells and normal glucose media for non-diabetic cells) could have made undermined the consistency and comparability of the results. HG or AGEs media are unlikely to fully replicate the complicated diabetic microenvironment as mentioned earlier in this thesis (253). Moreover, BM-MSCs isolated from animal models with short term exposure to diabetic microenvironment still exhibited altered osteogenic differentiation when cultured under normal conditions (253), and diabetes could induce a number of persistent epigenetic changes that remained after cell culture under normal glucose (640). This phenomena is described as 'metabolic memory', and could be in part responsible for diabetic complications seen in well controlled diabetic patients, because of earlier exposure to high glucose prior to diagnosis and treatment (640). Nevertheless, the impact of different culture systems on expanded diabetic BM-MSCs relative to uncultured cells remains to be ascertained.

Both diabetic and non-diabetic BM-MSCs showed colony forming abilities, slower proliferation rates in later passages and fitted the phenotypic pattern of MSCs as identified by ISCT, but without significant differences between both cell types. This in general is consistent with earlier investigations (246,247), as detailed in chapter 4 of this thesis. Moreover, the osteogenic differentiation assay has shown that both cell types have similar osteogenic potentials as evident by quantification of their mineralisation and expression of different osteogenic markers.

Nevertheless, statistically significant reduced expression of key periodontal markers, *POSTN* and *CEMP-1*, was detected in diabetic BM-MSCs at Wk1 basal and Wk3 osteogenic cultures respectively. While extensive studies investigated osteogenic differentiation and bone regeneration potentials of different types of stem cells resulting in well-established protocols and markers, induction of *in vitro* cementogenic differentiation of stem cells and achieving cementum regeneration in periodontal defects clinically, a key event for periodontal wound healing, are not fully established yet (641). *CEMP-1* was reported to stimulate proliferation, migration and multilineage differentiation of PDLSCs (642), and more recently was found to induce complete regeneration of PDL tissues in a rat model (643). Accordingly, it seems *CEMP-1* functions extend beyond being a marker of cementoblastic differentiation and could be a key molecule for inducing periodontal regeneration, both in health and under diabetic conditions. Indeed,

CEMP-1 (or its derived peptides) induced osteogenic differentiation of gingival fibroblasts (644), oral mucosal stem cells (645) and PDL cells (475), though its pro-osteogenic effects on BM-MSCs are not fully established.

The same can be true for POSTN, which has pro-osteogenic potentials (646,647), induces PDL cells migration and proliferation even under inflammatory conditions or bacterial LPS (648); and also can reverse the negative impact of HG (292) and AGEs (515) on osteogenic potentials of PDLSCs. Hence it could be an ideal candidate to be used in local drug delivery systems in periodontal lesions in patients with T2DM where it could promote periodontal regeneration through stimulation of native endogenous stem cells within these defects while protecting against different pathological elements of diabetic microenvironment. Equally, POSTN can be used to enhance regenerative potentials of stem cells transplanted into periodontal defects in diabetic patients. POSTN incorporated into collagen scaffolds enhanced proliferation, adhesion and ALP activity in the osteoblasts seeded onto those scaffolds (647). This ultimate clinical translation would go first through different phases of research, which is outlined in the 'Future Work' section.

Both diabetic and non-diabetic BM-MSCs in this thesis showed an *OPG/RANKL* ratio above 1, indicating their relative preference for bone deposition over bone resorption. Both cell populations also formed calcium deposits, the ultimate product of osteogenic differentiation, at comparable levels. Thus the lower expression levels of *CEMP-1* and *POSTN* may not hugely influence the overall mineralization capacities of diabetic BM-MSCs, but possibly their potentials to regenerate PDL tissues and cementum when transplanted to periodontal defects. Testing this hypothesis is detailed in the upcoming 'Future Work' section.

While different GFs have been used clinically in orthopaedics and periodontology, they do have their own limitations. For instance, while recombinant BMP-2 has been used on a relatively large scale in orthopaedics and to a lesser degree in dentistry, it was linked with postoperative complications, such as ectopic bone formation and possibly higher cancer risk (649). It is thus prudent to investigate other signalling cues for bone and periodontal regeneration. Because the IGF axis plays an important role in stem cell biology and bone regeneration, IGF axis genes would represent ideal candidates for this purpose. The data presented in this thesis showed that *IGFBP-2*, *-3* and *-4* showed statistically significant lower

expression levels in diabetic versus non-diabetic BM-MSCs at Wk1, Wk3 and Wk1 basal cultures. *IGFBP-1* also showed a trend of lower expression in diabetic versus non-diabetic BM-MSCs at T0, Wk1 basal and Wk2 osteogenic cultures.

Additionally, this thesis demonstrated that *IGF-1* was significantly downregulated in Wk2 osteogenic cultures of non-diabetic cells (with all other time-points of diabetic and non-diabetic BM-MSCs showing a similar trend), *IGFBP-3* was significantly downregulated in Wk3 osteogenic cultures of non-diabetic cells and Wk1 and Wk2 osteogenic cultures showing a similar trend (diabetic BM-MSCs failed to show any of these patterns); and that *IGFBP-2* showed a trend of upregulation during osteogenic differentiation of diabetic and non-diabetic BM-MSCs. These changes in *IGFBP-2* and *-3* expression are supported by similar previously published data reported using DPSCs (350) and *IGFBP-2* was also upregulated during osteogenic differentiation of AT-MSCs (650). Moreover, the data in this thesis showed *IGFBP-5* had a trend of downregulation in osteogenic cultures of both diabetic and non-diabetic BM-MSCs across all time-points. Therefore, there is a potential to use these molecules to boost and coordinate the osteogenic differentiation of MSCs in situations where they can be compromised, such as when isolated from donors of old age or with medical comorbidities. Recent reports suggest that members of the IGF axis can improve insulin resistance and glycaemic control or protect against obesity and diabetes including, *IGFBP-1* (320), *IGFBP-2* (651) and a combination of *IGF-1* and *IGFBP-3* (652). Thus further research is needed to confirm if the IGFs and their binding proteins could help achieve both goals, bone regeneration and metabolic homeostasis, simultaneously in diabetics.

Furthermore, the statistically significant lower gene expression levels of IGFBPs in diabetic versus non-diabetic BM-MSCs reported in this thesis were observed under basal cultures only, possibly indicating a 'rescuing' effect of the osteogenic media. Additionally, non-diabetic BM-MSCs showed a higher number of differentially expressed genes under osteogenic versus basal conditions (Appendix B), potentially representing in general a weaker response of diabetic BM-MSCs to osteogenic supplements.

Interestingly, *IGFBP-2*, *-3* and *-4* differential gene expression in diabetic and non-diabetic cells was not reflected on the protein levels, which could be explained by variation in mRNA stability levels or translation rates as well as post-translational

stability of these proteins. Consequently, further research into factors that might alter the concentration of these IGFbps, including IGFbps proteases (in particular PAPP-A and -A2), as well as their inhibitors (most notably STC-2), is needed. PAPP-A is a secreted enzyme potentially controlled by a number of cytokines, including IL-1 $\beta$ , -4 and -6 as well as TGF- $\beta$  and BMP-2 (653); and its transcription and protein levels can be assessed using qPCR and ELISA respectively. STC-2 is also a secreted protein with putative receptors that is potentially involved in calcium regulation, angiogenesis, glucose homeostasis, in addition to its more established role in regulating PAPP-A and IGFbp-4 activity (654). With more research suggesting a central role of IGF axis in development and regeneration of oral and dental tissues (655), it is prudent to investigate the expression of PAPP-A, -A2 and STC-2, as they would ultimately affect any IGF axis related therapeutics.

The release of IGFbp-2 and -4 was notably increased in osteogenic conditions compared to basal. For IGFbp-2, this was reflecting the changes seen on mRNA levels and confirms its pro-osteogenic effect (392,587). For IGFbp-4, the higher concentrations detected in osteogenic versus basal conditioned media were not related to the gene expression levels. IGFbp-4 role in osteogenesis has been considerably contentious, with local injections inducing and systemic administration inhibiting ALP activity (656). While *IGFBP-3* was downregulated in osteogenic cultures of non-diabetic cells, this was not the case for protein concentrations, and the discrepancies could indicate a possible role of IGFbps proteases and their inhibitors as outlined above.

Most of the literature on diabetic BM-MSCs, as well as a number of the results reported in this thesis, show no dramatic differences in diabetic cells compared to non-diabetic controls. Thus it could be the BM-MSCs niche rather than the cells *per se* that contributes to the different complications and pathologies attributed to diabetes. This includes but is not limited to angiogenic, endothelial and immune cells residing within the BM-MSCs niche. Indeed, BM adipocytes from diabetic donors favoured adipogenic over osteogenic differentiation of BM-MSCs through paracrine secretion of monocyte chemoattractant protein-1, a chemokine actively involved in adipose tissue inflammation in T2DM (250). Moreover, hyperglycaemia and obesity could induce inflammatory memory in hematopoietic

cells within the BM, which substantially contributes to development of diabetes and CVD (657).

In their review on microenvironmental modulation of stem cells, Zheng et al. (514) propose that stem cells based therapy could face double impairment: one resulting from the donor's systemic health (including but not limited to aging, lower levels of sex hormones in postmenopausal women, glucocorticoid therapy and diabetes) and another from the pathological inflammatory niche at the recipient sites (periodontitis for example). Interestingly, native stem cells within the periodontal defects (PDLSCs) would also be affected by both impairments. As a results, for both treatment strategies of periodontitis in diabetics (cytotherapy or tissue engineering using transplanted BM-MSCs and activation of endogenous PDLSCs), pharmacological intervention to rescue stem cells and restore their regenerative capacities seems almost inevitable. These include antioxidants, epigenetic regulation or targeting signalling pathways involved in tissue regeneration (514). The notion of 'perfect' MSCs is far from reality, as there would almost always be a compounding factor influencing MSCs therapeutic potentials, not only underlying local or systemic medical conditions but also aging, obesity, smoking, unhealthy diet or other life style related factors.

## **7.2 Future work**

The set of experiments presented in this thesis was conducted on BM-MSCs from diabetic patients, with the ultimate goal of their use in autologous stem cell based periodontal tissue engineering, and have demonstrated lower expression of *POSTN*, *CEMP-1* and 3 IGFbps on the gene level in diabetic compared to non-diabetic BM-MSCs. The first implication of these findings is to test whether these changes would be mirrored in diabetic PDLSCs. This will improve our understanding of the underlying molecular mechanisms of the association between diabetes and periodontal disease and address these possible deficiencies in diabetic PDLSCs to enhance *in situ* periodontal regeneration, depending on native resident stem cells rather than stem cell transplantation. Moreover, larger samples in these future studies could also allow for stratifying the diabetic donors into subgroups based on additional factors such as their glycaemic control, BMI, duration and medication of diabetes and association of diabetic complications such as CVD. This would help build a better understanding of how T2DM could impact BM-MSCs and PDLSCs.

IGF-1, -2 and all IGFBPs were detectable in ECM of PDL, and IGF1-R was expressed by PDL fibroblasts, suggesting that these stores of IGFs within ECM could exert a paracrine effect on PDL cells (364). Therefore, different members of the IGF axis could potentially be applied locally to improve periodontal regeneration in T2DM patients with periodontitis. Indeed, as mentioned earlier, IGFBP-5 has shown promising results in animal models of periodontitis (609), and IGF-1 has already been used clinically in non-diabetic patients with periodontal defects in combination with other GFs (375,376).

The multiple genes that showed differential expression in diabetic versus non-diabetic BM-MSCs or in osteogenic versus basal cultures in this thesis could be used to modulate differentiation of diabetic BM-MSCs into mineralising phenotype by adding recombinant human proteins of these molecules to cultures of diabetic cells. An experimental design comparing basal and osteogenic cultures with and without the molecule under investigation would allow for detection of any synergistic effects. While bone regeneration using gene therapy has been tested in limited clinical trials (658), using this approach to correct deficiencies of diabetic BM-MSCs could prove useful.

Though this thesis has shown lower gene expression levels of *POSTN* and *CEMP-1* in diabetic BM-MSCs, these findings need to be verified on the protein level. The results of IGFBPs expression discussed in chapter 6 of this thesis has clearly shown that mRNA and protein levels do not necessarily match. These lower expression levels of *POSTN* and *CEMP-1* in diabetic BM-MSCs may not hugely influence their osteogenic potentials (both diabetic and non-diabetic BM-MSCs expressed osteogenic markers and eventually formed mineralised deposits comparably in this thesis as well as in previous investigations (247,248)). However, these markers are more likely to influence differentiation of diabetic BM-MSCs into PDL fibroblasts and cementoblasts and subsequent formation of PDL tissue and cementum.

This hypothesis cannot be tested in monolayer cultures but in animal models where diabetic BM-MSCs could be transplanted into experimental periodontal defects and formation of new cementum and alveolar bone with well aligned PDL fibres in-between can be verified. These animal models include surgically created periodontal defects (659), ligature induced periodontal defects (660), or heterotopic defects where bovine bone and human dentine matrix were implanted

into mice to simulate periodontal defects (240). A number of T2DM animal models could be used for this purpose, including high fat feeding rats and ZDF rats (661). Alternatively, 3D models of periodontal tissues are under development for use in periodontal regeneration research (284). Moreover, BM-MSCs can be transplanted into these models as cell sheets, which have the extra advantage of ECM proteins serving both as a scaffold and as signalling molecules, superior handling characteristics and minimal manipulation (240).

Moreover, assessing osteogenic potentials and IGF axis expression in freshly isolated BM-MSCs from diabetic donors would reveal if uncultured cells mirror the changes observed in cultured BM-MSCs in this study. Alteration of crucial pathways in bone regeneration, senescence and phenotypic changes have been reported in culture expanded BM-MSCs compared to native cells (662). Furthermore, *in vitro* aging of BM-MSCs during their culture and expansion can be more detrimental on their multilineage differentiation and therapeutic potentials than donor aging or systemic morbidities, including diabetes (247).

This could be taken even further by using fluorescence based sorting of uncultured diabetic BM-MSC to enrich CD271<sup>+</sup> CD45<sup>-</sup> MSCs population, as the CD271<sup>+</sup> population was shown to contain BM-MSCs with higher proliferative and differentiating potentials (663). Furthermore, co-culturing BM-MSCs with other cells types normally present in BM such as adipocytes, which play a crucial role in tuning insulin resistance, under hyperglycaemic conditions has been tested earlier (664). It would be interesting to retest such models, but using BM-MSCs and adipocytes isolated from diabetics rather than HG simulatory cultures.

Next generation sequencing could also be used to explore genes differentially expressed in diabetic BM-MSCs. Most recently, RNA sequencing has shown that *IGF-1*, as well as *RUNX2*, *BMP-2*, *-4* and *-6*, were downregulated in alveolar bone BM-MSCs isolated from diabetic patients (665). As outlined in chapter 5 of this thesis, alveolar BM-MSCs from diabetic patients did show lower expression levels of key osteogenic markers (251), which is different from the data on knee joint BM-MSCs presented in this thesis. Thus, using one BM-MSCs population from diabetics for drawing generalised conclusions may not be ideal and therapeutic potentials of diabetic BM-MSCs from different tissues should be assessed individually.

Another path worth exploring would be culturing diabetic BM-MSCs on scaffolds for bone and periodontal tissue engineering. Considering the complexity of periodontal tissues, the rather limited size of periodontal defects (150), higher risk of postsurgical complications, such as flap dehiscence, delayed wound healing, postoperative swelling and bleeding in diabetics (131), injectable hydrogels in particular present attractive candidates for this purpose. Apart from their ease of preparation and low cost, they can be readily injected into periodontal defects on their own or loaded with drugs to function as local drugs delivery system (666).

While this thesis has focused on the osteogenic differentiation of diabetic BM-MSCs and the expression of periodontal markers and IGF axis genes, investigating other aspects of diabetic BM-MSCs behaviour that might influence their periodontal regenerative potentials is worth considering. For example, exploring whether the diabetic microenvironment alters the immunomodulatory characteristics of diabetic BM-MSCs. Moreover, as discussed earlier in this thesis, the periodontal defects where diabetic BM-MSCs would be transplanted represent an even more challenging microenvironment, given the bacterial origin of periodontitis and the host inflammatory response mediating a considerable part of periodontal tissues damage (667), as well as the heavy microbial load in the non-sterile oral cavity (284) (For instance, oral plaque from T2DM patients reduced clonogenicity but not expression of osteogenic marker in DPSCs (668)). While a number of studies explored the immunomodulatory characteristics of BM-MSCs isolated from T1DM patients (7), and AT-MSCs derived from T2DM patients showed lower expression levels of anti-inflammatory cytokines and weaker suppression of PBMCs proliferation (669), in addition to weaker suppression of lymphocytes proliferation and activation of M2 macrophages (670), this remains to be explored for BM-MSCs isolated from T2DM patients.

The ultimate goal of this research would be the clinical translation of both approaches: using POSTN, CEMP-1 and members of the IGF axis for *in situ* stimulation of niche PDLSCs or transplanted autogenous diabetic BM-MSCs into periodontal defects. Thus the above-mentioned experimental testing should, in due course, be followed by well-designed and carefully implemented randomised controlled trials to confirm if diabetic BM-MSCs are good candidates for periodontal regeneration in diabetic patients.

### 7.3 Limitations

BM-MSCs investigated in this study were isolated from osteoarthritic knee joints of patients undergoing knee replacement surgery. A major advantage of this method would be making use of cells and tissues that otherwise would go to medical waste. The approach of using MSCs from 'discarded' tissues is well documented, with multiple papers investigating therapeutic potentials of MSCs derived from amputated limbs with CLI (246,671), pulp of carious teeth (459,672), PDL tissues of teeth with periodontitis (673) and even burn tissue (674,675).

In fact, BM-MSCs from osteoarthritic hip joints could differentiate into chondrocytes upon proper stimulation and have been used to construct 3D hyaline cartilage (676). Although these chondrocytes had higher levels of *COL X* expression and subsequently formed hypertrophic rather than hyaline cartilage, this hypertrophy was inhibited by treating cultured cells with parathyroid hormone-related protein, which supports the concept of microenvironmental modification of MSCs discussed earlier. Furthermore, almost all fast growing clones established from BM-MSCs of femoral canal of patients with osteoarthritic knees displayed multilineage differentiation and expressed MSCs positive markers (677). Alternatively, BM-MSCs could have been isolated from non osteoarthritic joints of diabetic and non-diabetic patients undergoing surgeries for fracture fixation or other traumatic incidents, yet the availability of such samples is quite challenging and unpredictable.

This thesis did not include sample size calculation, which allows for calculating the required sample size from a statistical point of view. As discussed in the previous section, expression of osteogenic and periodontal markers in cultures of diabetic and non-diabetic BM-MSCs was not assessed on the protein level; and animal models of periodontal defects where the impact of diabetic BM-MSCs transplantation on periodontal regeneration can be verified through histologic examination, quantitative assessment of newly formed tissues and immunohistochemistry of different periodontal markers, were not included. Nonetheless, this was beyond the scope of this PhD project due to time limitations.

As outlined in chapter 1 of this thesis, craniofacial bones, including alveolar bone, are derived from the ectomesenchyme under influence of NCCs, while the long bones are mesodermal in origin (678). While the influence of embryonic origin on

MSCs osteogenic differentiation potentials is not fully clear (678), using BM-MSCs isolated from craniofacial, rather than long bones, could be more suited for periodontal regeneration.

Another limitation due to time constraints of this PhD project is the relatively small sample size (n=3 for each group) and the lack of technical replicates, which was not ideal for the robustness and reproducibility of the data and conclusions presented from a statistical standpoint. For instance, the interesting trends observed in gene expression of BM-MSCs in this thesis could have possibly reached statistical significance with a larger sample size. Thus, the findings of this thesis should be considered as exploratory and valuable preliminary clues for more comprehensive and larger studies in the future. Nonetheless, similar sample size was reported in multiple publications investigating MSCs therapeutic potentials (245,505,679).

Both non-diabetic and diabetic BM-MSCs donors included in this study were relatively old (Table 3-9), and therefore the presented results may not be fully generalizable to BM-MSCs isolated from younger donors; and this should be addressed in future studies as well. Furthermore, this thesis did not include information on a number of potential confounders, such as duration of diabetes and BMI in the diabetic donors. However, it should be noted that diabetic MSCs therapeutic potentials could be impacted by other confounders as well, such as CVD, kidney disease and lifestyle related factors including diet, alcohol intake, smoking and physical exercise.

As detailed in chapter 6 of this thesis, a considerable part of changes in the expression of IGF axis genes observed in this study could be attributed to the use of dexamethasone as an osteogenic supplement. Despite the fact that the combination of dexamethasone, glycerophosphate and ascorbic acid has been used extensively with different MSCs, including BM-MSCs, other osteogenic supplements, including FGF, vitamin D3, BMP-2 (464), TGF- $\beta$ , IGF-1, VEGF, hepatocyte growth factor (680), ECM proteins such as COL1, vitronectin, laminin and fibronectin (681) have also been used with BM-MSCs. Probing IGF axis expression in diabetic BM-MSCs cultured in media supplemented with one or more of these reagents, in comparison to the data presented herein, would help optimise osteogenic culture systems in future investigations.

Finally, there is some evidence that *in vitro* cell culture could cause epigenetic changes of BM-MSCs (682), as well as altered phenotype and accumulation of senescent cells (662). Using freshly isolated uncultured BM-MSCs could be a more robust alternative to culture expanded BM-MSCs to avoid these possible alterations induced by culture expansion.

## **7.4 Conclusions**

The findings of this thesis have shown that BM-MSCs isolated from T2DM patients could be suitable for autologous transplantation for periodontal and bone regeneration. However, with the limitations of this *in vitro* study, this should warrant further research on uncultured BM-MSCs and additional *in vivo* investigations. Secondly, diabetic BM-MSCs have shown lower expression levels of *POSTN* and *CEMP-1*, and these molecules could be targeted to boost the regenerative potentials of these cells. Diabetic BM-MSCs also showed lower expression levels of IGFBP-2, -3 and -4 at gene but not at protein levels, suggesting further research into IGFbps proteinases and their inhibitors in this cell population is needed. Finally, IGF-1, IGFBP-2, and -5 could prove useful to fine tune the osteogenic differentiation of BM-MSCs in general. These molecules (*POSTN*, *CEMP-1* and the IGF axis genes) could be the next generation of signalling cues used in periodontal regeneration and bone tissue engineering in general.

## References

1. Carmagnola D, Pellegrini G, Dellavia C, Rimondini L, Varoni E. Tissue engineering in periodontology: Biological mediators for periodontal regeneration. *Int J Artif Organs*. 2019;42(5):241–57.
2. Peng BY, Dubey NK, Mishra VK, Tsai FC, Dubey R, Deng WP, et al. Addressing stem cell therapeutic approaches in pathobiology of diabetes and its complications. *J Diabetes Res*. 2018;2018:1–16.
3. Kocher T, König J, Sylling W, Christiane B, Meisel P, Kocher T. Periodontal complications of hyperglycemia/diabetes mellitus: Epidemiologic complexity and clinical challenge. *Periodontol 2000*. 2018;78:59–97.
4. Villar CC, Cochran DL. Regeneration of Periodontal Tissues: Guided Tissue Regeneration. *Dent Clin North Am*. 2010;54(1):73–92.
5. Iviglia G, Kargozar S, Baino F. Biomaterials, current strategies, and novel nano-technological approaches for periodontal regeneration. *J Funct Biomater*. 2019;10(3).
6. Gay IC, Chen S, MacDougall M. Isolation and characterization of multipotent human periodontal ligament stem cells. *Orthod Craniofacial Res*. 2007;10:149–60.
7. Mahmoud M, Abu-Shahba N, Azmy O, El-Badri N. Impact of Diabetes Mellitus on Human Mesenchymal Stromal Cell Biology and Functionality: Implications for Autologous Transplantation. *Stem Cell Rev Reports*. 2019;15(2):194–217.
8. Gaubys A, Papeckys V, Pranskunas M. Use of Autologous Stem Cells for the Regeneration of Periodontal Defects in Animal Studies: a Systematic Review and Meta-Analysis. *J Oral Maxillofac Res*. 2018;9(2):e3.
9. de Jong T, Bakker AD, Everts V, Smit TH. The intricate anatomy of the periodontal ligament and its development: Lessons for periodontal regeneration. *J Periodontal Res*. 2017;52(6):965–74.
10. Andrei M, Dinischiotu A, Didilescu AC, Ionita D, Demetrescu I. Periodontal materials and cell biology for guided tissue and bone regeneration. *Ann Anat*. 2018;216:164–9.
11. Nuñez J, Vignoletti F, Caffesse RG, Sanz M. Cellular therapy in periodontal regeneration. *Periodontol 2000*. 2019;79:107–16.
12. Park CH, Kim KH, Rios HF, Lee YM, Giannobile W V., Seol YJ.

- Spatiotemporally controlled microchannels of periodontal mimic scaffolds. *J Dent Res.* 2014;93(12):1304–12.
13. Nanci A, Bosshardt DD. Structure of periodontal tissues in health and disease. *Periodontol 2000.* 2006;40:11–28.
  14. Pagni G, Pellegrini G, Giannobile W V., Rasperini G. Postextraction alveolar ridge preservation: Biological basis and treatments. *Int J Dent.* 2012;2012.
  15. Bartold M, Gronthos S, Haynes D, Ivanovski S. Mesenchymal stem cells and biologic factors leading to bone formation. *J Clin Periodontol.* 2019;46(S21):12–32.
  16. Sodek J, McKee MD. Molecular and cellular biology of alveolar bone. *Periodontol 2000.* 2000;24(1):99–126.
  17. Bosshardt DD. Are Cementoblasts a Subpopulation of Osteoblasts or a Unique Phenotype ? *J Dent Res.* 2005;84(5):390–406.
  18. Kalfas IH. Principles of bone healing. *Neurosurg Focus.* 2001;10(4).
  19. Karsenty G. The complexities of skeletal biology. *Nature.* 2003;423(6937):316–8.
  20. Rutkovskiy A, Stensløkken K-O, Vaage IJ. Osteoblast Differentiation at a Glance. *Med Sci Monit Basic Res.* 2016;22:95–106.
  21. Hasegawa T, Hongo H, Yamamoto T, Abe M, Yoshino H, Haraguchi-Kitakamae M, et al. Matrix Vesicle-Mediated Mineralization and Osteocytic Regulation of Bone Mineralization. *Int J Mol Sci.* 2022;23(17):9941.
  22. Florencio-Silva R, Sasso GR da S, Sasso-Cerri E, Simões MJ, Cerri PS. Biology of Bone Tissue: Structure, Function, and Factors That Influence Bone Cells. *Biomed Res Int.* 2015;2015.
  23. Uda Y, Azab E, Sun N, Shi C, Pajevic PD. Osteocyte Mechanobiology. *Curr Osteoporos Rep.* 2017;15:318–25.
  24. Divieti P, Krause DS. Osteocyte regulation of bone and blood. *Bone.* 2019;119:13–8.
  25. Edwards JR, Mundy GR. Advances in osteoclast biology: Old findings and new insights from mouse models. *Nat Rev Rheumatol.* 2011;7(4):235–43.
  26. Ono T, Nakashima T. Recent advances in osteoclast biology. *Histochem Cell Biol.* 2018;149(4):325–41.
  27. El-Zainy MA, Halawa AM, Saad FA. Effect of diabetes mellitus on cementum periodontal interface in Streptozotocin-induced diabetic rat

- model. *Futur Dent J.* 2018;4(2):181–8.
28. Yamamoto TTT, Hasegawa T, Yamamoto TTT, Hongo H, Amizuka N. Histology of human cementum: Its structure, function, and development. *Jpn Dent Sci Rev.* 2016;52(3):63–74.
  29. Zhao N, Foster BL, Bonewald LF. The Cementocyte - An Osteocyte Relative? *J Dent Res.* 2016;95(7):734–41.
  30. Bartold PM, Walsh LJ, Narayanan AS. Molecular and cell biology of the gingiva. *Periodontol 2000.* 2000;24(1):28–55.
  31. Ji S, Choi Y. Microbial and Host Factors That Affect Bacterial Invasion of the Gingiva. *J Dent Res.* 2020;99(9):1013–20.
  32. Yajima-Himuro S, Oshima M, Yamamoto G, Ogawa M, Furuya M, Tanaka J, et al. The junctional epithelium originates from the odontogenic epithelium of an erupted tooth. *Sci Rep.* 2014;4:1–7.
  33. Nakamura M. Histological and immunological characteristics of the junctional epithelium. *Jpn Dent Sci Rev.* 2018;54(2):59–65.
  34. Graf D, Malik Z, Hayano S, Mishina Y. Common mechanisms in development and disease: BMP signaling in craniofacial development. *Cytokine Growth Factor Rev.* 2016;27:129–39.
  35. Ouchi T, Nakagawa T. Mesenchymal stem cell-based tissue regeneration therapies for periodontitis. *Regen Ther.* 2020;14:72–8.
  36. Lesot H, Kieffer-Combeau S, Fausser JL, Meyer JM, Perrin-Schmitt F, Peterková R, et al. Cell-cell and cell-matrix interactions during initial enamel organ histomorphogenesis in the mouse. *Connect Tissue Res.* 2002;43(2–3):191–200.
  37. Li J, Parada C, Chai Y. Cellular and molecular mechanisms of tooth root development. *Development.* 2017;144:374–84.
  38. Nakatomi M, Morita I. Sonic Hedgehog Signaling is Important in Tooth Root Development. *J Dent Oral Heal.* 2006;85(5):427–31.
  39. Thomas HF. Root formation. *Int J Dev Biol.* 1995;39(1):231–7.
  40. Dang P, Tang Q, Nie M yuan, An Y, Dong R, Hua X dong, et al. Comparative gene expression profiles of dental follicle at different stages of periodontal development: Combined use of laser capture microdissection and microarray. *J Oral Biosci.* 2018;60(4):92–7.
  41. Zheng J, Chen S, Albiero ML, Vieira GHA, Wang J, Feng JQ, et al. Diabetes Activates Periodontal Ligament Fibroblasts via NF- $\kappa$ B In Vivo. *J Dent Res.*

- 2018;97(5):580–8.
42. Hajishengallis G. Periodontitis: From microbial immune subversion to systemic inflammation. *Nat Rev Immunol*. 2015;15(1):30–44.
  43. Frencken JE, Sharma P, Stenhouse L, Green D, Lavery D, Dietrich T. Global epidemiology of dental caries and severe periodontitis – a comprehensive review. *J Clin Periodontol*. 2017;44(Suppl. 18):S94–105.
  44. Bernabe E, Marcenes W, Hernandez CR, Bailey J, Abreu LG, Alipour V, et al. Global, Regional, and National Levels and Trends in Burden of Oral Conditions from 1990 to 2017: A Systematic Analysis for the Global Burden of Disease 2017 Study. *J Dent Res*. 2020;99(4):362–73.
  45. Vos T, Abajobir AA, Abbafati C, Abbas KM, Abate KH, Abd-Allah F, et al. Global, regional, and national incidence, prevalence, and years lived with disability for 328 diseases and injuries for 195 countries, 1990-2016: A systematic analysis for the Global Burden of Disease Study 2016. *Lancet*. 2017;390(10100):1211–59.
  46. Caton JG, Armitage G, Berglundh T, Chapple ILC, Jepsen S, Kornman KS, et al. A new classification scheme for periodontal and peri-implant diseases and conditions – Introduction and key changes from the 1999 classification. *J Periodontol*. 2018;89(S1):S1–8.
  47. Avila-Ortiz G, De Buitrago JG, Reddy MS. Periodontal Regeneration – Furcation Defects: A Systematic Review From the AAP Regeneration Workshop. *J Periodontol*. 2015;86(2-s):S108–30.
  48. Papapanou PN, Sanz M, Buduneli N, Dietrich T, Feres M, Fine DH, et al. Periodontitis: Consensus report of workgroup 2 of the 2017 World Workshop on the Classification of Periodontal and Peri-Implant Diseases and Conditions. *J Periodontol Res*. 2018;89(Suppl 1):S173–82.
  49. Armitage GC. Development of a classification system for periodontal diseases and conditions. *Ann Periodontol*. 1999;4(1):1–6.
  50. Dietrich T, Ower P, Tank M, West NX, Walter C, Needleman I, et al. Periodontal diagnosis in the context of the 2017 classification system of periodontal diseases and conditions – Implementation in clinical practice. *Br Dent J*. 2019;226(1):16–22.
  51. Socransky SS, Haffajee AD, Cugini MA, Smith C, Kent RL. Microbial complexes in subgingival plaque. *J Clin Periodontol*. 1998;25(2):134–44.
  52. Griffen AL, Beall CJ, Campbell JH, Firestone ND, Kumar PS, Yang ZK, et

- al. Distinct and complex bacterial profiles in human periodontitis and health revealed by 16S pyrosequencing. *ISME J.* 2012;6:1176–85.
53. Hajishengallis G, Lamont RJ. Beyond the red complex and into more complexity: The polymicrobial synergy and dysbiosis (PSD) model of periodontal disease etiology. *Mol Oral Microbiol.* 2012;27(6):409–19.
  54. Hajishengallis G. The inflammophilic character of the periodontitis-associated microbiota. *Mol Oral Microbiol.* 2014;29(6):248–57.
  55. Hajishengallis G. Immunomicrobial pathogenesis of periodontitis: keystones, pathobionts, and host response. *Trends Immunol.* 2014;35(1):3–11.
  56. Hajishengallis G, Korostoff JM. Revisiting the Page & Schroeder model: the good, the bad and the unknowns in the periodontal host response 40 years later. *Periodontol 2000.* 2017;75(1):116–51.
  57. Tsukasaki M, Takayanagi H. Osteoimmunology: evolving concepts in bone–immune interactions in health and disease. *Nat Rev Immunol.* 2019;19(10):626–42.
  58. Tsukasaki M. RANKL and osteoimmunology in periodontitis. Vol. 39, *Journal of Bone and Mineral Metabolism.* Springer Singapore; 2021. p. 82–90.
  59. AlQranei MS, Chellaiah MA. Osteoclastogenesis in periodontal diseases: Possible mediators and mechanisms. *J Oral Biosci.* 2020;(xxxx).
  60. Papapanou PN, Tonetti MS. Diagnosis and epidemiology of periodontal osseous lesions. *Periodontol 2000.* 2000;22(1):8–21.
  61. Sculean A, Stavropoulos A, Bosshardt DD. Self-regenerative capacity of intra-oral bone defects. *J Clin Periodontol.* 2019;46(Suppl. 21):70–81.
  62. Könönen E, Gursoy M, Gursoy UK. Periodontitis: A Multifaceted Disease of Tooth-Supporting Tissues. *J Clin Med.* 2019;8(8):1135.
  63. Mattila KJ, Nieminen MS, Valtonen V V., Rasi VP, Kesaniemi YA, Syrjala SL, et al. Association between dental health and acute myocardial infarction. *Br Med J.* 1989;298(6676):779–81.
  64. Hugoson A, Thorstensson H, Falitt H, Kuylentierna J. Periodontal conditions in insulin-dependent diabetics. *J Clin Periodontol.* 1989;16(4):215–23.
  65. Beck JD, Papapanou PN, Philips KH, Offenbacher S. Periodontal Medicine: 100 Years of Progress. *J Dent Res.* 2019;98(10):1053–62.

66. Monsarrat P, Blaizot A, Kémoun P, Ravaud P, Nabet C, Sixou M, et al. Clinical research activity in periodontal medicine: A systematic mapping of trial registers. *J Clin Periodontol*. 2016;43(5):390–400.
67. Herrera D, Molina A, Buhlin K, Klinge B. Periodontal diseases and association with atherosclerotic disease. *Periodontol 2000*. 2020;83(1):66–89.
68. Komine-Aizawa S, Aizawa S, Hayakawa S. Periodontal diseases and adverse pregnancy outcomes. *J Obstet Gynaecol Res*. 2019;45(1):5–12.
69. Figuero E, Han YW, Furuichi Y. Periodontal diseases and adverse pregnancy outcomes: Mechanisms. *Periodontol 2000*. 2020;83(1):175–88.
70. Deschamps-Lenhardt S, Martin-Cabezas R, Hannedouche T, Huck O. Association between periodontitis and chronic kidney disease: Systematic review and meta-analysis. *Oral Dis*. 2019;25(2):385–402.
71. Takeuchi K, Matsumoto K, Furuta M, Fukuyama S, Takeshita T, Ogata H, et al. Periodontitis Is Associated with Chronic Obstructive Pulmonary Disease. *J Dent Res*. 2019;98(5):534–40.
72. Cheng Z, Meade J, Mankia K, Emery P, Devine DA. Periodontal disease and periodontal bacteria as triggers for rheumatoid arthritis. *Best Pract Res Clin Rheumatol*. 2017;31(1):19–30.
73. de Oliveira Ferreira R, de Brito Silva R, Magno MB, Carvalho Almeida APCPS, Fagundes NCF, Maia LC, et al. Does periodontitis represent a risk factor for rheumatoid arthritis? A systematic review and meta-analysis. *Ther Adv Musculoskelet Dis*. 2019;11:1–16.
74. Pritchard AB, Crean SJ, Olsen I, Singhrao SK. Periodontitis, microbiomes and their role in Alzheimer's Disease. *Front Aging Neurosci*. 2017;9:336.
75. Dioguardi M, Crincoli V, Laino L, Alovise M, Sovereto D, Mastrangelo F, et al. The Role of Periodontitis and Periodontal Bacteria in the Onset and Progression of Alzheimer's Disease: A Systematic Review. *J Clin Med*. 2020;9(2):495.
76. Retzepi M, Calciolari E, Wall I, Lewis MP, Donos N. The effect of experimental diabetes and glycaemic control on guided bone regeneration: histology and gene expression analyses. *Clin Oral Implants Res*. 2018;29:139–54.
77. American Diabetes Association. 2. Classification and diagnosis of diabetes: Standards of medical care in diabetes - 2019. *Diabetes Care*.

- 2019;42(Suppl. 1):S13–28.
78. WHO. Classification of diabetes mellitus. 2019.
  79. Wu YY, Xiao E, Graves DT. Diabetes mellitus related bone metabolism and periodontal disease. *Int J Oral Sci.* 2015;7(2):63–72.
  80. Pociot F, Lernmark Å. Genetic risk factors for type 1 diabetes. *Lancet.* 2016;387(10035):2331–9.
  81. Rewers M, Ludvigsson J. Environmental risk factors for type 1 diabetes. *Lancet.* 2016;387(10035):2340–8.
  82. Chatterjee S, Khunti K, Davies MJ. Type 2 diabetes. *Lancet.* 2017;389(10085):2239–51.
  83. Forouhi NG, Wareham NJ. Epidemiology of diabetes. *Medicine (Baltimore).* 2019;47(1):22–7.
  84. Donath MY, Shoelson SE. Type 2 diabetes as an inflammatory disease. *Nat Rev Immunol.* 2011;11(2):98–107.
  85. Lontchi-Yimagou E, Sobngwi E, Matsha TE, Kengne AP. Diabetes mellitus and inflammation. *Curr Diab Rep.* 2013;13(3):435–44.
  86. Calle MC, Fernandez ML. Inflammation and type 2 diabetes. *Diabetes Metab.* 2012;38(3):183–91.
  87. Xu J, Xiong M, Hung B, Chen H. Advanced Glycation End Products Upregulate the Endoplasmic Reticulum Stress in Human Periodontal Ligament Cells. *J Periodontol.* 2014;86(3):440–7.
  88. Miranda C, Giner M, José Montoya M, Vázquez MA, Miranda MJ, Pérez-Cano R. Influence of high glucose and advanced glycation end-products (ages) levels in human osteoblast-like cells gene expression. *BMC Musculoskelet Disord.* 2016;17(377).
  89. Fadini GP, Ciciliot S, Albiero M. Concise Review: Perspectives and Clinical Implications of Bone Marrow and Circulating Stem Cell Defects in Diabetes. *Stem Cells.* 2017;35(1):106–16.
  90. Loomans CJM, Van Haperen R, Duijs JM, Verseyden C, De Crom R, Leenen PJM, et al. Differentiation of bone marrow-derived endothelial progenitor cells is shifted into a proinflammatory phenotype by hyperglycemia. *Mol Med.* 2009;15(5–6):152–9.
  91. Negrato CA, Tarzia O, Jovanović L, Eduardo L, Chinellato M. Periodontal disease and diabetes mellitus. *J App Oral Sci.* 2013;21(1):1–12.
  92. Kinane DF, Stathopoulou PG, Papapanou PN. Periodontal diseases. *Nat*

- Rev Dis Prim. 2017;3:1–14.
93. Xiao E, Mattos M, Vieira GHA, Chen S, Corrêa JD, Wu Y, et al. Diabetes Enhances IL-17 Expression and Alters the Oral Microbiome to Increase Its Pathogenicity. *Cell Host Microbe*. 2017;22:120–8.
  94. Shi B, Lux R, Klokkevold P, Chang M, Barnard E, Haake S, et al. The subgingival microbiome associated with periodontitis in type 2 diabetes mellitus. *ISME J*. 2020;14(2):519–30.
  95. Duarte PM, Bezerra JP, Miranda TS, Feres M, Chambrone L, Shaddox LM. Local levels of inflammatory mediators in uncontrolled type 2 diabetic subjects with chronic periodontitis. *J Clin Periodontol*. 2014;41(1):11–8.
  96. Patil VS, Patil VP, Gokhale N, Acharya A, Kangokar P. Chronic periodontitis in type 2 diabetes mellitus: Oxidative stress as a common factor in periodontal tissue injury. *J Clin Diagnostic Res*. 2016;10(4):BC12–6.
  97. Polak D, Shapira L. An update on the evidence for pathogenic mechanisms that may link periodontitis and diabetes. *J Clin Periodontol*. 2018;45(2):150–66.
  98. Waddington RJ, Moseley R, Embery G. Reactive oxygen species: A potential role in the pathogenesis of periodontal diseases. *Oral Dis*. 2000;6(3):138–51.
  99. Waddington RJ, Alraies A, Colombo JS, Sloan AJ, Okazaki J, Moseley R. Characterization of oxidative stress status during diabetic bone healing. *Cells Tissues Organs*. 2011;194(2–4):307–12.
  100. Graves DT, Ding Z, Yang Y. The impact of diabetes on periodontal diseases. *Periodontol 2000*. 2020;82(1):214–24.
  101. Retamal I, Hernández R, Velarde V, Oyarzún A, Martínez C, Julieta González M, et al. Diabetes alters the involvement of myofibroblasts during periodontal wound healing. *Oral Dis*. 2020;26(5):1062–71.
  102. Graziani F, Gennai S, Solini A, Petrini M. A systematic review and meta-analysis of epidemiologic observational evidence on the effect of periodontitis on diabetes An update of the EFP-AAP review. *J Clin Periodontol*. 2018;45(2):167–87.
  103. Isola G, Matarese G, Ramaglia L, Pedullà E, Rapisarda E, Iorio-Siciliano V. Association between periodontitis and glycosylated haemoglobin before diabetes onset: a cross-sectional study. *Clin Oral Investig*. 2020;24:2799–

2808.

104. Miranda TS, Heluy SL, Cruz DF, da Silva HDP, Feres M, Figueiredo LC, et al. The ratios of pro-inflammatory to anti-inflammatory cytokines in the serum of chronic periodontitis patients with and without type 2 diabetes and/or smoking habit. *Clin Oral Investig*. 2019;23(2):641–50.
105. Merchant AT, Georgantopoulos P, Howe CJ, Virani SS, Morales DA, Haddock KS. Effect of Long-Term Periodontal Care on Hemoglobin A1c in Type 2 Diabetes. *J Dent Res*. 2016;95(4):408–15.
106. Nazir MA. Prevalence of periodontal disease, its association with systemic diseases and prevention. *Int J Health Sci (Qassim)*. 2017;1(2):72–80.
107. Mougeot JLC, Stevens CB, Paster BJ, Brennan MT, Lockhart PB, Mougeot FKB. *Porphyromonas gingivalis* is the most abundant species detected in coronary and femoral arteries. *J Oral Microbiol*. 2017;9(1):1281562.
108. Kramer CD, Simas AM, He X, Ingalls RR, Weinberg EO, Attardo C. Distinct roles for dietary lipids and *Porphyromonas gingivalis* infection on atherosclerosis progression and the gut microbiota. *Anaerobe*. 2017;45:19–30.
109. Preshaw PM, Bissett SM. Periodontitis and diabetes. *Br Dent J*. 2019;227(7):577–84.
110. Preshaw PM, Taylor JJ, Jaedicke KM, De Jager M, Bikker JW, Selten W, et al. Treatment of periodontitis reduces systemic inflammation in type 2 diabetes. *J Clin Periodontol*. 2020;4.
111. Artese HPC, Foz AM, Rabelo MDS, Gomes GH, Orlandi M, Suvan J, et al. Periodontal therapy and systemic inflammation in type 2 diabetes mellitus: A meta-analysis. *PLoS One*. 2015;10(5):1–14.
112. Peng CH, Yang YS, Chan KC, Kornelius E, Chiou JY, Huang CN. Periodontal treatment and the risks of cardiovascular disease in patients with type 2 diabetes: A retrospective cohort study. *Intern Med*. 2017;56(9):1015–21.
113. West N, Chapple I, Claydon N, D’Aiuto F, Donos N, Ide M, et al. BSP implementation of European S3 - level evidence-based treatment guidelines for stage I-III periodontitis in UK clinical practice. *J Dent*. 2021;106:103562.
114. Cobb CM, Sottosanti JS. A re-evaluation of scaling and root planing. *J Periodontol*. 2021;92(10):1370–8.

115. Cobb CM. Clinical significance of non-surgical periodontal therapy: an evidence-based perspective of scaling and root planing. *J Clin Periodontol*. 2002;29(s2):22–32.
116. Naiff P, Carneiro V, Guimarães MDC. Importance of mechanical periodontal therapy in patients with diabetes type 2 and periodontitis. *Int J Dent*. 2018;2018.
117. Rees TS. Periodontal management of the patient with diabetes mellitus. *Periodontol 2000*. 2000;23:63–72.
118. Han J, Menicanin D, Gronthos S, Bartold PM. Stem cells, tissue engineering and periodontal regeneration. *Aust Dent J*. 2014;59(SUPPL. 1):117–30.
119. Bosshardt DD, Sculean A. Does periodontal tissue regeneration really work? *Periodontol 2000*. 2009;51(1):208–19.
120. Duarte PM, Feres M, Yassine LLS, Soares GMS, Miranda TS, Faveri M, et al. Clinical and microbiological effects of scaling and root planing, metronidazole and amoxicillin in the treatment of diabetic and non-diabetic subjects with periodontitis: A cohort study. *J Clin Periodontol*. 2018;45(11):1326–35.
121. Christgau M, Palitzsch KD, Schmalz G, Kreiner U, Frenzel S. Healing response to non-surgical periodontal therapy in patients with diabetes mellitus: Clinical, microbiological, and immunologic results. *J Clin Periodontol*. 1998;25(2):112–24.
122. Hsu YT, Nair M, Angelov N, Lalla E, Lee CT. Impact of diabetes on clinical periodontal outcomes following non-surgical periodontal therapy. *J Clin Periodontol*. 2019;46(2):206–17.
123. Lang NP, Salvi GE, Sculean A. Nonsurgical therapy for teeth and implants—When and why? *Periodontol 2000*. 2019;79(1):15–21.
124. Sallum EA, Ribeiro F V., Ruiz KS, Sallum AW. Experimental and clinical studies on regenerative periodontal therapy. *Periodontol 2000*. 2019;79(1):22–55.
125. Wu YC, Lin LK, Song CJ, Su YX, Tu YK. Comparisons of periodontal regenerative therapies: A meta-analysis on the long-term efficacy. *J Clin Periodontol*. 2017;44:511–9.
126. Moreno Rodríguez JA, Ortiz Ruiz AJ, Caffesse RG. Supra-alveolar attachment gain in the treatment of combined intra-suprabony periodontal

- defects by non-incised papillae surgical approach. *J Clin Periodontol*. 2019;46(9):927–36.
127. Jayakumar A, Rohini S, Naveen A, Haritha A, Reddy K. Horizontal alveolar bone loss: A periodontal orphan. *J Indian Soc Periodontol*. 2010;14(3):181.
128. Iorio-Siciliano V, Blasi A, Stratul SI, Ramaglia L, Octavia V, Salvi GE, et al. Healing of periodontal suprabony defects following treatment with open flap debridement with or without an enamel matrix derivative: A randomized controlled clinical study. *Clin Oral Investig*. 2021;25:1019–1027.
129. Susin C, Fiorini T, Lee J, De Stefano JA, Dickinson DP, Wikesjö UME. Wound healing following surgical and regenerative periodontal therapy. *Periodontol 2000*. 2015;68(1):83–98.
130. Graziani F, Gennai S, Cei S, Ducci F, Discepoli N, Carmignani A, et al. Does enamel matrix derivative application provide additional clinical benefits in residual periodontal pockets associated with suprabony defects? A systematic review and meta-analysis of randomized clinical trials. *J Clin Periodontol*. 2014;41:377–86.
131. Askar H, Di Gianfilippo R, Ravida A, Tattan M, Majzoub J, Wang HL. Incidence and severity of postoperative complications following oral, periodontal, and implant surgeries: A retrospective study. *J Periodontol*. 2019;90(11):1270–8.
132. Cho YD, Kim KH, Lee YM, Ku Y, Seol YJ. Periodontal wound healing and tissue regeneration: A narrative review. *Pharmaceuticals*. 2021;14(456).
133. Lee RSB, Hamlet SM, Ivanovski S. The influence of titanium surface characteristics on macrophage phenotype polarization during osseous healing in type I diabetic rats: a pilot study. *Clin Oral Implants Res*. 2017;28(10):e159–68.
134. Retzepi M, Lewis MP. Effect of diabetes and metabolic control on de novo bone formation following guided bone regeneration. *Clin Oral Implant Res*. 2010;21:71–9.
135. Corrêa MG, Gomes Campos ML, Marques MR, Casati MZ, Nociti FH, Sallum EA. Histometric Analysis of the Effect of Enamel Matrix Derivative on the Healing of Periodontal Defects in Rats With Diabetes. *J Periodontol*. 2013;84(9):1309–18.
136. Shirakata Y, Eliezer M, Ce N, Weinreb M, Dard M, Sculean A. Periodontal healing after application of enamel matrix derivative in surgical supra/

- infrabony periodontal defects in rats with streptozotocin-induced diabetes. *J Periodontal Res.* 2014;49:93–101.
137. Takeda K, Mizutani K, Matsuura T, Kido D, Mikami R, Noda M, et al. Periodontal regenerative effect of enamel matrix derivative in diabetes. *PLoS One.* 2018;13(11).
138. Nemtoi A, Danila V, Dragan E, Pasca S, Nemtoi A, Constantin M, et al. The Effects of Insulin and Strontium Ranelate on Guided Bone Regeneration in Diabetic Rats. *Rev Chim.* 2017;68(4):693–7.
139. Lee SB, Retzepi M, Petrie A, Hakimi AR, Schwarz F, Donos N. The effect of diabetes on bone formation following application of the GBR principle with the use of titanium domes. *Clin Oral Implants Res.* 2013;24(1):28–35.
140. Seshima F, Nishina M, Namba T, Saito A. Periodontal Regenerative Therapy in Patient with Chronic Periodontitis and Type 2 Diabetes Mellitus: A Case Report. *Bull Tokyo Dent Coll.* 2016;57(2):97–104.
141. Mizutani K, Shioyama H, Matsuura T, Mikami R, Takeda K, Izumi Y, et al. Periodontal regenerative therapy in patients with type 2 diabetes using minimally invasive surgical technique with enamel matrix derivative under 3-year observation: A prospective cohort study. *J Periodontol.* 2021;1–12.
142. Cimões R, Santiago LM, de França Caldas Júnior A, de Carvalho Farias Vajgel B, Perussolo J, Donos N. Treatment of intrabony periodontal defects in controlled diabetic patients with an enamel matrix derivative: a split-mouth randomized clinical trial. *Clin Oral Investig.* 2021;1–11.
143. Al Amri MD, Kellesarian SV, Al-Kheraif AA, Malmstrom H, Javed F, Romanos GE. Effect of oral hygiene maintenance on HbA1c levels and peri-implant parameters around immediately-loaded dental implants placed in type-2 diabetic patients: 2 years follow-up. *Clin Oral Implants Res.* 2016;27(11):1439–43.
144. Sghaireen MG, Alduraywish AA, Chandan Srivastava K, Shrivastava D, Patil SR, Habib S Al, et al. Comparative evaluation of dental implant failure among healthy and well-controlled diabetic patients—a 3-year retrospective study. *Int J Environ Res Public Health.* 2020;17(14):1–10.
145. Huynh-Ba G, Friedberg JR, Vogiatzi D, Ioannidou E. Implant Failure Predictors in the Posterior Maxilla: A Retrospective Study of 273 Consecutive Implants. *J Periodontol.* 2008;79(12):2256–61.
146. Erdogan Ö, Uçar Y, Tatli U, Sert M, Benlidayi ME, Evlice B. A clinical

- prospective study on alveolar bone augmentation and dental implant success in patients with type 2 diabetes. *Clin Oral Implants Res.* 2015;26(11):1267–75.
147. Naujokat H, Kunzendorf B, Wiltfang J. Dental implants and diabetes mellitus—a systematic review. *Int J Implant Dent.* 2016;2(1).
  148. Moraschini V, Barboza ESP, Peixoto GA. The impact of diabetes on dental implant failure: a systematic review and meta-analysis. *Int J Oral Maxillofac Surg.* 2016;45(10):1237–45.
  149. Langer R, Vacanti JP. Tissue Engineering. *Science* (80- ). 1993;260(5110):920–6.
  150. Park CH. Biomaterial-based approaches for regeneration of periodontal ligament and cementum using 3D platforms. *Int J Mol Sci.* 2019;20(18):4364.
  151. Staples RJ, Ivanovski S, Vaquette C. Fibre guiding scaffolds for periodontal tissue engineering. *J Periodontal Res.* 2020;55(3):1–11.
  152. Abou Neel EA, Chrzanowski W, Salih VM, Kim HW, Knowles JC. Tissue engineering in dentistry. *J Dent.* 2014;42(8):915–28.
  153. Orciani M, Fini M, Di Primio R, Mattioli-Belmonte M. Biofabrication and Bone Tissue Regeneration: Cell source, Approaches, and Challenges. *Front Bioeng Biotechnol.* 2017;5(17):1–15.
  154. Liang Y, Luan X, Liu X. Recent advances in periodontal regeneration: A biomaterial perspective. *Bioact Mater.* 2020;5(2):297–308.
  155. Chen X, Liu Y, Miao L, Wang Y, Ren S, Yang X, et al. Controlled release of recombinant human cementum protein 1 from electrospun multiphasic scaffold for cementum regeneration. *Int J Nanomedicine.* 2016;11:3145–58.
  156. Vaquette C, Fan W, Xiao Y, Hamlet S, Hutmacher DW, Ivanovski S. A biphasic scaffold design combined with cell sheet technology for simultaneous regeneration of alveolar bone/periodontal ligament complex. *Biomaterials.* 2012;33(22):5560–73.
  157. Vaquette C, Saifzadeh S, Farag A, Hutmacher DW, Ivanovski S. Periodontal Tissue Engineering with a Multiphasic Construct and Cell Sheets. *J Dent Res.* 2019;98(6):673–81.
  158. Sowmya S, Mony U, Jayachandran P, Reshma S, Kumar RA, Arzate H, et al. Tri-Layered Nanocomposite Hydrogel Scaffold for the Concurrent

- Regeneration of Cementum, Periodontal Ligament, and Alveolar Bone. *Adv Healthc Mater.* 2017;6(7):1–13.
159. Carter SSD, Costa PF, Vaquette C, Ivanovski S, Hutmacher DW, Malda J. Additive Biomanufacturing: An Advanced Approach for Periodontal Tissue Regeneration. *Ann Biomed Eng.* 2017;45(1):12–22.
  160. Rasperini G, Pilipchuk SP, Flanagan CL, Park CH, Pagni G, Hollister SJ, et al. 3D-printed Bioresorbable Scaffold for Periodontal Repair. *J Dent Res.* 2015;94(9):153S-157S.
  161. Morand DN, Davideau JL, Clauss F, Jessel N, Tenenbaum H, Huck O. Cytokines during periodontal wound healing: potential application for new therapeutic approach. *Oral Dis.* 2017;23(3):300–11.
  162. Osorio R, Alfonso-Rodríguez CA, Osorio E, Medina-Castillo AL, Alaminos M, Toledano-Osorio M, et al. Novel potential scaffold for periodontal tissue engineering. *Clin Oral Investig.* 2017;21(9):2695–707.
  163. Batool F, Morand DN, Thomas L, Bugueno IM, Aragon J, Irusta S, et al. Synthesis of a novel electrospun polycaprolactone scaffold functionalized with ibuprofen for periodontal regeneration: An in vitro and in vivo study. *Materials (Basel).* 2018;11(4):1–18.
  164. Liao Y, Li H, Shu R, Chen H, Zhao L, Song Z, et al. Mesoporous Hydroxyapatite/Chitosan Loaded With Recombinant-Human Amelogenin Could Enhance Antibacterial Effect and Promote Periodontal Regeneration. *Front Cell Infect Microbiol.* 2020;10:180.
  165. Bartold PM, Gronthos S. Standardization of Criteria Defining Periodontal Ligament Stem Cells. *J Dent Res.* 2017;96(5):487–90.
  166. Kargozar S, Mozafari M, Hamzehlou S, Milan PB, Hae-Won K, Baino F. Bone Tissue Engineering Using Human Cells : A Comprehensive Review on Recent Trends, Current Prospects, and Recommendations. *Appl Sci.* 2019;9(174):1–49.
  167. Yang JR, Hsu CW, Liao SC, Lin YT, Chen LR, Yuan K. Transplantation of embryonic stem cells improves the regeneration of periodontal furcation defects in a porcine model. *J Clin Periodontol.* 2013;40(4):364–71.
  168. Zhang Y, Li Y, Shi R, Zhang S, Liu H, Zheng Y, et al. Generation of tooth-periodontium complex structures using high-odontogenic potential dental epithelium derived from mouse embryonic stem cells. *Stem Cell Res Ther.* 2017;8(1):1–8.

169. Inanç B, Elçin AE, Elçin YM. Effect of osteogenic induction on the in vitro differentiation of human embryonic stem cells cocultured with periodontal ligament fibroblasts. *Artif Organs*. 2007;31(11):792–800.
170. Takahashi K, Yamanaka S. Induction of Pluripotent Stem Cells from Mouse Embryonic and Adult Fibroblast Cultures by Defined Factors. *Cell*. 2006;2:663–76.
171. Du M, Duan X, Yang P. Induced Pluripotent Stem Cells and Periodontal Regeneration. *Curr Oral Heal Reports*. 2015;2(4):257–65.
172. Radwan IA, Rady D, Abbass MMS, El Moshy S, Abubakr N, Dörfer CE, et al. Induced Pluripotent Stem Cells in Dental and Nondental Tissue Regeneration: A Review of an Unexploited Potential. *Stem Cells Int*. 2020;2020.
173. Wang P, Ma T, Guo D, Hu K, Shu Y, Xu HHK, et al. Metformin induces osteoblastic differentiation of human induced pluripotent stem cell-derived mesenchymal stem cells. *J Tissue Eng Regen Med*. 2018;12(2):437–46.
174. Duan X, Tu Q, Zhang J, Ye J, Sommer C, Mostoslavsky G, et al. Application of induced pluripotent stem (iPS) cells in periodontal tissue regeneration. *J Cell Physiol*. 2011;226(1):150–7.
175. Ma MS, Kannan V, Vries AE De, Czepiel M. Characterization and comparison of osteoblasts derived from mouse embryonic stem cells and induced pluripotent stem cells. *J Bone Miner Metab*. 2017;35(1):20–9.
176. Verfaillie CM. Adult stem cells : assessing the case for pluripotency. *Trends Cell Biol*. 2002;12(11):502–8.
177. Dominici M, Le Blanc K, Mueller I, Slaper-Cortenbach I, Marini FC, Krause DS, et al. Minimal criteria for defining multipotent mesenchymal stromal cells. The International Society for Cellular Therapy position statement. *Cytotherapy*. 2006;8(4):315–7.
178. Hernández-Monjaraz B, Santiago-Osorio E, Monroy-García A, Ledesma-Martínez E, Mendoza-Núñez VM. Mesenchymal stem cells of dental origin for inducing tissue regeneration in periodontitis: A mini-review. *Int J Mol Sci*. 2018;19(4).
179. Cristaldi M, Mauceri R, Campisi G, Pizzo G, Alessandro R, Tomasello L, et al. Growth and Osteogenic Differentiation of Discarded Gingiva-Derived Mesenchymal Stem Cells on a Commercial Scaffold. *Front Cell Dev Biol*. 2020;8(May):1–16.

180. Volponi AA, Sharpe PT. The tooth - A treasure chest of stem cells. *Br Dent J.* 2013;215(7):353–8.
181. Zhai Q, Dong Z, Wang W, Li B, Jin Y. Dental stem cell and dental tissue regeneration. *Front Med.* 2019;13(2):152–9.
182. Wang H, Ma D, Zhang X, Xu S, Ning T, Wu B. Comparative proteomic profiling of human dental pulp stem cells and periodontal ligament stem cells under in vitro osteogenic induction. *Arch Oral Biol.* 2018;89:9–19.
183. Khorsand A, Eslaminejad MB, Arabsolghar M, Paknejad M, Ghaedi B, Rokn AR, et al. Autologous Dental Pulp Stem Cells in Regeneration of Defect Created in Canine Periodontal Tissue. *J Oral Implantol.* 2013;39(4):433–43.
184. Liu L, Ling J, Wei X, Wu L, Xiao Y. Stem Cell Regulatory Gene Expression in Human Adult Dental Pulp and Periodontal Ligament Cells Undergoing Odontogenic/Osteogenic Differentiation. *J Endod.* 2009;35(10):1368–76.
185. Hu J, Cao Y, Xie Y, Wang H, Fan Z, Wang J, et al. Periodontal regeneration in swine after cell injection and cell sheet transplantation of human dental pulp stem cells following good manufacturing practice. *Stem Cell Res Ther.* 2016;7(1):1–11.
186. Ferrarotti F, Romano F, Gamba MN, Quirico A, Giraudi M, Audagna M, et al. Human intrabony defect regeneration with micrografts containing dental pulp stem cells: A randomized controlled clinical trial. *J Clin Periodontol.* 2018;45(7):841–50.
187. Li Y, Zhao S, Nan X, Wei H, Shi J, Li A, et al. Repair of human periodontal bone defects by autologous grafting stem cells derived from inflammatory dental pulp tissues. *Stem Cell Res Ther.* 2016;7(1):1–9.
188. Bassir SH, Wisitrasameewong W, Raanan J, Ghaffarigarakani S, Chung J, Freire M, et al. Potential for Stem Cell-Based Periodontal Therapy. *J Cell Physiol.* 2016;231(1):50–61.
189. Xie F, He J, Chen Y, Hu Z, Qin M, Hui T. Multi-lineage differentiation and clinical application of stem cells from exfoliated deciduous teeth. *Hum Cell.* 2020;33(2):295–302.
190. Miura M, Gronthos S, Zhao M, Lu B, Fisher LW, Robey PG, et al. SHED: Stem cells from human exfoliated deciduous teeth. *Proc Natl Acad Sci.* 2003;100(10):5807–12.
191. Seo BM, Sonoyama W, Yamaza T, Coppe C, Kikuri T, Akiyama K, et al.

- SHED repair critical-size calvarial defects in mice. *Oral Dis.* 2008;14(5):428–34.
192. Qiao YQ, Zhu LS, Cui SJ, Zhang T, Yang RL, Zhou YH. Local Administration of Stem Cells from Human Exfoliated Primary Teeth Attenuate Experimental Periodontitis in Mice. *Chinese J Dent Res.* 2019;22(3):157–63.
193. Chadipiralla K, Yochim JM, Bahuleyan B, Huang CYC, Garcia-Godoy F, Murray PE, et al. Osteogenic differentiation of stem cells derived from human periodontal ligaments and pulp of human exfoliated deciduous teeth. *Cell Tissue Res.* 2010;340(2):323–33.
194. Mori G, Ballini A, Carbone C, Oranger A, Brunetti G, di Benedetto A, et al. Osteogenic differentiation of dental follicle stem cells. *Int J Med Sci.* 2012;9(6):480–7.
195. Caracappa JD, Vincent S. The future in dental medicine : Dental stem cells are a promising source for tooth and tissue engineering. *J Stem Cell Res Ther Rev.* 2019;5(2):30–6.
196. Kang J, Fan W, Deng Q, He H, Huang F. Stem Cells from the Apical Papilla: A Promising Source for Stem Cell-Based Therapy. *Biomed Res Int.* 2019;2019.
197. Sonoyama W, Liu Y, Fang D, Yamaza T, Seo BM, Zhang C, et al. Mesenchymal stem cell-mediated functional tooth regeneration in Swine. *PLoS One.* 2006;1(1):1–8.
198. Li G, Han N, Zhang X, Yang H, Cao Y, Wang S, et al. Local Injection of Allogeneic Stem Cells from Apical Papilla Enhanced Periodontal Tissue Regeneration in Minipig Model of Periodontitis. *Biomed Res Int.* 2018;2018.
199. Fawzy El-Sayed KM, Dörfer CE. Gingival Mesenchymal Stem/Progenitor Cells: A Unique Tissue Engineering Gem. *Stem Cells Int.* 2016;2016.
200. Fawzy El-Sayed K, Paris S, Becker S, Neuschl M, De Buhr W, Salzer S, et al. Periodontal regeneration employing gingival margin-derived stem/progenitor cells: an animal study. *J Clin Periodontol.* 2012;39:861–70.
201. Fonticoli L, Rocca Y Della, Rajan TS, Murmura G, Trubiani O, Oliva S, et al. A Narrative Review : Gingival Stem Cells as a Limitless Reservoir for Regenerative Medicine. *Int J Mol Sci.* 2022;23.
202. Xu XY, Li X, Wang J, He XT, Sun HH, Chen FM. Concise Review:

- Periodontal Tissue Regeneration Using Stem Cells: Strategies and Translational Considerations. *Stem Cells Transl Med.* 2019;8:392–403.
203. Baksh D, Yao R, Tuan RS. Comparison of Proliferative and Multilineage Differentiation Potential of Human Mesenchymal Stem Cells Derived from Umbilical Cord and Bone Marrow. *Stem Cells.* 2007;25(6):1384–92.
204. Wang Q, Zhao G, Xing Z, Zhan J, Ma JIE. Comparative evaluation of the osteogenic capacity of human mesenchymal stem cells from bone marrow and umbilical cord tissue. *Exp Ther Med.* 2019;17:764–72.
205. A. J. Friedenstein, R. K. Chailakhjan KSL. The Development Of Fibroblast Colonies In Monolayer Cultures Of Guinea-Pig Bone Marrow And Spleen Cells. *Cell Tissue Kinet.* 1970;3:393–403.
206. Pittenger MF, Mackay AM, Beck SC, Jaiswal RK, Douglas R, Mosca JD, et al. Multilineage Potential of Adult Human Mesenchymal Stem Cells. *Science (80- ).* 1999;284:143–7.
207. Chan CKF, Gulati GS, Sinha R, Tompkins JV, Lopez M, Carter AC, et al. Identification of the Human Skeletal Stem Cell. *Cell.* 2018;175(1):43–56.
208. Aida Y, Kurihara H, Kato K. Wnt3a promotes differentiation of human bone marrow-derived mesenchymal stem cells into cementoblast-like cells. *Vitr Cell Dev Biol - Anim.* 2018;54:468–76.
209. Dawson JI, Kanczler J, Tare R, Kassem M, Oreffo ROC. Concise review: Bridging the gap: Bone regeneration using skeletal stem cell-based strategies-where are we now? *Stem Cells.* 2014;32(1):35–44.
210. Gómez-Barrena E, Rosset P, Gebhard F, Hernigou P, Baldini N, Rouard H, et al. Feasibility and safety of treating non-unions in tibia, femur and humerus with autologous, expanded, bone marrow-derived mesenchymal stromal cells associated with biphasic calcium phosphate biomaterials in a multicentric, non-comparative trial. *Biomaterials.* 2019;196:100–8.
211. Redondo LM, García V, Peral B, Verrier A, Becerra J, Sánchez A, et al. Repair of maxillary cystic bone defects with mesenchymal stem cells seeded on a cross-linked serum scaffold. *J Cranio-Maxillofacial Surg.* 2018;46(2):222–9.
212. Iwasaki K, Peng Y, Kanda R, Umeda M, Ishikawa I. Stem Cell Transplantation and Cell-Free Treatment for Periodontal Regeneration. *Int J Mol Sci.* 2022;23(3).
213. Hasegawa N, Kawaguchi H, Hirachi A, Takeda K, Mizuno N, Nishimura M,

- et al. Behavior of Transplanted Bone Marrow–Derived Mesenchymal Stem Cells in Periodontal Defects. *J Periodontol.* 2006;77(6):1003–7.
214. Zhou W, Mei L. Effect of autologous bone marrow stromal cells transduced with osteoprotegerin on periodontal bone regeneration in canine periodontal window defects. *Int J Periodontics Restor Dent.* 2012;32(5):174–81.
215. Cai X, Yang F, Yan X, Yang W, Yu N, Oortgiesen DAW, et al. Influence of bone marrow-derived mesenchymal stem cells pre-implantation differentiation approach on periodontal regeneration in vivo. *J Clin Periodontol.* 2015;42(4):380–9.
216. Bartold M, Ivanovski S. Stem Cell Applications in Periodontal Regeneration. *Dent Clin North Am.* 2022;66(1):53–74.
217. Baba S, Yamada Y, Komuro A, Yotsui Y, Umeda M, Shimuzutani K, et al. Phase I/II Trial of Autologous Bone Marrow Stem Cell Transplantation with a Three-Dimensional Woven-Fabric Scaffold for Periodontitis. *Stem Cells Int.* 2016;2016:1–7.
218. Apatzidou DA, Bakopoulou AA, Kouzi-Koliakou K, Karagiannis V, Konstantinidis A. A tissue-engineered biocomplex for periodontal reconstruction. A proof-of-principle randomized clinical study. *J Clin Periodontol.* 2021;48(8):1111–25.
219. Costa CA, Deliberador TM, Abuna RPF, Rodrigues TL, De Souza SLS, Palioto DB. Mesenchymal stem cells surpass the capacity of bone marrow aspirate concentrate for periodontal regeneration. *J Appl Oral Sci.* 2022;30:1–12.
220. Sharpe PT. Dental mesenchymal stem cells. *Development.* 2016;143:2273–80.
221. Leucht P, Kim JB, Amasha R, James AW, Girod S, Helms JA. Embryonic origin and Hox status determine progenitor cell fate during adult bone regeneration. *Development.* 2008;135(17):2845–54.
222. Akintoye SO, Lam T, Shi S, Brahim J, Collins MT, Robey PG. Skeletal site-specific characterization of orofacial and iliac crest human bone marrow stromal cells in same individuals. *Bone.* 2006;38(6):758–68.
223. Seo BM, Miura M, Gronthos S, Bartold PM, Batouli S, Brahim J, et al. Investigation of multipotent postnatal stem cells from human periodontal ligament. *Lancet.* 2004;364(9429):149–55.

224. Tomokiyo A, Wada N, Maeda H. Periodontal Ligament Stem Cells: Regenerative Potency in Periodontium. *Stem Cells Dev.* 2019;28(15):974–85.
225. Trubiani O, Pizzicannella J, Caputi S, Marchisio M, Mazzon E, Paganelli R, et al. Periodontal Ligament Stem Cells: Current Knowledge and Future Perspectives. *Stem Cells Dev.* 2019;28(15):995–1003.
226. Zhu W, Liang M. Periodontal ligament stem cells: Current status, concerns, and future prospects. *Stem Cells Int.* 2015;2015:1–11.
227. Zhang J, An Y, Gao LN, Zhang YJ, Jin Y, Chen FM. The effect of aging on the pluripotential capacity and regenerative potential of human periodontal ligament stem cells. *Biomaterials.* 2012;33(29):6974–86.
228. Trubiani O, Zalzal SF, Paganelli R, Marchisio M, Giancola R, Pizzicannella J. Expression Profile of the Embryonic Markers Nanog , Frizzled-9 Receptor in Human Periodontal Ligament Mesenchymal Stem Cells. *J Cell Physiol.* 2010;225:123–31.
229. Tomokiyo A, Yoshida S, Hamano S, Hasegawa D, Sugii H, Maeda H. Detection, Characterization, and Clinical Application of Mesenchymal Stem Cells in Periodontal Ligament Tissue. *Stem Cells Int.* 2018;2018.
230. Gay I, Cavender A, Peto D, Sun Z, Speer A, Cao H, et al. Differentiation of human dental stem cells reveals a role for microRNA-218. *J Periodontal Res.* 2014;49(1):110–20.
231. Liu W, Konermann A, Guo T, Jäger A, Zhang L, Jin Y. Canonical Wnt signaling differently modulates osteogenic differentiation of mesenchymal stem cells derived from bone marrow and from periodontal ligament under inflammatory conditions. *Biochim Biophys Acta.* 2014;1840(3):1125–34.
232. Wei F, Yang S, Guo Q, Zhang X, Ren D, Lv T, et al. MicroRNA-21 regulates Osteogenic Differentiation of Periodontal Ligament Stem Cells by targeting Smad5. *Sci Rep.* 2017;7(1):1–12.
233. Albiero ML, Amorim BR, Martins L, Casati MZ, Sallum EA, Nociti FH, et al. Exposure of periodontal ligament progenitor cells to lipopolysaccharide from escherichia coli changes osteoblast differentiation pattern. *J Appl Oral Sci.* 2015;23(2):145–52.
234. Mukhtar AH, Alqutub MN. Osteogenic Potential of Periodontal Ligament Stem Cells Cultured in Osteogenic and Regular Growth Media: Confocal and Scanning Electron Microscope Study. *J Contemp Dent Pract.*

2020;21(7):776–80.

235. Yamada S, Tauchi T, Awata T, Maeda K, Kajikawa T, Yanagita M, et al. Characterization of a novel periodontal ligament-specific periostin isoform. *J Dent Res*. 2014;93(9):891–7.
236. Komaki M, Iwasaki K, Arzate H, Narayanan AS, Izumi Y, Morita I. Cementum protein 1 (CEMP1) induces a cementoblastic phenotype and reduces osteoblastic differentiation in periodontal ligament cells. *J Cell Physiol*. 2012;227(2):649–57.
237. Chen F ming, Zhao Y min, Wu H, Deng Z hong, Wang Q tao, Zhou W, et al. Enhancement of periodontal tissue regeneration by locally controlled delivery of insulin-like growth factor-I from dextran-co-gelatin microspheres. *J Control Release*. 2006;114(2):209–22.
238. Gao LN, An Y, Lei M, Li B, Yang H, Lu H, et al. The effect of the coumarin-like derivative osthole on the osteogenic properties of human periodontal ligament and jaw bone marrow mesenchymal stem cell sheets. *Biomaterials*. 2013;34(38):9937–51.
239. Iwata T, Yamato M, Zhang Z, Mukobata S, Washio K, Ando T, et al. Validation of human periodontal ligament-derived cells as a reliable source for cytotherapeutic use. *J Clin Periodontol*. 2010;37(12):1088–99.
240. Zhang H, Liu S, Zhu B, Xu Q, Ding Y, Jin Y. Composite cell sheet for periodontal regeneration: crosstalk between different types of MSCs in cell sheet facilitates complex periodontal-like tissue regeneration. *Stem Cell Res Ther*. 2016;7(1):1–15.
241. Tsumanuma Y, Iwata T, Washio K, Yoshida T, Yamada A, Takagi R, et al. Comparison of different tissue-derived stem cell sheets for periodontal regeneration in a canine 1-wall defect model. *Biomaterials*. 2011;32(25):5819–25.
242. Kim S-H, Kim K-H, Seo B-M, Koo K-T, Kim T-I, Seol Y-J, et al. Alveolar Bone Regeneration by Transplantation of Periodontal Ligament Stem Cells and Bone Marrow Stem Cells in a Canine Peri-Implant Defect Model: A Pilot Study. *J Periodontol*. 2009;80(11):1815–23.
243. Zhang J, Li ZG, Si YM, Chen B, Meng J. The difference on the osteogenic differentiation between periodontal ligament stem cells and bone marrow mesenchymal stem cells under inflammatory microenvironments. *Differentiation*. 2014;88(4–5):97–105.

244. Phadnis SM, Ghaskadbi SM, Hardikar AA, Bhonde RR. Mesenchymal stem cells derived from bone marrow of diabetic patients portrait unique markers influenced by the diabetic microenvironment. *Rev Diabet Stud.* 2009;6(4):260–70.
245. Gabr MM, Zakaria MM, Refaie AF, Ismail AM, Abou-El-Mahasen MA, Ashamallah SA, et al. Insulin-producing cells from adult human bone marrow mesenchymal stem cells control streptozotocin-induced diabetes in nude mice. *Cell Transplant.* 2013;22(1):133–45.
246. Brewster L, Robinson S, Wang R, Griffiths S, Li H, Peister A, et al. Expansion and angiogenic potential of mesenchymal stem cells from patients with critical limb ischemia. *J Vasc Surg.* 2017;65(3):826-838.e1.
247. Andrzejewska A, Catar R, Schoon J, Qazi TH, Sass FA, Jacobi D, et al. Multi-Parameter Analysis of Biobanked Human Bone Marrow Stromal Cells Shows Little Influence for Donor Age and Mild Comorbidities on Phenotypic and Functional Properties. *Front Immunol.* 2019;10(2472).
248. Cassidy FC, Shortiss C, Murphy CG, Kearns SR, Curtin W, Buitl C De, et al. Impact of Type 2 Diabetes Mellitus on Human Bone Marrow Stromal Cell Number and Phenotypic Characteristics. *Int J Mol Sci.* 2020;21:1–20.
249. Flouzat-Lachaniette CH, Heyberger C, Bouthors C, Roubineau F, Chevallier N, Rouard H, et al. Osteogenic progenitors in bone marrow aspirates have clinical potential for tibial non-unions healing in diabetic patients. *Int Orthop.* 2016;40(7):1375–9.
250. Ferland-McCollough D, Maselli D, Spinetti G, Sambataro M, Sullivan N, Blom A, et al. MCP-1 feedback loop between adipocytes and mesenchymal stromal cells causes fat accumulation and contributes to hematopoietic stem cell rarefaction in the bone marrow of patients with diabetes. *Diabetes.* 2018;67(7):1380–94.
251. Sun R, Liang C, Sun Y, Xu Y, Geng W, Li J. Effects of metformin on the osteogenesis of alveolar BMSCs from diabetic patients and implant osseointegration in rats. *Oral Dis.* 2021;28:1170–80.
252. Liang C, Liu X, Liu C, Xu Y, Geng W, Li J. Integrin  $\alpha 10$  regulates adhesion, migration, and osteogenic differentiation of alveolar bone marrow mesenchymal stem cells in type 2 diabetic patients who underwent dental implant surgery. *Bioengineered.* 2022;13(5):13252–68.
253. Ribot J, Denoëud C, Frescaline G, Landon R, Petite H, Pavon-Djavid G, et

- al. Experimental type 2 diabetes differently impacts on the select functions of bone marrow-derived multipotent stromal cells. *Cells*. 2021;10(2):268.
254. Doxey DL, Nares S, Park B, Trieu C, Cutler CW, Iacopino AM. Diabetes-induced impairment of macrophage cytokine release in a rat model: Potential role of serum lipids. *Life Sci*. 1998;63(13):1127–36.
255. Kato H, Taguchi Y, Tominaga K, Kimura D, Yamawaki I, Noguchi M, et al. High Glucose Concentrations Suppress the Proliferation of Human Periodontal Ligament Stem Cells and Their Differentiation Into Osteoblasts. *J Periodontol*. 2016;87(4).
256. Dohl J, Foldi J, Heller J, Gasier HG, Deuster PA, Yu T. Acclimation of C2C12 myoblasts to physiological glucose concentrations for in vitro diabetes research. *Life Sci*. 2018;211:238–44.
257. José VS de S, Monnerat G, Guerra B, Paredes BD, Kasai-Brunswick TH, Carvalho ACC de, et al. Bone-Marrow-Derived Mesenchymal Stromal Cells (MSC) from Diabetic and Nondiabetic Rats Have Similar Therapeutic Potentials. *Arq Bras Cardiol*. 2017;579–89.
258. Li X, Liu N, Gu B, Hu W, Li Y, Guo B, et al. BMAL1 regulates balance of osteogenic–osteoclastic function of bone marrow mesenchymal stem cells in type 2 diabetes mellitus through the NF- $\kappa$ B pathway. *Mol Biol Rep*. 2018;45(6):1691–704.
259. Okuda M, Taguchi Y, Takahashi S, Umeda AT and M. Effects of High Glucose for Hard Tissue Formation on Type II Diabetes Model Rat Bone Marrow Cells In Vitro. *J Hard Tissue Biol*. 2015;24(1):77–84.
260. Qian C, Zhu C, Yu W, Jiang X, Zhang F. High-fat diet/low-dose streptozotocin-induced type 2 diabetes in rats impacts osteogenesis and Wnt signaling in bone marrow stromal cells. *PLoS One*. 2015;10(8):1–15.
261. Jiang ZL, Jin H, Liu ZS, Liu MY, Cao XF, Jiang YY, et al. Lentiviral-mediated Shh reverses the adverse effects of high glucose on osteoblast function and promotes bone formation via Sonic hedgehog signaling. *Mol Med Rep*. 2019;20(4):3265–75.
262. Al-Qarakhli AMA, Yusop N, Waddington RJ, Moseley R. Effects of high glucose conditions on the expansion and differentiation capabilities of mesenchymal stromal cells derived from rat endosteal niche. *BMC Mol Cell Biol*. 2019;20(1):1–18.
263. Xu J, Huang Z, Lin L, Fu M, Song Y, Shen Y, et al. MiRNA-130b is required

- for the ERK/FOXO1 pathway activation-mediated protective effects of isosorbide dinitrate against mesenchymal stem cell senescence induced by high glucose. *Int J Mol Med*. 2015;35(1):59–71.
264. Zhang D, Lu H, Chen Z, Wang Y, Lin J, Xu S, et al. High glucose induces the aging of mesenchymal stem cells via Akt/mTOR signaling. *Mol Med Rep*. 2017;16(2):1685–90.
265. Yang K, Wang XQ, He YS, Lu L, Chen QJ, Liu J, et al. Advanced glycation end products induce chemokine/cytokine production via activation of p38 pathway and inhibit proliferation and migration of bone marrow mesenchymal stem cells. *Cardiovasc Diabetol*. 2010;9(1):1–10.
266. Kim S, Kwon J. COMP-Ang1 inhibits apoptosis as well as improves the attenuated osteogenic differentiation of mesenchymal stem cells induced by advanced glycation end products. *Biochim Biophys Acta - Gen Subj*. 2013;1830(10):4928–34.
267. Ying X, Chen X, Liu H, Nie P, Shui X, Shen Y, et al. Silibinin alleviates high glucose-suppressed osteogenic differentiation of human bone marrow stromal cells via antioxidant effect and PI3K/Akt signaling. *Eur J Pharmacol*. 2015;765:394–401.
268. Chang TC, Hsu MF, Wu KK. High glucose induces bone marrow-derived mesenchymal stem cell senescence by upregulating autophagy. *PLoS One*. 2015;10(5):1–15.
269. Li YM, Schilling T, Benisch P, Zeck S, Meissner-Weigl J, Schneider D, et al. Effects of high glucose on mesenchymal stem cell proliferation and differentiation. *Biochem Biophys Res Commun*. 2007;363(1):209–15.
270. Dhanasekaran M, Indumathi S, Rajkumar JS, Sudarsanam D. Effect of high glucose on extensive culturing of mesenchymal stem cells derived from subcutaneous fat, omentum fat and bone marrow. *Cell Biochem Funct*. 2013;31(1):20–9.
271. Shiomi K, Yamawaki I, Taguchi Y, Kimura D, Umeda M. Osteogenic effects of glucose concentration for human bone marrow stromal cells after stimulation with *Porphyromonas gingivalis* lipopolysaccharide. *J Hard Tissue Biol*. 2020;29(1):17–24.
272. Qu B, Gong K, Yang HS, Li YG, Jiang T, Zeng ZM, et al. MiR-449 overexpression inhibits osteogenic differentiation of bone marrow mesenchymal stem cells via suppressing Sirt1/Fra-1 pathway in high

- glucose and free fatty acids microenvironment. *Biochem Biophys Res Commun.* 2018;496(1):120–6.
273. Bian Y, Ma X, Wang R, Yuan H, Chen N, Du Y. Human amnion-derived mesenchymal stem cells promote osteogenesis of human bone marrow mesenchymal stem cells against glucolipotoxicity. *FEBS Open Bio.* 2019;9:74–81.
274. Wang Y, Huang L, Qin Z, Yuan H, Li B, Pan Y, et al. Parathyroid hormone ameliorates osteogenesis of human bone marrow mesenchymal stem cells against glucolipotoxicity through p38 MAPK signaling. *IUBMB Life.* 2021;73(1):213–22.
275. Lu YQ, Lu Y, Li HJ, Cheng XB. Effect of advanced glycosylation end products (AGEs) on proliferation of human bone marrow mesenchymal stem cells (MSCs) in vitro. *Vitr Cell Dev Biol - Anim.* 2012;48:599–602.
276. Deng X, Xu M, Shen M, Cheng J. Effects of Type 2 Diabetic Serum on Proliferation and Osteogenic Differentiation of Mesenchymal Stem Cells. *J Diabetes Res.* 2018;2018.
277. Rezaabakhsh A, Cheraghi O, Nourazarian A, Hassanpour M, Kazemi M, Ghaderi S, et al. Type 2 Diabetes Inhibited Human Mesenchymal Stem Cells Angiogenic Response by Over-Activity of the Autophagic Pathway. *J Cell Biochem.* 2017;118(6):1518–30.
278. Assem M, Kamal S, Sabry D, Soliman N, Aly RM. Preclinical Assessment of the Proliferation Capacity of Gingival and Periodontal Ligament Stem Cells from Diabetic Patients. *Maced J Med Sci.* 2018;6(2):254–9.
279. Liu Q, Hu C, Zhou C, Cui X, Yang K, Deng C. DKK1 rescues osteogenic differentiation of mesenchymal stem cells isolated from periodontal ligaments of patients with diabetes mellitus induced periodontitis. *Sci Rep.* 2015;5:13142.
280. Hobbs HC, Rowe DJ, Johnson PW. Periodontal Ligament Cells From Insulin- Dependent Diabetics Exhibit Altered Alkaline Phosphatase Activity in Response to Growth Factors. *J Periodontol.* 1999;70(7):736–42.
281. Sundaram MN, Sowmya S, Deepthi S, Bumgardener JD, Jayakumar R. Bilayered construct for simultaneous regeneration of alveolar bone and periodontal ligament. *J Biomed Mater Res - Part B Appl Biomater.* 2016;104(4):761–70.
282. Park SB, An SY, Han WJ, Park JT. Three-dimensional measurement of

- periodontal surface area for quantifying inflammatory burden. *J Periodontal Implant Sci.* 2017;47(3):154–64.
283. Khadre A, Raif EL, Junaid S, Goudouri OM, Refaat W, Ramadan A, et al. A bilayered tissue engineered in vitro model simulating the tooth periodontium. *Eur Cells Mater.* 2021;41:232–45.
284. El-Gendy R, Junaid S, Lam SKL, Elson KM, Tipper JL, Hall RM, et al. Developing a Tooth in situ Organ Culture Model for Dental and Periodontal Regeneration Research. *Front Bioeng Biotechnol.* 2021;8.
285. Koch F, Meyer N, Valdec S, Jung RE, Mathes SH. Development and application of a 3D periodontal in vitro model for the evaluation of fibrillar biomaterials. *BMC Oral Health.* 2020;20(1):1–12.
286. Zhen L, Jiang X, Chen Y, Fan D. MiR-31 is involved in the high glucose-suppressed osteogenic differentiation of human periodontal ligament stem cells by targeting *Satb2*. *Am J Transl Res.* 2017;9(5):2384–93.
287. Liu Z, Chen T, Sun W, Yuan Z, Yu M, Chen G, et al. DNA Demethylation Rescues the Impaired Osteogenic Differentiation Ability of Human Periodontal Ligament Stem Cells in High Glucose. *Sci Rep.* 2016;6:1–12.
288. Guo Z, Chen R, Zhang F, Ding M, Wang P. Exendin-4 relieves the inhibitory effects of high glucose on the proliferation and osteoblastic differentiation of periodontal ligament stem cells. *Arch Oral Biol.* 2018;91:9–16.
289. Zheng DH, Han ZQ, Wang XX, Ma D, Zhang J. Erythropoietin attenuates high glucose-induced oxidative stress and inhibition of osteogenic differentiation in periodontal ligament stem cell (PDLSCs). *Chem Biol Interact.* 2019;305:40–7.
290. Zhan D, Guo L, Zheng L. Inhibition of the receptor for advanced glycation promotes proliferation and repair of human periodontal ligament fibroblasts in response to high glucose via the NF- $\kappa$ B signaling pathway. *Arch Oral Biol.* 2018;87:86–93.
291. Kim SY, Lee JY, Park YD, Kang KL, Lee JC, Heo JS. Hesperetin Alleviates the Inhibitory Effects of High Glucose on the Osteoblastic Differentiation of Periodontal Ligament Stem Cells. *PLoS One.* 2013;8(6):1–11.
292. Yan Y, Zhang H, Liu L, Chu Z, Ge Y, Wu J, et al. Periostin reverses high glucose-inhibited osteogenesis of periodontal ligament stem cells via AKT pathway. *Life Sci.* 2020;242.
293. Deng C, Sun Y, Liu H, Wang W, Wang J, Zhang F. Selective adipogenic

- differentiation of human periodontal ligament stem cells stimulated with high doses of glucose. *PLoS One*. 2018;13(7):1–12.
294. Bhattarai G, Min CK, Jeon YM, Bashyal R, Poudel SB, Kook SH, et al. Oral supplementation with p-coumaric acid protects mice against diabetes-associated spontaneous destruction of periodontal tissue. *J Periodontal Res*. 2019;54(6):690–701.
  295. Kim HS, Park JW, Yeo S II, Choi BJ, Suh JY. Effects of high glucose on cellular activity of periodontal ligament cells in vitro. *Diabetes Res Clin Pract*. 2006;74(1):41–7.
  296. Liu J, Jiang Y, Mao J, Gu B, Liu H, Fang B. High levels of glucose induces a dose-dependent apoptosis in human periodontal ligament fibroblasts by activating caspase-3 signaling pathway. *Appl Biochem Biotechnol*. 2013;170(6):1458–71.
  297. Luo H, Zhu W, Mo W, Liang M. High-glucose concentration aggravates TNF-alpha-induced cell viability reduction in human CD146-positive periodontal ligament cells via TNFR-1 gene demethylation. *Cell Biol Int*. 2020;44(12):2383–94.
  298. Wu Y, Liu F, Zhang X, Shu L. Insulin modulates cytokines expression in human periodontal ligament cells. *Arch Oral Biol*. 2014;59(12):1301–6.
  299. Seubbuk S, Sritanaudomchai H, Kasetsuwan J, Surarit R. High glucose promotes the osteogenic differentiation capability of human periodontal ligament fibroblasts. *Mol Med Rep*. 2017;15(5):2788–94.
  300. Guo Z, Gan S, Cao C, Fu R, Cao S, Xie C, et al. Advanced glycosylated end products restrain the osteogenic differentiation of the periodontal ligament stem cell. *J Dent Sci*. 2019;1–6.
  301. Mei YM, Li L, Wang XQ, Zhang M, Zhu LF, Fu YW, et al. AGEs induces apoptosis and autophagy via reactive oxygen species in human periodontal ligament cells. *J Cell Biochem*. 2019;1–16.
  302. Wang Z, Wang X, Zhang L, Wang B, Xu B, Zhang J. GLP-1 inhibits PKC $\beta$ 2 phosphorylation to improve the osteogenic differentiation potential of hPDLSCs in the AGE microenvironment. *J Diabetes Complications*. 2020;34(3):107495.
  303. Zhang LN, Wang XX, Wang Z, Li KY, Xu BH, Zhang J. Berberine improves advanced glycation end products-induced osteogenic differentiation responses in human periodontal ligament stem cells through the canonical

- Wnt/ $\beta$ -catenin pathway. *Mol Med Rep.* 2019;19(6):5440–52.
304. Fang H, Yang K, Tang P, Zhao N, Ma R, Luo X, et al. Glycosylation end products mediate damage and apoptosis of periodontal ligament stem cells induced by the JNK-mitochondrial pathway. *Aging (Albany NY).* 2020;12(13):12850–68.
  305. Yang N, Li Y, Wang G, Ding Y, Jin Y, Xu Y. Tumor necrosis factor- $\alpha$  suppresses adipogenic and osteogenic differentiation of human periodontal ligament stem cell by inhibiting miR-21/Spry1 functional axis. *Differentiation.* 2017;97:33–43.
  306. Yuan J, Wang X, Ma D, Gao H, Zheng D, Zhang J. Resveratrol rescues TNF- $\alpha$ -induced inhibition of osteogenesis in human periodontal ligament stem cells via the ERK1/2 pathway. *Mol Med Rep.* 2020;21:2085–94.
  307. Jiang C, Wang Q, Song M, Wang M, Zhao L, Huang Y. Coronarin D affects TNF- $\alpha$  induced proliferation and osteogenic differentiation of human periodontal ligament stem cells. *Arch Oral Biol.* 2019;108:104519.
  308. Yang H, Gao L, An Y, Hu C, Jin F, Zhou J. Comparison of mesenchymal stem cells derived from gingival tissue and periodontal ligament in different incubation conditions. *Biomaterials.* 2013;34:7033–47.
  309. Raja S, Byakod G, Pudukalkatti P. Growth factors in periodontal regeneration. *Int J Dent Hyg.* 2009;7(2):82–9.
  310. Zhou WL, Li LL, Qiu XR, An Q, Li MH. Effects of Combining Insulin-like Growth Factor 1 and Platelet-derived Growth Factor on Osteogenesis around Dental Implants. *Chinese J Dent Res.* 2017;20(2):105–9.
  311. Dereka XE, Markopoulou CE, Vrotsos IA. Role of growth factors on periodontal repair. *Growth Factors.* 2006;24(4):260–7.
  312. Huang Z, Ren PG, Ma T, Smith RL, Goodman SB. Modulating osteogenesis of mesenchymal stem cells by modifying growth factor availability. *Cytokine.* 2010;51(3):305–10.
  313. Stavropoulos A, Wikesjö UME. Growth and differentiation factors for periodontal regeneration: A review on factors with clinical testing. *J Periodontal Res.* 2012;47(5):545–53.
  314. Ausenda F, Rasperini G, Acunzo R, Gorbunkova A, Pagni G. New perspectives in the use of biomaterials for periodontal regeneration. *Materials (Basel).* 2019;12(13).
  315. Deifenderfer DL, Osyczka AM, Reilly GC, Leboy PS. BMP responsiveness

- in human mesenchymal stem cells. *Connect Tissue Res.* 2003;44(1):305–11.
316. Hjortebjerg R, Laugesen E, Hoyem P, Oxvig C, Stausbøl-Gron B, Knudsen ST, et al. The IGF system in patients with type 2 diabetes: Associations with markers of cardiovascular target organ damage. *Eur J Endocrinol.* 2017;176(5):521–31.
317. Sesti G, Sciacqua A, Cardellini M, Marini MA, Maio R, Vatrano M, et al. Plasma concentration of IGF-I is independently associated with insulin sensitivity in subjects with different degrees of glucose tolerance. *Diabetes Care.* 2005;28(1):120–5.
318. Clemmons DR, Sleevi M, Allan G, Sommer A. Effects of combined recombinant insulin-like growth factor (IGF)-I and IGF binding protein-3 in type 2 diabetic patients on glycemic control and distribution of IGF-I and IGF-II among serum binding protein complexes. *J Clin Endocrinol Metab.* 2007;92(7):2652–8.
319. Balducci, Stefano, Sacchetti, Massimo, Haxhi, Jonida, Orlando, Giorgio, D'Errico, Valeria, Fallucca, Sara, Menini, Stefano, Pugliese G. Physical Exercise as therapy for type II diabetes. *Diabetes Metab Res Rev.* 2014;32(30):13–23.
320. Haywood NJ, Cordell PA, Tang KY, Makova N, Yuldasheva NY, Imrie H, et al. Insulin-like growth factor binding protein 1 could improve glucose regulation and insulin sensitivity through its RGD domain. *Diabetes.* 2017;66(2):287–99.
321. Haywood NJ, Slater TA, Matthews CJ, Wheatcroft SB. The insulin like growth factor and binding protein family: Novel therapeutic targets in obesity & diabetes. *Mol Metab.* 2019;19:86–96.
322. Schreiber I, Dörpholz G, Ott CE, Kragesteen B, Schanze N, Lee CT, et al. BMPs as new insulin sensitizers: Enhanced glucose uptake in mature 3T3-L1 adipocytes via PPAR $\gamma$  and GLUT4 upregulation. *Sci Rep.* 2017;7(1):1–13.
323. Slaaby R, Schäffer L, Lautrup-Larsen I, Andersen AS, Shaw AC, Mathiasen IS, et al. Hybrid receptors formed by insulin receptor (IR) and insulin-like growth factor I receptor (IGF-IR) have low insulin and high IGF-1 affinity irrespective of the IR splice variant. *J Biol Chem.* 2006;281(36):25869–74.
324. Lawrence MC, McKern NM, Ward CW. Insulin receptor structure and its

- implications for the IGF-1 receptor. *Curr Opin Struct Biol.* 2007;17(6):699–705.
325. Al-Khafaji H, Noer PR, Alkharobi H, Alhodhodi A, Meade J, El-Gendy R, et al. A characteristic signature of insulin-like growth factor (IGF) axis expression during osteogenic differentiation of human dental pulp cells (hDPCs): Potential co-ordinated regulation of IGF action. *Growth Horm IGF Res.* 2018;42–43:14–21.
326. Dixit M, Poudel SB, Yakar S. Effects of GH/IGF axis on bone and cartilage. *Mol Cell Endocrinol.* 2021;519.
327. Ranke MB. Insulin-like growth factor binding-protein-3 (IGFBP-3). *Best Pract Res Clin Endocrinol Metab.* 2015;701–11.
328. Bach L. 40 YEARS OF IGF1: IGF-binding proteins. *J Mol Endocrinol.* 2018;61(1):T11–28.
329. Al-Kharobi H, El-Gendy RO, Devine DA, Beattie J. The role of the insulin-like growth factor (IGF) axis in osteogenic and odontogenic differentiation. *Cell Mol Life Sci.* 2014;71:1469–76.
330. Brahmkhatri VP, Prasanna C, Atreya HS. Insulin-Like Growth Factor System in Cancer : Novel Targeted Therapies. 2015;2015.
331. Lerner UH, Kindstedt E, Lundberg P. The critical interplay between bone resorbing and bone forming cells. *J Clin Periodontol.* 2019;46(S21):33–51.
332. Kawai M, Rosen CJ. The Insulin-Like Growth Factor System in Bone. Basic and Clinical Implications. *Endocrinol Metab Clin North Am.* 2012;41(2):323–33.
333. LeRoith D, Yakar S. Mechanisms of disease: Metabolic effects of growth hormone and insulin-like growth factor 1. *Nat Clin Pract Endocrinol Metab.* 2007;3(3):302–10.
334. Saeed H, Qiu W, Li C, Flyvbjerg A, Abdallah BM, Kassem M. Telomerase activity promotes osteoblast differentiation by modulating IGF-signaling pathway. *Biogerontology.* 2015;16(6):733–45.
335. Bahamonde M, Misra M. Potential applications for rhIGF-I : Bone disease and IGF-I. *Growth Horm IGF Res.* 2020;52:101317.
336. van Doorn J. Insulin-like growth factor-II and bioactive proteins containing a part of the E-domain of pro-insulin-like growth factor-II. *BioFactors.* 2020;46(4):563–78.
337. Yakar S, Werner H, Rosen CJ. 40 years of IGF1: Insulin-like growth factors:

- Actions on the skeleton. *J Mol Endocrinol*. 2018;61:T115–37.
338. Clemmons DR. Modifying IGF1 activity: An approach to treat endocrine disorders, atherosclerosis and cancer. *Nat Rev Drug Discov*. 2007;6(10):821–33.
339. Xu Y, Kong GW, Menting JG, Margetts MB, Delaine CA, Jenkin LM, et al. How ligand binds to the type 1 insulin-like growth factor receptor. *Nat Commun*. 2018;9(821).
340. Fowlkes JL, R CB, Thrailkill KM. Contributions of the Insulin/Insulin-Like Growth Factor-1 Axis to Diabetic Osteopathy. *J Diabetes Metab*. 2011;1(3):1–14.
341. Torrente Y, Bella P, Tripodi L, Villa C, Farini A. Role of Insulin-Like Growth Factor Receptor 2 across Muscle Homeostasis: Implications for Treating Muscular Dystrophy. *Cells*. 2020;9(2):1–12.
342. Heald AH, Cruickshank JK, Riste LK, Cade JE, Anderson S, Greenhalgh A, et al. Close relation of fasting insulin-like growth factor binding protein-1 (IGFBP-1) with glucose tolerance and cardiovascular risk in two populations. *Diabetologia*. 2001;44:333–9.
343. Zheng W, Lai Y, Jin P, Gu W, Zhou Q, Wu X. Association of circulating IGFBP1 level with the severity of coronary artery lesions in patients with unstable angina. *Dis Markers*. 2017;2017.
344. Hou L, He Q. Inhibition of IGFBP1 induction enhances the radiosensitivity of colon cancer cells in vitro. *Int J Clin Exp Pathol*. 2016;9(8):8759–66.
345. Ceccarini G, Pelosini C, Ferrari F, Magno S, Vitti J, Salvetti G, et al. Serum IGF-binding protein 2 (IGFBP-2) concentrations change early after gastric bypass bariatric surgery revealing a possible marker of leptin sensitivity in obese subjects. *Endocrine*. 2019;2:86–93.
346. Amin S, Riggs BL, Atkinson EJ, Oberg AL, Melton LJ, Khosla S. A potentially deleterious role of IGFBP-2 on bone density in aging men and women. *J Bone Miner Res*. 2004;19(7):1075–83.
347. Amin S, Riggs BL, Melton LJ, Achenbach SJ, Atkinson EJ, Khosla S. High serum IGFBP-2 is predictive of increased bone turnover in aging men and women. *J Bone Miner Res*. 2007;22(6):799–807.
348. Takenouchi Y, Ohshima M, Yamaguchi Y, Nishida T, Senda N, Idesawa M, et al. Insulin-like growth factor-binding protein-2 and -3 in gingival crevicular fluid. *J Periodontal Res*. 2010;45(6):803–8.

349. Gang Xi, Xinchun Shen, Clifford J Rosen and DRC. IRS-1 Functions as a Molecular Scaffold to Coordinate IGF-I/ IGFBP-2 Signaling During Osteoblast Differentiation. *J Bone Min Res.* 2016;31(6):1300–14.
350. Alkharobi H, Alhodhodi A, Hawsawi Y, Alkafaji H, Devine D, El-gendy R, et al. IGFBP-2 and -3 co-ordinately regulate IGF1 induced matrix mineralisation of differentiating human dental pulp cells. *Stem Cell Res.* 2016;17(3):517–22.
351. Baxter RC. Signalling pathways involved in antiproliferative effects of IGFBP-3: A review. *J Clin Pathol - Mol Pathol.* 2001;54(3):145–8.
352. Allard JB, Duan C. IGF-Binding Proteins: Why Do They Exist and Why Are There So Many? *Front Endocrinol (Lausanne).* 2018;9(117):1–12.
353. Gillberg P, Olofsson H, Mallmin H, Blum WF, Ljunghall S, Nilsson AG. Bone mineral density in femoral neck is positively correlated to circulating insulin-like growth factor (IGF)-I and IGF-binding protein (IGFBP)-3 in Swedish men. *Calcif Tissue Int.* 2002;70(1):22–9.
354. Yamaguchi T, Kanatani M, Yamauchi M, Kaji H, Sugishita T, Baylink DJ, et al. Serum levels of insulin-like growth factor (IGF); IGF-binding proteins-3, -4, and -5; and their relationships to bone mineral density and the risk of vertebral fractures in postmenopausal women. *Calcif Tissue Int.* 2006;78(1):18–24.
355. Harb AN, Holtfreter B, Friedrich N, Wallaschofski H, Nauck M, Albers M, et al. Association between the insulin-like growth factor axis in serum and periodontitis in the Study of Health in Pomerania: An exploratory study. *J Clin Periodontol.* 2012;39(10):931–9.
356. Beattie J, Al-Khafaji H, Noer PR, Alkharobi HE, Alhodhodi A, Meade J, et al. Insulin-like Growth Factor-Binding Protein Action in Bone Tissue: A key Role for Pregnancy-Associated Plasma Protein-A. *Front Endocrinol (Lausanne).* 2018;9(31):1–10.
357. Maridas DE, DeMambro VE, Le PT, Nagano K, Baron R, Mohan S, et al. IGFBP-4 regulates adult skeletal growth in a sex-specific manner. *J Endocrinol.* 2017;233(1):131–44.
358. Simon CM, Rauskolb S, Gunnensen JM, Holtmann B, Drepper C, Dombert B, et al. Dysregulated IGFBP5 expression causes axon degeneration and motoneuron loss in diabetic neuropathy. *Acta Neuropathol.* 2015;130(3):373–87.

359. Duan C, Allard JB. Insulin-Like Growth Factor Binding Protein-5 in Physiology and Disease. *Front Endocrinol (Lausanne)*. 2020;11(100):1–13.
360. Beattie J, Allan GJ, Lochrie JD, Flint DJ. Insulin-like growth factor-binding protein-5 (IGFBP-5): A critical member of the IGF axis. *Biochem J*. 2006;395(1):1–19.
361. Bach LA. Current ideas on the biology of IGFBP-6: More than an IGF-II inhibitor? *Growth Horm IGF Res*. 2016;30–31:81–6.
362. Bach LA. Recent insights into the actions of IGFBP-6. *J Cell Commun Signal*. 2015;9(2):189–200.
363. Liso A, Capitanio N, Gerli R, Conese M. From fever to immunity: A new role for IGFBP-6? *J Cell Mol Med*. 2018;22(10):4588–96.
364. Götz W, Heinen M, Lossdörfer S, Jäger A. Immunohistochemical localization of components of the insulin-like growth factor system in human permanent teeth. *Arch Oral Biol*. 2006;51(5):387–95.
365. Reckenbeil J, Kraus D, Stark H, Rath-Deschner B, Jäger A, Wenghoefer M, et al. Insulin-like growth factor 1 (IGF1) affects proliferation and differentiation and wound healing processes in an inflammatory environment with p38 controlling early osteoblast differentiation in periodontal ligament cells. *Arch Oral Biol*. 2017;73:142–50.
366. Han X, Amar S. Role of Insulin-Like Growth Factor-1 Signaling in Dental Fibroblast Apoptosis. *J Periodontol*. 2003;74(8):1176–82.
367. Konermann A, Lossdörfer S, Jäger A, Chen Y, Götz W. Autoregulation of insulin-like growth factor 2 and insulin-like growth factor-binding protein 6 in periodontal ligament cells in vitro. *Ann Anat*. 2013;195(6):527–32.
368. Lynch SE, Williams RC, Poison AM, Howell TH, Reddy MS, Zappa UE, et al. A combination of platelet-derived and insulin-like growth factors enhances periodontal regeneration. *J Clin Periodontol*. 1989;16(8):545–8.
369. Rutherford RB, Niekrash CE, Kennedy JE, Charette MF. Platelet-derived and insulin-like growth factors stimulate regeneration of periodontal attachment in monkeys. *J Periodontal Res*. 1992;27(4):285–90.
370. Giannobile W V., Hernandez RA, Finkelman RD, Ryan S, Kiritsy CP, D'Andrea M, et al. Comparative effects of platelet-derived growth factor-BB and insulin-like growth factor-I, individually and in combination, on periodontal regeneration in *Macaca fascicularis*. *J Periodontal Res*.

- 1996;31:301–12.
371. Gamal AY, Mailhot JM, Garnick JJ, Newhouse R, Sharawy MM. Human periodontal ligament fibroblast response to PDGF-BB and IGF-1 application on tetracycline HCl conditioned root surfaces. *J Clin Periodontol.* 1998;25(5):404–12.
372. Selvig KA, Wikesjö UME, Bogle GC, Finkelman RD. Impaired early bone formation in periodontal fenestration defects in dogs following application of insulin-like growth factor (II). Basic fibroblast growth factor and transforming growth factor beta 1. *J Clin Periodontol.* 1994;21(6):380–5.
373. Fang Y, Wang LP, Du FL, Liu WJ, Ren GL. Effects of insulin-like growth factor I on alveolar bone remodeling in diabetic rats. *J Periodontal Res.* 2013;48(2):144–50.
374. Han N, Zhang F, Li G, Zhang X, Lin X, Yang H, et al. Local application of IGFBP5 protein enhanced periodontal tissue regeneration via increasing the migration, cell proliferation and osteo/dentinogenic differentiation of mesenchymal stem cells in an inflammatory niche. *Stem Cell Res Ther.* 2017;8(210):1–13.
375. Howell TH, Fiorellini JP, Paquette DW, Offenbacher S, Giannobile W V., Lynch SE. A Phase I/II Clinical Trial to Evaluate a Combination of Recombinant Human Platelet-Derived Growth Factor-BB and Recombinant Human Insulin-Like Growth Factor-I in Patients with Periodontal Disease. *J Periodontol.* 1997;68(12):1186–93.
376. Devi R, Dixit J. Clinical Evaluation of Insulin like Growth Factor-I and Vascular Endothelial Growth Factor with Alloplastic Bone Graft Material in the Management of Human Two Wall Intra- Osseous Defects. *J Clin Diagnostic Res.* 2016;10(9):41–6.
377. Walsh S, Jefferiss CM, Stewart K, Beresford JN. IGF-I does not affect the proliferation or early osteogenic differentiation of human marrow stromal cells. *Bone.* 2003;33(1):80–9.
378. Reible B, Schmidmaier G, Moghaddam A, Westhauser F, Induce P-, Differentiation O, et al. Insulin-Like Growth Factor-1 as a Possible Alternative to Bone Morphogenetic Protein-7 to Induce Osteogenic Differentiation of Human Mesenchymal Stem Cells in Vitro. *Int J Mol Sci.* 2018;19(1674):1–15.
379. Reible B, Schmidmaier G, Prokscha M, Moghaddam A, Westhauser F.

- Continuous stimulation with differentiation factors is necessary to enhance osteogenic differentiation of human mesenchymal stem cells in-vitro. *Growth Factors*. 2017;35(4–5):179–88.
380. Celil AB, Campbell PG. BMP-2 and insulin-like growth factor-I mediate osterix (Osx) expression in human mesenchymal stem cells via the MAPK and protein kinase D signaling pathways. *J Biol Chem*. 2005;280(36):31353–9.
381. Wu L, Zhang G, Guo C, Pan Y. Intracellular Ca<sup>2+</sup> signaling mediates IGF-1-induced osteogenic differentiation in bone marrow mesenchymal stem cells. *Biochem Biophys Res Commun*. 2020;527(1):200–6.
382. Chen CY, Tseng KY, Lai YL, Chen YS, Lin FH, Lin S. Overexpression of insulin-like growth factor 1 enhanced the osteogenic capability of aging bone marrow mesenchymal stem cells. *Theranostics*. 2017;7(6):1598–611.
383. Scavo LM, Karas M, Murray M, Leroith D. Insulin-like growth factor-I stimulates both cell growth and lipogenesis during differentiation of human mesenchymal stem cells into adipocytes. *J Clin Endocrinol Metab*. 2004;89(7):3543–53.
384. James AW. Review of Signaling Pathways Governing MSC Osteogenic and Adipogenic Differentiation. *Scientifica (Cairo)*. 2013;2013:684736.
385. Min SK, Kim M, Park J-B. Insulin-like growth factor 2-enhanced osteogenic differentiation of stem cell spheroids by regulation of Runx2 and Col1 expression. *Exp Ther Med*. 2021;21(4):2–7.
386. Ortiz CO, Chen BK, Bale LK, Overgaard MT, Oxvig C, Conover CA. Transforming Growth Factor- $\beta$  Regulation of the Insulin-Like Growth Factor Binding Protein-4 Protease System in Cultured Human Osteoblasts. *J Bone Miner Res*. 2003;18(6):1066–72.
387. Xue P, Wu X, Zhou L, Ma H, Wang Y, Liu Y, et al. IGF1 promotes osteogenic differentiation of mesenchymal stem cells derived from rat bone marrow by increasing TAZ expression. *Biochem Biophys Res Commun*. 2013;433(2):226–31.
388. Rico-Llanos GA, Becerra J, Visser R. Insulin-like growth factor-1 (IGF-1) enhances the osteogenic activity of bone morphogenetic protein-6 (BMP-6) in vitro and in vivo, and together have a stronger osteogenic effect than when IGF-1 is combined with BMP-2. *J Biomed Mater Res - Part A*. 2017;105(7):1867–75.

389. Myers TJ, Yan Y, Granero-Molto F, Weis JA, Longobardi L, Li T, et al. Systemically delivered insulin-like growth factor-I enhances mesenchymal stem cell-dependent fracture healing. *Growth Factors*. 2012;30(4):230–41.
390. Khan M, Akhtar S, Mohsin S, N. Khan S, Riazuddin S. Growth factor preconditioning increases the function of diabetes-impaired mesenchymal stem cells. *Stem Cells Dev*. 2011;20(1):67–75.
391. Xi G, Rosen CJ, Clemmons DR. IGF-I and IGFBP-2 stimulate AMPK activation and autophagy, which are required for osteoblast differentiation. *Endocrinology*. 2016;157(1):268–81.
392. Xi G, D'Costa S, Wai C, Xia SK, Cox ZC, Clemmons DR. IGFBP-2 stimulates calcium/calmodulin-dependent protein kinase kinase 2 activation leading to AMP-activated protein kinase induction which is required for osteoblast differentiation. *J Cell Physiol*. 2019;234(12):23232–42.
393. Xi G, Demambro VE, D'costa S, Xia SK, Cox ZC, Rosen CJ, et al. Estrogen Stimulation of Pleiotrophin Enhances Osteoblast Differentiation and Maintains Bone Mass in IGFBP-2 Null Mice. *Endocrinology*. 2020;161(4):1–13.
394. Eguchi K, Akiba Y, Akiba N, Nagasawa M, Cooper LF, Uoshima K. Insulin-like growth factor binding Protein-3 suppresses osteoblast differentiation via bone morphogenetic protein-2. *Biochem Biophys Res Commun*. 2018;507(1–4):465–70.
395. Xian L, Wu X, Pang L, Lou M, Rosen CJ, Qiu T, et al. Matrix IGF-1 maintains bone mass by activation of mTOR in mesenchymal stem cells. *Nat Med*. 2012;18(7).
396. Haase HR, Clarkson RW, Waters MJ, Bartold PM. Growth factor modulation of mitogenic responses and proteoglycan synthesis by human periodontal fibroblasts. *J Cell Physiol*. 1998;174:353–61.
397. Palioto DB, Coletta RD, Graner E, Joly JC, de Lima AFM. The Influence of Enamel Matrix Derivative Associated With Insulin-Like Growth Factor-I on Periodontal Ligament Fibroblasts. *J Periodontol*. 2004;75(4):498–504.
398. Okubo K, Kobayashi M, Takiguchi T, Takada T, Ohazama A, Okamatsu Y, et al. Participation of endogenous IGF-I and TGF- $\beta$ 1 with enamel matrix derivative-stimulated cell growth in human periodontal ligament cells. *J Periodontal Res*. 2003;38(1):1–9.

399. Parkar MH, Tonetti M. Gene Expression Profiles of Periodontal Ligament Cells Treated With Enamel Matrix Proteins In Vitro: Analysis Using cDNA Arrays. *J Periodontol.* 2004;75(11):1539–46.
400. Yang J, Zhou J, Cui B, Yu T. Evaluation of hypoxia on the expression of miR-646/IGF-1 signaling in human periodontal ligament cells (hPDLs). *Med Sci Monit.* 2018;24:5282–91.
401. Pumklin J, Manokawinchoke J, Bhalang K, Pavasant P. Intermittent Compressive Stress Enhanced Insulin-Like Growth Factor-1 Expression in Human Periodontal Ligament Cells. *Int J Cell Biol.* 2015;2015.
402. Ochiai H, Okada S, Saito A, Hoshi K, Yamashita H, Takato T, et al. Inhibition of insulin-like growth factor-1 (IGF-1) expression by prolonged transforming growth factor- $\beta$ 1 (TGF- $\beta$ 1) administration suppresses osteoblast differentiation. *J Biol Chem.* 2012;287(27):22654–61.
403. Yu Y, Mu J, Fan Z, Lei G, Yan M, Wang S, et al. Insulin-like growth factor 1 enhances the proliferation and osteogenic differentiation of human periodontal ligament stem cells via ERK and JNK MAPK pathways. *Histochem Cell Biol.* 2012;137(4):513–25.
404. Li X, Yao J, Wu J, Du X, Jing W, Liu L. Roles of PRF and IGF-1 in promoting alveolar osteoblast growth and proliferation and molecular mechanism. *Int J Clin Exp Pathol.* 2018;11(7):3294–301.
405. Han X, Amar S. IGF-1 Signaling Enhances Cell Survival in Periodontal Ligament Fibroblasts vs. Gingival Fibroblasts. *J Dent Res.* 2003;454–9.
406. Lossdörfer S, Abuduwali N, Jäger A. Bone Morphogenetic Protein-7 Modifies the Effects of Insulin-Like Growth Factors and Intermittent Parathyroid Hormone (1-34) on Human Periodontal Ligament Cell Physiology In Vitro. *J Periodontol.* 2011;82(6):900–8.
407. Nemoto E, Shimonishi M, Nitta Y, Shimauchi H. The involvement of platelet-derived growth factor receptors and insulin-like growth factor-1 receptors signaling during mineralized nodule formation by human periodontal ligament cells. *J Periodontal Res.* 2004;39(6):388–97.
408. Xi K, Peng C. Insulin-like growth factor-1 promotes proliferation, migration and osteoblasts differentiation of periodontal ligament stem cells via activating PI3K/AKT signal pathway. *Int J Clin Exp Pathol.* 2017;10(6):6674–82.
409. Matsubara T, Suardita K, Ishii M, Sugiyama M, Igarashi A, Oda R, et al.

- Alveolar bone marrow as a cell source for regenerative medicine: Differences between alveolar and iliac bone marrow stromal cells. *J Bone Miner Res.* 2005;20(3):399–409.
410. Amable PR, Teixeira MVT, Carias RBV, Granjeiro JM, Borojevic R. Identification of appropriate reference genes for human mesenchymal cells during expansion and differentiation. *PLoS One.* 2013;8(9).
411. Winning L, El Karim IA, Lundy FT. A Comparative Analysis of the Osteogenic Potential of Dental Mesenchymal Stem Cells. *Stem Cells Dev.* 2019;28(15):1050–8.
412. Neve A, Corrado A, Cantatore FP. Osteocalcin: Skeletal and extra-skeletal effects. *J Cell Physiol.* 2013;228(6):1149–53.
413. Sato M, Aoki H, Nakamura T, Onodera S, Yamaguchi A, Saito A, et al. Effects of intermittent treatment with parathyroid hormone (PTH) on osteoblastic differentiation and mineralization of mouse induced pluripotent stem cells in a 3D culture model. *J Periodontal Res.* 2020;1–10.
414. Cobo T, Vilorio CG, Solares L, Fontanil T, González-Chamorro E, De Carlos F, et al. Role of periostin in adhesion and migration of bone remodeling cells. *PLoS One.* 2016;11(1):1–19.
415. Sowmya S, Chennazhi KP, Arzate H, Jayachandran P, Nair S V., Jayakumar R. Periodontal Specific Differentiation of Dental Follicle Stem Cells into Osteoblast, Fibroblast, and Cementoblast. *Tissue Eng - Part C Methods.* 2015;21(10):1044–58.
416. Martin JT. Historically significant events in the discovery of RANK/RANKL/OPG. *World J Orthop.* 2013;4(4):186–97.
417. Alkharobi HE, Al-Khafaji H, Beattie J, Devine DA, El-Gendy R. Insulin-Like Growth Factor Axis Expression in Dental Pulp Cells Derived From Carious Teeth. *Front Bioeng Biotechnol.* 2018;6(36).
418. Koffi KA, Doublier S, Ricort J-M, Babajko S, Nassif A, Isaac J. The Role of GH/IGF Axis in Dento-Alveolar Complex from Development to Aging and Therapeutics: A Narrative Review. *Cells.* 2021;10(1181).
419. Jones E, English A, Churchman SM, Kouroupis D, Boxall SA, Kinsey S, et al. Large-scale extraction and characterization of CD271+ multipotential stromal cells from trabecular bone in health and osteoarthritis: Implications for bone regeneration strategies based on uncultured or minimally cultured multipotential stromal cells. *Arthritis Rheum.* 2010;62(7):1944–54.

420. Campbell TM, Churchman SM, Gomez A, McGonagle D, Conaghan PG, Ponchel F, et al. Mesenchymal Stem Cell Alterations in Bone Marrow Lesions in Patients With Hip Osteoarthritis. *Arthritis Rheumatol.* 2016;68(7):1648–59.
421. Ilas DC, Baboolal TG, Churchman SM, Jones WG, Giannoudis P V., Bühring HJ, et al. The osteogenic commitment of CD271+CD56+ bone marrow stromal cells (BMSCs) in osteoarthritic femoral head bone. *Sci Rep.* 2020;10(1):1–14.
422. El-Jawhari JJ, Ganguly P, Jones E, Giannoudis P V. Bone marrow multipotent mesenchymal stromal cells as autologous therapy for osteonecrosis: Effects of age and underlying causes. *Bioengineering.* 2021;8(5).
423. Russell T, Watad A, Bridgewood C, Rowe H, Khan A, Rao A, et al. Il-17a and TNF modulate normal human spinal enthesal bone and soft tissue mesenchymal stem cell osteogenesis, adipogenesis, and stromal function. *Cells.* 2021;10(2):1–18.
424. Owston HE, Ganguly P, Tronci G, Russell SJ, Giannoudis P V., Jones EA. Colony Formation, Migratory, and Differentiation Characteristics of Multipotential Stromal Cells (MSCs) from “Clinically Accessible” Human Periosteum Compared to Donor-Matched Bone Marrow MSCs. *Stem Cells Int.* 2019;2019.
425. Perfetto SP, Chattopadhyay PK, Roederer M. Seventeen-colour flow cytometry: Unravelling the immune system. *Nat Rev Immunol.* 2004;4(8):648–55.
426. Adan A, Alizada G, Kiraz Y, Baran Y, Nalbant A. Flow cytometry: basic principles and applications. *Crit Rev Biotechnol.* 2017;37(2):163–76.
427. Baumgarth N, Roederer M. A practical approach to multicolor flow cytometry for immunophenotyping. *J Immunol Methods.* 2000;243:77–97.
428. Colgan SP, Eltzschig HK, Eckle T, Thompson LF. Physiological roles for ecto-5'-nucleotidase (CD73). *Purinergic Signal.* 2006;2(2):351–60.
429. Jiang D, Rinkevich Y. Defining skin fibroblastic cell types beyond CD90. *Front Cell Dev Biol.* 2018;6(OCT):1–3.
430. Mark P, Kleinsorge M, Gaebel R, Lux CA, Toelk A, Pittermann E, et al. Human mesenchymal stem cells display reduced expression of CD105 after culture in serum-free medium. *Stem Cells Int.* 2013;2013.

431. Heideveld E, Masiello F, Marra M, Esteghamat F, Yağcı N, von Lindern M, et al. CD14+ cells from peripheral blood positively regulate hematopoietic stem and progenitor cell survival resulting in increased erythroid yield. *Haematologica*. 2015;100(11):1396–406.
432. Xian B, Zhang Y, Peng Y, Huang J, Li W, Wang W, Zhang M, Li K, Zhang H, Zhao M LX. Adult Human Peripheral Blood Mononuclear Cells Are Capable of Producing Neurocyte or Photoreceptor- Like Cells That Survive in Mouse Eyes After Preinduction With Neonatal Retina. *Stem Cells Transl Med*. 2016;5(11):1525–1524.
433. Roederer M. Spectral compensation for flow cytometry: Visualization artifacts, limitations, and caveats. *Cytometry*. 2001;45(3):194–205.
434. Herzenberg LA, Tung J, Moore WA, Herzenberg LA, Parks DR. Interpreting flow cytometry data: a guide for the perplexed. *Nat Immunol*. 2006;7(7):681–5.
435. Etheridge SL, Spencer GJ, Heath DJ, Genever PG. Expression Profiling and Functional Analysis of Wnt Signaling Mechanisms in Mesenchymal Stem Cells. *Stem Cells*. 2004;22:849–60.
436. Kasahara T, Miyazaki T, Nitta H, Ono A, Miyagishima T, Nagao T, et al. Evaluation of methods for duration of preservation of RNA quality in rat liver used for transcriptome analysis. *J Toxicol Sci*. 2006;31(5):509–19.
437. Ruan C, Wang W, Gu B. Detection of alkaline phosphatase using surface-enhanced raman spectroscopy. *Anal Chem*. 2006;78(10):3379–84.
438. Hsiao JK, Tsai CP, Chung TH, Hung Y, Yao M, Liu HM, et al. Mesoporous silica nanoparticles as a delivery system of gadolinium for effective human stem cell tracking. *Small*. 2008;4(9):1445–52.
439. Gregory CA, Gunn WG, Peister A, Prockop DJ. An Alizarin red-based assay of mineralization by adherent cells in culture: Comparison with cetylpyridinium chloride extraction. *Anal Biochem*. 2004;329(1):77–84.
440. Garibyan L, Avashia N. Polymerase chain reaction. *J Invest Dermatol*. 2013;133(3):1–4.
441. Santos CF dos, Sakai VT, Machado MA de AM, Schippers DN, Greene AS. Reverse transcription and polymerase chain reaction: principles and applications in dentistry. *J Appl Oral Sci*. 2004;12(1):1–11.
442. Yousefi A-M, James PF, Akbarzadeh R, Subramanian A, Flavin C, Oudadesse H. Prospect of Stem Cells in Bone Tissue Engineering: A

- Review. *Stem Cells Int.* 2016;2016.
443. Xu J, Zuo C. The Fate Status of Stem Cells in Diabetes and its Role in the Occurrence of Diabetic Complications. *Front Mol Biosci.* 2021;8:745035.
  444. Jones WG, El-Jawhari JJ, Brockett CL, Korla L, Ktistakis I, Jones E. Multipotential stromal cells in the talus and distal tibia in ankle osteoarthritis – Presence, potency and relationships to subchondral bone changes. *J Cell Mol Med.* 2021;25(1):259–71.
  445. Sakaguchi Y, Sekiya I, Yagishita K, Muneta T. Comparison of human stem cells derived from various mesenchymal tissues: Superiority of synovium as a cell source. *Arthritis Rheum.* 2005;52(8):2521–9.
  446. Siegel G, Kluba T, Hermanutz-Klein U, Bieback K, Northoff H, Schäfer R. Phenotype, donor age and gender affect function of human bone marrow-derived mesenchymal stromal cells. *BMC Med.* 2013;11(1).
  447. Stolzing A, Jones E, McGonagle D, Scutt A. Age-related changes in human bone marrow-derived mesenchymal stem cells: Consequences for cell therapies. *Mech Ageing Dev.* 2008;129(3):163–73.
  448. Inoue O, Usui S, Takashima S ichiro, Nomura A, Yamaguchi K, Takeda Y, et al. Diabetes impairs the angiogenic capacity of human adipose-derived stem cells by reducing the CD271+ subpopulation in adipose tissue. *Biochem Biophys Res Commun.* 2019;517(2):369–75.
  449. Zhai W, Yong D, El-Jawhari JG, Cuthbert R, McGonagle D, Naing MW, et al. Identification of senescent cells in multipotent mesenchymal stromal cell cultures: Current methods and future directions. *Cytotherapy.* 2019;21(8):803–19.
  450. Zhang P, Zhang H, Lin J, Xiao T, Xu R, Fu Y, et al. Insulin impedes osteogenesis of BMSCs by inhibiting autophagy and promoting premature senescence via the TGF- $\beta$ 1 pathway. *Aging (Albany NY).* 2020;12(3):2084–100.
  451. Yin M, Zhang Y, Yu H, Li X. Role of Hyperglycemia in the Senescence of Mesenchymal Stem Cells. *Front Cell Dev Biol.* 2021;9:665412.
  452. Perfetto SP, Chattopadhyay PK, Lamoreaux L, Nguyen R, Ambrozak D, Koup RA, et al. Amine reactive dyes: An effective tool to discriminate live and dead cells in polychromatic flow cytometry. *J Immunol Methods.* 2006;313(1–2):199–208.
  453. Min WK, Bae JS, Park BC, Jeon IH, Jin HK, Son MJ, et al. Proliferation and

- osteoblastic differentiation of bone marrow stem cells: Comparison of vertebral body and iliac crest. *Eur Spine J.* 2010;19(10):1753–60.
454. Li Y, Wu Q, Yujia W, Li L, Bu H, Bao J. Senescence of mesenchymal stem cells. *Int J Mol Med.* 2017;39(4):775–82.
455. Glyn-Jones S, Palmer AJR, Agricola R, Price AJ, Vincent TL, Weinans H, et al. Osteoarthritis. *Lancet.* 2015;386:376–87.
456. Stiehler M, Rauh J, Bünger C, Jacobi A, Vater C, Schildberg T, et al. In vitro characterization of bone marrow stromal cells from osteoarthritic donors. *Stem Cell Res.* 2016;16:782–9.
457. Maecker HT, Trotter J. Flow cytometry controls, instrument setup, and the determination of positivity. *Cytom Part A.* 2006;69(9):1037–42.
458. Dentelli P, Barale C, Togliatto G, Trombetta A, Olgasi C, Gili M, et al. A diabetic milieu promotes OCT4 and NANOG production in human visceral-derived adipose stem cells. *Diabetologia.* 2013;56(1):173–84.
459. Alkharobi H, Beattie J, Meade J, Devine D, El-Gendy R. Dental Pulp Cells Isolated from Teeth with Superficial Caries Retain an Inflammatory Phenotype and Display an Enhanced Matrix Mineralization Potential. *Front Physiol.* 2017;8(244).
460. El-Jawhari JJ, Ganguly P, Churchman S, Jones E, Giannoudis P V. The Biological Fitness of Bone Progenitor Cells in Reamer/Irrigator/Aspirator Waste. *J Bone Joint Surg Am.* 2019;101(23):2111–9.
461. Ganguly P, Burska AN, Davis CLM, El-Jawhari JJ, Giannoudis P V., Jones EA. Intrinsic Type 1 Interferon (IFN1) Profile of Uncultured Human Bone Marrow CD45low CD271+ Multipotential Stromal Cells (BM-MSCs): The Impact of Donor age, Culture Expansion and IFN $\alpha$  and IFN $\beta$  Stimulation. *Biomedicines.* 2020;8(7):214.
462. Hoemann CD, El-Gabalawy H, McKee MD. In vitro osteogenesis assays: Influence of the primary cell source on alkaline phosphatase activity and mineralization. *Pathol Biol.* 2009;57(4):318–23.
463. Makhluif HA, Mueller SM, Mizuno S, Glowacki J. Age-related decline in osteoprotegerin expression by human bone marrow cells cultured in three-dimensional collagen sponges. *Biochem Biophys Res Commun.* 2000;268(3):669–72.
464. Mostafa NZ, Fitzsimmons R, Major PW, Adesida A, Jomha N, Jiang H, et al. Osteogenic differentiation of human mesenchymal stem cells cultured

- with dexamethasone, vitamin D3, basic fibroblast growth factor, and bone morphogenetic protein-2. *Connect Tissue Res.* 2012;53(2):117–31.
465. Zhao ZY, Yang L, Mu X, Xu L, Yu X, Jiao Y, et al. Cajanine promotes osteogenic differentiation and proliferation of human bone marrow mesenchymal stem cells. *Adv Clin Exp Med.* 2019;28(1):45–50.
466. Churchman SM, Boxall SA, McGonagle D, Jones EA. Predicting the Remaining Lifespan and Cultivation-Related Loss of Osteogenic Capacity of Bone Marrow Multipotential Stromal Cells Applicable across a Broad Donor Age Range. *Stem Cells Int.* 2017;2017.
467. Jeon RH, Lee WJ, Son YB, Bharti D, Shivakumar SB, Lee SL, et al. PPIA, HPRT1, and YWHAZ Genes Are Suitable for Normalization of mRNA Expression in Long-Term Expanded Human Mesenchymal Stem Cells. *Biomed Res Int.* 2019;2019.
468. Riedel G, Rüdric U, Fekete-Drimusz N, Manns MP, Vondran FWR, Bock M. An extended  $\Delta$ CT-method facilitating normalisation with multiple reference genes suited for quantitative RT-PCR analyses of human hepatocyte-like cells. *PLoS One.* 2014;9(3):2–6.
469. Komaki M, Karakida T, Abe M, Oida S, Mimori K, Iwasaki K, et al. Twist negatively regulates osteoblastic differentiation in human periodontal ligament cells. *J Cell Biochem.* 2007;100(2):303–14.
470. Saito Y, Yoshizawa T, Takizawa F, Ikegame M, Ishibashi O, Okuda K, et al. A cell line with characteristics of the periodontal ligament fibroblasts is negatively regulated for mineralization and Runx2/Cbfa1/Osf2 activity, part of which can be overcome by bone morphogenetic protein-2. *J Cell Sci.* 2002;115(21):4191–200.
471. Zhu Y, Jia Y, Wang Y, Xu J, Chai Y. Impaired Bone Regenerative Effect of Exosomes Derived from Bone Marrow Mesenchymal Stem Cells in Type 1 Diabetes. *Stem Cells Transl Med.* 2019;8(6):593–605.
472. Kono K, Maeda H, Fujii S, Tomokiyo A, Yamamoto N, Wada N, et al. Exposure to transforming growth factor- $\beta$ 1 after basic fibroblast growth factor promotes the fibroblastic differentiation of human periodontal ligament stem/progenitor cell lines. *Cell Tissue Res.* 2013;352(2):249–63.
473. Pi SH, Lee SK, Hwang YS, Choi MG, Lee SK, Kim EC. Differential expression of periodontal ligament-specific markers and osteogenic differentiation in human papilloma virus 16-immortalized human gingival

- fibroblasts and periodontal ligament cells. *J Periodontal Res.* 2007;42(2):104–13.
474. Wang ZS, Feng ZH, Wu GF, Bai SZ, Dong Y, Chen FM, et al. The use of platelet-rich fibrin combined with periodontal ligament and jaw bone mesenchymal stem cell sheets for periodontal tissue engineering. *Sci Rep.* 2016;6(1):1–5.
475. Hoz L, Romo E, Zeichner-David M, Sanz M, Nuñez J, Gaitán L, et al. Cementum protein 1 (CEMP1) induces differentiation by human periodontal ligament cells under three-dimensional culture conditions. *Cell Biol Int.* 2012;36(2):129–36.
476. Jia D, Heersche JNM. Expression of insulin-like growth factor system constituents in differentiating rat osteoblastic cell populations. *Growth Horm IGF Res.* 2002;12(6):399–410.
477. Palmieri V, Barba M, Di Pietro L, Conti C, De Spirito M, Lattanzi W, et al. Graphene oxide induced osteogenesis quantification by in-situ 2d-fluorescence spectroscopy. *Int J Mol Sci.* 2018;19(11):1–9.
478. Kim MS, Noh WC, Kim YG, Kim JY, Park JW, Suh JY. Effect of rhBMP-2 on mineralization of human periodontal ligament cells under high glucose conditions in vitro. *Int J Diabetes Dev Ctries.* 2015;35(2):108–14.
479. Grellier M, Bordenave L, Amédée J. Cell-to-cell communication between osteogenic and endothelial lineages: implications for tissue engineering. *Trends Biotechnol.* 2009;27(10):562–71.
480. De Amorim FPLG, Ornelas SS, Diniz SF, Batista AC, Da Silva TA. Imbalance of RANK, RANKL and OPG expression during tibial fracture repair in diabetic rats. *J Mol Histol.* 2008;39(4):401–8.
481. Villarreal-Ramírez E, Moreno A, Mas-Oliva J, Chávez-Pacheco JL, Narayanan AS, Gil-Chavarría I, et al. Characterization of recombinant human cementum protein 1 (hrCEMP1): Primary role in biomineralization. *Biochem Biophys Res Commun.* 2009;384(1):49–54.
482. Kook SH, Hwang JM, Park JS, Kim EM, Heo JS, Jeon YM, et al. Mechanical force induces type I collagen expression in human periodontal ligament fibroblasts through activation of ERK/JNK and AP-1. *J Cell Biochem.* 2009;106(6):1060–7.
483. Wei Y, Ye Q, Tang Z, Tian G, Zhu Q, Gao H, et al. Calcitonin induces collagen synthesis and osteoblastic differentiation in human periodontal

- ligament fibroblasts. *Arch Oral Biol.* 2017;74:114–22.
484. Horiuchi K, Amizuka N, Takeshita S, Takamatsu H, Katsuura M, Ozawa H, et al. Identification and characterization of a novel protein, periostin, with restricted expression to periosteum and periodontal ligament and increased expression by transforming growth factor  $\beta$ . *J Bone Miner Res.* 1999;14(7):1239–49.
485. Wilde J, Yokozeki M, Terai K, Kudo A, Moriyama K. The divergent expression of periostin mRNA in the periodontal ligament during experimental tooth movement. *Cell Tissue Res.* 2003;312(3):345–51.
486. Fujii S, Maeda H, Wada N, Tomokiyo A, Saito M, Akamine A. Investigating a clonal human periodontal ligament progenitor/stem cell line in vitro and in vivo. *J Cell Physiol.* 2008;215(3):743–9.
487. Marchesan JT, Scanlon CS, Soehren S, Matsuo M, Kapila YL, Teresa J, et al. Implications of cultured periodontal ligament cells for the clinical and experimental setting: A review. *Arch Oral Biol.* 2011;56(10):933–43.
488. Franke S, Ruster C, Pester J, Hofmann G, Oelzner P, Wolf G. Advanced glycation end products affect growth and function of osteoblasts. *Clin Exp Rheumatol.* 2011;29(4):650–60.
489. Kočí Z, Turnovcová K, Dubský M, Baranovičová L, Holáň V, Chudíčková M, et al. Characterization of human adipose tissue-derived stromal cells isolated from diabetic patient's distal limbs with critical ischemia. *Cell Biochem Funct.* 2014;32(7):597–604.
490. Vimalraj S. Alkaline phosphatase: Structure, expression and its function in bone mineralization. *Gene.* 2020;754:144855.
491. Vimalraj S, Arumugam B, Miranda PJ, Selvamurugan N. Runx2: Structure, function, and phosphorylation in osteoblast differentiation. *Int J Biol Macromol.* 2015;78:202–8.
492. Tarkkonen K, Hieta R, Kytölä V, Nykter M, Kiviranta R. Comparative analysis of osteoblast gene expression profiles and Runx2 genomic occupancy of mouse and human osteoblasts in vitro. *Gene.* 2017;626:119–31.
493. Komori T. Runx2, an inducer of osteoblast and chondrocyte differentiation. *Histochem Cell Biol.* 2018;149(4):313–23.
494. Babey ME, Ewing SK, Strotmeyer ES, Napoli N, Schafer AL, Vittinghoff E, et al. No Evidence of Association Between Undercarboxylated Osteocalcin

- and Incident Type 2 Diabetes. *J Bone Miner Res.* 2022;1–9.
495. Zoch ML, Clemens TL, Riddle RC. New insights into the biology of osteocalcin. *Bone.* 2016;82:42–9.
496. Moser SC, van der Eerden BCJ. Osteocalcin — A versatile bone-derived hormone. *Front Endocrinol (Lausanne).* 2019;10(JAN):4–9.
497. Kato H, Taguchi Y, Tominaga K, Umeda M, Tanaka A. Porphyromonas gingivalis LPS inhibits osteoblastic differentiation and promotes pro-inflammatory cytokine production in human periodontal ligament stem cells. *Arch Oral Biol.* 2014;59(2):167–75.
498. Villafán-Bernal JR, Sánchez-Enríquez S, Muñoz-Valle JF. Molecular modulation of osteocalcin and its relevance in diabetes. *Int J Mol Med.* 2011;28(3):283–93.
499. Conte A, Ghiraldini B, Casarin RC, Casati MZ, Pimentel SP, Cirano FR, et al. Impact of type 2 diabetes on the gene expression of bone-related factors at sites receiving dental implants. *Int J Oral Maxillofac Surg.* 2015;44(10):1302–8.
500. Hempel U, Müller K, Preissler C, Noack C, Boxberger S, Dieter P, et al. Human Bone Marrow Stromal Cells: A Reliable, Challenging Tool for in Vitro Osteogenesis and Bone Tissue Engineering Approaches. *Stem Cells Int.* 2016;2016.
501. Liu J, Zhao Z, Ruan J, Weir MD, Ma T, Ren K, et al. Stem cells in the periodontal ligament differentiated into osteogenic, fibrogenic and cementogenic lineages for the regeneration of the periodontal complex. *J Dent.* 2020;92:103259.
502. Fang Y, Xue Z, Zhao L, Yang X, Yang Y, Zhou X, et al. Calycosin stimulates the osteogenic differentiation of rat calvarial osteoblasts by activating the IGF1R/PI3K/Akt signaling pathway. *Cell Biol Int.* 2019;43(3):323–32.
503. Picke AK, Salbach-Hirsch J, Hintze V, Rother S, Rauner M, Kascholke C, et al. Sulfated hyaluronan improves bone regeneration of diabetic rats by binding sclerostin and enhancing osteoblast function. *Biomaterials.* 2016;96:11–23.
504. Nakamura S, Ito T, Okamoto K, Mima T, Uchida K, Siddiqui YD, et al. Acceleration of bone regeneration of horizontal bone defect in rats using collagen-binding basic fibroblast growth factor combined with collagen scaffolds. *J Periodontol.* 2019;90(9):1043–52.

505. Abuarqoub D, Zaza R, Aslam N, Jafar H, Zalloum S, Atoom R, et al. The Role of Biodentine™ on the Odontogenic / Osteogenic Differentiation of Human Dental Pulp Stem Cells. *Appl Sci*. 2021;11(7563).
506. Egusa H, Iida K, Kobayashi M, Lin TY, Zhu M, Zuk PA, et al. Downregulation of extracellular matrix-related gene clusters during osteogenic differentiation of human bone marrow- and adipose tissue-derived stromal cells. *Tissue Eng*. 2007;13(10):2589–600.
507. Açıl Y, Ghoniem AA, Gülses A, Kisch T, Stang F, Wiltfang J, et al. Suppression of osteoblast-related genes during osteogenic differentiation of adipose tissue derived stromal cells. *J Cranio-Maxillofacial Surg*. 2017;45(1):33–8.
508. Takeshita S, Kikuno R, Tezuka K, Amann E. Osteoblast-specific factor 2: Cloning of a putative bone adhesion protein with homology with the insect protein fasciclin I. *Biochem J*. 1993;294(1):271–8.
509. Bornstein P, Sage EH. Matricellular proteins: extracellular modulators of cell function. *Curr Opin Cell Biol*. 2002;14(5):608–16.
510. González-González L, Alonso J. Periostin: A matricellular protein with multiple functions in cancer development and progression. *Front Oncol*. 2018;8:225.
511. Merle B, Garnero P. The multiple facets of periostin in bone metabolism. *Osteoporos Int*. 2012;23(4):1199–212.
512. Sirisereephap K, Maekawa T, Tamura H, Hiyoshi T, Domon H, Isono T, et al. Osteoimmunology in Periodontitis: Local Proteins and Compounds to Alleviate Periodontitis. *Int J Mol Sci*. 2022;23(10).
513. Romanos GE, Asnani KP, Hingorani D, Deshmukh VL. PERIOSTIN: Role in Formation and Maintenance of Dental Tissues. *J Cell Physiol*. 2014;229(1):1–5.
514. Zheng C, Chen J, Liu S, Jin Y. Stem cell-based bone and dental regeneration: a view of microenvironmental modulation. *Int J Oral Sci*. 2019;11(3):1–15.
515. Wang QN, Yan YZ, Zhang XZ, Lv JX, Nie HP, Wu J, et al. Rescuing effects of periostin in advanced glycation end-products (AGEs) caused osteogenic and oxidative damage through AGE receptor mediation and DNA methylation of the CALCA promoter. *Chem Biol Interact*. 2022;354:109835.
516. Han L, Gong S, Wang R, Liu S, Wang B, Chen G, et al. Knockdown of

- POSTN Inhibits Osteogenic Differentiation of Mesenchymal Stem Cells From Patients With Steroid-Induced Osteonecrosis. *Front Cell Dev Biol.* 2020;8:606289.
517. Dandona P, Aljada A, Bandyopadhyay A. Inflammation the link between insulin resistance, obesity and diabetes. *Trends Immunol.* 2004;25(1):4–7.
518. Oguntibeju OO. Type 2 diabetes mellitus, oxidative stress and inflammation: examining the links. *Int J Physiol Pathophysiol Pharmacol.* 2019;11(3):45–63.
519. Rohm T V., Meier DT, Olefsky JM, Donath MY. Inflammation in obesity, diabetes, and related disorders. *Immunity.* 2022;55(1):31–55.
520. Alvarez-Pérez MA, Narayanan S, Zeichner-David M, Rodríguez Carmona B, Arzate H. Molecular cloning, expression and immunolocalization of a novel human cementum-derived protein (CP-23). *Bone.* 2006;38(3):409–19.
521. Kim JE, Kim TG, Lee YH, Yi HK. Phelligrin D maintains the function of periodontal ligament cells through autophagy in glucose-induced oxidative stress. *J Periodontal Implant Sci.* 2020;50(5):291–302.
522. Gokhan K, Keklikoglu N, Buyukertan M. The comparison of the thickness of the cementum layer in type 2 diabetic and non-diabetic patients. *J Contemp Dent Pract.* 2004;5(2):124–33.
523. Kadokura H, Yamazaki T, Masuda Y, Kato Y, Hasegawa A, Sakagami H, et al. Establishment of a primary culture system of human periodontal ligament cells that differentiate into cementum protein 1-expressing cementoblast-like cells. *In Vivo (Brooklyn).* 2019;33(2):349–52.
524. Li S, Shao J, Zhou Y, Friis T, Yao J, Shi B, et al. The impact of Wnt signalling and hypoxia on osteogenic and cementogenic differentiation in human periodontal ligament cells. *Mol Med Rep.* 2016;14(6):4975–82.
525. Hong HH, Hong A, Wang CC, Huang EW, Chiang CC, Yen TH, et al. Calcitriol exerts a mineralization-inductive effect comparable to that of vitamin C in cultured human periodontium cells. *Am J Transl Res.* 2019;11(4):2304–16.
526. Leibbrandt A, Penninger JM. RANK/RANKL: Regulators of immune responses and bone physiology. *Ann N Y Acad Sci.* 2008;1143:123–50.
527. Walsh MC, Choi Y. Biology of the RANKL-RANK-OPG system in immunity, bone, and beyond. *Front Immunol.* 2014;5:511.

528. Boyce BF, Xing L. Biology of RANK, RANKL, and osteoprotegerin. *Arthritis Res Ther.* 2007;9(SUPPL.1):S1.
529. Xu J, Yue F, Wang J, Chen L, Qi W. High glucose inhibits receptor activator of nuclear factor- $\kappa$ B ligand-induced osteoclast differentiation via downregulation of v-ATPase V0 subunit d2 and dendritic cell-specific transmembrane protein. *Mol Med Rep.* 2015;11(2):865–70.
530. Simonet WS, Lacey DL, Dunstan CR, Kelley M, Chang MS, Lüthy R, et al. Osteoprotegerin: A novel secreted protein involved in the regulation of bone density. *Cell.* 1997;89(2):309–19.
531. Ateeq H, Zia A, Husain Q, Khan MS, Ahmad M. Effect of inflammation on bones in diabetic patients with periodontitis via RANKL/OPG system-A review. *J Diabetes Metab Disord.* 2022;(0123456789).
532. Ono T, Hayashi M, Sasaki F, Nakashima T. RANKL biology: Bone metabolism, the immune system, and beyond. *Inflamm Regen.* 2020;40(1):1–16.
533. Bjerre M. Osteoprotegerin (OPG) as a biomarker for diabetic cardiovascular complications. *Springerplus.* 2013;2(1):1–6.
534. Boyce BF, Xing L. Functions of RANKL/RANK/OPG in bone modeling and remodeling. *Arch Biochem Biophys.* 2008;473(2):139–46.
535. Tetè S, Vinci R, Zizzari VL, Zara S, La Scala V, Cataldi A, et al. Maxillary sinus augmentation procedures through equine-derived biomaterial or calvaria autologous bone: Immunohistochemical evaluation of OPG/RANKL in humans. *Eur J Histochem.* 2013;57(1):60–5.
536. Zhang L, Ding Y, Rao GZ, Miao D. Effects of IL-10 and glucose on expression of OPG and RANKL in human periodontal ligament fibroblasts. *Brazilian J Med Biol Res.* 2016;49(4):1–6.
537. Feng Y, Liu J qiang, Liu H chen. AMP-activated protein kinase acts as a negative regulator of high glucose-induced RANKL expression in human periodontal ligament cells. *Chin Med J (Engl).* 2012;125(18):3298–304.
538. Sassi F, Buondonno I, Luppi C, Spertino E, Stratta E, Di Stefano M, et al. Type 2 diabetes affects bone cells precursors and bone turnover. *BMC Endocr Disord.* 2018;18(1):1–8.
539. Simpson A, Petnga W, Macaulay VM, Weyer-Czernilofsky U, Bogenrieder T. Insulin-Like Growth Factor (IGF) Pathway Targeting in Cancer: Role of the IGF Axis and Opportunities for Future Combination Studies. *Target*

- Oncol. 2017;12:571–97.
540. Katagiri W, Osugi M, Kawai T, Hibi H. First-in-human study and clinical case reports of the alveolar bone regeneration with the secretome from human mesenchymal stem cells. *Head Face Med.* 2016;12(1):1–10.
  541. Fowlkes JL, Nyman JS, Bunn RC, Jo C, Wahl EC, Liu L, et al. Osteo-promoting effects of insulin-like growth factor I (IGF-I) in a mouse model of type 1 diabetes. *Bone.* 2013;57(1):36–40.
  542. Uchimura T, Hollander JM, Nakamura DS, Liu Z, Rosen CJ, Georgakoudi I, et al. An essential role for IGF2 in cartilage development and glucose metabolism during postnatal long bone growth. *Development.* 2017;144:3533–46.
  543. Ma S, Liu G, Jin L, Pang X, Wang Y, Wang Z, et al. IGF-1/IGF-1R/hsa-let-7c axis regulates the committed differentiation of stem cells from apical papilla. *Sci Rep.* 2016;6:36922.
  544. Kelley KM, Oh Y, Gargosky SE, Gucev Z, Matsumoto T, Hwa V, et al. Insulin-like growth factor-binding proteins (IGFBPs) and their regulatory dynamics. *Int J Biochem Cell Biol.* 1996;28(6):619–37.
  545. Kveiborg M, Flyvbjerg A, Rattan SIS, Kassem M. Changes in the insulin-like growth factor-system may contribute to in vitro age-related impaired osteoblast functions. *Exp Gerontol.* 2000;35(8):1061–74.
  546. Aonuma H, Ogura N, Kamino Y, Ito K, Kondoh T. Microarray analysis of human dental follicle cells in osteogenic differentiation -Gene expression of IGF-II and IGFBP-2 during osteogenic differentiation. *J Hard Tissue Biol.* 2009;18(1):27–34.
  547. Strohbach C, Kleinman S, Linkhart T, Amaar Y, Chen ST, Mohan S, et al. Potential involvement of the interaction between insulin-like growth factor binding protein (IGFBP)-6 and LIM mineralization protein (LMP)-1 in regulating osteoblast differentiation. *J Cell Biochem.* 2008;104(5):1890–905.
  548. Okazaki R, Conover CA, Harris SA, Spelsberg TC, Riggs LB. Normal human osteoblast-like cells consistently express genes for insulin-like growth factors I and II but transformed human osteoblast cell lines do not. *J Bone Miner Res.* 1995;10(5):788–95.
  549. Yan L, Sun S, Qu L. Insulin-like growth factor-1 promotes the proliferation and odontoblastic differentiation of human dental pulp cells under high

- glucose conditions. *Int J Mol Med*. 2017;40(4):1253–60.
550. Khan M, Ali F, Mohsin S, Akhtar S, Mehmood A, Choudhery MS, et al. Preconditioning diabetic mesenchymal stem cells with myogenic medium increases their ability to repair diabetic heart. *Stem Cell Res Ther*. 2013;4(3).
551. Zhao YF, Zeng DL, Xia LG, Zhang SM, Xu LY, Jiang XQ, et al. Osteogenic potential of bone marrow stromal cells derived from streptozotocin-induced diabetic rats. *Int J Mol Med*. 2013;31(3):614–20.
552. McCarthy AD, Etcheverry SB, Cortizo AM. Effect of advanced glycation endproducts on the secretion of insulin-like growth factor-I and its binding proteins: Role in osteoblast development. *Acta Diabetol*. 2001;38(3):113–22.
553. Delany AM, Durant D, Canalis E. Glucocorticoid suppression of IGF I transcription in osteoblasts. *Mol Endocrinol*. 2001;15(10):1781–9.
554. Birnbaum RS, Bowsher RR, Wiren KM. Changes in IGF-I and -II expression and secretion during the proliferation and differentiation of normal rat osteoblasts. *J Endocrinol*. 1995;144(2):251–9.
555. Thrailkill KM, Siddhanti SR, Fowlkes JL, Quarles LD. Differentiation of MC3T3-E1 Osteoblasts is associated with temporal changes in the expression of IGF-I and IGF-BPs. *Bone*. 1995;17(3):307–13.
556. Palermo C, Manduca P, Gazzero E, Foppiani L, Segat D, Barreca A. Potentiating role of IGF-BP-2 on IGF-II-stimulated alkaline phosphatase activity in differentiating osteoblasts. *Am J Physiol - Endocrinol Metab*. 2004;286:E648–E657.
557. Wang S, Mu J, Fan Z, Yu Y, Yan M, Lei G, et al. Insulin-like growth factor 1 can promote the osteogenic differentiation and osteogenesis of stem cells from apical papilla. *Stem Cell Res*. 2012;8(3):346–56.
558. MOCHIZUKI H, HAKEDA Y, WAKATSUKI N, USUI N, AKASHI S, SATO T, et al. Insulin-Like Growth Factor-I Supports Formation and Activation of Osteoclasts. *Endocrinology*. 1992;131(3).
559. Peng JX, Guan XY, Li GH, Zhong JL, Song JK, Xiao LL, et al. Recombinant human insulin-like growth factor-1 promotes osteoclast formation and accelerates orthodontic tooth movement in rats. *J Appl Oral Sci*. 2021;29:e20200791.
560. Fiorelli G, Formigli L, Zecchi Orlandini S, Gori F, Falchetti A, Morelli A, et

- al. Characterization and function of the receptor for IGF-I in human preosteoclastic cells. *Bone*. 1996;18(3):269–76.
561. Wang Y, Nishida S, Elalieh HZ, Long RK, Halloran BP, Bikle DD. Role of IGF-I signaling in regulating osteoclastogenesis. *J Bone Miner Res*. 2006;21(9):1350–8.
562. Fang J, Zhang X, Chen X, Wang Z, Zheng S, Cheng Y, et al. The role of insulin-like growth factor-1 in bone remodeling: A review. *Int J Biol Macromol*. 2023;238(January):124125.
563. Ismayilnajadteymurabadi H, Konukoglu D. The relationship between IGF-2, IGFBP-2, and IGFBP-3 levels in patients suffering from pre-diabetes. *J Biol Regul Homeost Agents*. 2018;32(1):63–8.
564. Heo YR, Kang CW, Cha YS. L-Carnitine changes the levels of insulin-like growth factors (IGFs) and IGF binding proteins in streptozotocin-induced diabetic rat. *J Nutr Sci Vitaminol (Tokyo)*. 2001;47:329–34.
565. Han HJ, Park SH. Alteration of the gene and protein levels of insulin-like growth factors in streptozotocin-induced diabetic male rats. *J Vet Med Sci*. 2006;68(5):413–9.
566. Fanganiello RD, Ishiy FAA, Kobayashi GS, Alvizi L, Sunaga DY, Passos-Bueno MR. Increased in vitro osteopotential in SHED associated with higher IGF2 expression when compared with hASCs. *Stem Cell Rev Reports*. 2015;11(4):635–44.
567. Hardouin SN, Guo R, Romeo PH, Nagy A, Aubin JE. Impaired mesenchymal stem cell differentiation and osteoclastogenesis in mice deficient for Igf2-P2 transcripts. *Development*. 2011;138(2):203–13.
568. DeChiara TM, Efstratiadis A, Robertsen EJ. A growth-deficiency phenotype in heterozygous mice carrying an insulin-like growth factor II gene disrupted by targeting. *Nature*. 1990;345(6270):78–80.
569. Gicquel C, Rossignol S, Cabrol S, Houang M, Steunou V, Barbu V, et al. Epimutation of the telomeric imprinting center region on chromosome 11p15 in Silver-Russell syndrome. *Nat Genet*. 2005;37(9):1003–7.
570. Lee H, Min SK, Park Y-H, Park J. The Role of Insulin-Like Growth Factor-2 on the Cellular Viability and Differentiation to the Osteogenic Lineage and Mineralization of Stem Cells Cultured on Deproteinized Bovine Bone Mineral. *Appl Sci*. 2020;10(16):5471.
571. Chen PC, Kuo YC, Chuong CM, Huang YH. Niche Modulation of IGF-1R

- Signaling: Its Role in Stem Cell Pluripotency, Cancer Reprogramming, and Therapeutic Applications. *Front Cell Dev Biol.* 2021;8:625943.
572. Jiang R, Wang M, Shen X, Huang S, Han J, Li L, et al. SUMO1 modification of IGF-1R combining with SNAI2 inhibited osteogenic differentiation of PDLSCs stimulated by high glucose. *Stem Cell Res Ther.* 2021;12(1):1–20.
573. Menssen A, Häupl T, Sittinger M, Delorme B, Charbord P, Ringe J. Differential gene expression profiling of human bone marrow-derived mesenchymal stem cells during adipogenic development. *BMC Genomics.* 2011;12:1–17.
574. Liu GX, Ma S, Li Y, Yu Y, Zhou YX, Lu YD, et al. Hsa-let-7c controls the committed differentiation of IGF-1-treated mesenchymal stem cells derived from dental pulps by targeting IGF-1R via the mapk pathways. *Exp Mol Med.* 2018;50(4).
575. Brouwer-Visser J, Huang GS. IGF2 signaling and regulation in cancer. *Cytokine Growth Factor Rev.* 2015;26(3):371–7.
576. Jehle PM, Jehle DR, Mohan S, Böhm BO, Bo BO, Böhm BO. Serum levels of insulin-like growth factor system components and relationship to bone metabolism in type 1 and type 2 diabetes mellitus patients. *J Endocrinol.* 1998;159(2):297–306.
577. Rajpathak SN, Gunter MJ, Wylie-Rosett J, Ho GYF, Kaplan RC, Muzumdar R, et al. The role of insulin-like growth factor-I and its binding proteins in glucose homeostasis and type 2 diabetes. *Diabetes Metab Res Rev.* 2009;25:3–12.
578. Wang X, Wei W, Krzeszinski JY, Wang Y, Wan Y, Xunde Wang, Wei Wei, Jing Y. Krzeszinski, Yubao Wang and YW. A Liver-Bone Endocrine Relay by IGFBP1 Promotes Osteoclastogenesis and Mediates FGF21-Induced Bone Resorption. *Cell Metab.* 2015;22(5):811–24.
579. Pye SR, Almusalam B, Boonen S, Vanderschueren D, Borghs H, Gielen E, et al. Influence of Insulin-Like Growth Factor Binding Protein (IGFBP)-1 and IGFBP-3 on bone health: Results from the european male ageing study. *Calcif Tissue Int.* 2011;88(6):503–10.
580. Lundin H, Sääf M, Strender LE, Nyren S, Johansson SE, Salminen H. High Serum Insulin-Like Growth Factor-Binding Protein 1 (IGFBP-1) is Associated with High Fracture Risk Independent of Insulin-Like Growth

- Factor 1 (IGF-I). *Calcif Tissue Int.* 2016;99(4):333–9.
581. Slater T, Haywood NJ, Matthews C, Cheema H, Wheatcroft SB. Insulin-like growth factor binding proteins and angiogenesis: from cancer to cardiovascular disease. *Cytokine Growth Factor Rev.* 2019;46:28–35.
582. Li T, Forbes ME, Fuller GN, Li J, Yang X, Zhang W. IGFBP2: integrative hub of developmental and oncogenic signaling network. *Oncogene.* 2020;39(11):2243–57.
583. Martin A, Komada MR, Sane DC. Abnormal angiogenesis in diabetes mellitus. *Med Res Rev.* 2003;23(2):117–45.
584. Dzhoyashvili NA, Efimenko AY, Kochegura TN, Kalinina NI, Koptelova N V., Sukhareva OY, et al. Disturbed angiogenic activity of adipose-derived stromal cells obtained from patients with coronary artery disease and diabetes mellitus type 2. *J Transl Med.* 2014;12(1):1–13.
585. Rezaie J, Mehranjani MS, Rahbarghazi R, Shariatzadeh MA. Angiogenic and Restorative Abilities of Human Mesenchymal Stem Cells Were Reduced Following Treatment With Serum From Diabetes Mellitus Type 2 Patients. *J Cell Biochem.* 2018;119(1):524–35.
586. Kim YS, Kang HJ, Hong MH, Kang WS, Choe N, Kook H, et al. Angiopoietin-like 4 is involved in the poor angiogenic potential of high glucose-insulted bone marrow stem cells. *Korean Circ J.* 2014;44(3):177–83.
587. Xi G, Wai C, DeMambro V, Rosen CJ, Clemmons DR. IGFBP-2 directly stimulates osteoblast differentiation. *J Bone Miner Res.* 2014;29(11):2427–38.
588. Cheng SL, Zhang SF, Mohan S, Lecanda F, Fausto A, Hunt AH, et al. Regulation of insulin-like growth factors I and II and their binding proteins in human bone marrow stromal cells by dexamethasone. *J Cell Biochem.* 1998;71(3):449–58.
589. Hamidouche Z, Fromigué O, Ringe J, Häupl T, Marie PJ. Crosstalks between integrin alpha 5 and IGF2/IGFBP2 signalling trigger human bone marrow-derived mesenchymal stromal osteogenic differentiation. *BMC Cell Biol.* 2010;11.
590. Fisher MC, Meyer C, Garber G, Dealy CN. Role of IGFBP2, IGF-I and IGF-II in regulating long bone growth. *Bone.* 2005;37(6):741–50.
591. Demambro VE, Maile L, Wai C, Kawai M, Cascella T, Rosen CJ, et al.

- Insulin-like growth factor-binding protein-2 is required for osteoclast differentiation. *J Bone Miner Res.* 2012;27(2):390–400.
592. Okuyama T, Kyohara M, Terauchi Y, Shirakawa J. The roles of the IGF axis in the regulation of the metabolism: Interaction and difference between insulin receptor signaling and IGF-I receptor signaling. *Int J Mol Sci.* 2021;22(13).
593. Cordain L, Eades MR, Eades MD. Hyperinsulinemic diseases of civilization: More than just Syndrome X. *Comp Biochem Physiol - A Mol Integr Physiol.* 2003;136:95–112.
594. Touskova V, Trachta P, Kavalkova P, Drapalova J, Haluzikova D, Mraz M, et al. Serum concentrations and tissue expression of components of insulin-like growth factor-axis in females with type 2 diabetes mellitus and obesity: The influence of very-low-calorie diet. *Mol Cell Endocrinol.* 2012;361(1–2):172–8.
595. Baxter RC. Insulin-like growth factor binding protein-3 (IGFBP-3): Novel ligands mediate unexpected functions. *J Cell Commun Signal.* 2013;7(3):179–89.
596. Villafuerte BC, Koop BL, Pao C-I, Phillips LS. Glucocorticoid Regulation of Insulin-Like Growth Factor-Binding Protein-3. *Endocrinology.* 1995;136(5):1928–33.
597. Valentinis B, Bhala A, DeAngelis T, Baserga R, Cohen P. The human insulin-like growth factor (IGF) binding protein-3 inhibits the growth of fibroblasts with a targeted disruption of the IGF-I receptor gene. *Mol Endocrinol.* 1995;9(3):361–7.
598. Nishimura I, Hisanaga R, Sato T, Arano T, Nomoto S. Effect of osteogenic differentiation medium on proliferation and differentiation of human mesenchymal stem cells in three-dimensional culture with radial flow bioreactor. *Regen Ther.* 2015;2:24–31.
599. Firth SM, Baxter RC. Cellular actions of the insulin-like growth factor binding proteins. *Endocr Rev.* 2002;23(6):824–54.
600. Martin JL, Baxter RC. Signalling pathways of insulin-like growth factors (IGFs) and IGF binding protein-3. *Growth Factors.* 2011;29(6):235–44.
601. Jacot TA, Clemmons DR. Effect of glucose on insulin-like growth factor binding protein-4 proteolysis. *Endocrinology.* 1998;139(1):44–50.
602. Ahmad T, Ugarph-Morawski A, Lewitt MS, Li J, Sääf M, Brismar K. Diabetic

- osteopathy and the IGF system in the Goto-Kakizaki rat. *Growth Horm IGF Res.* 2008;18(5):404–11.
603. Hjortebjerg R. IGFBP-4 and PAPP-A in normal physiology and disease. *Growth Horm IGF Res.* 2018;41:7–22.
604. Li H, Yu S, Hao F, Sun X, Zhao J, Xu Q, et al. Insulin-like growth factor binding protein 4 inhibits proliferation of bone marrow mesenchymal stem cells and enhances growth of neurospheres derived from the stem cells. *Cell Biochem Funct.* 2018;36(6):331–41.
605. Zhang M, Faugere MC, Malluche H, Rosen CJ, Chernausek SD, Clemens TL. Paracrine Overexpression of IGFBP-4 in Osteoblasts of Transgenic Mice Decreases Bone Turnover and Causes Global Growth Retardation. *J Bone Miner Res.* 2003;18(5):836–43.
606. MIYAKOSHI N, QIN X, KASUKAWA Y, RICHMAN C, SRIVASTAVA AK, BAYLINK DJ, et al. Systemic Administration of Insulin-Like Growth Factor (IGF)-Binding Protein-4 (IGFBP-4) Increases Bone Formation Parameters in Mice by Increasing IGF Bioavailability via an IGFBP-4 Protease-Dependent Mechanism. *Endocrinology.* 2001;142(6):2641–8.
607. Ning Y, Schuller AGP, Conover CA, Pintar JE. Insulin-like growth factor (IGF) binding protein-4 is both a positive and negative regulator of IGF activity in vivo. *Mol Endocrinol.* 2008;22(5):1213–25.
608. Moyer-Mileur LJ, Slater H, Jordan KC, Murray MA. IGF-1 and IGF-binding proteins and bone mass, geometry, and strength: Relation to metabolic control in adolescent girls with type 1 diabetes. *J Bone Miner Res.* 2008;23(12):1884–91.
609. Liu D, Wang Y, Jia Z, Wang L, Wang J, Yang D, et al. Demethylation of IGFBP5 by Histone Demethylase KDM6B Promotes Mesenchymal Stem Cell-Mediated Periodontal Tissue Regeneration by Enhancing Osteogenic Differentiation and Anti-Inflammation Potentials. *Stem Cells.* 2015 Aug 1;33:2523–36.
610. Abdallah BM. Osteoblast differentiation of NIH3T3 fibroblasts is associated with changes in the IGF-I/IGFBP expression pattern. *Cell Mol Biol Lett.* 2006;11(4):461–74.
611. Hao J, Yang H, Cao Y, Zhang C, Fan Z. IGFBP5 enhances the dentinogenesis potential of dental pulp stem cells via JNK and Erk signalling pathways. *J Oral Rehabil.* 2020;47(12):1557–65.

612. Yin P, Xu Q, Duan C. Paradoxical actions of endogenous and exogenous insulin-like growth factor-binding protein-5 revealed by RNA interference analysis. *J Biol Chem.* 2004;279(31):32660–6.
613. Schedlich LJ, Muthukaruppan A, O'Han MK, Baxter RC. Insulin-like growth factor binding protein-5 interacts with the vitamin D receptor and modulates the vitamin D response in osteoblasts. *Mol Endocrinol.* 2007;21(10):2378–90.
614. Durant D, Pereira RMR, Canalis E. Overexpression of insulin-like growth factor binding protein-5 decreases osteoblastic function in vitro. *Bone.* 2004;35(6):1256–62.
615. Mukherjee A, Rotwein P. Insulin-like growth factor-binding protein-5 inhibits osteoblast differentiation and skeletal growth by blocking insulin-like growth factor actions. *Mol Endocrinol.* 2008;22(5):1238–50.
616. Aboalola D, Han VKM. Insulin-Like Growth Factor Binding Protein-6 Alters Skeletal Muscle Differentiation of Human Mesenchymal Stem Cells. *Stem Cells Int.* 2017;2017.
617. Bach LA. IGFBP-6 five years on; not so “forgotten”? *Growth Horm IGF Res.* 2005;15(3):185–92.
618. Iosef C, Vilk G, Gkourasas T, Lee KJ, Chen BPC, Fu P, et al. Insulin-like growth factor binding protein-6 (IGFBP-6) interacts with DNA-end binding protein Ku80 to regulate cell fate. *Cell Signal.* 2010;22(7):1033–43.
619. Götz W, Lossdörfer S, Krüger U, Braumann B, Jäger A. Immunohistochemical localization of insulin-like growth factor-II and its binding protein-6 in human epithelial cells of Malassez. *Eur J Oral Sci.* 2003;111(1):26–33.
620. Viereck V, Siggelkow H, Pannem R, Bräulke T, Scharf JG, Kübler B. Alteration of the insulin-like growth factor axis during in vitro differentiation of the human osteosarcoma cell line HOS 58. *J Cell Biochem.* 2007;102(1):28–40.
621. Massoner P, Ladurner Rennau M, Heidegger I, Kloss-Brandstätter A, Summerer M, Reichhart E, et al. Expression of the IGF axis is decreased in local prostate cancer but enhanced after benign prostate epithelial differentiation and TGF- $\beta$  treatment. *Am J Pathol.* 2011;179(6):2905–19.
622. Spentzos D, Cannistra SA, Grall F, Levine DA, Pillay K, Libermann TA, et al. IGF axis gene expression patterns are prognostic of survival in epithelial

- ovarian cancer. *Endocr Relat Cancer*. 2007;14(3):781–90.
623. Milne M, Quail JM, Rosen CJ, Baran DT. Insulin-like growth factor binding proteins in femoral and vertebral bone marrow stromal cells: Expression and regulation by thyroid hormone and dexamethasone. *J Cell Biochem*. 2001;81(2):229–40.
624. Payne SH. The utility of protein and mRNA correlation. *Trends Biochem Sci*. 2015;40(1):1–3.
625. Vogel C, Marcotte EM. Insights into the regulation of protein abundance from proteomic and transcriptomic analyses. *Nat Rev Genet*. 2012;13(4):227–32.
626. Wegler C, Ölander M, Wiśniewski JR, Lundquist P, Zettl K, Åsberg A, et al. Global variability analysis of mRNA and protein concentrations across and within human tissues. *NAR Genomics Bioinforma*. 2020;2(1):1–11.
627. Maier T, Güell M, Serrano L. Correlation of mRNA and protein in complex biological samples. *FEBS Lett*. 2009;583(24):3966–73.
628. Buccitelli C, Selbach M. mRNAs, proteins and the emerging principles of gene expression control. *Nat Rev Genet*. 2020;21(10):630–44.
629. Mohan S, Baylink DJ. IGF-binding proteins are multifunctional and act via IGF-dependent and -independent mechanisms. *J Endocrinol*. 2002;175(1):19–31.
630. Frystyk J, Skjærbæk C, Vestbo E, Fisker S, Ørskov H. Circulating levels of free insulin-like growth factors in obese subjects: The impact of type 2 diabetes. *Diabetes Metab Res Rev*. 1999;15(5):314–22.
631. Song F, Zhou XX, Hu Y, Li G, Wang Y. The Roles of Insulin-Like Growth Factor Binding Protein Family in Development and Diseases. *Adv Ther*. 2021;38(2):885–903.
632. Kobberø SD, Gajhede M, Mirza OA, Kløverpris S, Kjær TR, Mikkelsen JH, et al. Structure of the proteolytic enzyme PAPP-A with the endogenous inhibitor stanniocalcin-2 reveals its inhibitory mechanism. *Nat Commun*. 2022;13(1):1–16.
633. Collett-Solberg PF, Cohen P. The role of the insulin-like growth factor binding proteins and the IGFBP proteases in modulating IGF action. *Endocrinol Metab Clin North Am*. 1996;25(3):591–614.
634. Barrios V, Chowen JA, Martín-Rivada Á, Guerra-Cantera S, Pozo J, Yakar S, et al. Pregnancy-associated plasma protein (PAPP)-A2 in physiology

- and disease. *Cells*. 2021;10(12).
635. Bunn RC, Fowlkes JL. Insulin-like growth factor binding protein proteolysis. *Trends Endocrinol Metab*. 2003;14(4):176–81.
636. Oxvig C. The role of PAPP-A in the IGF system: location, location, location. *J Cell Commun Signal*. 2015;9:177–87.
637. Arthur A, Gronthos S. Clinical application of bone marrow mesenchymal stem/stromal cells to repair skeletal tissue. *Int J Mol Sci*. 2020;21(24):1–27.
638. Hernigou P, Guissou I, Homma Y, Poignard A, Chevallier N, Rouard H, et al. Percutaneous injection of bone marrow mesenchymal stem cells for ankle non-unions decreases complications in patients with diabetes. *Int Orthop*. 2015;39(8):1639–43.
639. Zhang H, Fu X, Zhang S, Li Q, Chen Y, Liu H, et al. Strategy of Stem Cell Transplantation for Bone Regeneration with Functionalized Biomaterials and Vascularized Tissues in Immunocompetent Mice. *ACS Biomater Sci Eng*. 2022;8(4):1656–66.
640. Reddy MA, Zhang E, Natarajan R. Epigenetic mechanisms in diabetic complications and metabolic memory. *Diabetologia*. 2015;58(3):443–55.
641. Grzesik WJ, Narayanan a S, Hill C. Cementum and Periodontal Wound Healing and Regeneration. *Crit Rev Oral Biol Med*. 2002;13(6):474–84.
642. Arzate H, Zeichner-David M, Mercado-Celis G. Cementum proteins : role in periodontium formation and regeneration. *Periodontol* 2000. 2015;67:211–33.
643. Hoz L, López S, Zeichner-David M, Arzate H. Regeneration of rat periodontium by cementum protein 1-derived peptide. *J Periodontal Res*. 2021;56(6):1223–32.
644. Carmona-Rodríguez B, Álvarez-Pérez MA, Narayanan AS, Zeichner-David M, Reyes-Gasga J, Molina-Guarneros J, et al. Human Cementum Protein 1 induces expression of bone and cementum proteins by human gingival fibroblasts. *Biochem Biophys Res Commun*. 2007;358(3):763–9.
645. Arroyo R, López S, Romo E, Montoya G, Hoz L, Pedraza C, et al. Carboxy-terminal cementum protein 1-derived peptide 4 (Cemp1-p4) promotes mineralization through wnt/ $\beta$ -catenin signaling in human oral mucosa stem cells. *Int J Mol Sci*. 2020;21(4).
646. Wu Z, Dai W, Wang P, Zhang X, Tang Y, Liu L, et al. Periostin promotes

- migration, proliferation, and differentiation of human periodontal ligament mesenchymal stem cells. *Connect Tissue Res.* 2018;59(2):108–19.
647. Mohanarangam S, Victor DJ, Sangeetha S, PSG P. The influence of periostin on osteoblastic adhesion and proliferation on collagen matrices - An in vitro study. *J Indian Soc Periodontol.* 2021;25:480–4.
648. Wang Z, An J, Zhu D, Chen H, Lin A, Kang J, et al. Periostin: an emerging activator of multiple signaling pathways. *J Cell Commun Signal.* 2022;16(4):515–30.
649. Poon B, Kha T, Tran S, Dass CR. Bone morphogenetic protein-2 and bone therapy: Successes and pitfalls. *J Pharm Pharmacol.* 2016;68(2):139–47.
650. Feng Z, Su X, Wang T, Guo S. Identification of Biomarkers That Modulate Osteogenic Differentiation in Mesenchymal Stem Cells Related to Inflammation and Immunity: A Bioinformatics-Based Comprehensive Study. *Pharmaceuticals.* 2022;15(9):1–28.
651. Wheatcroft SB, Kearney MT, Shah AM, Ezzat VA, Miell JR, Modo M, et al. IGF-Binding Protein-2 Protects Against the Development of Obesity and Insulin Resistance. *Diabetes.* 2007;56:285–94.
652. Regan FM, Williams RM, McDonald A, Umpleby AM, Acerini CL, Rahilly SO, et al. Treatment with Recombinant Human Insulin-Like Growth Factor (rhIGF)-I/rhIGF Binding Protein-3 Complex Improves Metabolic Control in Subjects with Severe Insulin Resistance. *J Clin Endocrinol Metab.* 2010;95(5):2113–22.
653. Conover CA. Key questions and answers about pregnancy-associated plasma protein-A. *Trends Endocrinol Metab.* 2012;23(5):242–9.
654. Joshi AD. New Insights Into Physiological and Pathophysiological Functions of Stanniocalcin 2. *Front Endocrinol (Lausanne).* 2020;11:172.
655. Koffi KAA, Doublier S, Ricort J-MM, Babajko S, Nassif A, Isaac J. The role of GH/IGF axis in dento-alveolar complex from development to aging and therapeutics: A narrative review. *Cells.* 2021;10(5):1–29.
656. Miyakoshi N, Richman C, Qin X, Baylink DJ, Mohan S. Effects of recombinant insulin-like growth factor-binding protein-4 on bone formation parameters in mice. *Endocrinology.* 1999;140(12):5719–28.
657. Mitroulis I, Hajishengallis G, Chavakis T. Bone marrow inflammatory memory in cardiometabolic disease and inflammatory comorbidities. *Cardiovasc Res.* 2023;1–12.

658. Wilkinson P, Bozo IY, Braxton T, Just P, Jones E, Deev R V., et al. Systematic Review of the Preclinical Technology Readiness of Orthopedic Gene Therapy and Outlook for Clinical Translation. *Front Bioeng Biotechnol.* 2021;9:626315.
659. Bizenjima T, Seshima F, Ishizuka Y, Takeuchi T, Kinumatsu T, Saito A. Fibroblast growth factor-2 promotes healing of surgically created periodontal defects in rats with early, streptozotocin-induced diabetes via increasing cell proliferation and regulating angiogenesis. *J Clin Periodontol.* 2015;42(1):62–71.
660. Zhang Y, Xiong Y, Chen X, Chen C, Zhu Z, Li L. Therapeutic effect of bone marrow mesenchymal stem cells pretreated with acetylsalicylic acid on experimental periodontitis in rats. *Int Immunopharmacol.* 2018;54(14):320–8.
661. King AJF. The use of animal models in diabetes research. *Br J Pharmacol.* 2012;166(3):877–94.
662. Churchman SM, Ponchel F, Boxall SA, Cuthbert R, Kouroupis D, Roshdy T, et al. Transcriptional profile of native CD271+ multipotential stromal cells: Evidence for multiple fates, with prominent osteogenic and wnt pathway signaling activity. *Arthritis Rheum.* 2012;64(8):2632–43.
663. Mabuchi Y, Morikawa S, Harada S, Niibe K, Suzuki S, Renault-Mihara F, et al. LNGFR+THY-1+VCAM-1hi+ cells reveal functionally distinct subpopulations in mesenchymal stem cells. *Stem Cell Reports.* 2013;1:152–65.
664. Torri E, Rinkera, Taymour M. Hammoudia, Melissa L. Kempa, Hang Lub and JST. Interactions between Mesenchymal Stem Cells, Adipocytes, and Osteoblasts in a 3D Tri-Culture Model of Hyperglycemic Conditions in the Bone Marrow Microenvironment. *Integr Biol.* 2014;6(3):324–37.
665. Ayilavarapu S, Doctor A, Lee CT, Tribble GD, Chiu Y, Weltman RL, et al. Altered human alveolar bone gene expression in type 2 diabetes—A cross-sectional study. *J Periodontal Res.* 2022;57(1):142–51.
666. Zhao X, Yang Y, Yu J, Ding R, Pei D, Zhang Y, et al. Injectable hydrogels with high drug loading through B–N coordination and ROS-triggered drug release for efficient treatment of chronic periodontitis in diabetic rats. *Biomaterials.* 2022;282:121387.
667. Hajishengallis G. New developments in neutrophil biology and

- periodontitis. *Periodontol 2000*. 2020;82(1):78–92.
668. Bordin A, Pagano F, Scaccia E, Saccucci M, Voza I, Incerti N, et al. Oral plaque from type 2 diabetic patients reduces the clonogenic capacity of dental pulp-derived mesenchymal stem cells. *Stem Cells Int*. 2019;2019.
669. Aliakbari S, Mohammadi M, Rezaee MA, Amini AA, Fakhari S, Rahmani MR. Impaired immunomodulatory ability of type 2 diabetic adipose-derived mesenchymal stem cells in regulation of inflammatory condition in mixed leukocyte reaction. *EXCLI J*. 2019;18:852–65.
670. Serena C, Keiran N, Ceperuelo-Mallafre V, Ejarque M, Fradera R, Roche K, et al. Obesity and Type 2 Diabetes Alters the Immune Properties of Human Adipose Derived Stem Cells. *Stem Cells*. 2016;34(10):2559–73.
671. Morris AD, Dalal S, Li H, Brewster LP. Human diabetic mesenchymal stem cells from peripheral arterial disease patients promote angiogenesis through unique secretome signatures. *Surgery*. 2018;163:870–6.
672. Louvrier A, Euvrard E, Nicod L, Rolin G, Gindraux F, Pazart L, et al. Odontoblastic differentiation of dental pulp stem cells from healthy and carious teeth on an original PCL-based 3D scaffold. *Int Endod J*. 2018;51:e252–63.
673. Tang HN, Xia Y, Yu Y, Wu RX, Gao LN, Chen FM. Stem cells derived from “inflamed” and healthy periodontal ligament tissues and their sheet functionalities: A patient-matched comparison. *J Clin Periodontol*. 2016;43(1):72–84.
674. Natesan S, Wrice NL, Baer DG, Christy RJ. Debrided skin as a source of autologous stem cells for wound repair. *Stem Cells*. 2011;29(8):1219–30.
675. Amini-Nik S, Dolp R, Eylert G, Datu AK, Parousis A, Blakeley C, et al. Stem cells derived from burned skin - The future of burn care. *EBioMedicine*. 2018;37:509–20.
676. Kafienah W, Mistry S, Dickinson SC, Sims TJ, Learmonth I, Hollander AP. Three-dimensional cartilage tissue engineering using adult stem cells from osteoarthritis patients. *Arthritis Rheum*. 2007;56(1):177–87.
677. Mareddy S, Crawford R, Brooke G, Xiao Y. Clonal isolation and characterization of bone marrow stromal cells from patients with osteoarthritis. *Tissue Eng*. 2007;13(4):819–29.
678. Srinivasan A, Teo N, Poon KJ, Tiwari P, Ravichandran A, Wen F, et al. Comparative Craniofacial Bone Regeneration Capacities of Mesenchymal

- Stem Cells Derived from Human Neural Crest Stem Cells and Bone Marrow. *ACS Biomater Sci Eng.* 2021;7(1):207–21.
679. Suliman S, Ali HRW, Karlsen TA, Amiaud J, Mohamed-Ahmed S, Layrolle P, et al. Impact of humanised isolation and culture conditions on stemness and osteogenic potential of bone marrow derived mesenchymal stromal cells. *Sci Rep.* 2019;9(1):1–18.
680. Blahnova VH, Filova E, Dankova J, Rampichova M. Combinations of growth factors for human mesenchymal stem cell proliferation and osteogenic differentiation. *Bone Jt Res.* 2020;9(7):412–20.
681. Huang CH, Chen MH, Young TH, Jeng JH, Chen YJ. Interactive effects of mechanical stretching and extracellular matrix proteins on initiating osteogenic differentiation of human mesenchymal stem cells. *J Cell Biochem.* 2009;108(6):1263–73.
682. Ghazanfari R, Zacharaki Di, Li H, Ching Lim H, Soneji S, Scheduling S. Human Primary Bone Marrow Mesenchymal Stromal Cells and Their in vitro Progenies Display Distinct Transcriptional Profile Signatures. *Sci Rep.* 2017;7(1):1–10.

# Appendix

## Appendix A: Ethical approval of samples collection

The Leeds Teaching Hospitals   
NHS Trust

Ref: Amy Dickinson

17/07/2014

Professor Dennis McGonagle  
Rheumatology Department  
Chapel Allerton Hospital  
Chapeltown Road  
Leeds  
LS7 4SA

Research & Development

Leeds Teaching Hospitals NHS Trust  
34 Hyde Terrace  
Leeds  
LS2 9LN

Tel: 0113 392 2878  
Fax: 0113 392 6397

r&d@leedsth.nhs.uk  
www.leedsth.nhs.uk

Dear Professor Dennis McGonagle

Re: NHS Permission at LTHT for: Collection of joint Mesenchymal Stem Cells by aspiration, biopsy, joint retrieval at arthroplasty or by synovium agitation during arthroscopy  
LTHT R&D Number: RR14/11102 (100077/WY)  
REC: 14/YH/0087

I confirm that *NHS Permission for research* has been granted for this project at The Leeds Teaching Hospitals NHS Trust (LTHT). NHS Permission is granted based on the information provided in the documents listed below. All amendments (including changes to the research team) must be submitted in accordance with guidance in IRAS. Any change to the status of the project must be notified to the R&D Department.

Permission is granted on the understanding that the study is conducted in accordance with the *Research Governance Framework for Health and Social Care*, ICH GCP (if applicable) and NHS Trust policies and procedures available at <http://www.leedsth.nhs.uk>

This permission is granted only on the understanding that you comply with the requirements of the *Framework* as listed in the attached sheet "Conditions of Approval".

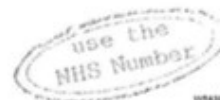
If you have any queries about this approval please do not hesitate to contact the R&D Department on telephone 0113 392 2878.

### Indemnity Arrangements

The Leeds Teaching Hospitals NHS Trust participates in the NHS risk pooling scheme administered by the NHS Litigation Authority 'Clinical Negligence Scheme for NHS Trusts' for: (i) medical professional and/or medical malpractice liability; and (ii) general liability. NHS Indemnity for negligent harm is extended to researchers with an employment contract (substantive or honorary) with the Trust. The Trust

Chairman Mike Collier CBE Chief Executive Maggie Boyle

The Leeds Teaching Hospitals incorporating:  
Chapel Allerton Hospital Leeds Dental Institute Seacroft Hospital  
St James's University Hospital The General Infirmary at Leeds Wharfedale Hospital



W14280

## Appendix B: Summary of qPCR results

**Table A: Statistically significant differences of gene expression in non-diabetic and diabetic BM-MSCs**

Gene	T0	B	O
<i>POSTN</i>	--	--	↓D, Wk3 (p=0.02)
<i>CEMP-1</i>	--	↓D, Wk1 (p=0.04)	--
<i>IGFBP-2</i>	--	↓D, Wk1 (p=0.02)	--
<i>IGFBP-3</i>	--	↓D, Wk3 (p=0.04)	--
<i>IGFBP-4</i>	--	↓D, Wk1 (p=0.049)	--

B: Basal, D: Diabetic, ND: Non-diabetic, O: Osteogenic, --: No change, ↑: upregulation, ↓: downregulation

**Table B: Trends of differences in gene expression in non-diabetic and diabetic BM-MSCs**

Gene	T0	B	O
<i>ALPL</i>	--	↓D, Wk3	--
<i>RUNX2</i>	--	↓D, Wk3	--
<i>POSTN</i>	↓D	↓D, Wk3	--
<i>CEMP-1</i>	--	--	↓D, Wk1
<i>IGFBP-1</i>	↓D	↓D, Wk1	↓D, Wk2
<i>IGFBP-3</i>	--	↓D, Wk2	--

B: Basal, D: Diabetic, ND: Non-diabetic, O: Osteogenic, --: No change, ↑: upregulation, ↓: downregulation

**Table C: Statistically significant differences in basal versus osteogenic cultures of non-diabetic and diabetic BM-MSCs**

Gene	ND	D
<i>IGF-1</i>	↓O, Wk2 (p=0.01)	--
<i>IGFBP-3</i>	↓O, Wk3 (p=0.045)	--

B: Basal, D: Diabetic, ND: Non-diabetic, O: Osteogenic, --: No change, ↑: upregulation, ↓: downregulation

**Table D: Trends of differences in basal versus osteogenic cultures of non-diabetic and diabetic BM-MSCs**

Gene	ND	D
<i>ALPL</i>	↑O, Wk1	↑O, Wk1 and Wk3
<i>RUNX2</i>	↑O, Wk1	↑O, Wk3
<i>COL1</i>	↓O, Wk3	↓O, Wk3
<i>POSTN</i>	↓O, Wk 2	--
<i>CEMP-1</i>	--	↑O, Wk 3
<i>IGF-1</i>	↓O, Wk1 and 3	↓O, Wk1, 2 and 3
<i>IGF-2</i>	↑O, Wk1	--
<i>IGFBP-1</i>	↓O, Wk1	--
<i>IGFBP-2</i>	↑O, Wk2 and Wk3	↑O, Wk1 and Wk3
<i>IGFBP-3</i>	↓O, Wk1, Wk2	--
<i>IGFBP-4</i>	↓O, Wk2	--
<i>IGFBP-5</i>	↓O, Wk1, 2 and 3	↓O, Wk1, 2 and 3
<i>IGFBP-6</i>	↓O,Wk3	--

B: Basal, D: Diabetic, ND: Non-diabetic, O: Osteogenic, --: No change, ↑: upregulation, ↓: downregulation

## Appendix C: List of presentations

1. Nancy Hussein, Josie Meade, Hemant Pandit, Elena Jones and Reem El-Gendy. Stem cells based periodontal regeneration in diabetics: challenges and potentials. Leeds Brasilia symposium (online), 12 May 2021 (Oral presentation).
2. Nancy Hussein, Josie Meade, Hemant Pandit, Elena Jones and Reem El-Gendy. Dental Tissue Engineering Using Diabetic Bone Marrow Mesenchymal Stromal Cells. Tissue and Cell Engineering Society (TCES) virtual conference, University of Edinburgh, 6-7 July 2021 (Poster presentation).
3. Nancy Hussein, Josie Meade, Hemant Pandit, Elena Jones and Reem El-Gendy. The Effect of Diabetes on Osteogenic Differentiation of Mesenchymal Stromal Cells (MSCs). British Society for Oral and Dental Research (BSODR) Annual Meeting, University of Birmingham, 1-3 September 2021 (Oral presentation).
4. Nancy Hussein, Josie Meade, Hemant Pandit, Elena Jones and Reem El-Gendy. Investigating the Role of Insulin-like Growth Factor Axis in Osteogenic Differentiation of Diabetic BM-MSCs. Joint Tissue and Cell Engineering Society (TCES) and Centre for doctoral training (CDT) conference, University of Birmingham, 13-15 June 2022 (Poster presentation).
5. Nancy Hussein, Josie Meade, Hemant Pandit, Elena Jones and Reem El-Gendy. Expression of Periodontal Markers in diabetic BM-MSCs. White Rose Biomaterials and Tissue Engineering Group Annual Meeting, University of York, 19 December 2022 (Oral presentation).
6. Nancy Hussein, Josie Meade, Hemant Pandit, Elena Jones and Reem El-Gendy. Role of IGF axis in Bone Tissue Engineering using Diabetic BM-MSCs. Tissue Engineering and Regenerative Medicine International Society (TERMIS) European Chapter Meeting 2023, Manchester, 28-31 March 2023 (Poster presentation).